

Synthesis and Reactivity of Lanthanide(II) Hydrides

Supplementary Materials

Supplementary material to a Thesis submitted to Victoria University of
Wellington in partial fulfilment of the requirements for the degree of Doctor of
Philosophy

by

Georgia M. Richardson



VICTORIA UNIVERSITY OF
WELLINGTON
TE HERENGA WAKA

Te Herenga Waka – Victoria University of Wellington 2024

Contents Table

| | |
|--|----|
| 1.0 Materials and Methods | 5 |
| 1.1 General Experimental Procedures..... | 5 |
| 1.2 Single Crystal X-ray Diffraction Analysis | 5 |
| 2.0 Chapter Two Experimental | 7 |
| 2.1 Synthetic, Spectroscopic and Analytical Data | 7 |
| [(BDI ^{Dipep})YbI] ₂ (2.1) | 7 |
| [(BDI ^{Dipep})YbN(SiMe ₃) ₂] (2.2) | 11 |
| [(BDI ^{Dipep})YbH] ₂ (2.4) | 16 |
| [(BDI ^{Dipep})YbH(THF)] ₂ (2.5) | 19 |
| Attempted synthesis of [(BDI ^{Dipep})YbEt] ₂ | 23 |
| (BDI ^{Dicyp})H (2.7) | 26 |
| [2-(2-cyclohexenyl)aniline] (2.8) | 30 |
| [2,6-di-(2-cyclohexenyl)aniline] (2.9) | 30 |
| [2,6-di-cyclohexylaniline] (2.10) | 31 |
| (BDI ^{Dicyp})K (2.11) | 32 |
| [(BDI ^{Dicyp})YbI] ₂ (2.12) | 36 |
| [(BDI ^{Dicyp})YbCH(SiMe ₃) ₂] (2.13) | 40 |
| [(BDI ^{Dicyp})YbH] ₂ (2.14) | 44 |
| [{(BDI ^{Dipp})Yb} ₃ P ₇] (2.15) | 46 |
| [(BDI ^{Dipep})Yb(THF)P ₄ Yb(THF)(BDI ^{Dipep})] (2.16) | 51 |
| [(BDI ^{Dicyp})Yb(P ₄)Yb(BDI ^{Dicyp})] (2.17) | 56 |
| [(BDI ^{Dipp})Yb(μ-C ₈ H ₈)Yb(BDI ^{Dipp})] (2.18) | 58 |
| [(BDI ^{Dipp})Yb(μ-C ₈ H ₈)] (2.19) | 62 |
| [(BDI ^{Dipp})(Et ₂ O)Yb(μ-C ₁₄ H ₁₀)Yb(OEt ₂)(BDI ^{Dipp})] (2.20) | 66 |
| [(BDI ^{Dipp})(Et ₂ O)Yb(μ-C ₁₀ H ₈)Yb(OEt ₂)(BDI ^{Dipp})] (2.21) | 70 |
| [(BDI ^{Dicyp})Yb(μ-C ₈ H ₈)Yb(BDI ^{Dicyp})] (2.22) | 74 |

| | |
|--|-----|
| $[(\text{BDI}^{\text{DicyP}})\text{Yb}(\mu\text{-C}_{14}\text{H}_{10})\text{Yb}(\text{BDI}^{\text{DicyP}})]$ (2.23) | 76 |
| 2.2 Single Crystal X-ray Diffraction Analysis | 78 |
| 2.2.1 Crystal Structure Data and Refinement Details | 78 |
| 2.3 Computational Details | 86 |
| 3.0 Chapter Three Experimental | 88 |
| 3.1 Synthetic, Spectroscopic and Analytical Data | 88 |
| $\text{K}[\text{Eu}(\text{HMDS})_3]$ (3.1) | 88 |
| $[\text{Eu}(\text{HMDS})_2(\text{Et}_2\text{O})]$ (3.2) | 89 |
| Attempted Synthesis of $[(\text{BDI}^{\text{DipeP}})\text{EuN}(\text{SiMe}_3)_2]$ | 90 |
| $[(\text{BDI}^{\text{DipeP}})\text{EuI}]_2$ (3.4) | 91 |
| Attempted Synthesis of $[(\text{BDI}^{\text{DipeP}})\text{EuN}(\text{SiMe}_3)_2]$ | 94 |
| Attempted Synthesis of $[(\text{BDI}^{\text{DipeP}})\text{EuN}(\text{SiMe}_3)_2]$ | 95 |
| Attempted Synthesis of $[(\text{BDI}^{\text{DipeP}})\text{EuCH}(\text{SiMe}_3)_2]$ | 96 |
| Attempted synthesis of $[(\text{BDI}^{\text{DipeP}})\text{EuH}]_2$ | 98 |
| $[(\text{BDI}^{\text{DicyP}})\text{Eu}(\text{I})_2\text{Eu}(\text{THF})(\text{BDI}^{\text{DicyP}})]$ (3.10) | 100 |
| $[(\text{BDI}^{\text{DicyP}})\text{EuCH}(\text{SiMe}_3)_2]$ (3.11) | 103 |
| $[(\text{BDI}^{\text{DicyP}})\text{EuN}(\text{SiMe}_3)_2]$ (3.13) | 106 |
| $[(\text{BDI}^{\text{DicyP}})\text{EuH}]_2$ (3.14) | 108 |
| $[(\text{BDI}^{\text{DicyP}})\text{Eu}(\text{DIC})]$ (3.15) | 110 |
| $(\text{BDI}^{\text{Dipp,DicyP}})\text{H}$ (3.16) | 112 |
| $(\text{BDI}^{\text{Dipp,DicyP}})\text{K}$ (3.17) | 117 |
| $[(\text{BDI}^{\text{Dipp,DicyP}})\text{EuI}]_2$ (3.18) | 121 |
| $[(\text{BDI}^{\text{Dipp,DicyP}})\text{EuCH}(\text{SiMe}_3)_2]$ (3.19) | 123 |
| $[(\text{BDI}^{\text{Dipp,DicyP}})\text{EuH}]$ (3.20) | 126 |
| $[(\text{BDI}^{\text{Dipp,TCHP}})\text{EuI}]_2$ (3.21) | 128 |
| $[(\text{BDI}^{\text{Dipp,TCHP}})\text{EuCH}(\text{SiMe}_3)_2(\text{THF})]$ (3.22) | 131 |
| $[(\text{BDI}^{\text{Dipp,TCHP}})\text{EuH}]$ (3.23) | 134 |

| | |
|---|-----|
| [(BDI ^{Dicyp})Eu(μ-COT)Eu(BDI ^{Dicyp})] (3.24)..... | 136 |
| [(BDI ^{Dipp,Dicyp})Eu(μ-COT)Eu(BDI ^{Dipp,Dicyp})] (3.25)..... | 139 |
| [(BDI ^{Dipp,TCHP})(THF)Eu(μ-COT)Eu(THF)(BDI ^{Dipp,TCHP})] (3.26) | 142 |
| [(BDI ^{Dicyp})Eu(μ-C ₁₄ H ₁₀)Eu(BDI ^{Dicyp})] (3.27)..... | 145 |
| [(BDI ^{Dicyp})Eu(OCHPh ₂)(THF)] ₂ (3.28)..... | 146 |
| [(BDI ^{Dicyp}) ₂ Eu(DMAP) ₃] (3.29) | 147 |
| [(2,6-di- ^t Bu-4-MePhO) ₂ Eu(THF) ₃] (3.30)..... | 148 |
| 3.2 Single Crystal X-ray Diffraction Analysis | 149 |
| 3.2.1 Crystal Structure Data and Refinement Details | 149 |
| 4.0 Chapter Four Experimental..... | 159 |
| 4.1 Synthetic, Spectroscopic and Analytic Data..... | 159 |
| [(BDI ^{Dicyp})SmI] ₂ (4.1) | 159 |
| [(BDI ^{Dicyp})SmCH(SiMe ₃) ₂] (4.2) | 164 |
| [(BDI ^{Dicyp})Sm(μ-C ₆ H ₆)Sm(BDI ^{Dicyp})] (4.3) | 169 |
| [(BDI ^{Dicyp})Sm(μ-C ₇ H ₈)Sm(BDI ^{Dicyp})] (4.4) | 174 |
| [(BDI ^{Dicyp})Sm(μ-C ₆ H ₈ Si)Sm(BDI ^{Dicyp})] (4.5) | 179 |
| Attempted synthesis of [(BDI ^{Dicyp})Sm(μ-C ₈ H ₁₀)Sm(BDI ^{Dicyp})]..... | 184 |
| [(BDI ^{Dicyp})Sm(μ-C ₈ H ₈)] (4.7)..... | 185 |
| [(BDI ^{Dicyp})Sm(μ-C ₂₈ H ₂₁)] (4.8)..... | 191 |
| [(BDI ^{Dicyp})(THF)Sm(μ-C ₆₀)Sm(THF)(BDI ^{Dicyp})] (4.9)..... | 193 |
| [(BDI ^{Dicyp})Sm(μ-C ₁₄ H ₁₀)Sm(BDI ^{Dicyp})] (4.10)..... | 194 |
| Attempted synthesis of [(BDI ^{Dicyp})Sm(μ-C ₁₀ H ₈)Sm(BDI ^{Dicyp})]..... | 196 |
| 4.2 Single Crystal X-ray Diffraction Analysis | 197 |
| 4.2.1 Crystal Structure Data and Refinement Details | 197 |
| 4.3 Solid-State Magnetic Susceptibility Measurements | 203 |
| 4.4 Computational Details | 206 |
| 5.0 References..... | 211 |

1.0 Materials and Methods

1.1 General Experimental Procedures

All manipulations were performed under a dry, oxygen-free argon atmosphere using standard Schlenk-line techniques, or in a conventional nitrogen-filled glovebox. Hexane, toluene, diethyl ether (Et₂O) and tetrahydrofuran (THF) were obtained from a PureSolv MD 5 system and stored over activated 5 Å molecular sieves prior to use. NMR spectra were recorded using a JEOL 500 MHz spectrometer, operating at 500 MHz (¹H), 126 MHz (¹³C) or 202 MHz (³¹P). Spectra were recorded at 298 K (unless stated otherwise) with proton and carbon chemical shifts being referenced internally to residual solvent resonances. Coupling constants are quoted in Hz. Data processing was performed with MestReNova software suites. Elemental analyses were performed at Elemental Microanalysis Ltd (UK). Infrared spectra were recorded on a Bruker Alpha FTIR spectrometer. GC–MS analyses, conducted by Assoc. Prof. Robert Keyzers, were carried out using a Shimadzu QP2010-Plus gas chromatograph–mass spectrometer equipped with an AOC-20i auto injector. GC–MS analyses used helium as the carrier gas. Mass spectra were obtained at 70 eV in positive ion mode, scanning at *m/z* 40–600 every 0.3 s. The ion source was held at 200 °C, while the MS-transfer line was at 305 °C. Compound identity was determined using both retention time and mass spectral fragmentation patterns. Samples were introduced (1 μL) into a glass split/splitless liner at 270 °C. Separations were performed using a Restek RXI-5Sil-MS column (30 m × 0.25 mm × 0.25 μm) with a 20:1 split injection using constant carrier gas flow (linear velocity 43.4 cm/s; 1.43 mL/min). The initial oven temperature was 50 °C, held for 2 min, after which a temperature ramp of 10 °C/min to 350 °C was used, with a final hold of 5 min (total analysis time 37 min).¹ [(BDI^{Dipp})YbH]₂,² (BDI^{Dipep})H³ and (BDI^{Dipp}.TCHP)H⁴ were all prepared according to literature procedures. The procedure for [2,6-di-cyclohexylaniline] has been reported in the literature but was prepared according to an updated methodology, with the help from Assoc. Prof. Joanne Harvey and Brooke Nicholls.^{1,5} Bis(trimethylsilyl)methane, phenylsilane, 1,4-cyclohexadiene (1,4-CHD), cyclooctatetraene (COT) and all other chemicals were purchased from Sigma Aldrich and used without further purification.

1.2 Single Crystal X-ray Diffraction Analysis

Most compounds presented in this Thesis were collected on an Agilent SuperNova diffractometer fitted with an EOS S2 detector, by either Georgia M. Richardson or Dr Mathew D. Anker. Datasets were collected using CuKα radiation ($\lambda = 1.54184$ Å) at the indicated temperature (120 K or 150 K).⁶ Compound **3.14** was transported to the Australian Synchrotron

(ANSTO, Melbourne) and mounted on the Macromolecular Crystallography (MX2) beamline by Dr Mathew D. Anker and Dr. Matthew J. Evans. Data was collected using CuK α radiation ($\lambda = 0.71073 \text{ \AA}$) at 100 K. All structures were solved by Dr. Scott A. Cameron on Olex2,⁷ using direct methods with SHELXS⁸ and refined on F² using full matrix least-squares procedures with the SHELXL refinement package.⁹

2.0 Chapter Two Experimental

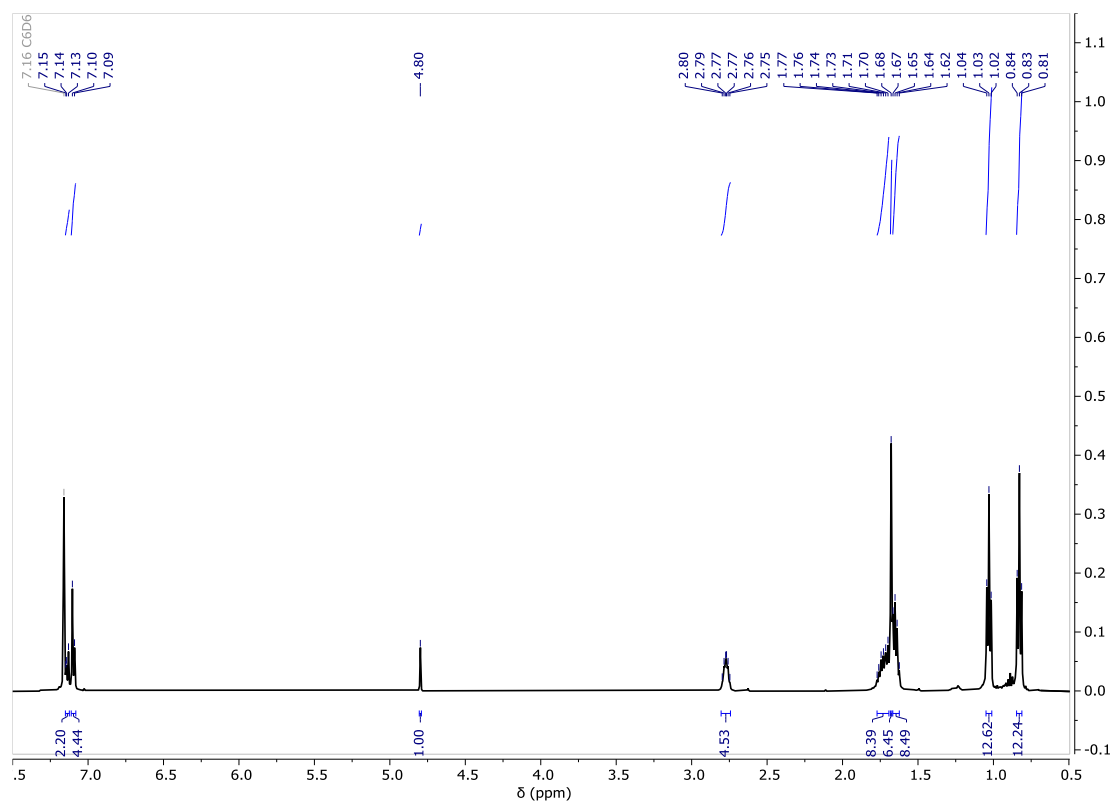
2.1 Synthetic, Spectroscopic and Analytical Data

[(BDI^{Dipep})YbI]₂ (2.1)

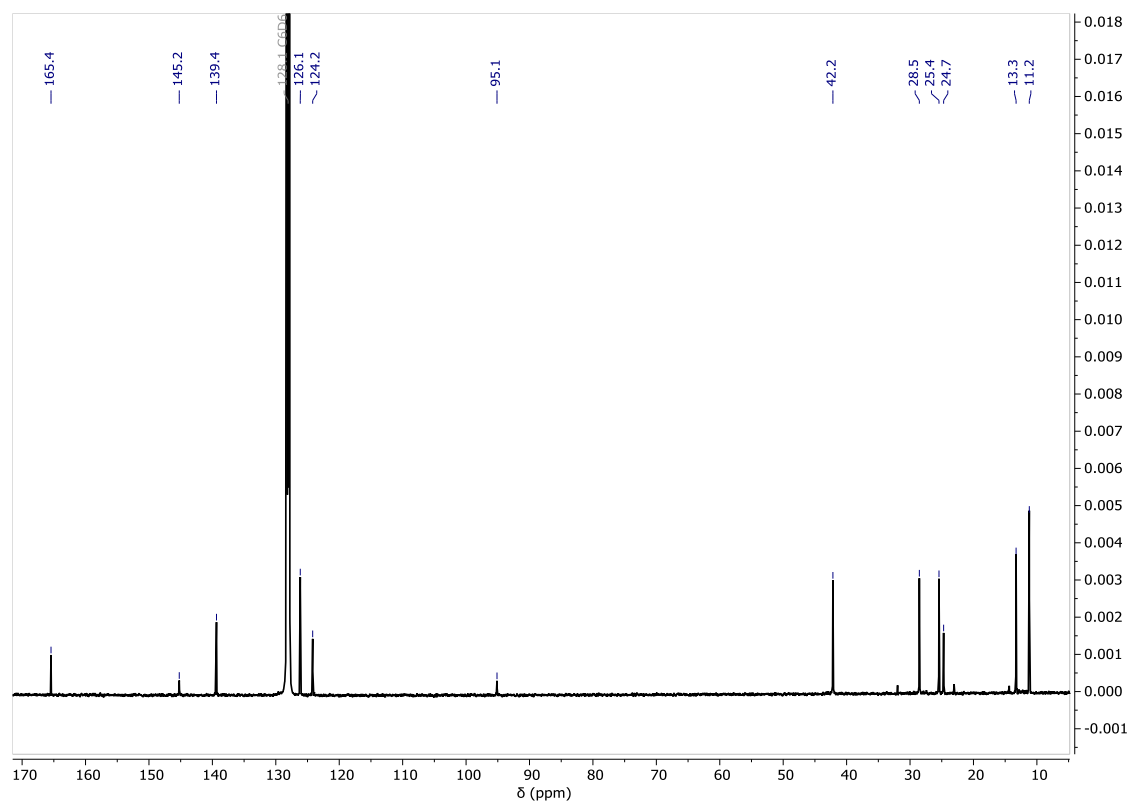
A pale brown Et₂O solution of (BDI^{Dipep})K (1560 mg, 2.70 mmol) was added to a scintillation vial containing a pale yellow suspension of YbI₂ (1170 mg, 2.70 mmol) in Et₂O and left to stir at room temperature for 48h. The mixture was filtered through Celite, and the solvent removed *in vacuo* from the resultant dark red solution to generate the crude product as a red solid. Deep red crystals suitable for X-ray diffraction analysis were obtained from a saturated pentane solution at room temperature (Isolated yield: 1658 mg, 74%).

¹H NMR (500 MHz, C₆D₆) δ 7.13 (m, 2H, ArH), 7.09 (m, 4H, ArH), 4.80 (s, 1H, NC(CH₃)CH), 2.77 (m, 4H, CH(CH₂CH₃)₂), 1.73 (m, 8H, CH(CH₂CH₃)₂), 1.68 (s, 6H, NC(CH₃)CH), 1.64 (m, 8H, CH(CH₂CH₃)₂), 1.03, 0.83 (t, *J* = 7.2 Hz, 12H, CH(CH₂CH₃)₂).

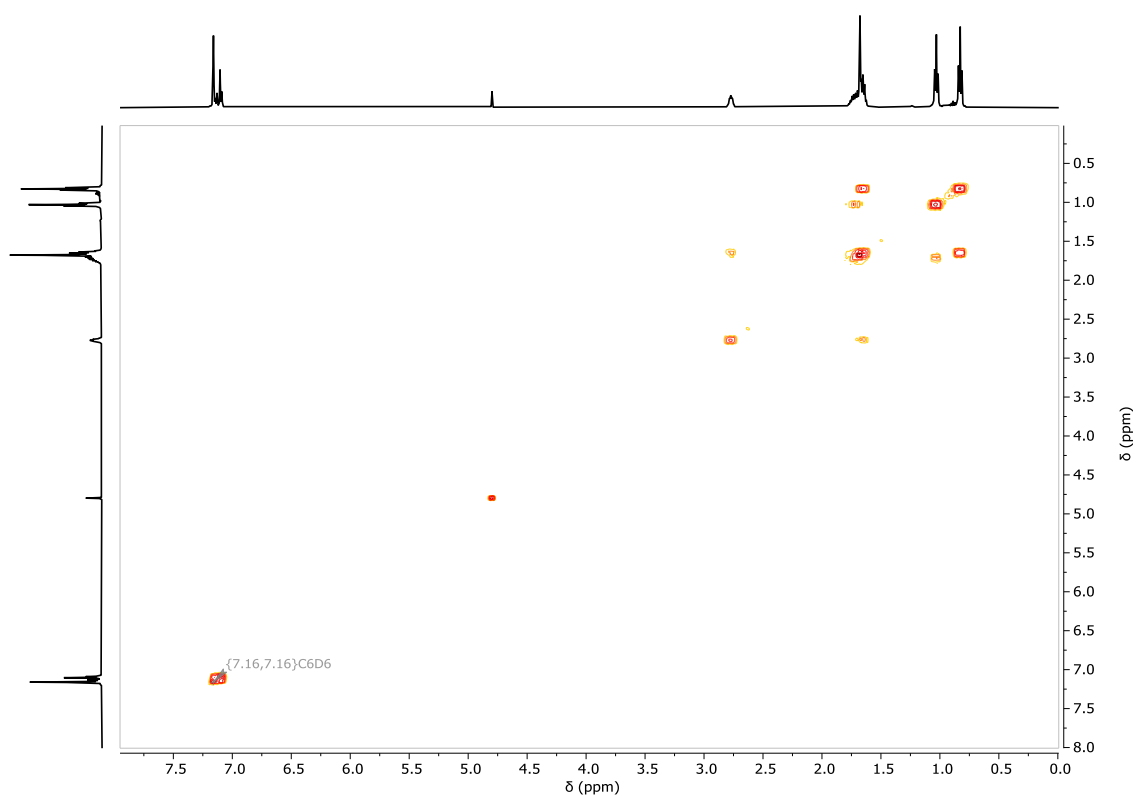
¹³C{¹H} NMR (126 MHz, C₆D₆) δ 165.4 (NC(CH₃)CH), 145.2 (C_{ipso}), 139.4 (C_{ortho}), 126.1 (C_{para}), 124.2 (C_{meta}), 95.1 (NC(CH₃)CH), 42.2 (CH(CH₂CH₃)₂), 28.5, 25.4 (CH(CH₂CH₃)₂), 24.7 (NC(CH₃)CH), 13.3, 11.2 (CH(CH₂CH₃)₂).



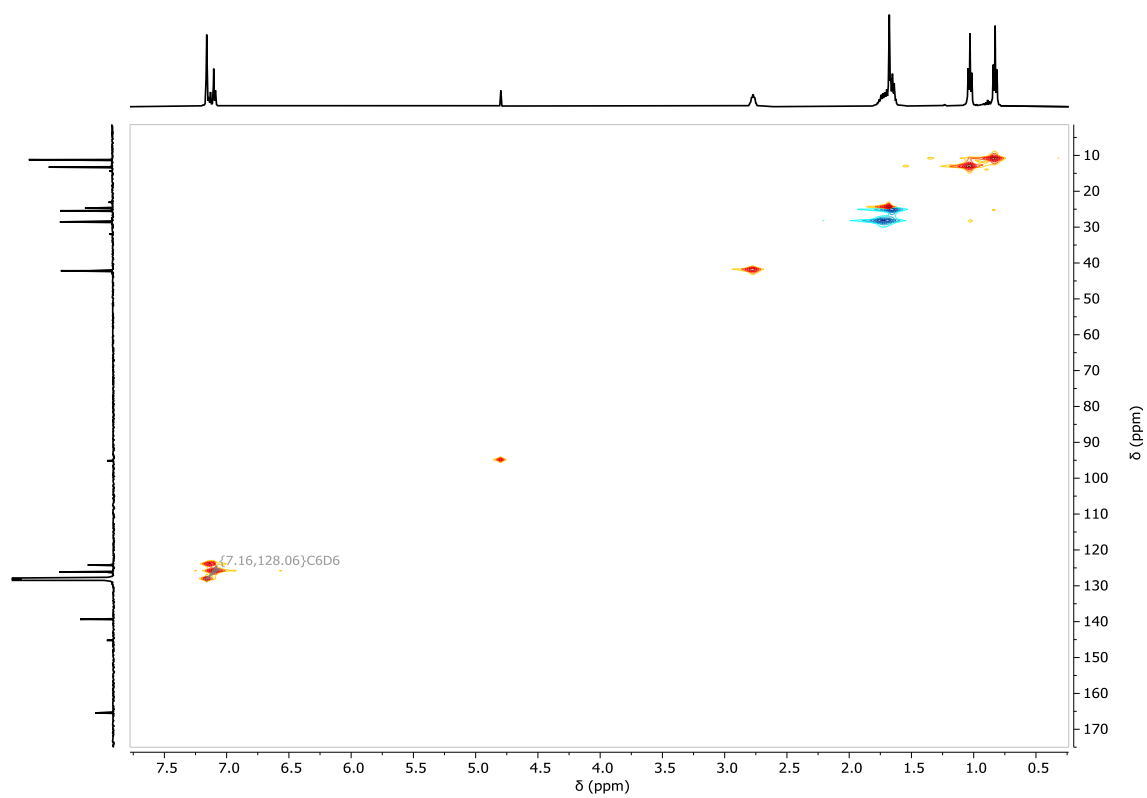
Supplementary Figure 2.1. ¹H NMR spectrum (500 MHz, C₆D₆) of [(BDI^{Dipep})YbI]₂ (2.1).



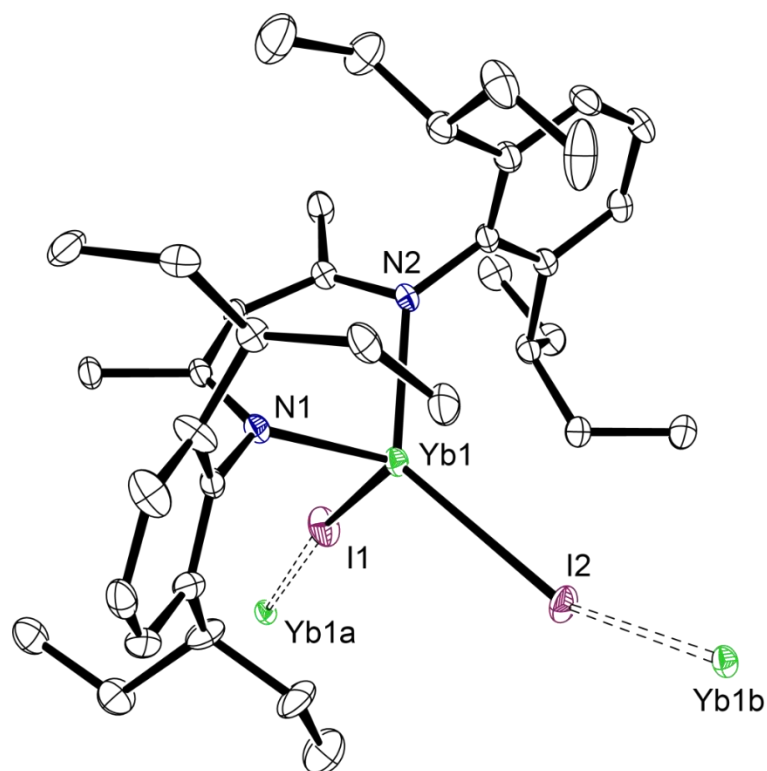
Supplementary Figure 2.2. ¹³C{¹H} NMR spectrum (126 MHz, C₆D₆) of [(BDI^{Dipep})YbI]₂ (2.1).



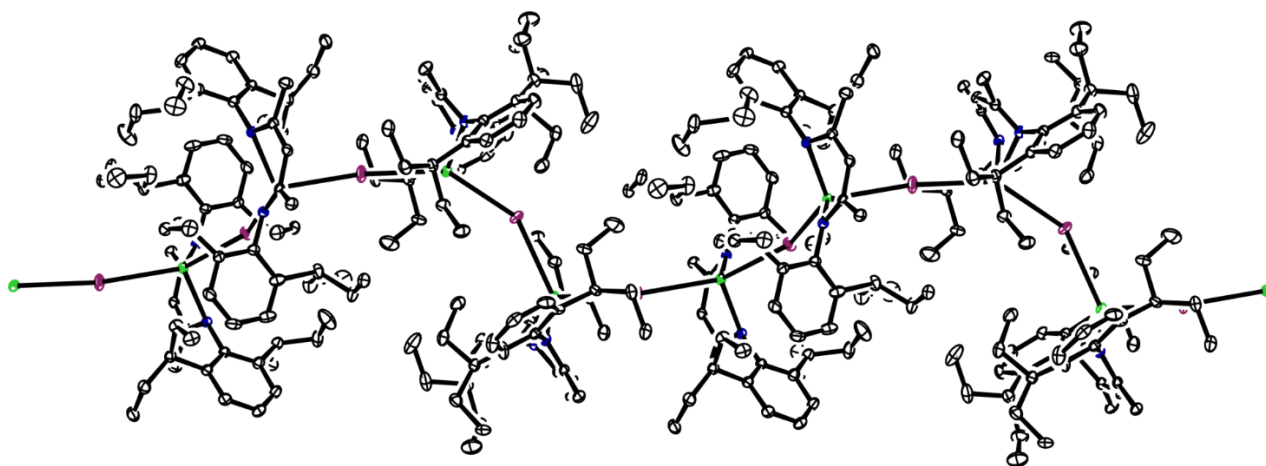
Supplementary Figure 2.3. ^1H - ^1H COSY NMR spectrum (500 MHz, C_6D_6) of $[(\text{BDI}^{\text{Dipep}})\text{YbI}]_2$ (**2.1**).



Supplementary Figure 2.4. ^1H - ^{13}C HSQC NMR spectrum (500 MHz, C_6D_6) of $[(\text{BDI}^{\text{Dipep}})\text{YbI}]_2$ (**2.1**).



Supplementary Figure 2.5. Ortep representation (30% probability ellipsoids) of $[(\text{BDI}^{\text{Dipep}})\text{YbI}]_2$ (**2.1**). Hydrogen atoms have been omitted for clarity.



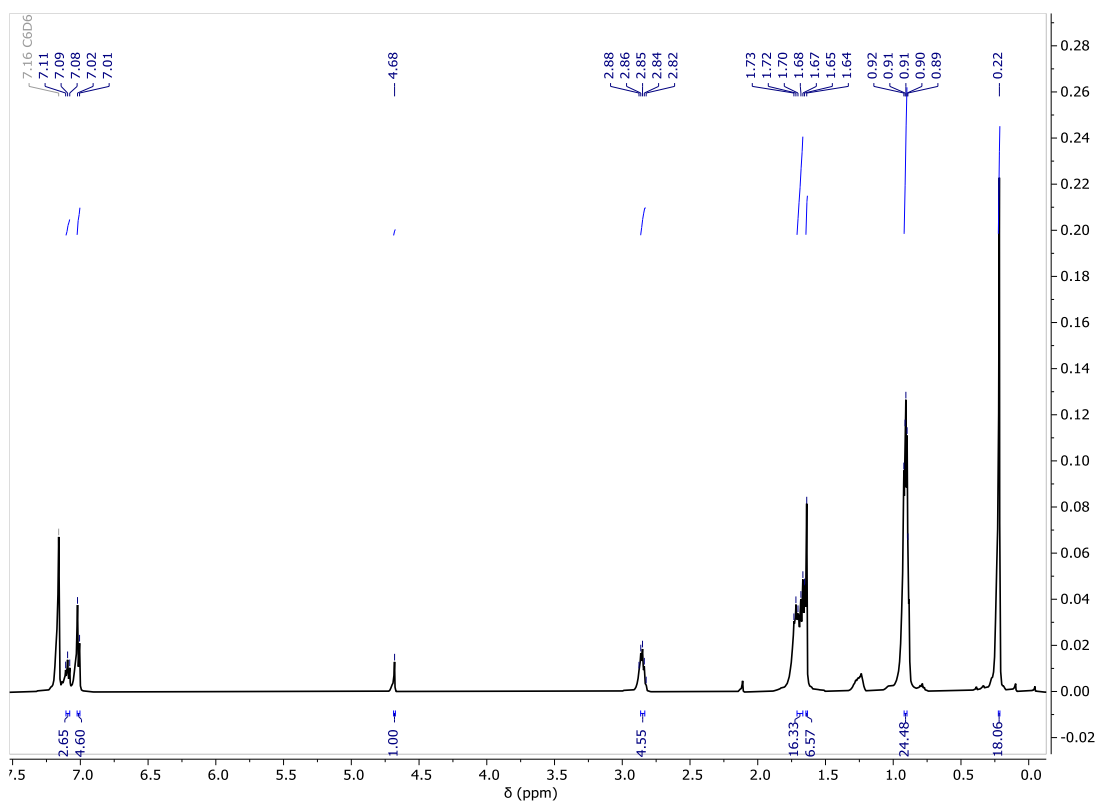
Supplementary Figure 2.6. Ortep representation (30% probability ellipsoids) of the pseudo polymer of $[(\text{BDI}^{\text{Dipep}})\text{YbI}]_2$ (**2.1**). Hydrogen atoms have been omitted for clarity.

[(BDI^{Dipep})YbN(SiMe₃)₂] (2.2)

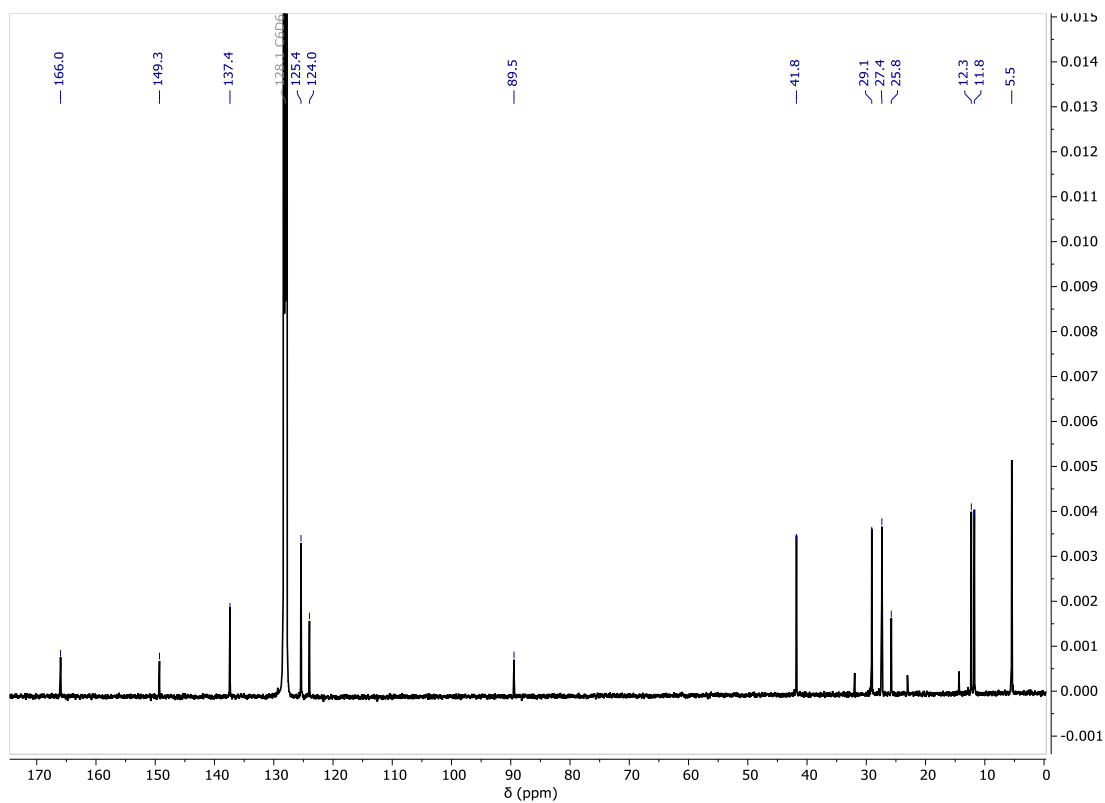
A red toluene solution of [(BDI^{Dipep})YbI]₂ (300 mg, 0.18 mmol) was added to a scintillation vial containing a toluene solution of K[N(SiMe₃)₂] (72 mg, 0.34 mmol) and was left to stir for ca. 48h at room temperature. The mixture was filtered through Celite, and the solvent removed *in vacuo* from the resultant dark brown-red solution, generating the crude product as a red solid. Deep red crystals suitable for X-ray diffraction analysis were obtained from a saturated hexane solution at room temperature (Isolated yield: 209 mg, 71%).

¹H NMR (500 MHz, C₆D₆) δ 7.09 (t, *J* = 7.2 Hz, 2H, Ar*H*), 7.01 (m, 4H, Ar*H*), 4.68 (s, 1H, NC(CH₃)CH), 2.85 (m, 4H, CH(CH₂CH₃)₂), 1.68 (m, 16H, CH(CH₂CH₃)₂), 1.64 (s, 6H, NC(CH₃)CH), 0.91 (m, 24H, CH(CH₂CH₃)₂ overlapping CH(CH₂CH₃)₂), 0.22 (s, 18H, N(SiMe₃)₂).

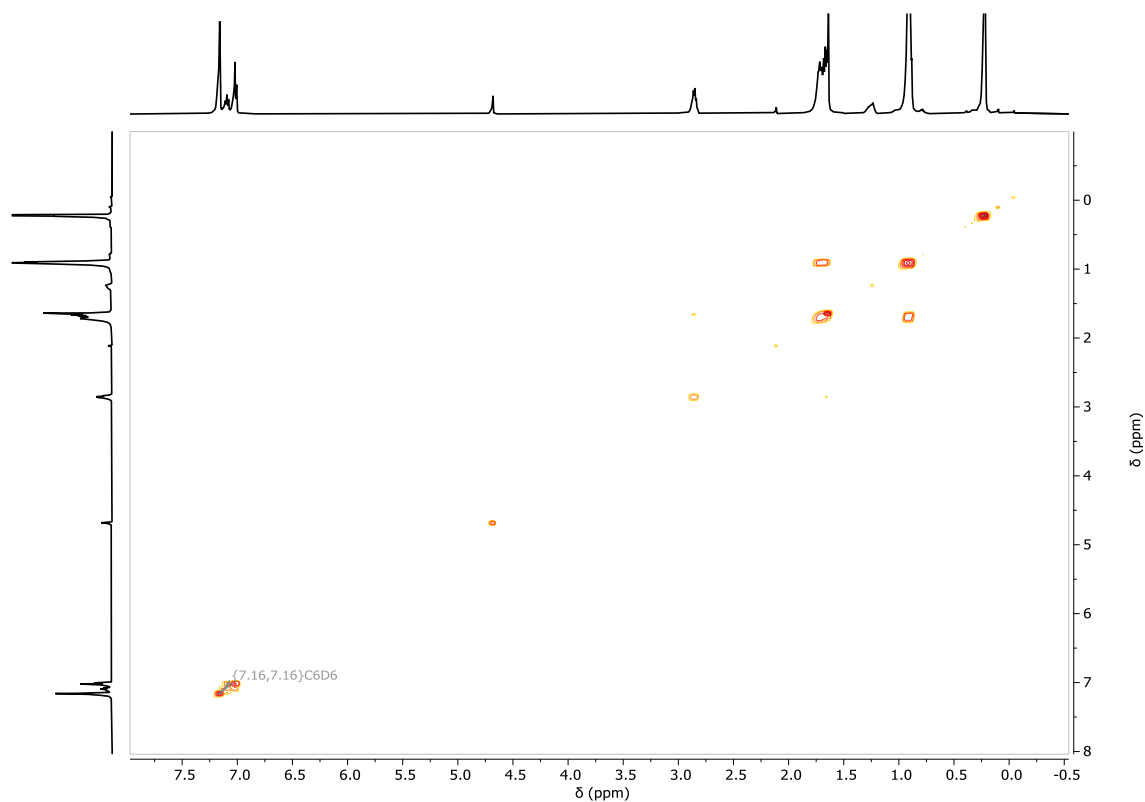
¹³C{¹H} NMR (126 MHz, C₆D₆) δ 166.0 (NC(CH₃)CH), 149.3 (C_{ipso}), 137.4 (C_{ortho}), 125.4 (C_{para}), 124.0 (C_{meta}), 89.5 (NC(CH₃)CH), 41.8 (CH(CH₂CH₃)₂), 29.1, 27.4 CH(CH₂CH₃)₂), 25.8 NC(CH₃)CH), 12.3, 11.8 (CH(CH₂CH₃)₂ overlapping CH(CH₂CH₃)₂), 5.5 (N(SiMe₃)₂).



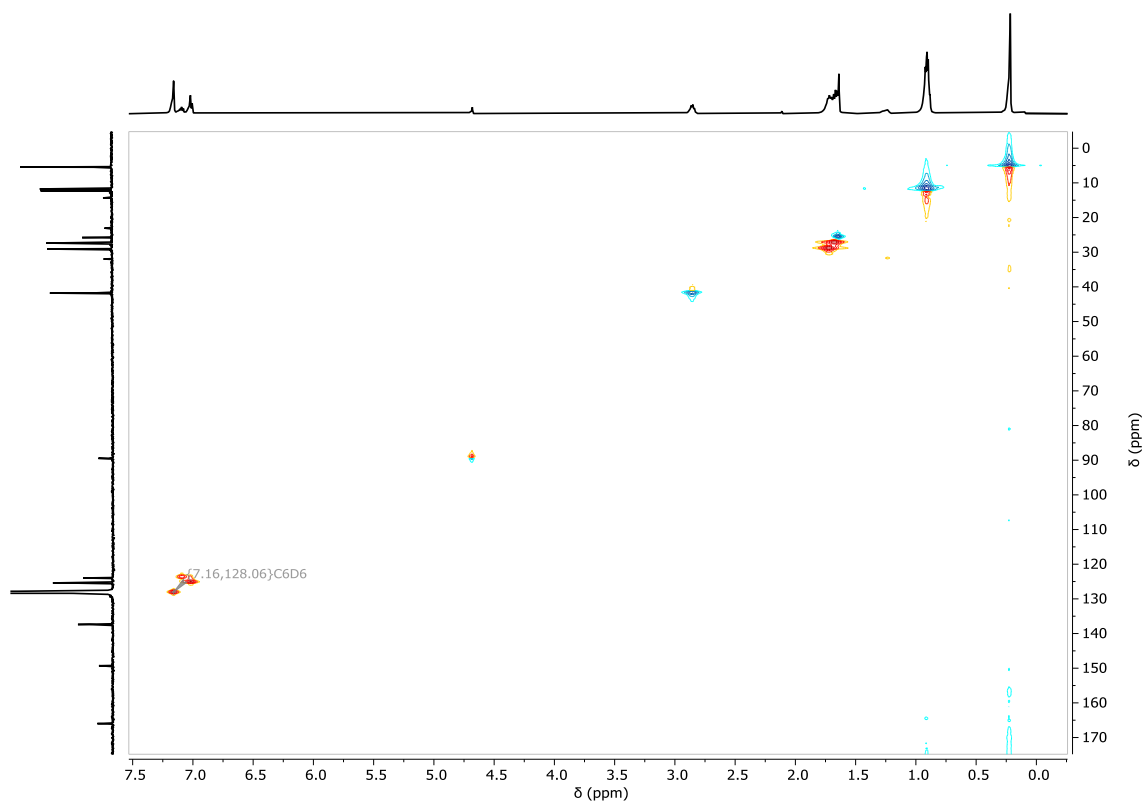
Supplementary Figure 2.7. ¹H NMR spectrum (500 MHz, C₆D₆) of [(BDI^{Dipep})YbN(SiMe₃)₂] (**2.2**).



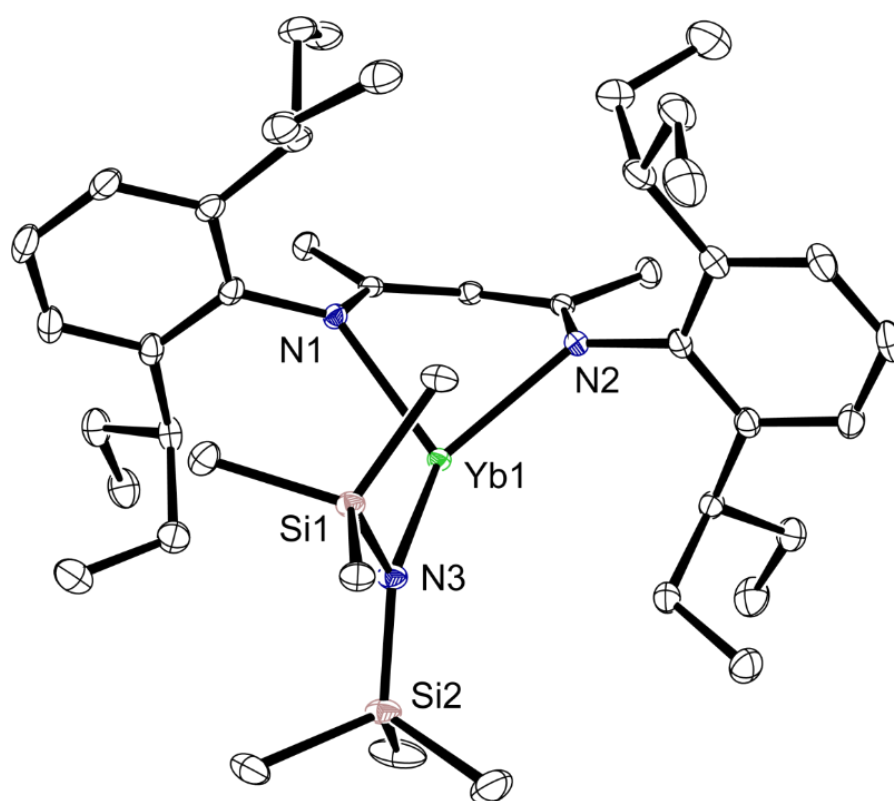
Supplementary Figure 2.8. ¹³C{¹H} NMR spectrum (126 MHz, C₆D₆) of [(BDI^{Dipep})YbN(SiMe₃)₂] (**2.2**).



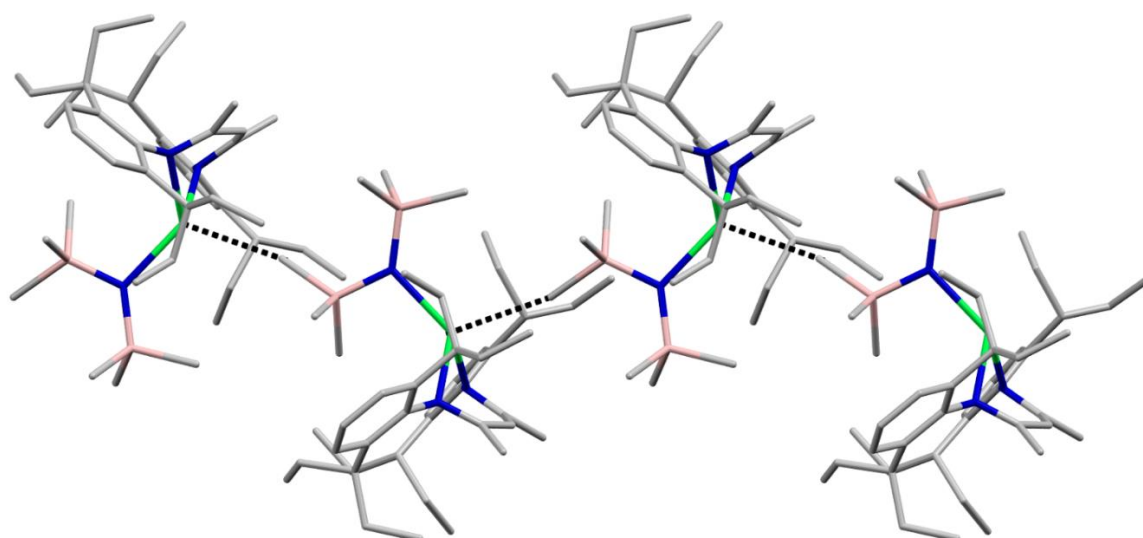
Supplementary Figure 2.9. ^1H - ^1H COSY NMR spectrum (500 MHz, C_6D_6) of $[(\text{BDI}^{\text{Dipep}})\text{YbN}(\text{SiMe}_3)_2]$ (**2.2**).



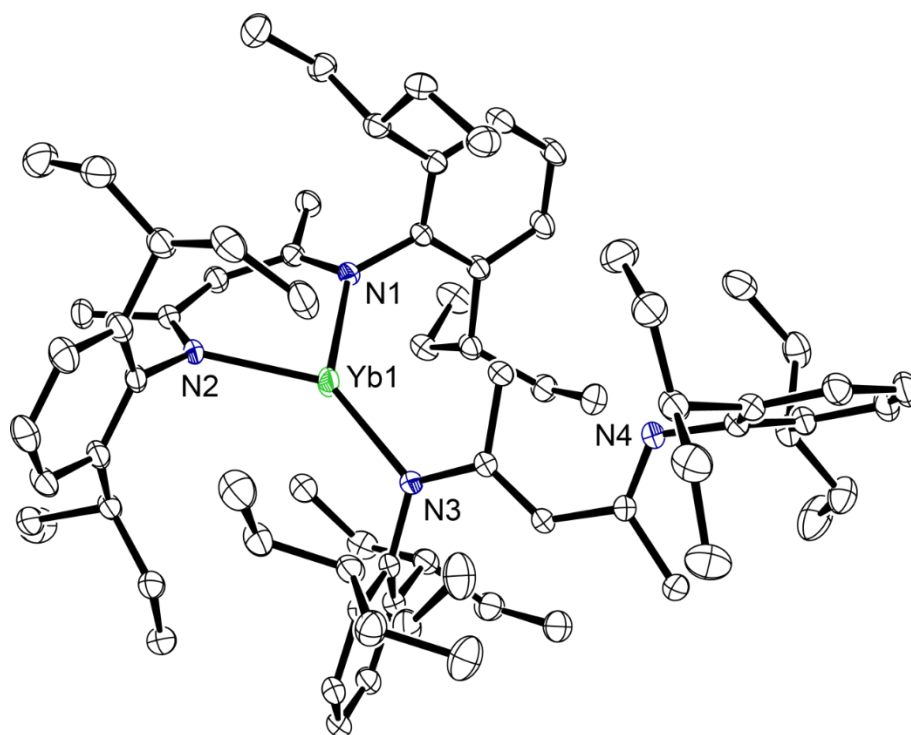
Supplementary Figure 2.10. ^1H - ^{13}C HSQC NMR spectrum (500 MHz, C_6D_6) of $[(\text{BDI}^{\text{Dipep}})\text{YbN}(\text{SiMe}_3)_2]$ (**2.2**).



Supplementary Figure 2.11. Ortep representation (30% probability ellipsoids) of $[(\text{BDI}^{\text{Dipep}})\text{YbN}(\text{SiMe}_3)_2]$ (**2.2**). Hydrogen atoms have been omitted for clarity.



Supplementary Figure 2.12. Ortep representation (30% probability ellipsoids) of the pseudo polymer of $[(\text{BDI}^{\text{Dipep}})\text{YbN}(\text{SiMe}_3)_2]$ (**2.2**). Hydrogen atoms have been omitted for clarity.



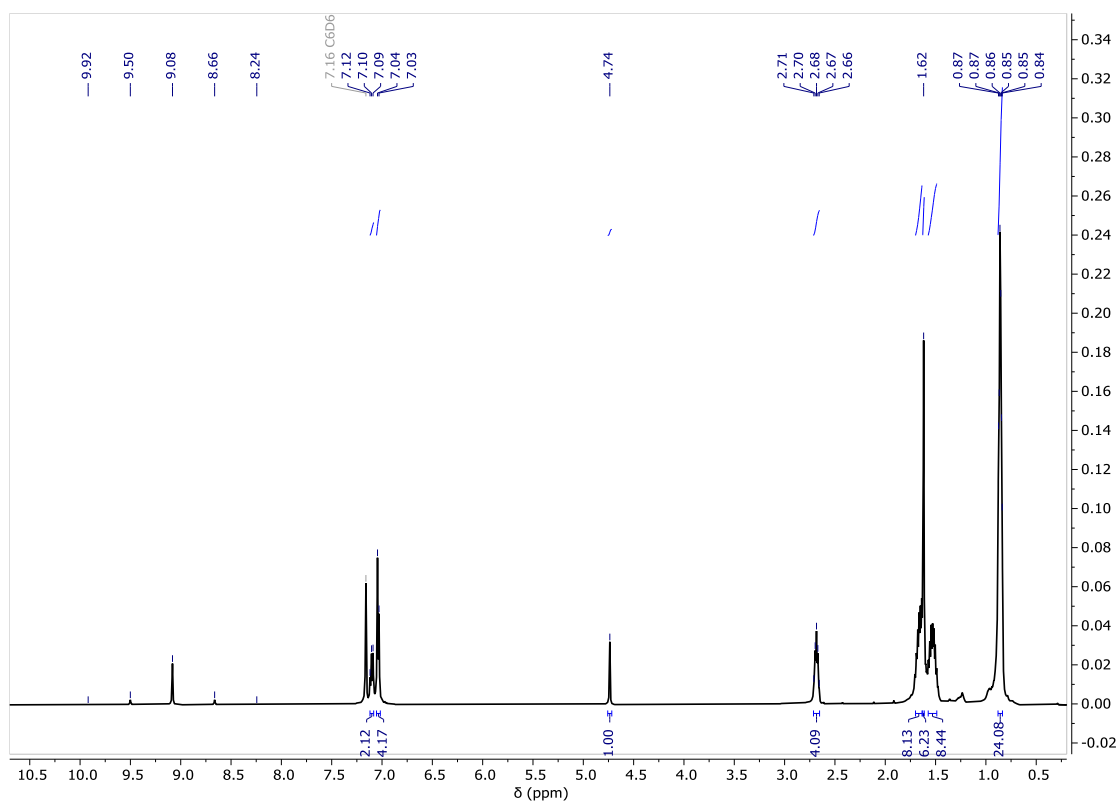
Supplementary Figure 2.13. Ortep representation (30% probability ellipsoids) of $[(\text{BDI}^{\text{Dipep}})_2\text{Yb}]$ (**2.3**), obtained through attempts at synthesising **2.4**. Hydrogen atoms have been omitted for clarity.

[(BDI^{Dipep})YbH]₂ (2.4)

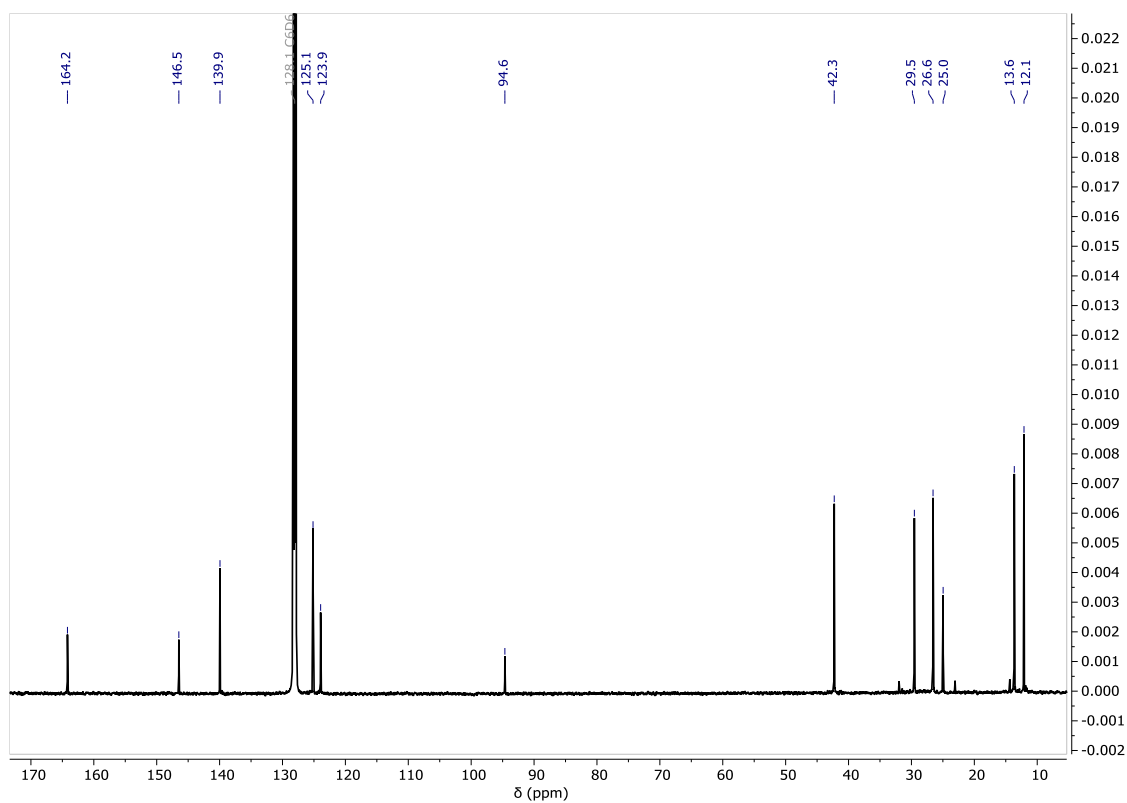
A colourless C₆D₆ solution of PhSiH₃ (151 mg, 1.40 mmol) was added to a red C₆D₆ solution of [(BDI^{Dipep})YbN(SiMe₃)₂] (119 mg, 0.14 mmol) in an NMR tube fitted with a J. Youngs tap. The reaction mixture was left to heat overnight at 60 °C to generate a brown solution. The volatiles were removed under vacuum to cleanly generate the crude product as a brown solid.

¹H NMR (500 MHz, C₆D₆) δ 9.08 (quint, *J* = 418 Hz, 1H, YbH), 7.10 (t, *J* = 7.5 Hz, 2H, ArH), 7.03 (d, *J* = 7.4 Hz, 4H, ArH), 4.74 (s, 1H, NC(CH₃)CH), 2.68 (quint, *J* = 6.6 Hz, 4H, CH(CH₂CH₃)₂), 1.66 (m, 8H, CH(CH₂CH₃)₂), 1.62 (s, 6H, NC(CH₃)CH), 1.53 (m, 8H, CH(CH₂CH₃)₂), 0.85 (m, 24H, CH(CH₂CH₃)₂ overlapping CH(CH₂CH₃)₂).

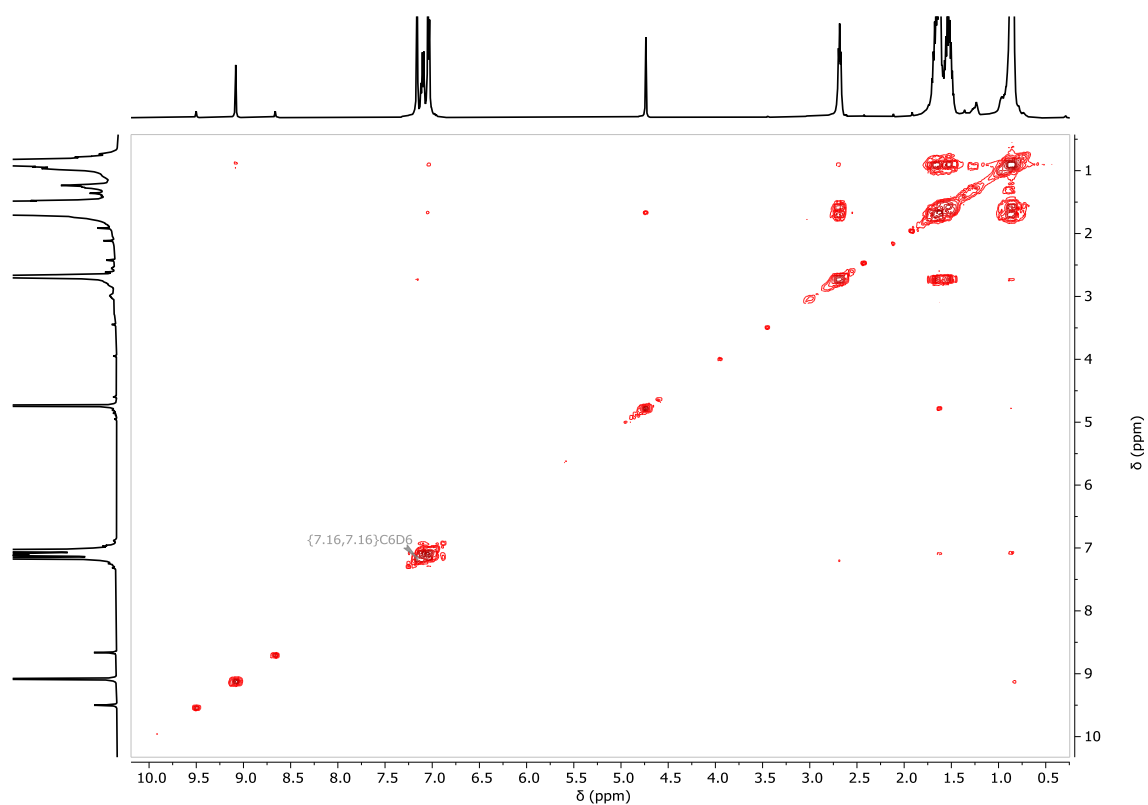
¹³C{¹H} NMR (126 MHz, C₆D₆) δ 164.2 (NC(CH₃)CH), 146.5 (C_{ipso}), 139.9 (C_{ortho}), 125.1 (C_{para}), 123.9 (C_{meta}), 94.6 (NC(CH₃)CH), 42.3 (CH(CH₂CH₃)₂), 29.5, 26.6 CH(CH₂CH₃)₂, 25.0 NC(CH₃)CH, 13.6, 12.1 (CH(CH₂CH₃)₂).



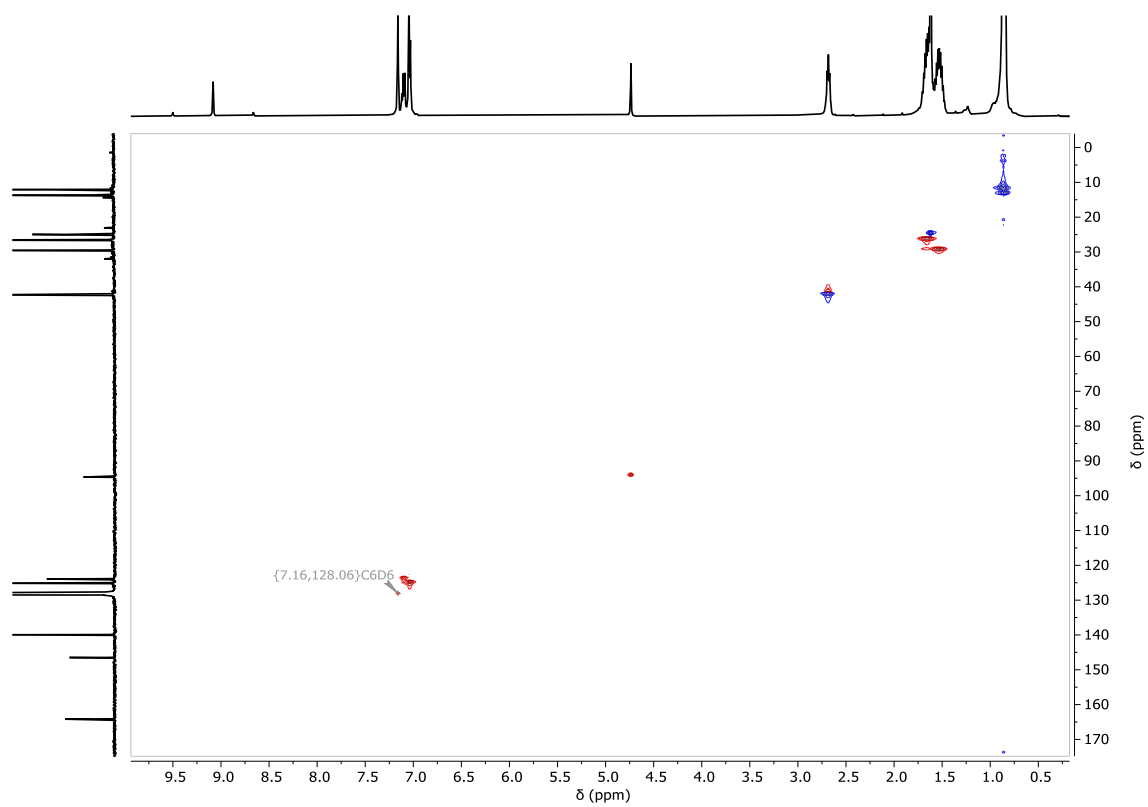
Supplementary Figure 2.14. ¹H NMR spectrum (500 MHz, C₆D₆) of [(BDI^{Dipep})YbH]₂ (**2.4**).



Supplementary Figure 2.15. ¹³C{¹H} NMR spectrum (126 MHz, C₆D₆) of [(BDI^{Dipep})YbH]₂ (**2.4**).



Supplementary Figure 2.16. ^1H – ^1H COSY NMR spectrum (500 MHz, C_6D_6) of $[(\text{BDI}^{\text{Dipep}})\text{YbH}]_2$ (**2.4**).



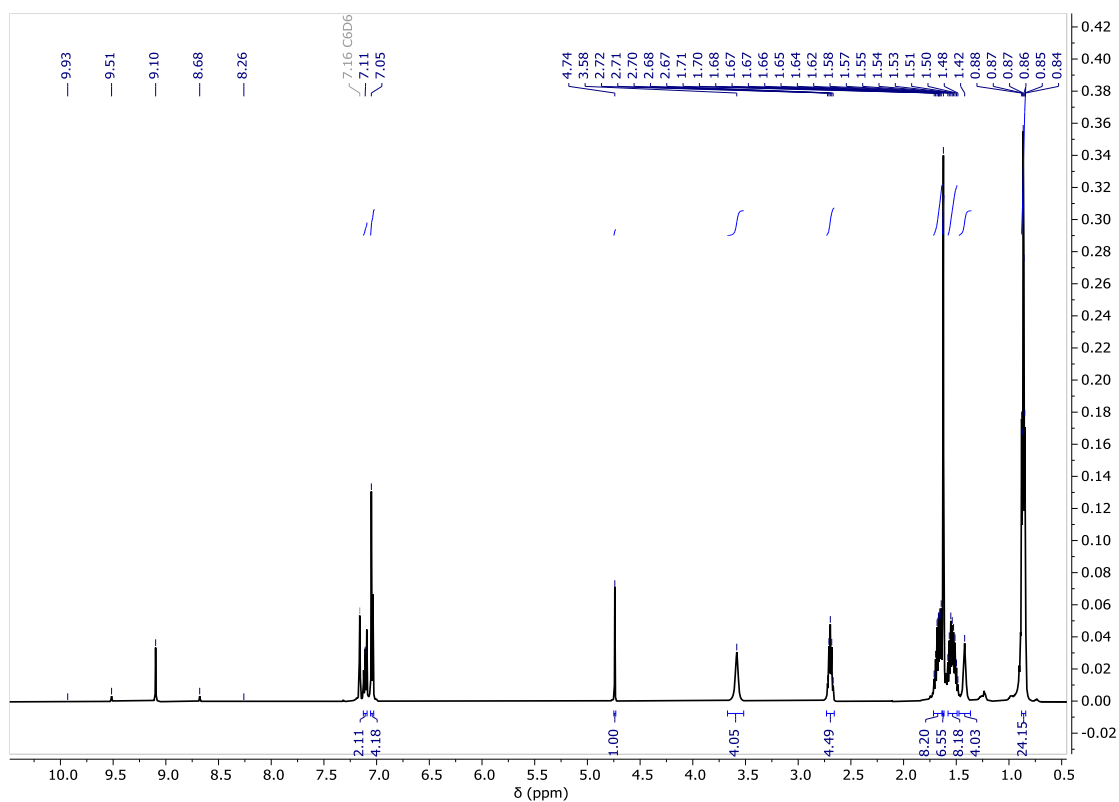
Supplementary Figure 2.17. ^1H – ^{13}C HSQC NMR spectrum (500 MHz, C_6D_6) of $[(\text{BDI}^{\text{Dipep}})\text{YbH}]_2$ (**2.4**).

[(BDI^{Dipep})YbH(THF)]₂ (2.5)

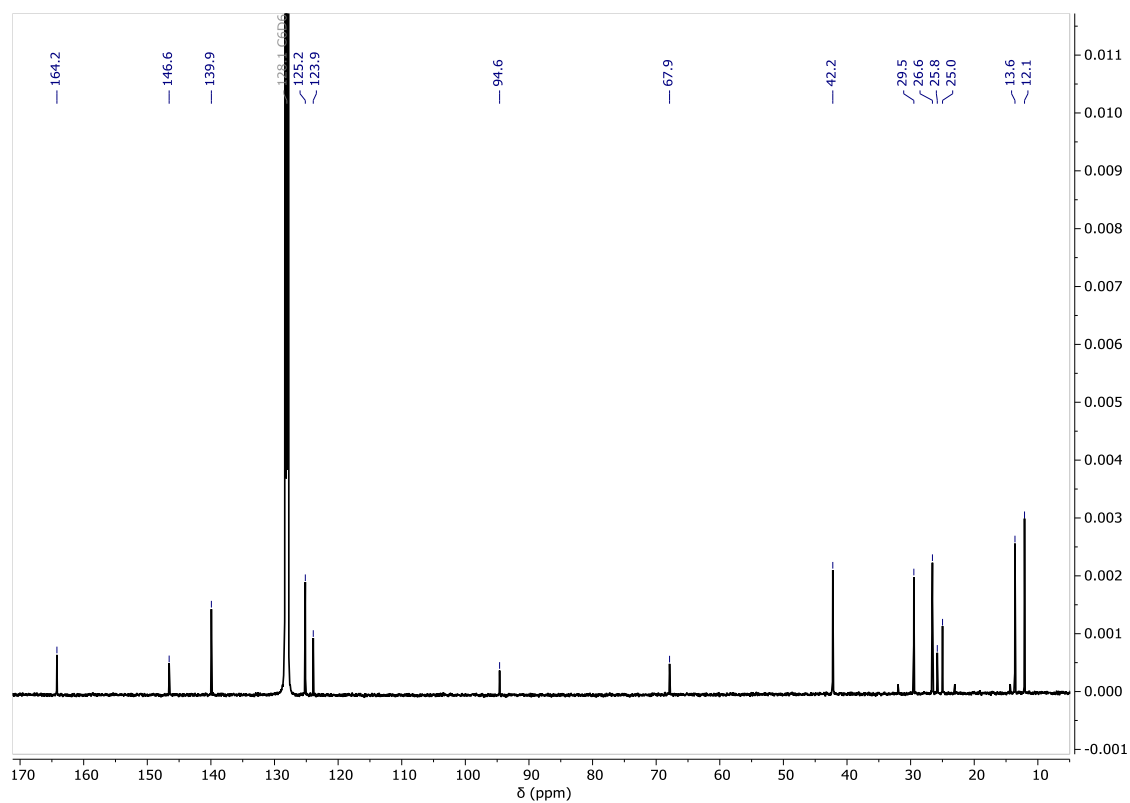
A colourless toluene solution of PhSiH₃ (1070 mg, 9.90 mmol) was added to a red toluene solution of [(BDI^{Dipep})YbN(SiMe₃)₂] (854 mg, 0.99 mmol) in an ampoule and the reaction mixture was left to heat overnight at 60 °C to generate a brown solution. The volatiles were removed under vacuum to generate the crude product as a brown solid. Crystallisation from a saturated hexane solution at room temperature afforded brown crystals suitable for an X-ray diffraction experiment (Isolated yield: 553 mg, 72%).

¹H NMR (500 MHz, C₆D₆) δ 9.10 (quint, *J* = 418 Hz, 1H, YbH), 7.11 (t, *J* = 7.4 Hz, 2H, ArH), 7.04 (d, *J* = 7.3 Hz, 4H, ArH), 4.74 (s, 1H, NC(CH₃)CH), 3.58 (br, 4H, THF), 2.70 (quint, *J* = 6.5 Hz, 4H, CH(CH₂CH₃)₂), 1.67 (m, 8H, CH(CH₂CH₃)₂), 1.62 (s, 6H, NC(CH₃)CH), 1.54 (m, 8H, CH(CH₂CH₃)₂), 1.42 (br, 4H, THF), 0.86 (m, 24H, CH(CH₂CH₃)₂ overlapping CH(CH₂CH₃)₂).

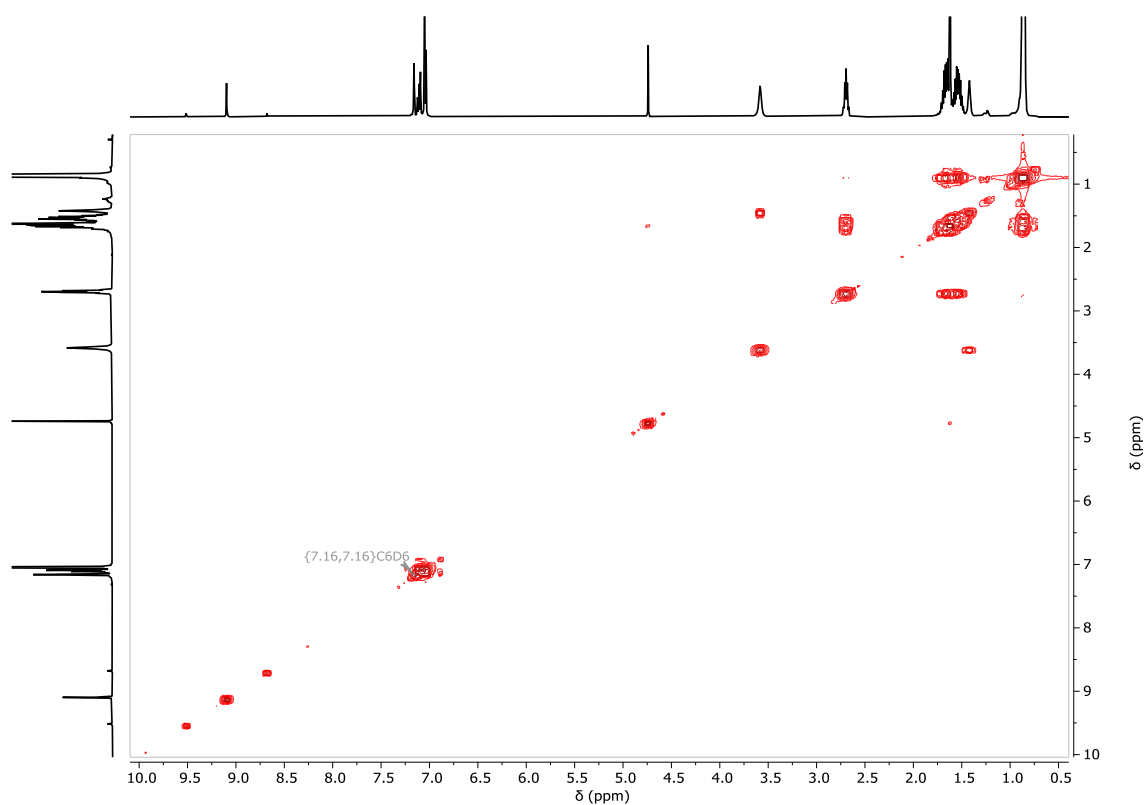
¹³C{¹H} NMR (126 MHz, C₆D₆) δ 164.2 (NC(CH₃)CH), 146.6 (C_{ipso}), 139.9 (C_{ortho}), 125.2 (C_{para}), 123.9 (C_{meta}), 94.6 (NC(CH₃)CH), 67.9 (THF), 42.2 (CH(CH₂CH₃)₂), 29.5, 26.6 CH(CH₂CH₃)₂, 25.8 (THF), 25.0 NC(CH₃)CH, 13.6, 12.1 (CH(CH₂CH₃)₂).



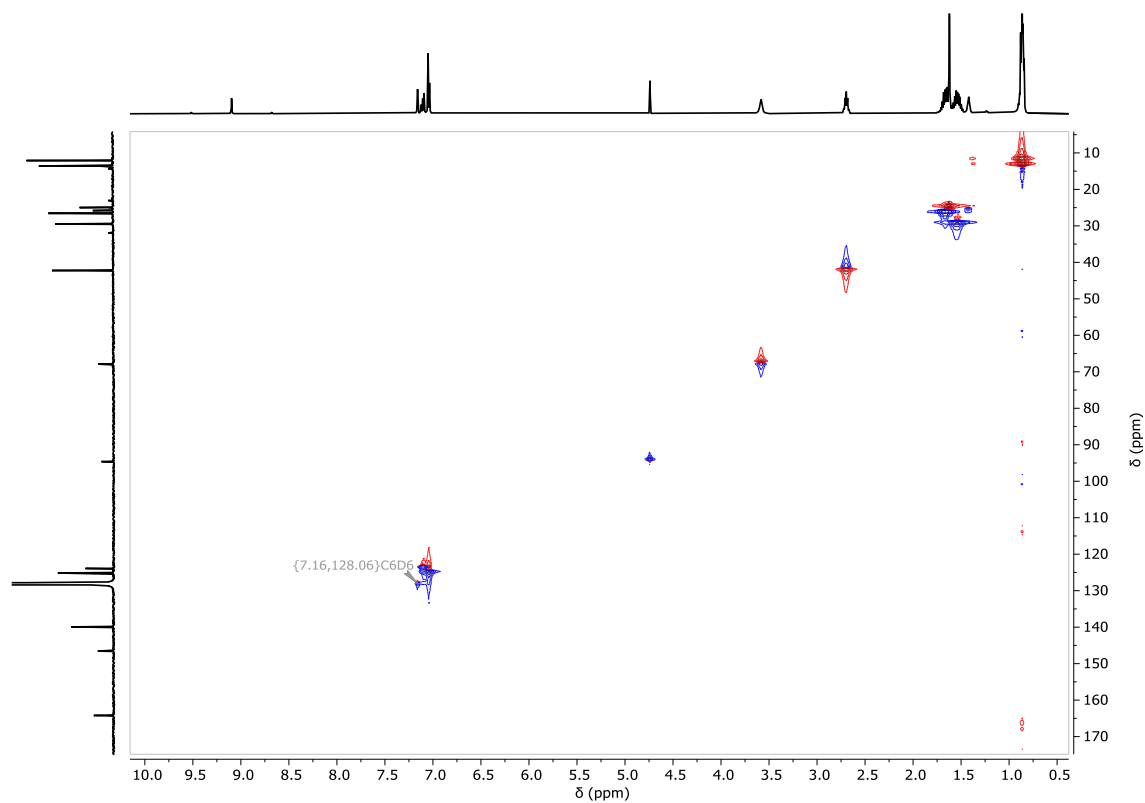
Supplementary Figure 2.18. ¹H NMR spectrum (500 MHz, C₆D₆) of [(BDI^{Dipep})YbH(THF)]₂ (**2.5**).



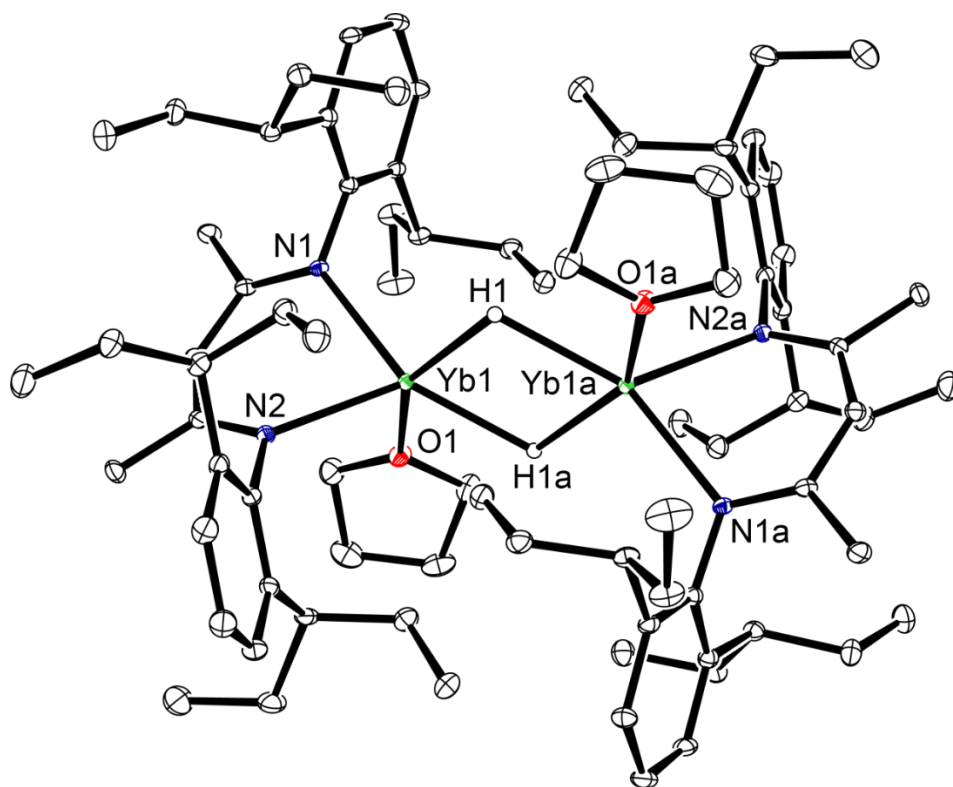
Supplementary Figure 2.19. ¹³C{¹H} NMR spectrum (126 MHz, C₆D₆) of [(BDI^{Dipep})YbH(THF)]₂ (**2.5**).



Supplementary Figure 2.20. ^1H - ^1H COSY NMR spectrum (500 MHz, C_6D_6) of $[(\text{BDI}^{\text{Dipep}})\text{YbH}(\text{THF})]_2$ (**2.5**).



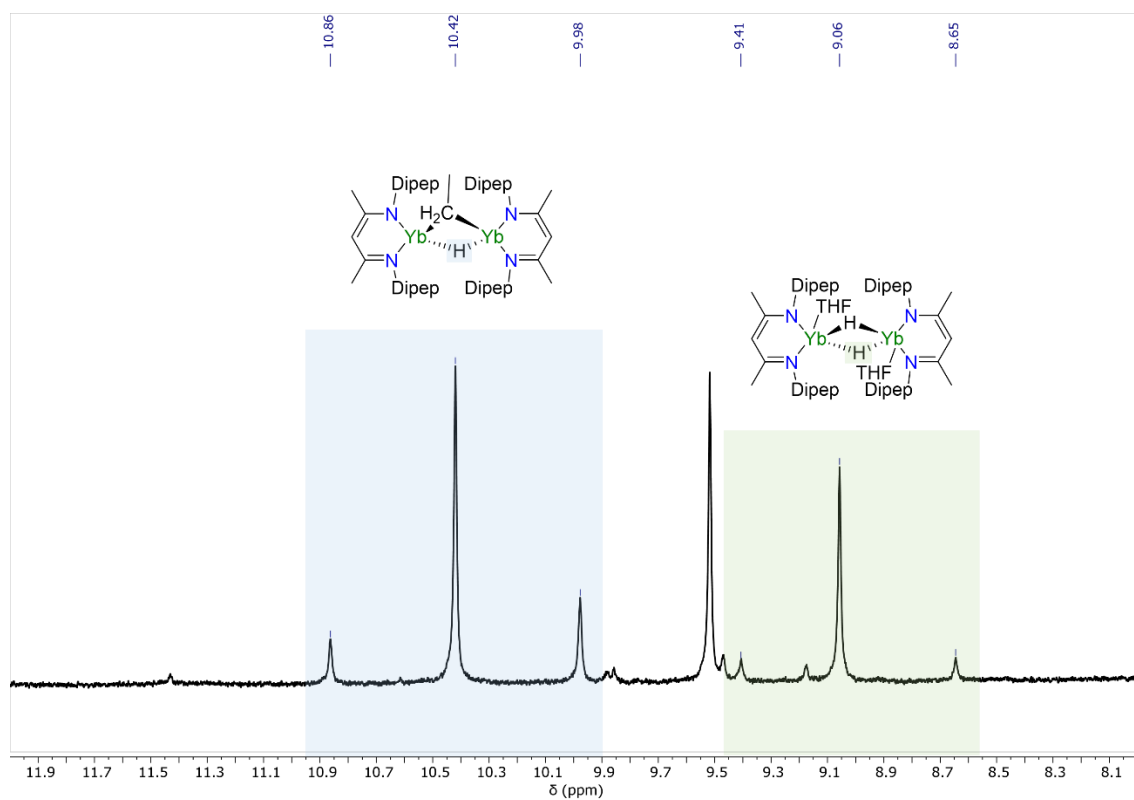
Supplementary Figure 2.21. ^1H - ^{13}C HSQC NMR spectrum (500 MHz, C_6D_6) of $[(\text{BDI}^{\text{Dipep}})\text{YbH}(\text{THF})]_2$ (**2.5**).



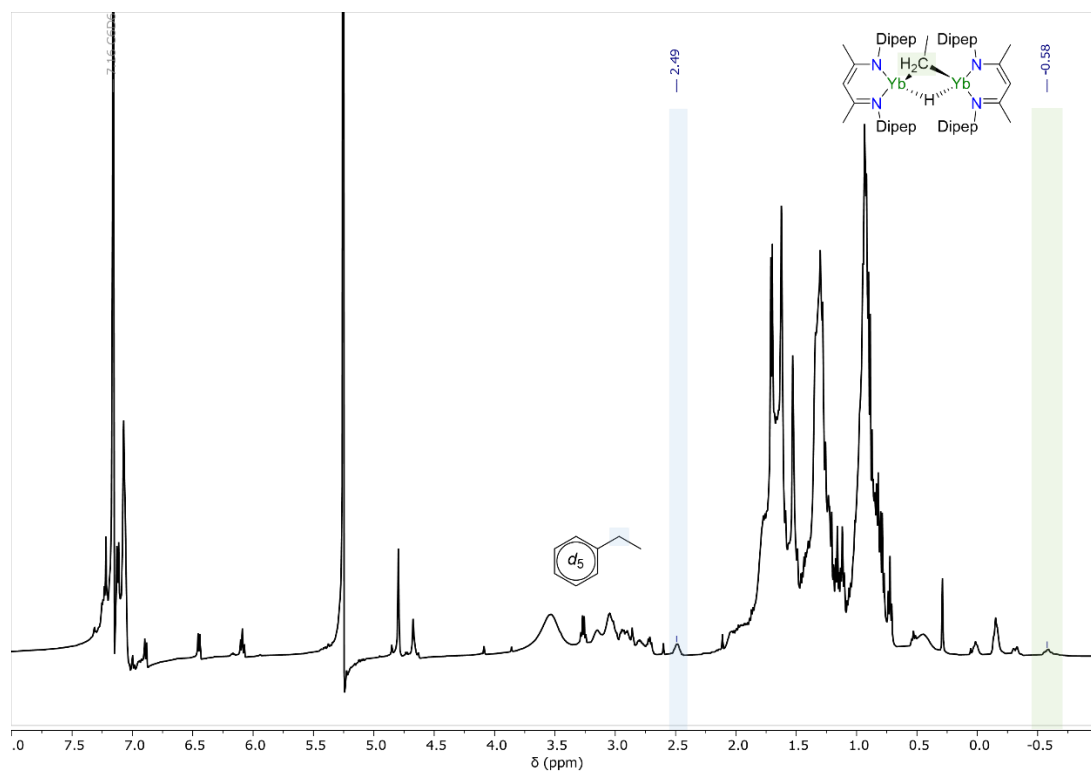
Supplementary Figure 2.22. Ortep representation (30% probability ellipsoids) of $[(\text{BDI}^{\text{Dipep}})\text{YbH}(\text{THF})]_2$ (**2.5**). Hydrogen atoms (except bridging H1 and H1a) have been omitted for clarity.

Attempted synthesis of $[(\text{BDI}^{\text{Dipep}})\text{YbEt}]_2$

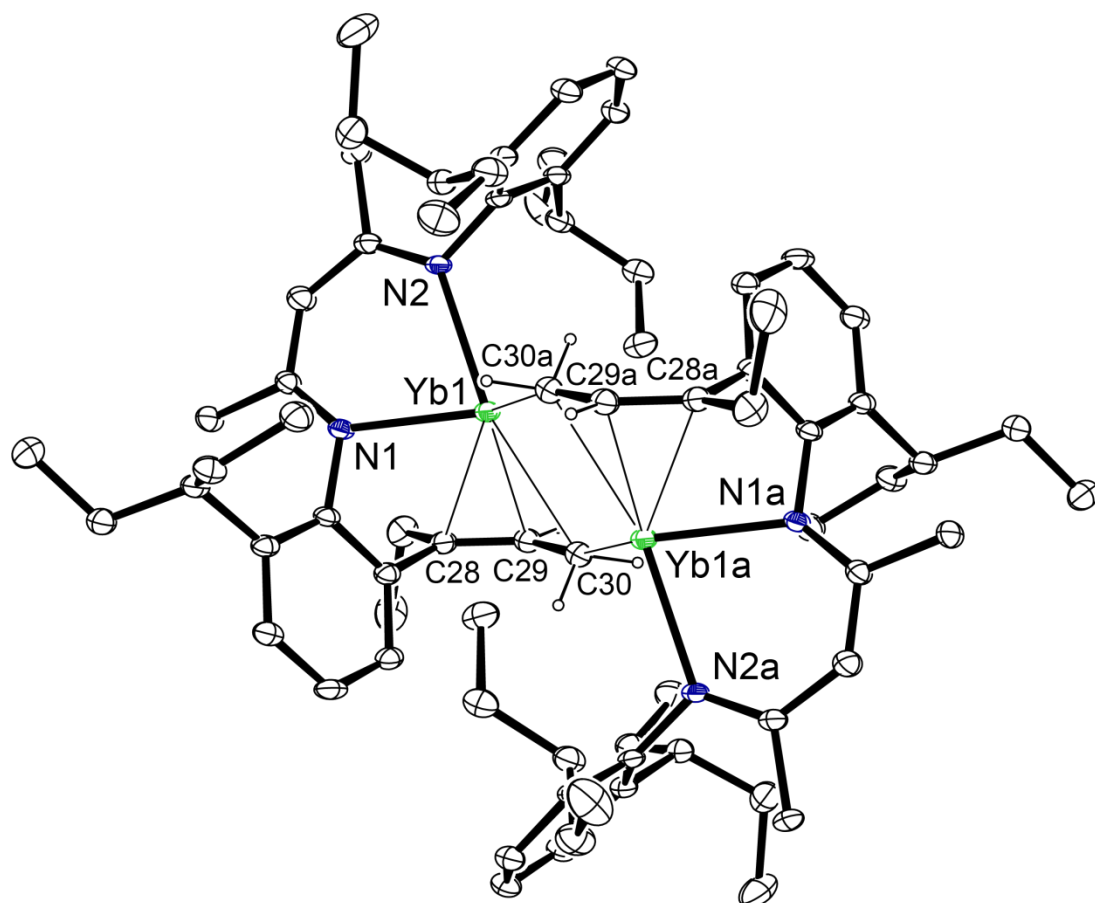
$[(\text{BDI}^{\text{Dipep}})\text{YbH}(\text{THF})]_2$ (100 mg, 0.06 mmol) was dissolved in C_6D_6 in an NMR tube fitted with a J. Youngs tap and degassed *via* three freeze-pump-thaw cycles on a Schlenk line. The mixture was exposed to one atmosphere of ethene gas at room temperature, with the presence of ethene confirmed through an initial ^1H NMR spectrum recorded immediately after exposure. The reaction mixture was left at room temperature for ca. 1h. The volatiles were removed *in vacuo*, the crude product re-dissolved into a pentane: toluene solvent mix and left to crystallise at room temperature, affording brown crystals suitable for an X-ray diffraction experiment.



Supplementary Figure 2.23. Close up of the ^1H NMR spectrum (500 MHz, C_6D_6) recorded after exposure of **2.5** to ethene gas at room temperature, highlighting the two Yb-H resonances present.



Supplementary Figure 2.24. ^1H NMR spectrum (500 MHz, C_6D_6) of the crude reaction solution, 1h at room temperature after exposure of **2.5** to ethene gas.



Supplementary Figure 2.25. Ortep representation (30% probability ellipsoids) of compound **2.6**, isolated from the attempted synthesis of $[(\text{BDI}^{\text{Dipep}})\text{YbEt}]_2$. Hydrogen atoms (except those on C29, C29a, C30 and C30a) have been omitted for clarity.

(BDI^{Dicyp})H (2.7)

a) Acetylacetone (500 mg, 4.99 mmol), *p*-toluenesulfonic acid monohydrate (949 mg, 4.99 mmol) and two molar equivalents of 2,6-dicyclohexylaniline (2571 mg, 9.99 mmol) were dissolved in toluene and refluxed with a Dean-Stark condenser for 10 days. After the resultant red solution was cooled to room temperature, triethylamine (504.9 mg, 4.99 mmol) was added, and the mixture stirred for 1h. The organic phase was washed twice with water, dried over MgSO₄ and the solvent was removed under vacuum. The resultant red-brown solid was washed with methanol until the solution became colourless, yielding the pure product as a pale beige powder. Recrystallisation from a saturated toluene solution afforded colourless crystals suitable for an X-ray diffraction experiment (1460 mg, 50%).

b) Acetylacetone (4570 mg, 45.65 mmol), *p*-toluenesulfonic acid monohydrate (8683 mg, 45.65 mmol) and two molar equivalents of 2,6-dicyclohexylaniline (23,502 mg, 91.30 mmol) were dissolved in anhydrous toluene in a round bottom flask and the Ar_(g) was bubbled through the mixture for 30 minutes. The mixture was then refluxed with a Dean-Stark condenser for 1 day under an inert atmosphere. After the resultant red solution was cooled to room temperature, triethylamine (4619 mg, 45.65 mmol) was added, and the mixture stirred for 1h. The organic phase was washed once with water then twice with brine, dried over MgSO₄ and the solvent was removed under vacuum. The resultant red-brown solid was heated into the minimum volume of methanol and left to cool, yielding the product as a pale beige powder (Isolated yield: 21,410 mg, 82%)

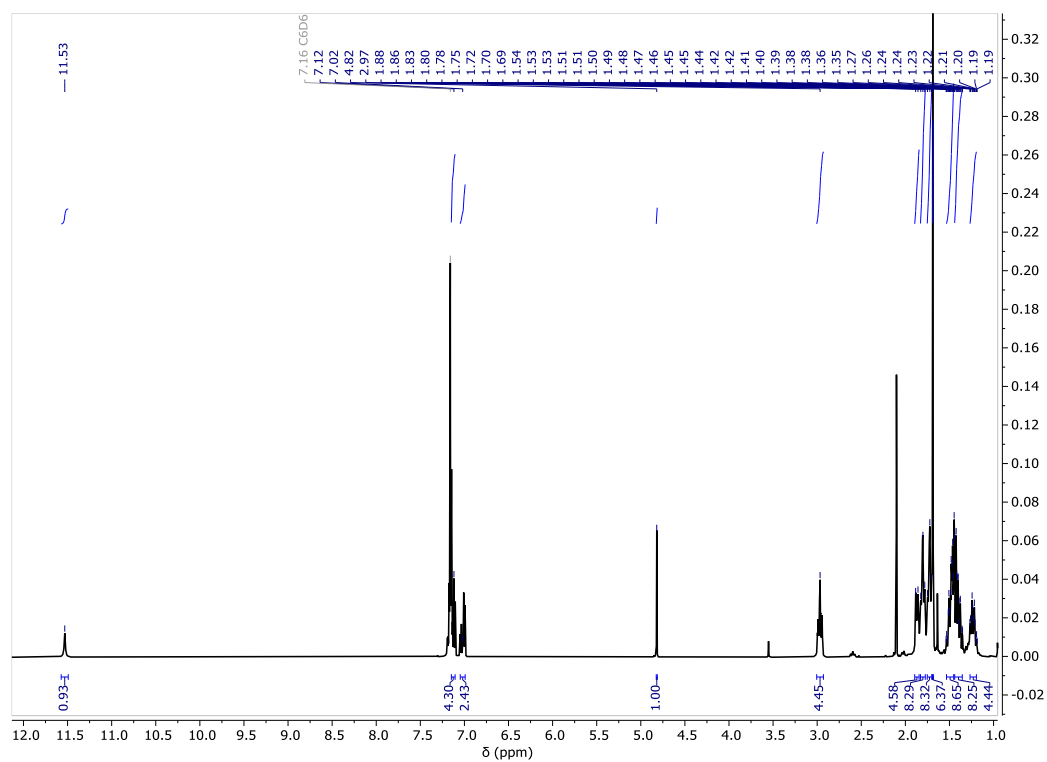
¹H NMR (500 MHz, C₆D₆) δ 11.53 (s, 1H, NH), 7.12 (m, 4H, ArH), 7.02 (m, 2H, ArH), 4.82 (s, 1H, NC(CH₃)CH), 2.97 (m, 4H, Cy-CH), 1.88 (m, 4H, Cy-CH₂), 1.80 (m, 8H, Cy-CH₂), 1.72 (m, 8H, Cy-CH₂), 1.69 (s, 6H, NC(CH₃)CH), 1.48 (m, 8H, Cy-CH₂), 1.41 (m, 8H, Cy-CH₂), 1.22 (m, 4H, Cy-CH₂).

¹³C{¹H} NMR (126 MHz, C₆D₆) δ 161.2 (NC(CH₃)CH), 141.8 (C_{ipso}), 141.5 (C_{ortho}), 125.5 (C_{para}), 124.7 (C_{meta}), 94.8 (NC(CH₃)CH), 39.2 (Cy-CH), 35.0 (Cy-CH₂ overlapping Cy-CH₂), 34.4 (Cy-CH), 27.6 (Cy-CH₂ overlapping Cy-CH₂), 27.5 (Cy-CH₂), 26.7 (Cy-CH₂), 21.3 (NC(CH₃)CH).

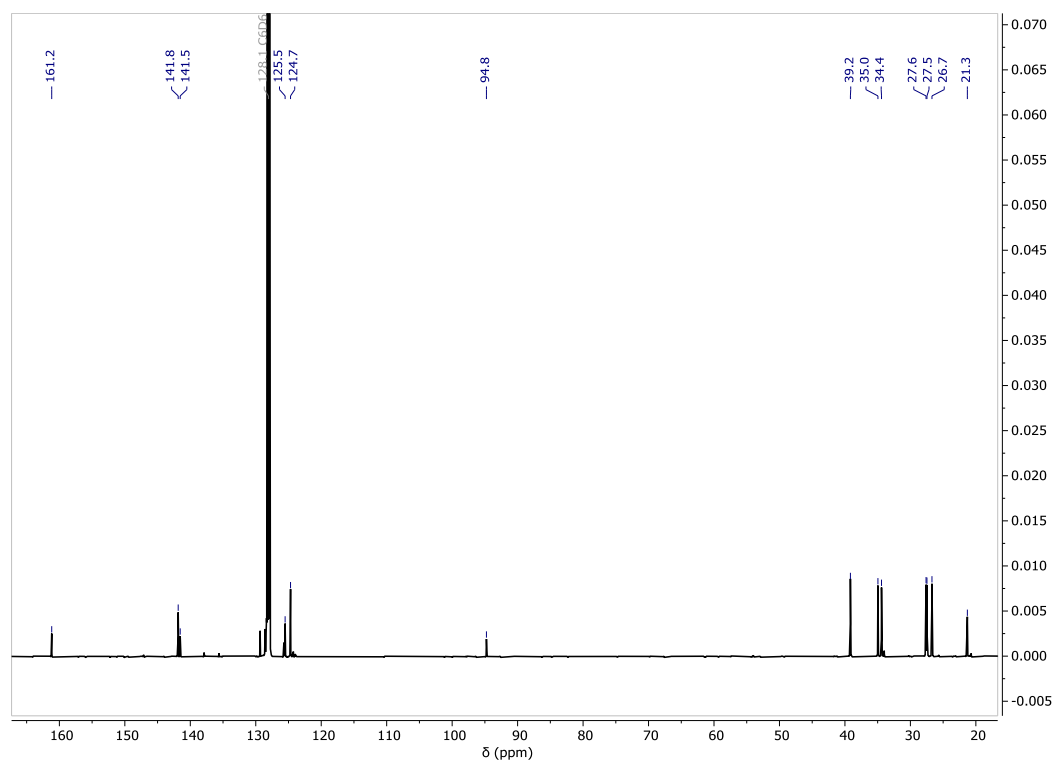
Elemental Analysis for [(BDI^{Dicyp})H] (578.93 g mol⁻¹):

Calculated: C, 85.06; H, 10.10; N, 4.84%.

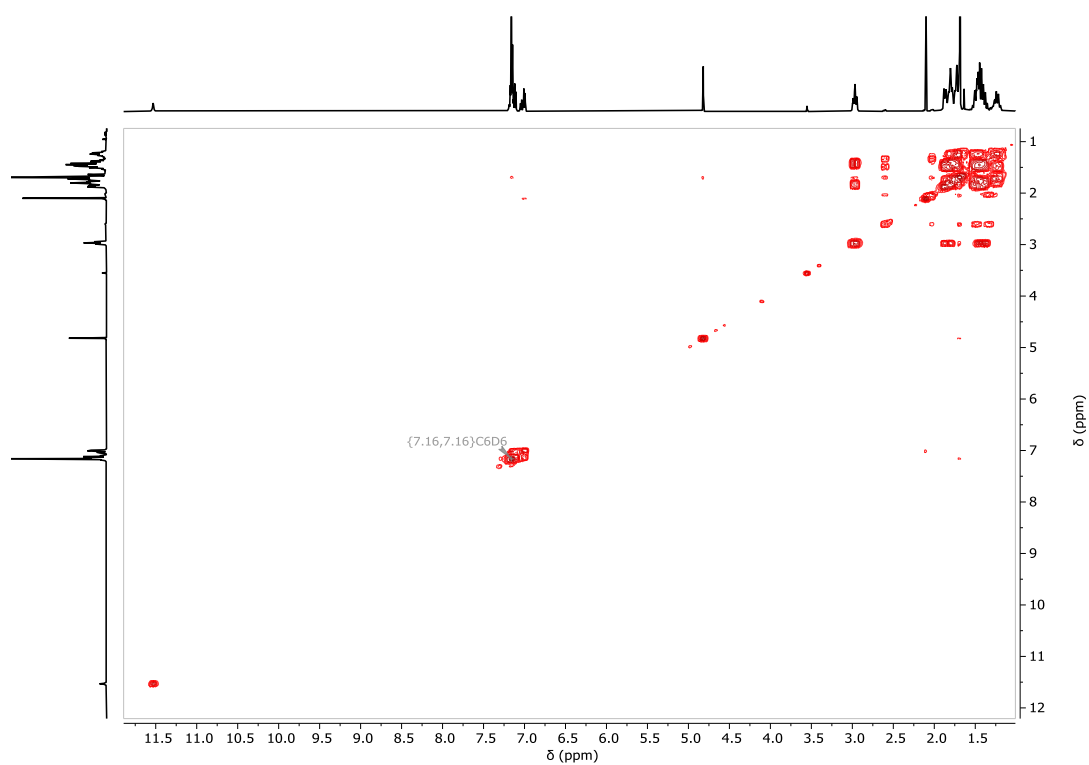
Found: C, 83.78; H, 10.10; N, 4.74%.



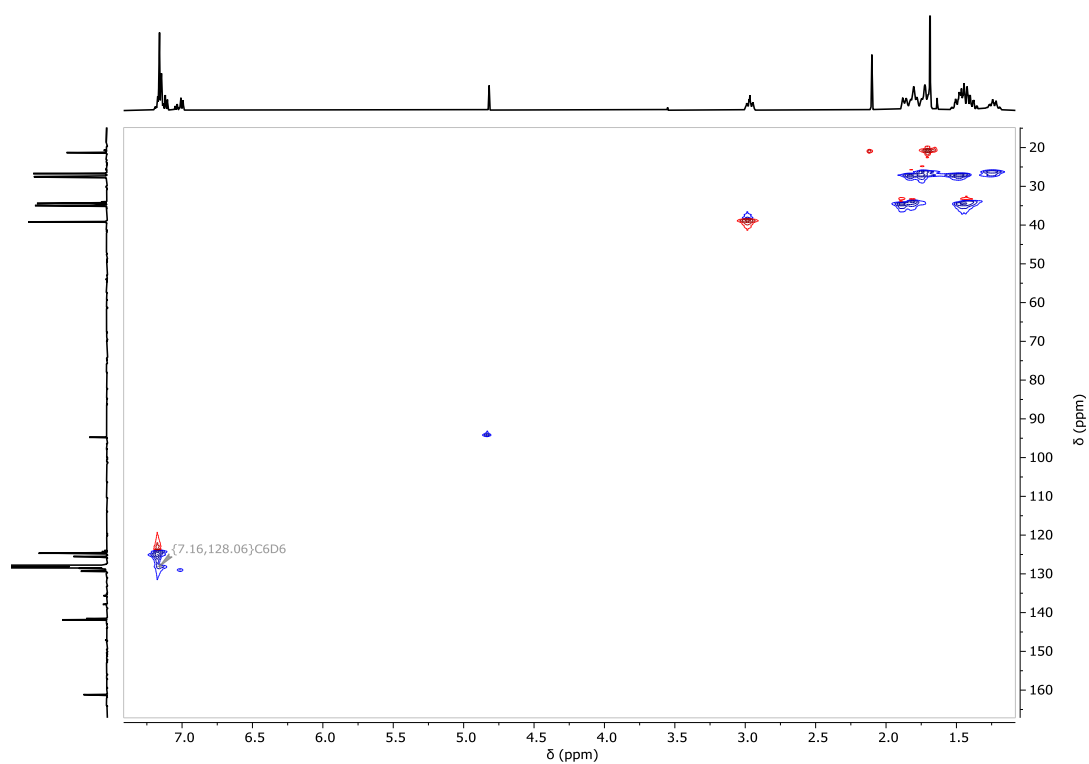
Supplementary Figure 2.26. ¹H NMR spectrum (500 MHz, C₆D₆) of (BDI^{Dicyp})H (**2.7**).



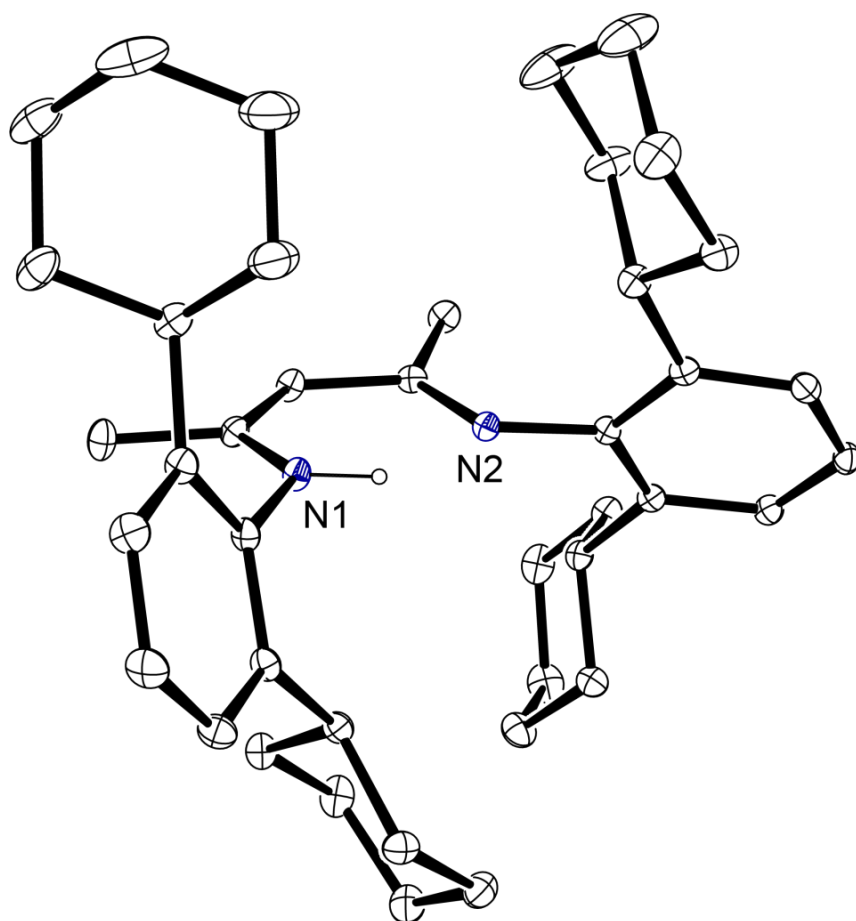
Supplementary Figure 2.27. ¹³C{¹H} NMR spectrum (126 MHz, C₆D₆) of (BDI^{Dicyp})H (**2.7**).



Supplementary Figure 2.28. ^1H - ^1H COSY NMR spectrum (500 MHz, C_6D_6) of $(\text{BDI}^{\text{Dicyp}})\text{H}$ (**2.7**).



Supplementary Figure 2.29. ^1H - ^{13}C HSQC NMR spectrum (500 MHz, C_6D_6) of $(\text{BDI}^{\text{Dicyp}})\text{H}$ (**2.7**).



Supplementary Figure 2.30. Ortep representation (ellipsoid 30% probability) of (BDI^{Dicyclopentadienyl})H (**2.7**). Hydrogen atoms (except on N1) have been omitted for clarity.

[2-(2-cyclohexenyl)aniline] (2.8)

Aniline (1010 g, 10.85 mol) (50 – 100 °C, ca. 0.02 mbar) was freshly distilled into a round bottom Schlenk flask, fitted with a pressure dropping funnel and cooled in an ice/water bath. While cool, 3-bromocyclohexene (250 mL, 2.17 mol) was added dropwise under a positive pressure of argon. The flask was then fitted with a water condenser and refluxed at 150 °C overnight. Distilled water was added whilst the mixture was still hot, transferred to a beaker containing ice and basified with sodium hydroxide pellets. The mixture was then transferred to a separating funnel and extracted with diethyl ether. The organic layer was dried with potassium hydroxide pellets, filtered and the solvent removed under reduced pressure to give a brown oil. 2-(2-cyclohexenyl)aniline (110 – 150 °C, ca. 0.02 mbar) was purified *via* vacuum distillation and isolated as a pale yellow oil (Isolated yield: 282 g, 75 %).

Multinuclear NMR analysis matches the literature.⁵

[2,6-di-(2-cyclohexenyl)aniline] (2.9)

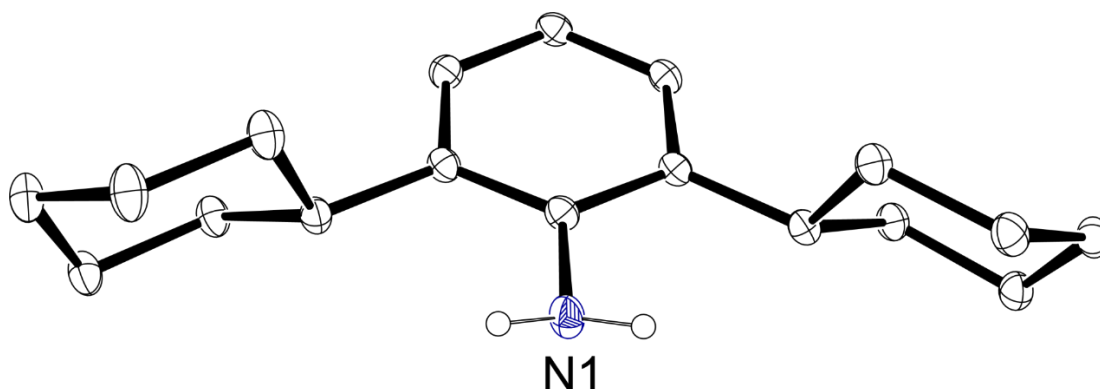
A multi-necked round bottom flask containing freshly distilled 2-(2-cyclohexenyl)aniline (282 g, 1.63 mol) (110 – 150 °C, ca. 0.02 mbar) was fitted with a pressure dropping funnel and a mechanical stirrer. The flask was cooled in an ice/water bath and 3-bromocyclohexene (62 mL, 0.54 mol) was added dropwise under a positive pressure of argon. The dropping funnel was swapped for a water condenser fitted with an argon balloon and the mixture was refluxed at 150 °C for 4 hours. Distilled water was added whilst the mixture was still hot, transferred to a beaker containing ice and basified with sodium hydroxide pellets. The mixture was then transferred to a separating funnel and extracted with diethyl ether. The organic layer was dried with potassium hydroxide pellets, filtered and the solvent removed under reduced pressure to give a brown oil. 2,6-di-(2-cyclohexenyl)aniline (155 – 190 °C, ca. 0.02 mbar) was purified *via* vacuum distillation and isolated as a pale yellow oil (Isolated yield: 108 g, 78 %).

Multinuclear NMR analysis matches the literature.⁵

[2,6-di-cyclohexylaniline] (2.10)

Freshly distilled 2,6-di-(2-cyclohexenyl)aniline (40 g, 0.16 mol) and Pd/C (10 w/w%, 2 g) was added into Fischer-Porter round bottom flask with methanol. The system was evacuated, purged with argon and re-evacuated. This was repeated thrice. The system was then purged with H_{2(g)} and re-evacuated once more before charging with H_{2(g)}. The mixture was left to stir under a H_{2(g)} atmosphere at room temperature for 1 day, resulting in the precipitation of a pale solid. The precipitate was re-dissolved by adding DCM solvent and the solution was filtered through Celite to remove Pd/C. The filtrate was dried under vacuum to give a pale pink powder. Colourless crystals suitable for an X-ray diffraction experiment were obtained from a saturated toluene: hexane solution at room temperature (Isolated yield: 24 g, 58%).

Multinuclear NMR analysis matches the literature.⁵



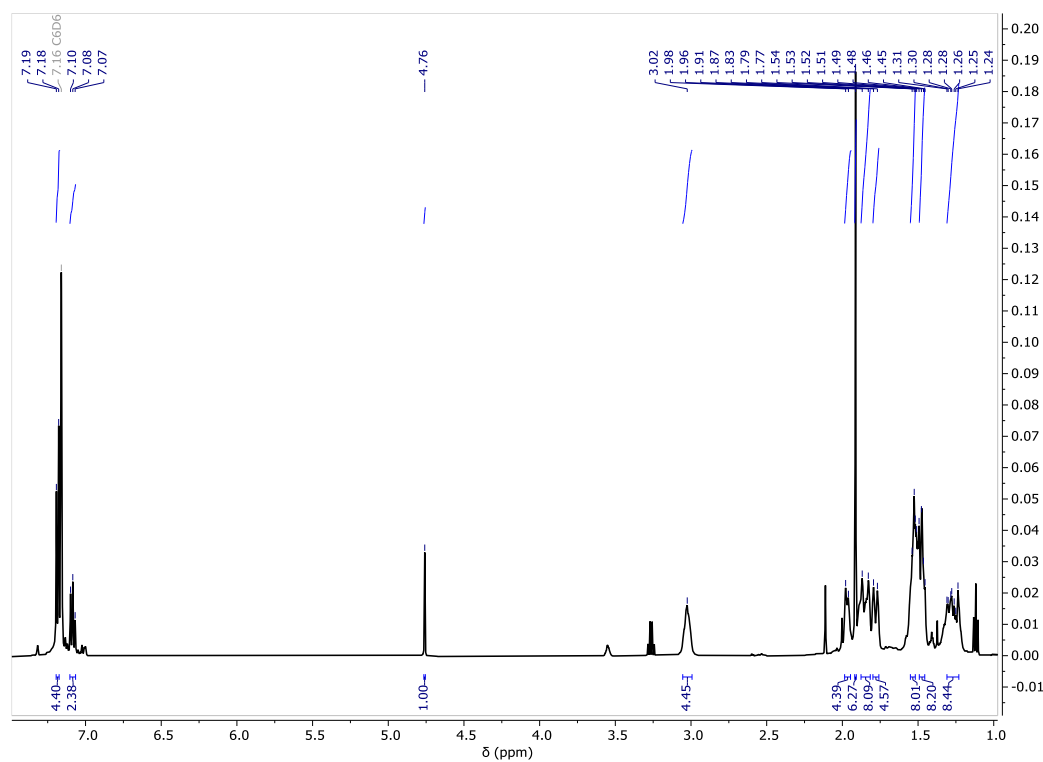
Supplementary Figure 2.31. Ortep representation (ellipsoid 30% probability) of [2,6-di-cyclohexylaniline] (2.10). Hydrogen atoms (except those on N1) have been omitted for clarity.

(BDI^{Dicyp})K (2.11)

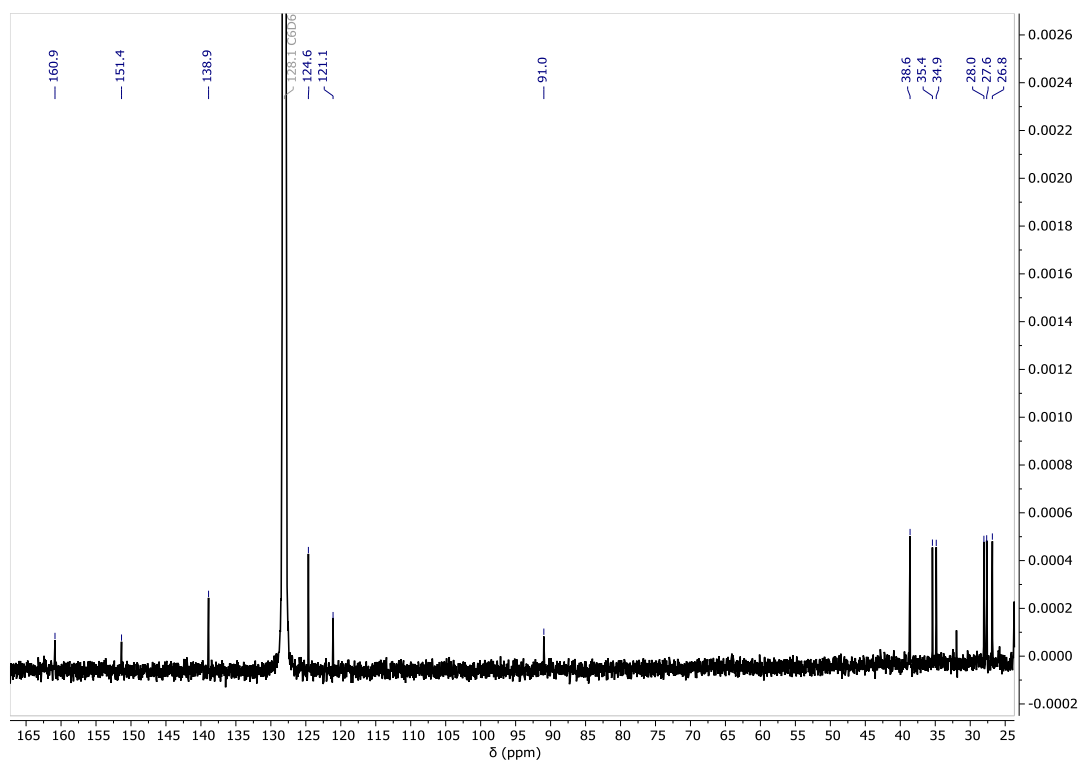
A colourless toluene solution containing (BDI^{Dicyp})H (436 mg, 0.75 mmol) was added to a Schlenk flask containing KHMDS (149 mg, 0.75 mmol) in toluene and left to stir at room temperature for 48h, affording a beige precipitate. The solution was decanted, the solid washed with hexane solvent before drying under vacuum to give the product as a light brown powder. Colourless crystals suitable for an X-ray diffraction experiment was obtained from a diethyl ether solution at room temperature (Isolated yield: 442 mg, 95%).

¹H NMR (500 MHz, C₆D₆) δ 11.53 (s, 1H, *NH*), 7.12 (m, 4H, *ArH*), 7.02 (m, 2H, *ArH*), 4.82 (s, 1H, NC(CH₃)CH), 2.97 (m, 4H, Cy-CH), 1.88 (m, 4H, Cy-CH₂), 1.80 (m, 8H, Cy-CH₂), 1.72 (m, 8H, Cy-CH₂), 1.69 (s, 6H, NC(CH₃)CH), 1.48 (m, 8H, Cy-CH₂), 1.41 (m, 8H, Cy-CH₂), 1.22 (m, 4H, Cy-CH₂).

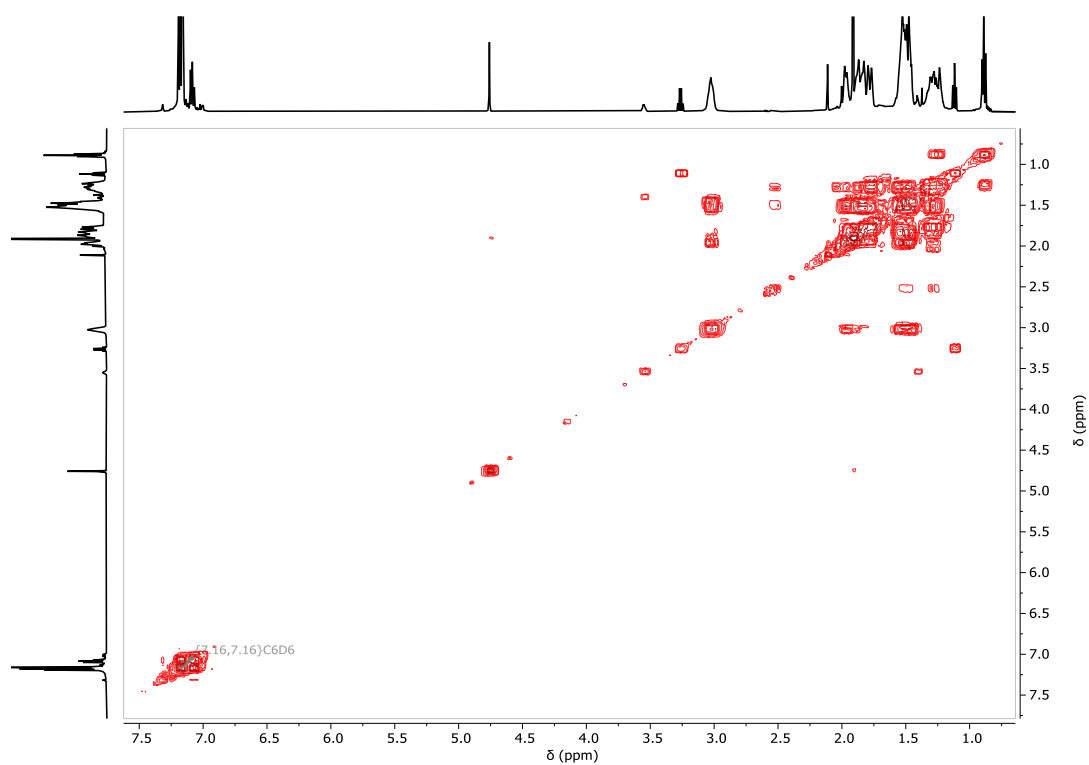
¹³C{¹H} NMR (126 MHz, C₆D₆) δ 161.2 (NC(CH₃)CH), 141.8 (C_{ipso}), 141.5 (C_{ortho}), 125.5 (C_{para}), 124.7 (C_{meta}), 94.8 (NC(CH₃)CH), 39.2 (Cy-CH), 35.0 (Cy-CH₂ overlapping Cy-CH₂), 34.4 (Cy-CH), 27.6 (Cy-CH₂ overlapping Cy-CH₂), 27.5 (Cy-CH₂), 26.7 (Cy-CH₂), 21.3 (NC(CH₃)CH).



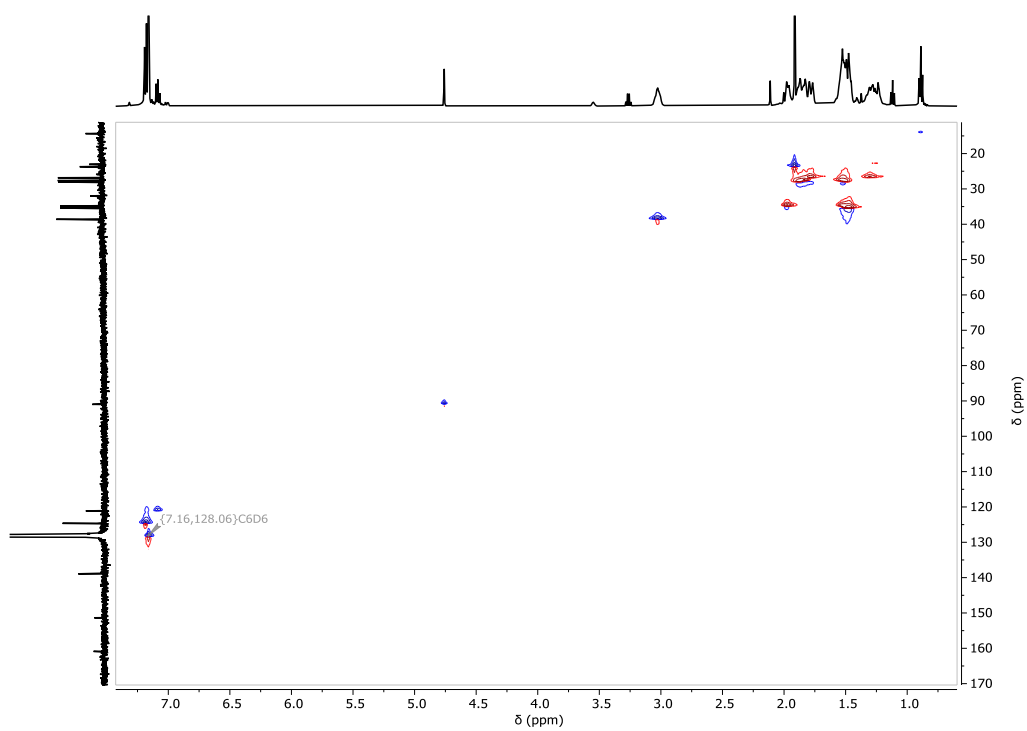
Supplementary Figure 2.32. ^1H NMR spectrum (500 MHz, C_6D_6) of $(\text{BDI}^{\text{Dicyl}})\text{K}$ (**2.11**).



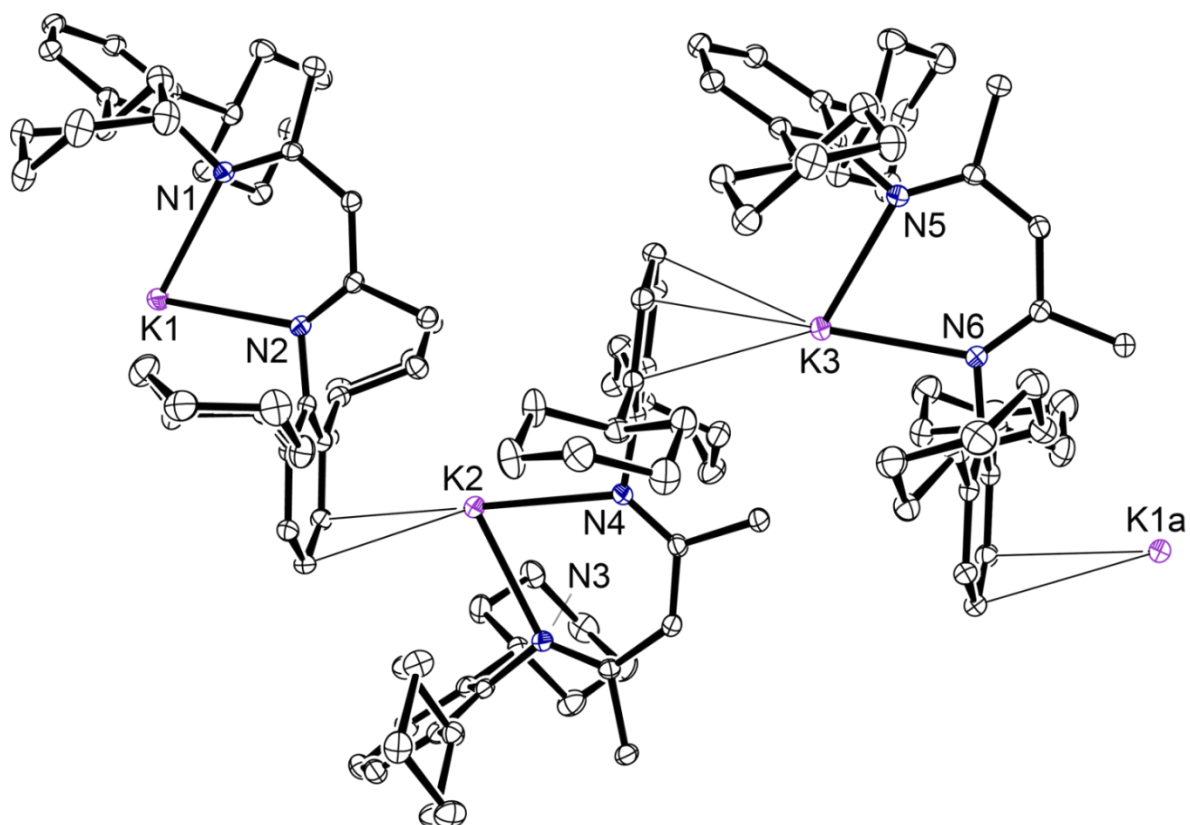
Supplementary Figure 2.33. $^{13}\text{C}\{^1\text{H}\}$ NMR spectrum (126 MHz, C_6D_6) of $(\text{BDI}^{\text{Dicyl}})\text{K}$ (**2.11**).



Supplementary Figure 2.34. ^1H - ^1H COSY spectrum (500 MHz, C_6D_6) of (BDI^{Dicyl})K (2.11).



Supplementary Figure 2.35. ^1H - ^{13}C HSQC spectrum (500 MHz, C_6D_6) of (BDI^{Dicyl})K (2.11).



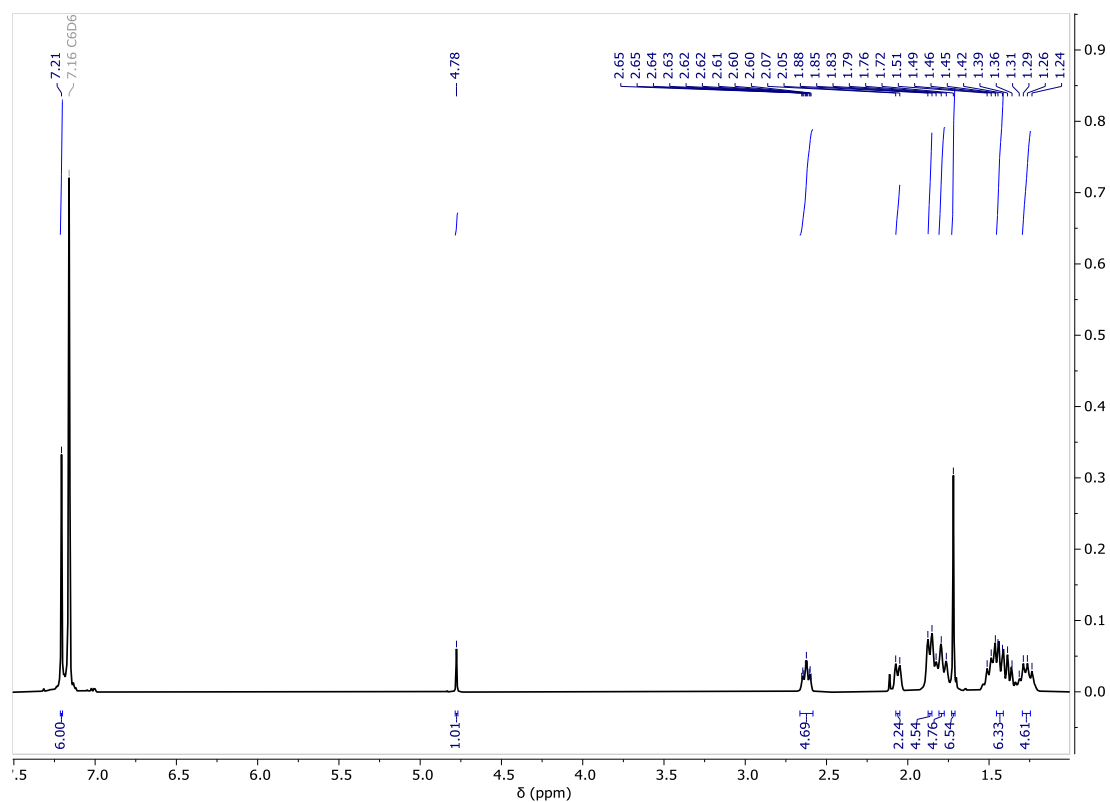
Supplementary Figure 2.36. Ortep representation (ellipsoid 30% probability) of (BDI^{Dicyclopentadienyl})K (**2.11**). Hydrogen atoms have been omitted for clarity.

[(BDI^{Dicyp})YbI]₂ (2.12)

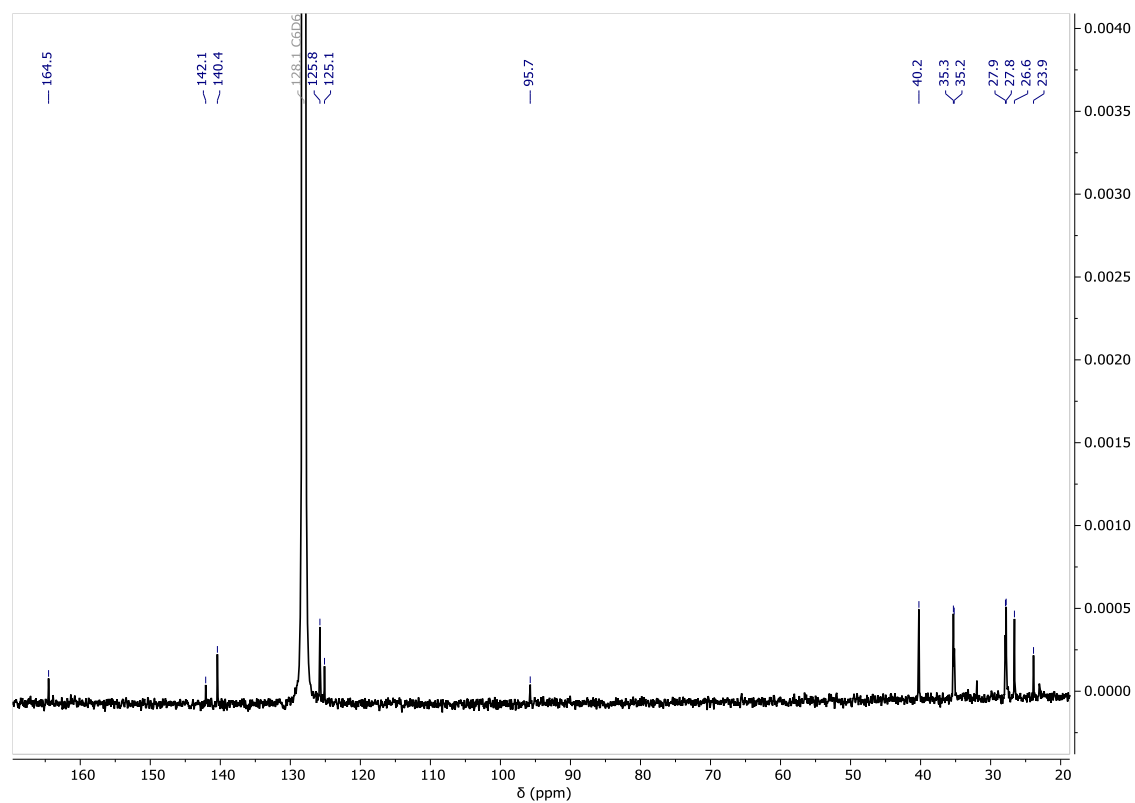
A pale brown THF solution of (BDI^{Dicyp})K (1120 mg, 1.80 mmol) was added to a scintillation vial containing a pale yellow suspension of YbI₂ (1267 mg, 2.0 mmol) in THF and left to stir at room temperature for 4h. The solvent removed *in vacuo* from the resultant dark red solution, filtered through Celite, and re-dried to generate the crude product as a red solid. Deep red crystals suitable for X-ray diffraction analysis were obtained from a saturated pentane solution at room temperature (Isolated yield: 1115 mg, 70%).

¹H NMR (500 MHz, C₆D₆) δ 7.21 (s, 6H, ArH), 4.78 (s, 1H, NC(CH₃)CH), 2.62 (m, 4H, Cy-CH), 2.06 (m, 2H, Cy-CH₂), 1.86 (m, 4H, Cy-CH₂), 1.79 (m, 4H, Cy-CH₂), 1.72 (s, 6H, NC(CH₃)CH), 1.46 (m, 6H, Cy-CH₂ overlapping Cy-CH₂), 1.27 (m 4H, Cy-CH₂)

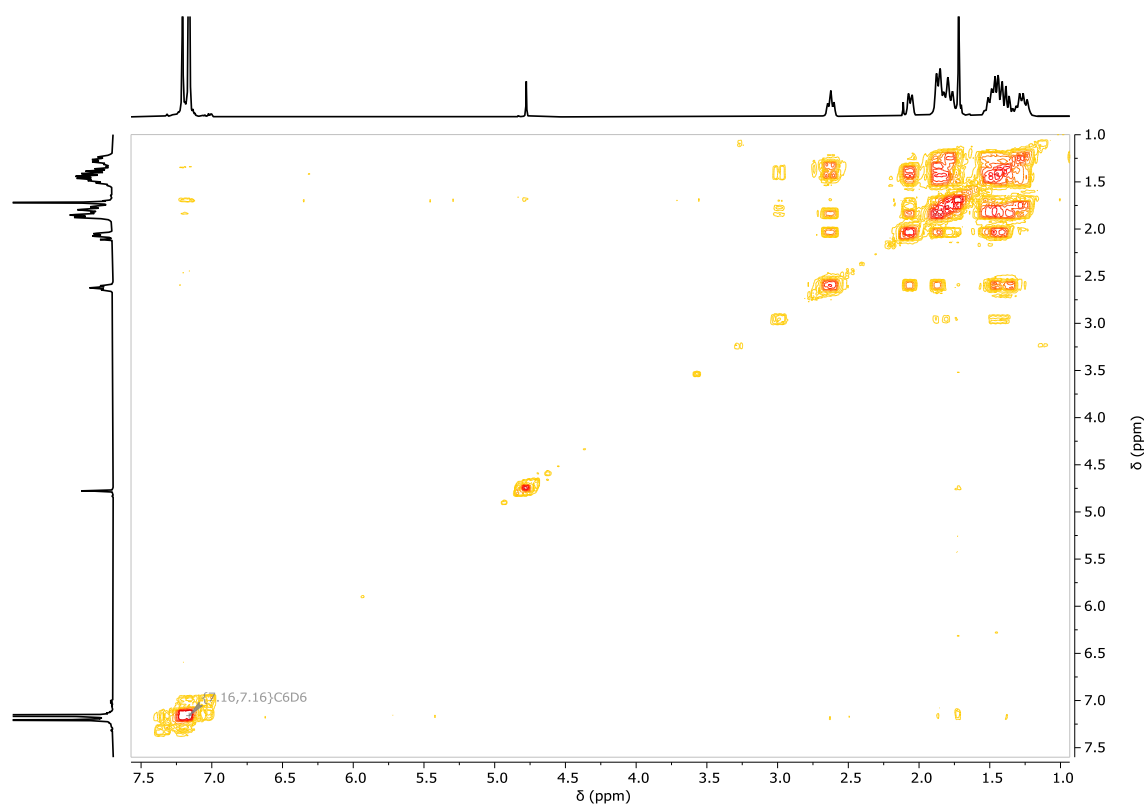
¹³C{¹H} NMR (126 MHz, C₆D₆) δ 164.5 (NC(CH₃)CH), 142.1 (C_{ipso}), 140.4 (C_{ortho}), 125.8 (C_{para}), 125.1 (C_{meta}), 95.7 (NC(CH₃)CH), 40.2 (Cy-CH), 35.3 (Cy-CH₂), 35.2 (Cy-CH₂ overlapping Cy-CH₂), 27.9, 27.8 (Cy-CH₂), 26.6 (Cy-CH₂ overlapping Cy-CH₂), 23.9 (NC(CH₃)CH)



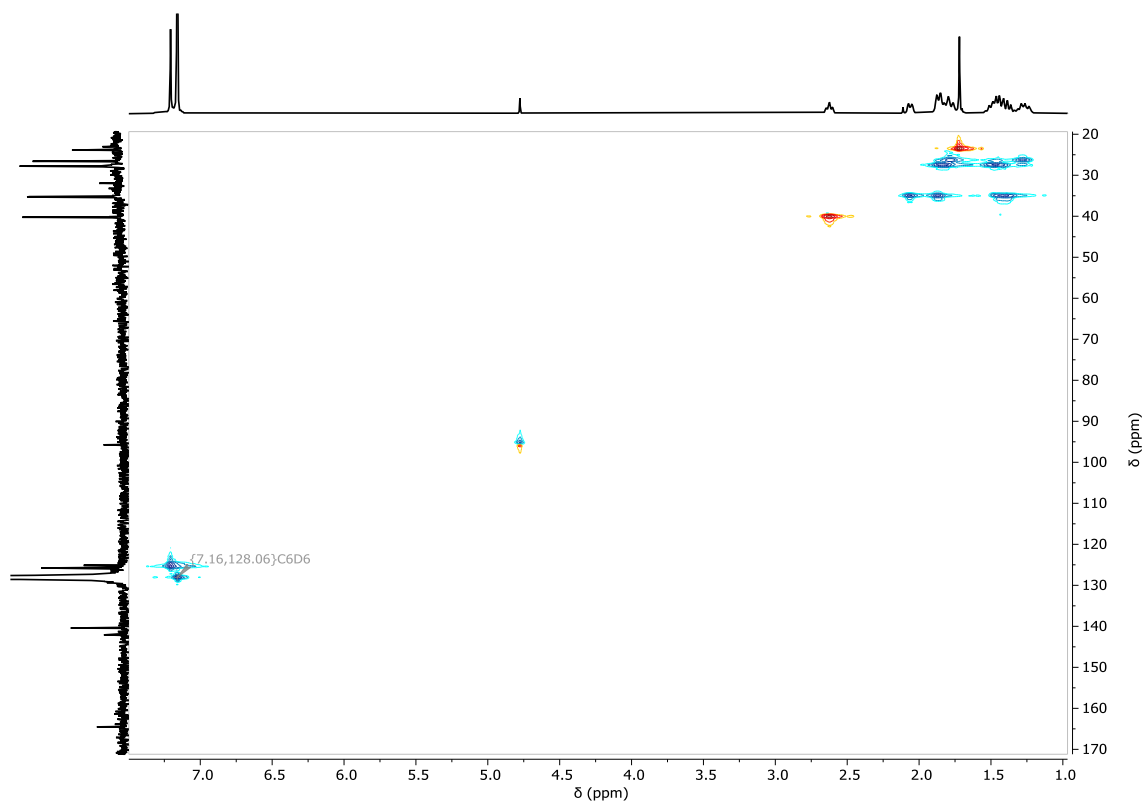
Supplementary Figure 2.37. ¹H NMR spectrum (500 MHz, C₆D₆) of [(BDI^{Dicyl})YbI]₂ (2.12).



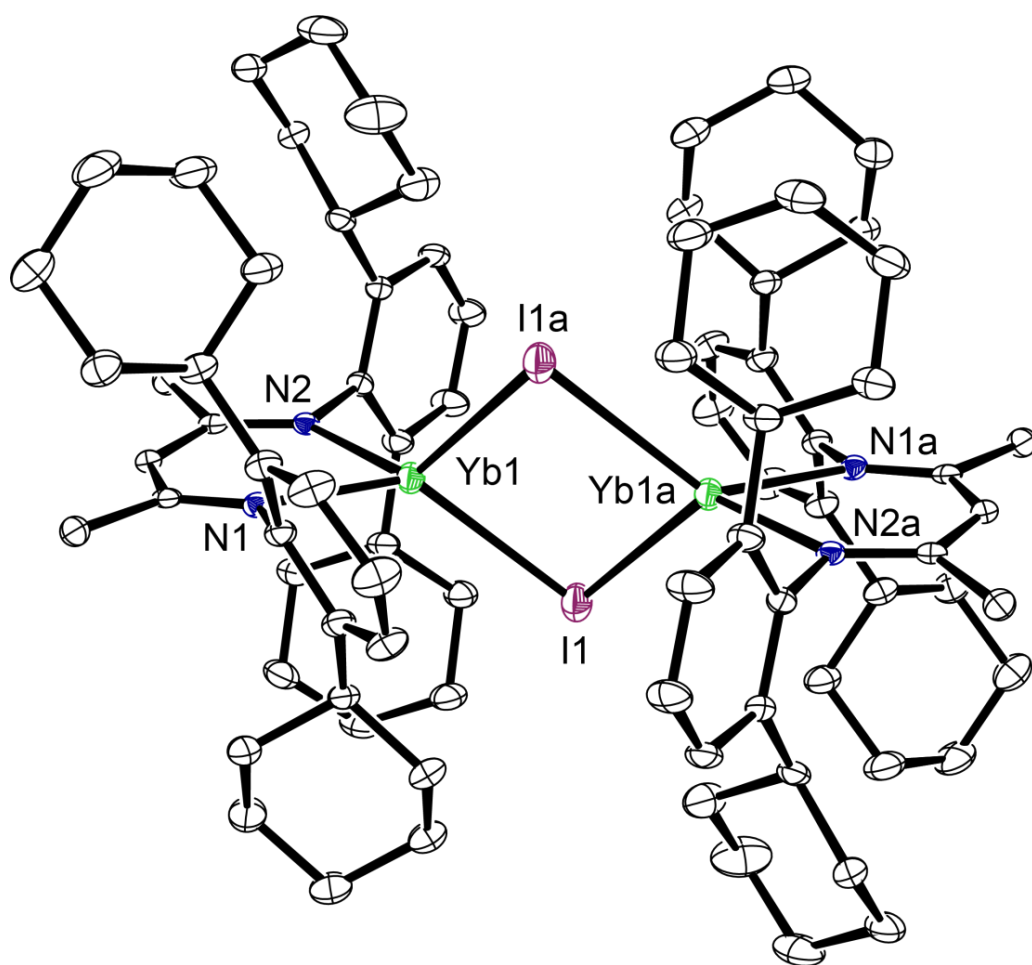
Supplementary Figure 2.38. ¹³C{¹H} NMR spectrum (126 MHz, C₆D₆) of [(BDI^{Dicyl})YbI]₂ (2.12).



Supplementary Figure 2.39. ^1H - ^1H COSY NMR spectrum (500 MHz, C_6D_6) of $[(\text{BDI}^{\text{Dicyl}})\text{YbI}]_2$ (**2.12**).



Supplementary Figure 2.40. ^1H - ^{13}C HSQC NMR spectrum (500 MHz, C_6D_6) of $[(\text{BDI}^{\text{Dicyl}})\text{YbI}]_2$ (**2.12**).



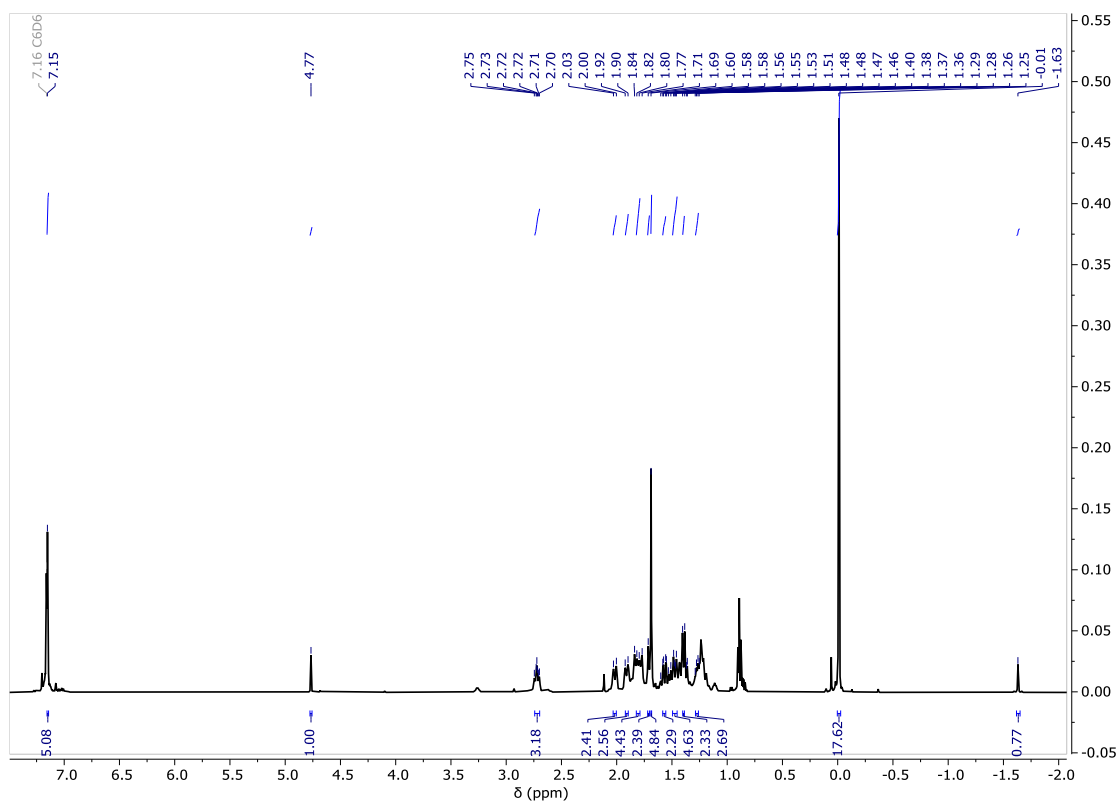
Supplementary Figure 2.41. Ortep representation (30% probability ellipsoids) of $[(BDI^{Dicyl})YbI]_2$ (2.12). Hydrogen atoms have been omitted for clarity.

[(BDI^{Dicyp})YbCH(SiMe₃)₂] (2.13)

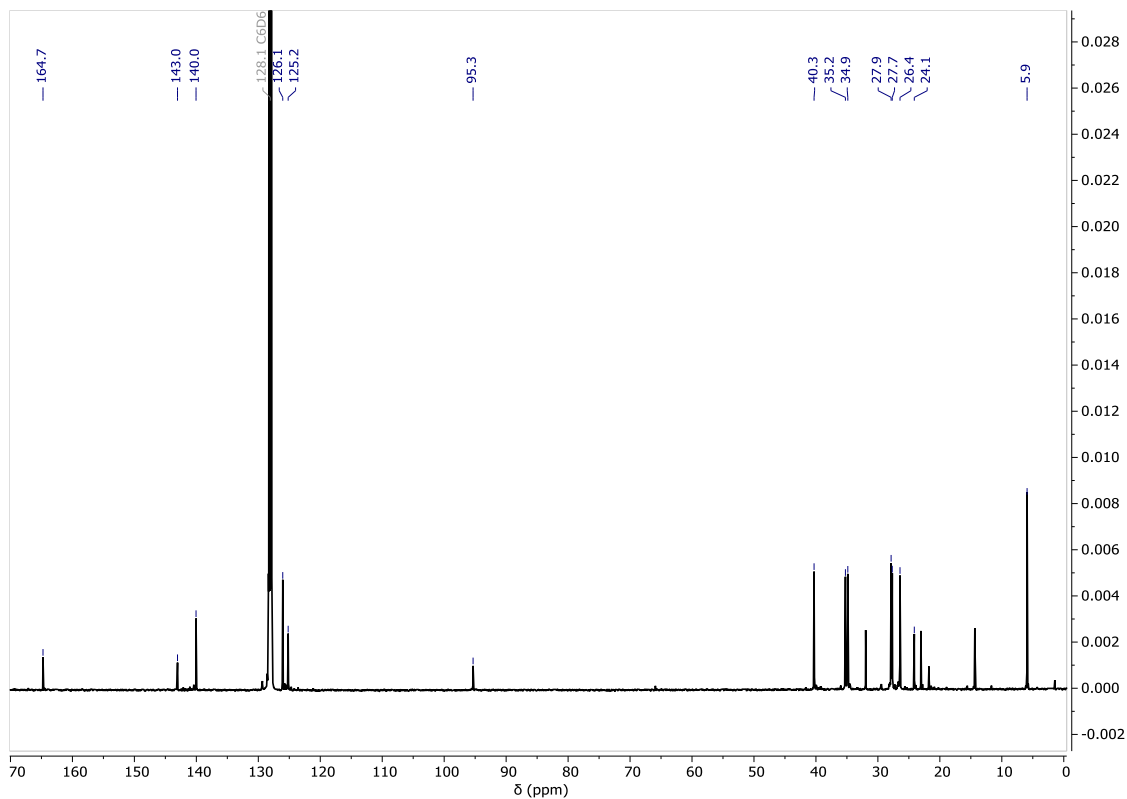
A red toluene solution of [(BDI^{Dicyp})YbI]₂ (1364 mg, 0.78 mmol) was added to a scintillation vial containing a toluene solution of K[CH(SiMe₃)₂] (308 mg, 1.50 mmol) and was left to stir for ca. 48h at room temperature. The mixture was filtered through Celite, and the solvent removed *in vacuo* from the resultant dark brown-red solution, generating the crude product as a red solid. Deep red crystals suitable for X-ray diffraction analysis were obtained from a saturated hexane solution at room temperature (Isolated yield: 556.7 mg, 78%).

¹H NMR (500 MHz, C₆D₆) δ 7.15 (s, 6H, ArH), 4.77 (s, 1H, NC(CH₃)CH), 2.72 (m, 4H, Cy-CH), 1.68 (m, 12H, CH(CH₂CH₃)₂), 2.01 (m, 2H, Cy-CH₂), 1.91 (m, 2H, Cy-CH₂), 1.81 (m, 4H, Cy-CH₂), 1.71 (br, 2H, Cy-CH₂), 1.69 (s, 6H, NC(CH₃)CH), 1.57 (m, 2H, Cy-CH₂), 1.48 (m, 4H, Cy-CH₂), 1.38 (m, 2H, Cy-CH₂), 1.28 (m, 2H, Cy-CH₂), -0.01 (s, 18H, CH(SiMe₃)₂), -1.63 (s, 1H, CH(SiMe₃)₂).

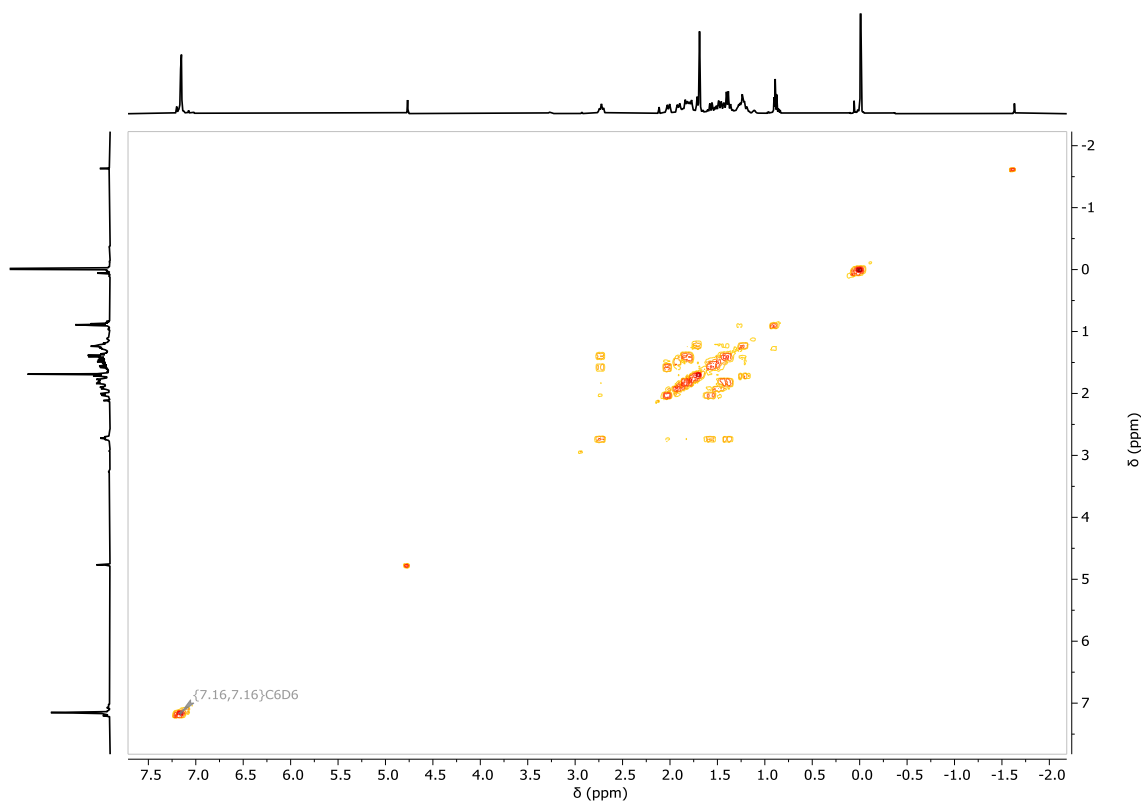
¹³C{¹H} NMR (126 MHz, C₆D₆) δ 164.7 (NC(CH₃)CH), 143.0 (C_{ipso}), 140.0 (C_{ortho}), 126.1 (C_{para}), 125.2 (C_{meta}), 95.3 (NC(CH₃)CH), 40.3 (Cy-CH), 35.2 (Cy-CH₂ overlapping Cy-CH₂), 34.9 (Cy-CH₂ overlapping Cy-CH₂), 27.9 (Cy-CH₂), 27.7 (Cy-CH₂ overlapping Cy-CH₂), 26.4 (Cy-CH₂ overlapping Cy-CH₂), 24.1 NC(CH₃)CH, 5.9 (CH(SiMe₃)₂).



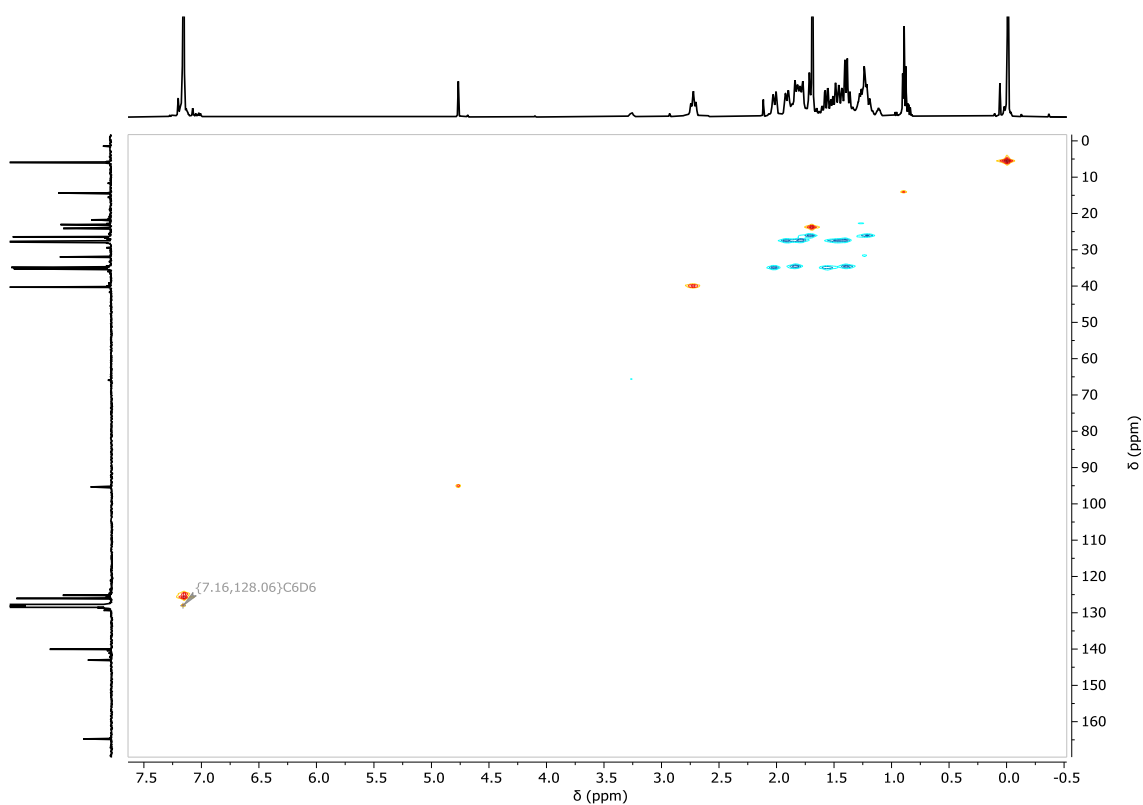
Supplementary Figure 2.42. ¹H NMR spectrum (500 MHz, C₆D₆) of [(BDI^{Dicyclopentadienyl})YbCH(SiMe₃)₂] (**2.13**).



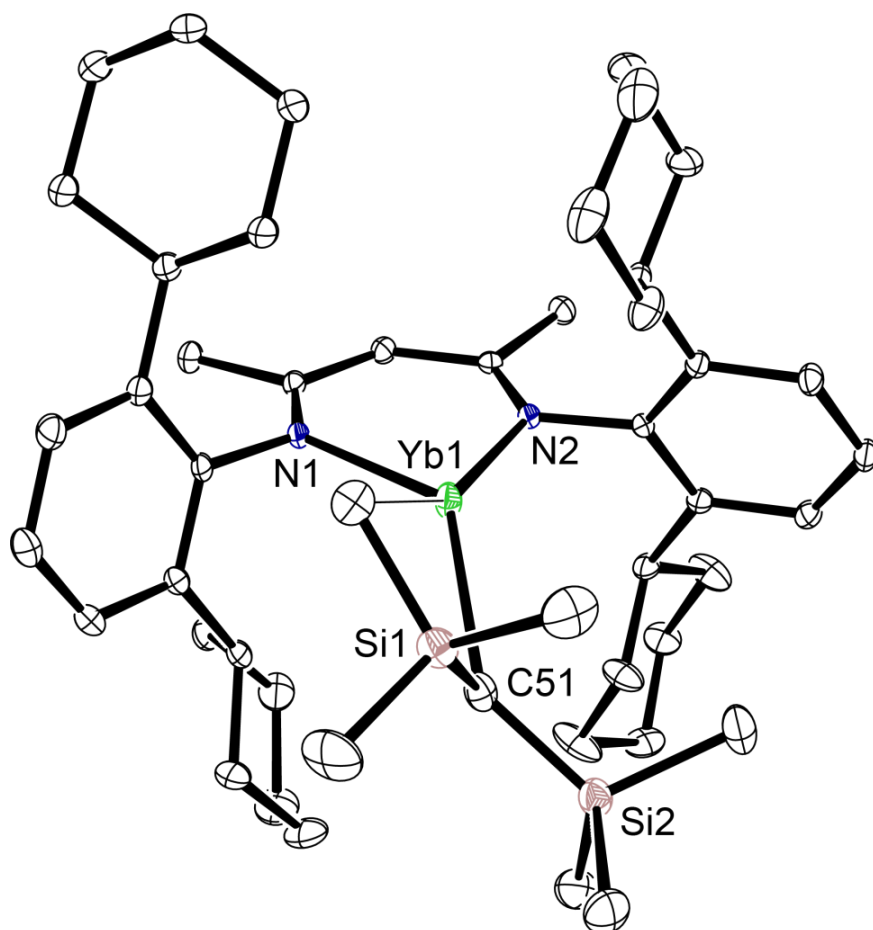
Supplementary Figure 2.43. ¹³C{¹H} NMR spectrum (126 MHz, C₆D₆) of [(BDI^{Dicyclopentadienyl})YbCH(SiMe₃)₂] (**2.13**).



Supplementary Figure 2.44. ^1H - ^1H COSY NMR spectrum (500 MHz, C_6D_6) of $[(\text{BDI}^{\text{Dicyclopentadienyl}})\text{YbCH}(\text{SiMe}_3)_2]$ (**2.13**).



Supplementary Figure 2.45. ^1H - ^{13}C HSQC NMR spectrum (500 MHz, C_6D_6) of $[(\text{BDI}^{\text{Dicyclopentadienyl}})\text{YbCH}(\text{SiMe}_3)_2]$ (**2.13**).

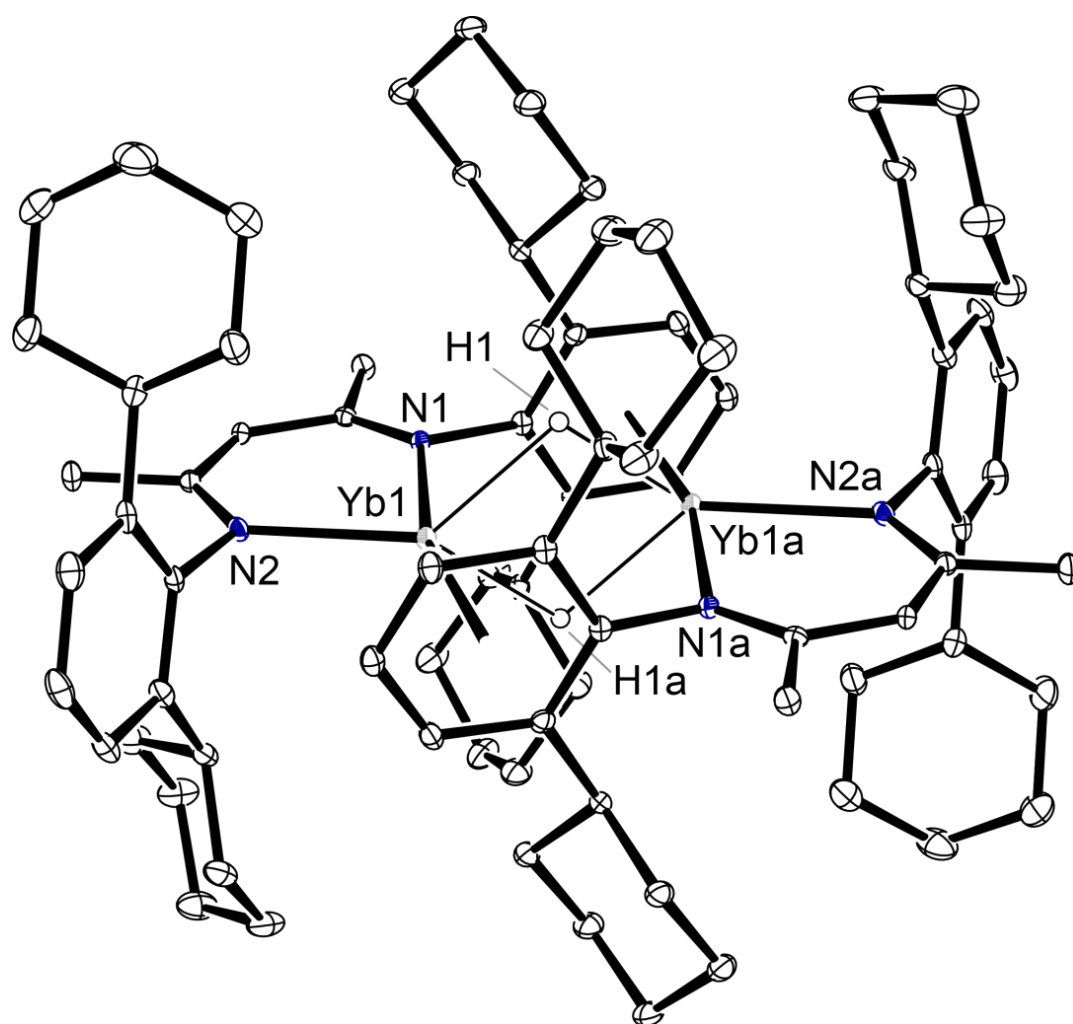


Supplementary Figure 2.46. Ortep representation (30% probability ellipsoids) of $[(\text{BDI}^{\text{DicyP}})\text{YbCH}(\text{SiMe}_3)_2]$ (**2.13**). Hydrogen atoms have been omitted for clarity.

[(BDI^{Dicyp})YbH]₂ (2.14)

A buffer toluene solution was gently layered on top of an orange toluene solution containing [(BDI^{Dicyp})YbCH(SiMe₃)₂] (556 mg, 0.61 mmol). A concentrated toluene containing 1,4-cyclohexadiene (98 mg, 1.22 mmol) was then gently layered on top of the buffer solution and the vial was left unmoved at room temperature with the vial lid cracked open. Small dark crystals suitable for a single crystal X-ray diffraction experiment were obtained over the course of 2 days (Isolated yield: 380.5 mg, 83%)

The insoluble nature of [(BDI^{Dicyp})YbH]₂ hampered characterisation by multinuclear NMR spectroscopic techniques.



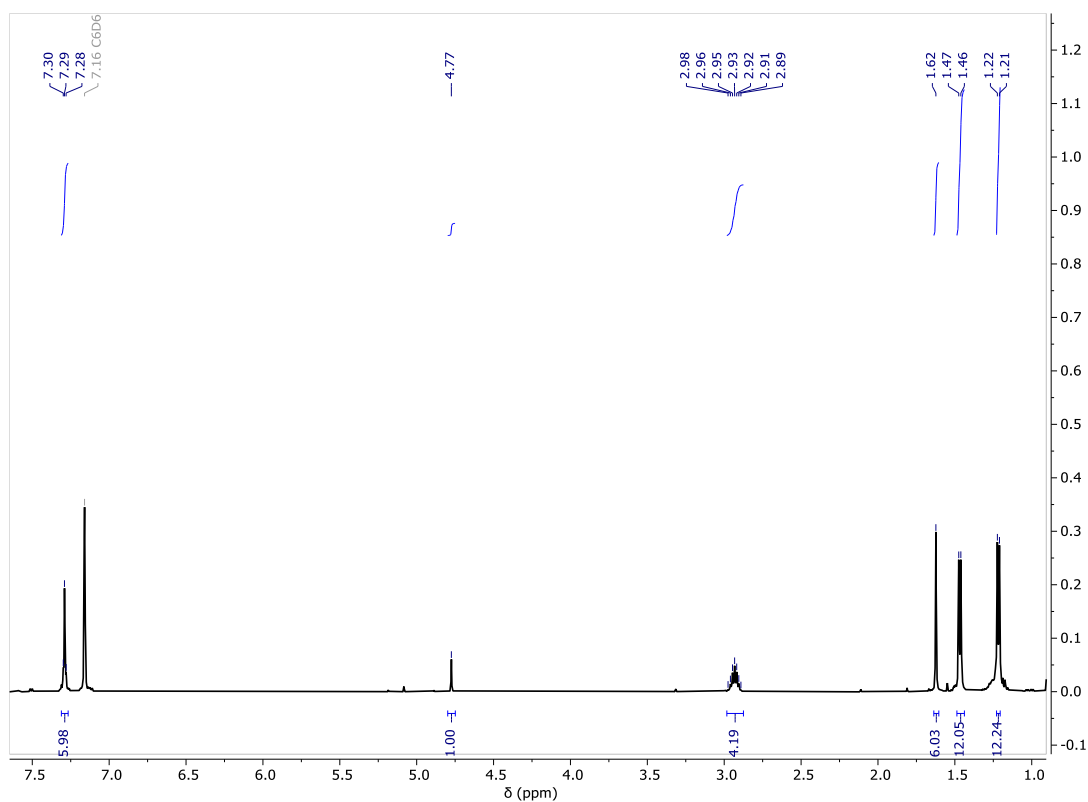
Supplementary Figure 2.47. Ortep representation (30% probability ellipsoids) of $[(\text{BDI}^{\text{Dicyl}})\text{YbH}]_2$ (**2.14**). Hydrogen atoms (except bridging H1 and H1a) have been omitted for clarity.

[{(BDI^{Dipp})Yb}₃P₇] (2.15)

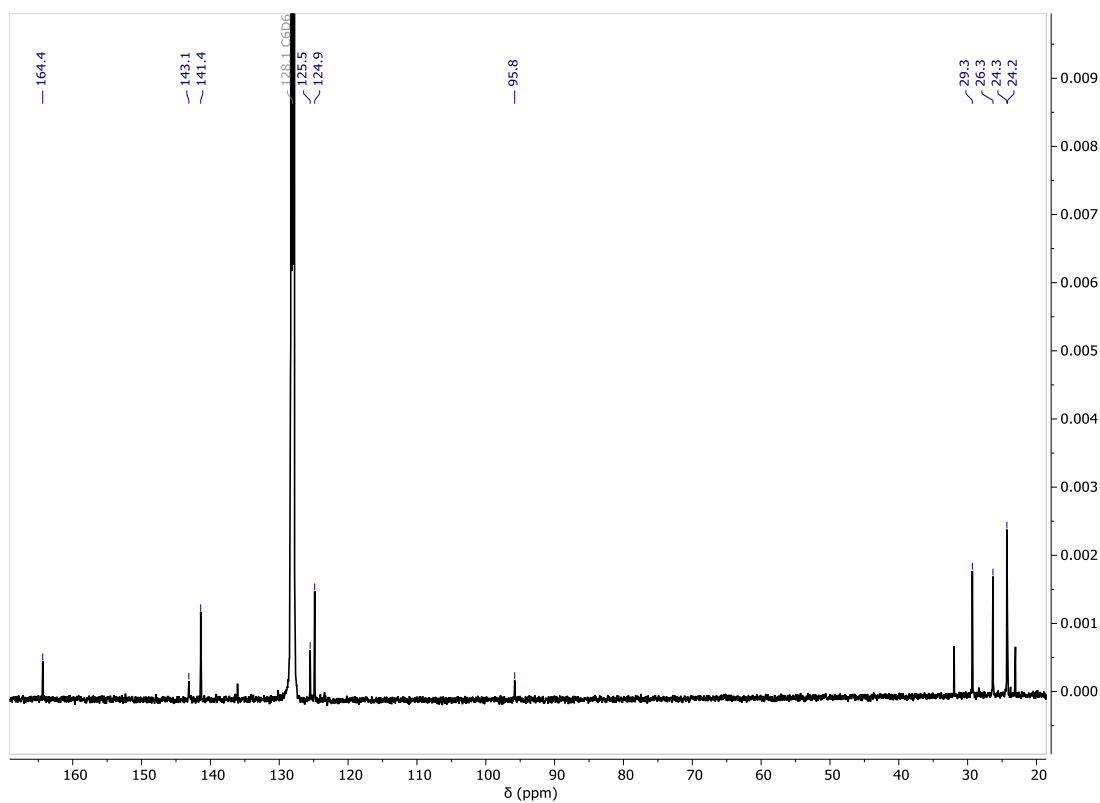
Addition of P₄ (6.86 mg, 0.06 mmol) to a J. Youngs tap NMR tube containing a black C₆D₆ solution [(BDI^{Dipp})YbH]₂ (65.5 mg, 0.06 mmol) resulted in a dark red solution almost immediately, with residual [(BDI^{Dipp})YbH]₂ reacting after 24h at room temperature. The solvent was removed *in vacuo* and the crude product re-dissolved into hexane. The mixture was filtered, concentrated, and crystallised at room temperature to afford red crystals suitable for X-ray diffraction analysis (Isolated yield: 16 mg, 44%).

¹H NMR (500 MHz, C₆D₆) δ 7.29 (m, 6H, ArH), 4.77 (s, 1H, NC(CH₃)CH), 2.93 (sept, 4H, *J* = 6.7 Hz, CH(CH₃)₂), 1.62 (s, 6H, NC(CH₃)CH), 1.47 (d, 12H, *J* = 6.8 Hz, CH(CH₃)₂), 1.22 (d, 12H, *J* = 6.8 Hz, CH(CH₃)₂).

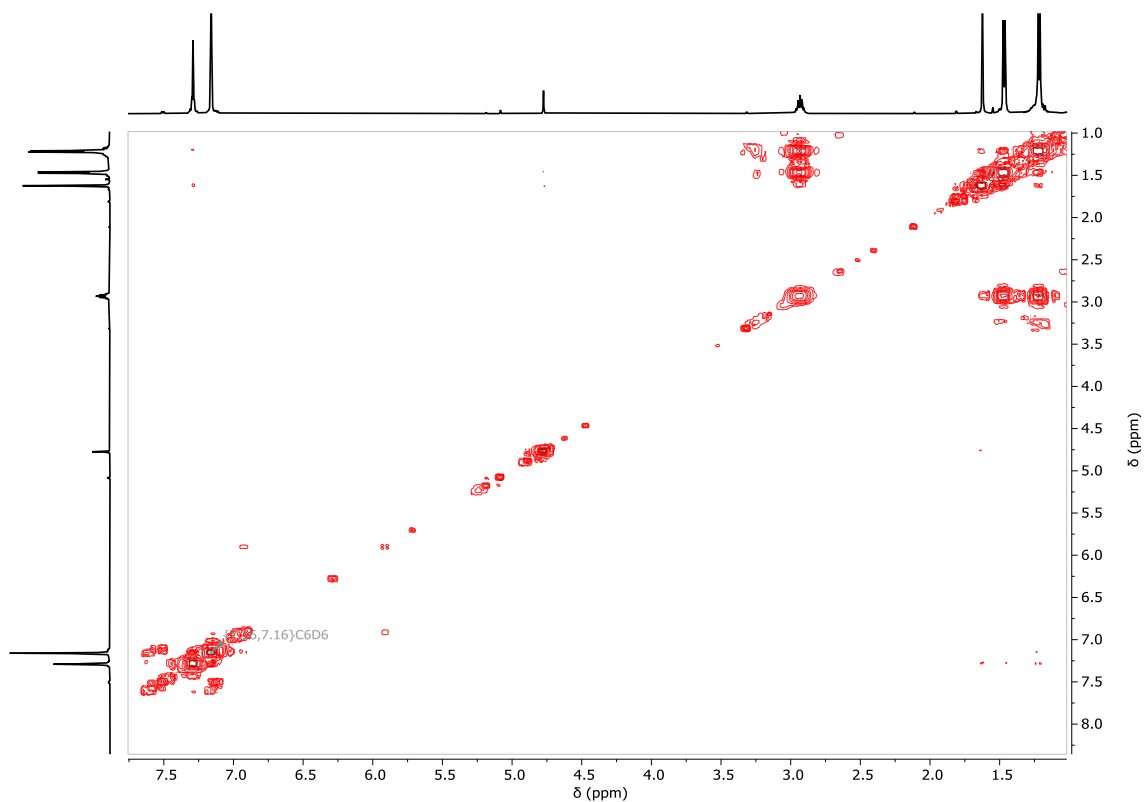
¹³C{¹H} NMR (126 MHz, C₆D₆) δ 164.4 (NC(CH₃)CH), 143.1 (C_{ipso}), 141.4 (C_{ortho}), 125.5 (C_{para}), 124.9 (C_{meta}), 95.8 (NC(CH₃)CH), 29.3 (CH(CH₃)₂), 26.3, 24.3 CH(CH₃)₂, 24.2 NC(CH₃)CH).



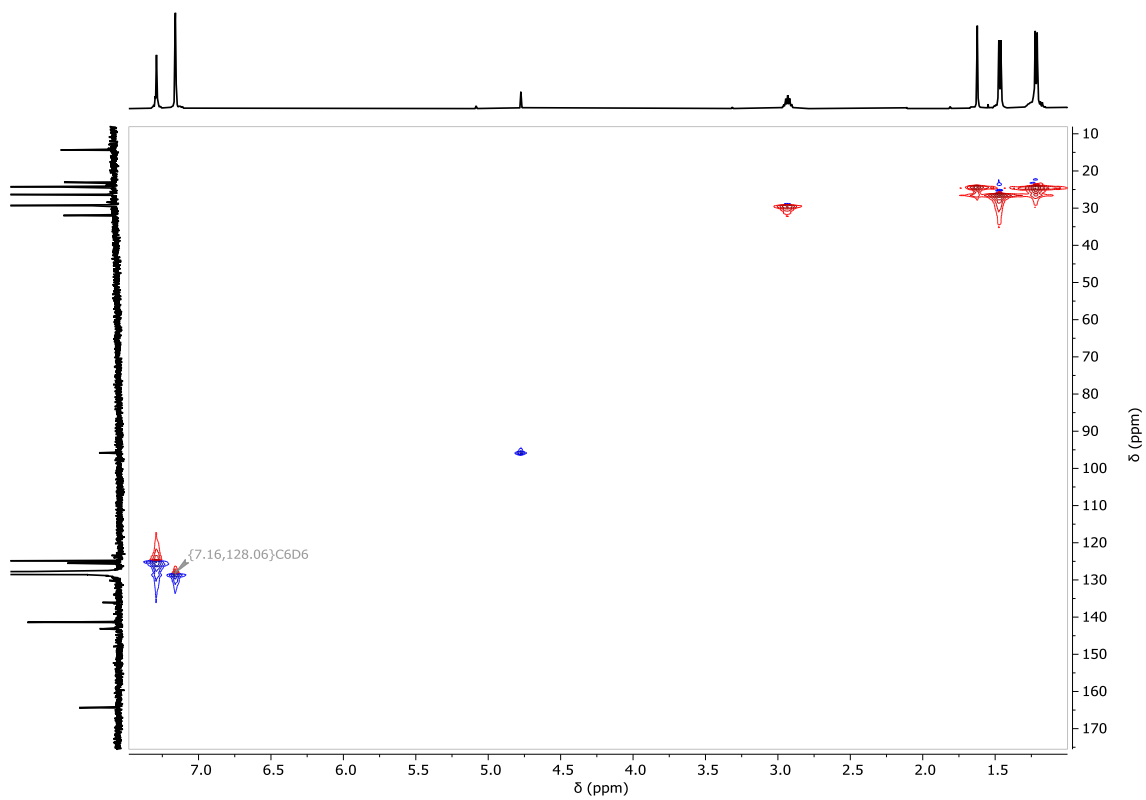
Supplementary Figure 2.48. ¹H NMR spectrum (500 MHz, C₆D₆) of [{(BDI^{Dipp})Yb}₃P₇] (2.15).



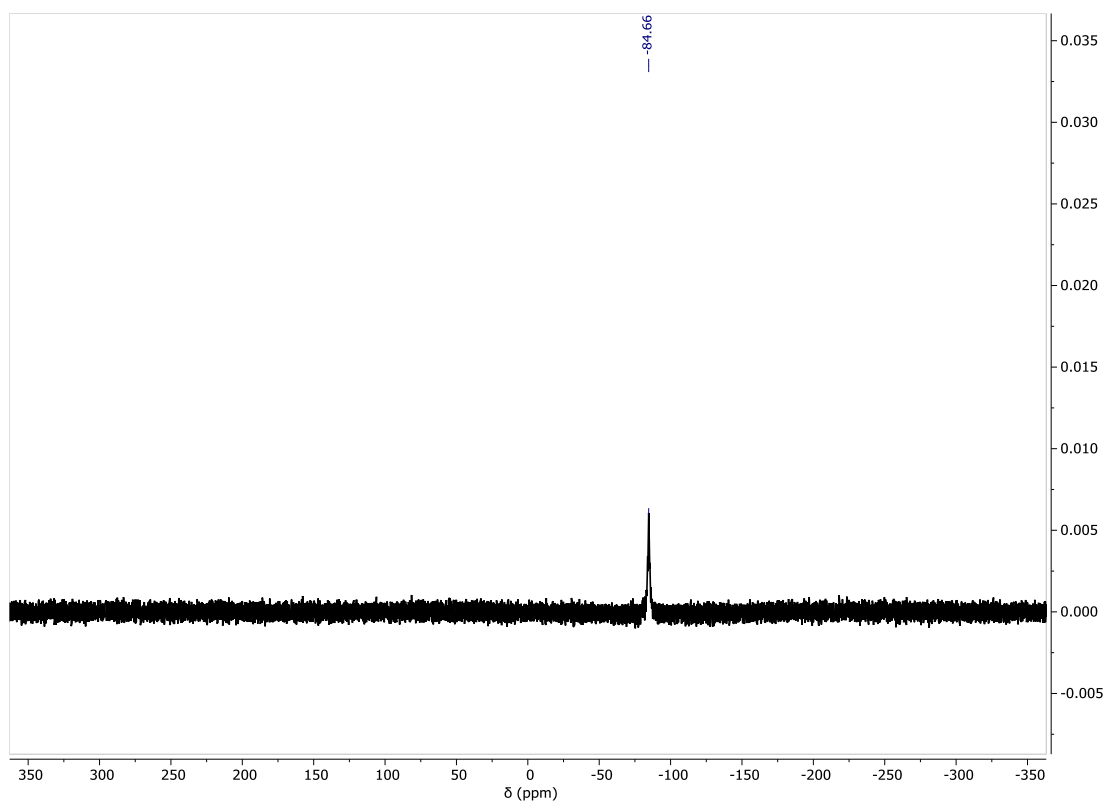
Supplementary Figure 2. 49. ¹³C{¹H} NMR spectrum (126 MHz, C₆D₆) of [{(BDI^{Dipp})Yb}₃P₇] (2.15).



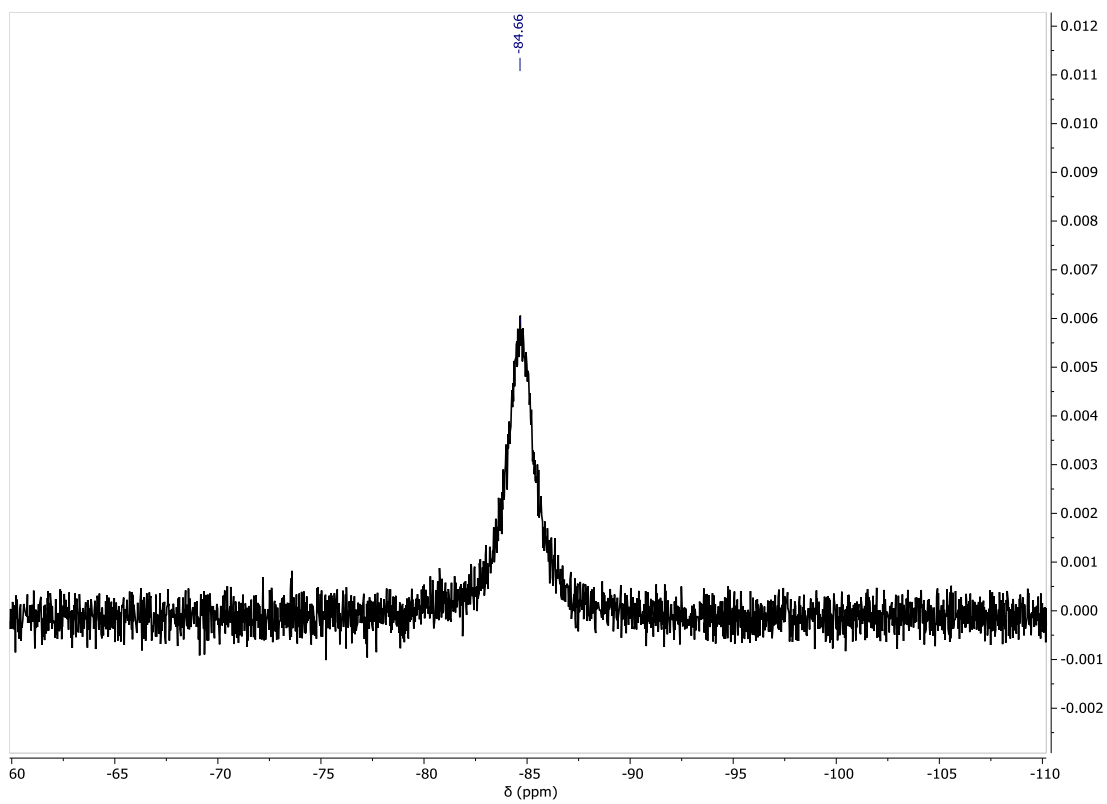
Supplementary Figure 2.50. ^1H - ^1H COSY NMR spectrum (500 MHz, C_6D_6) of $[\{(\text{BDI}^{\text{Dipp}})\text{Yb}\}_3\text{P}_7]$ (**2.15**).



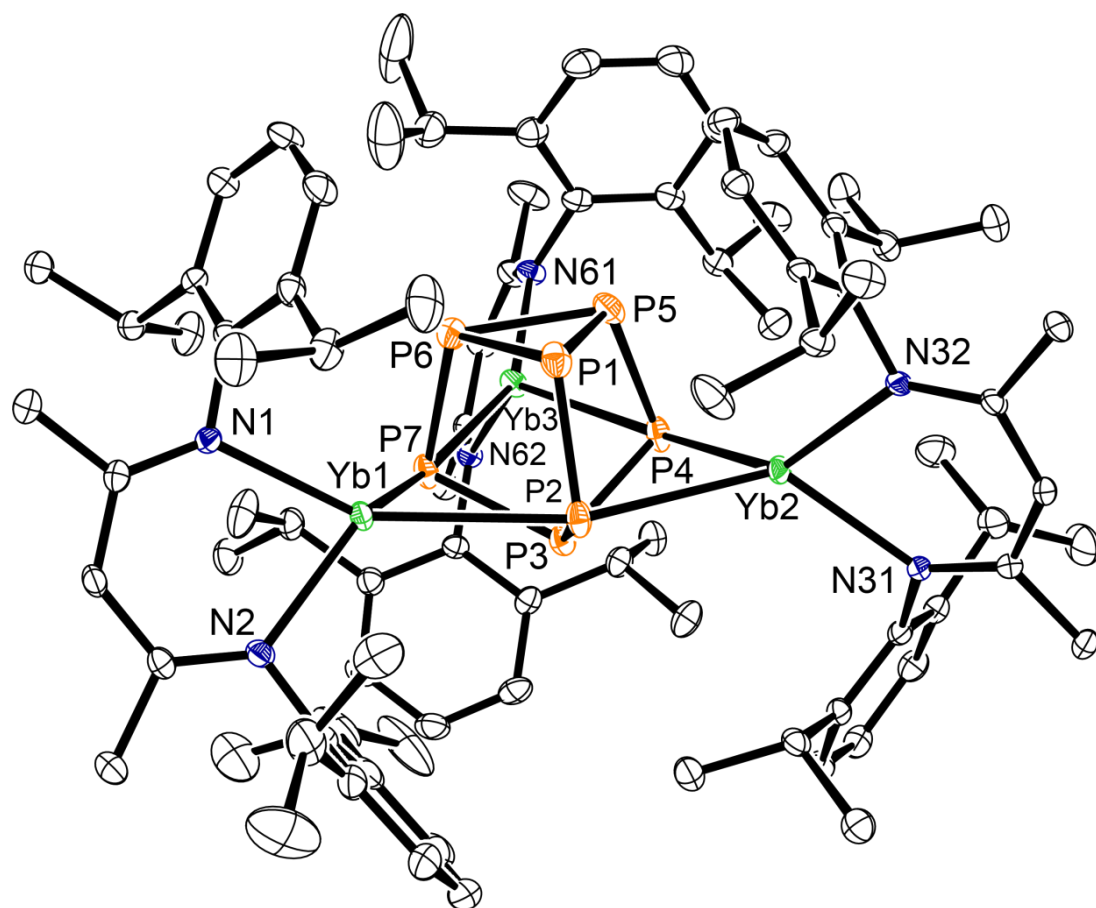
Supplementary Figure 2.51. ^1H - ^{13}C HSQC NMR spectrum (500 MHz, C_6D_6) of $[\{(\text{BDI}^{\text{Dipp}})\text{Yb}\}_3\text{P}_7]$ (**2.15**).



Supplementary Figure 2.52. ^{31}P NMR spectrum (202 MHz, C_6D_6) of $[(\text{BDI}^{\text{Dipp}})\text{Yb}]_3\text{P}_7$ (**2.15**).



Supplementary Figure 2.53. Close up of the single phosphorus environment in the ^{31}P NMR spectrum (202 MHz, C_6D_6) of $[(\text{BDI}^{\text{Dipp}})\text{Yb}]_3\text{P}_7$ (**2.15**).



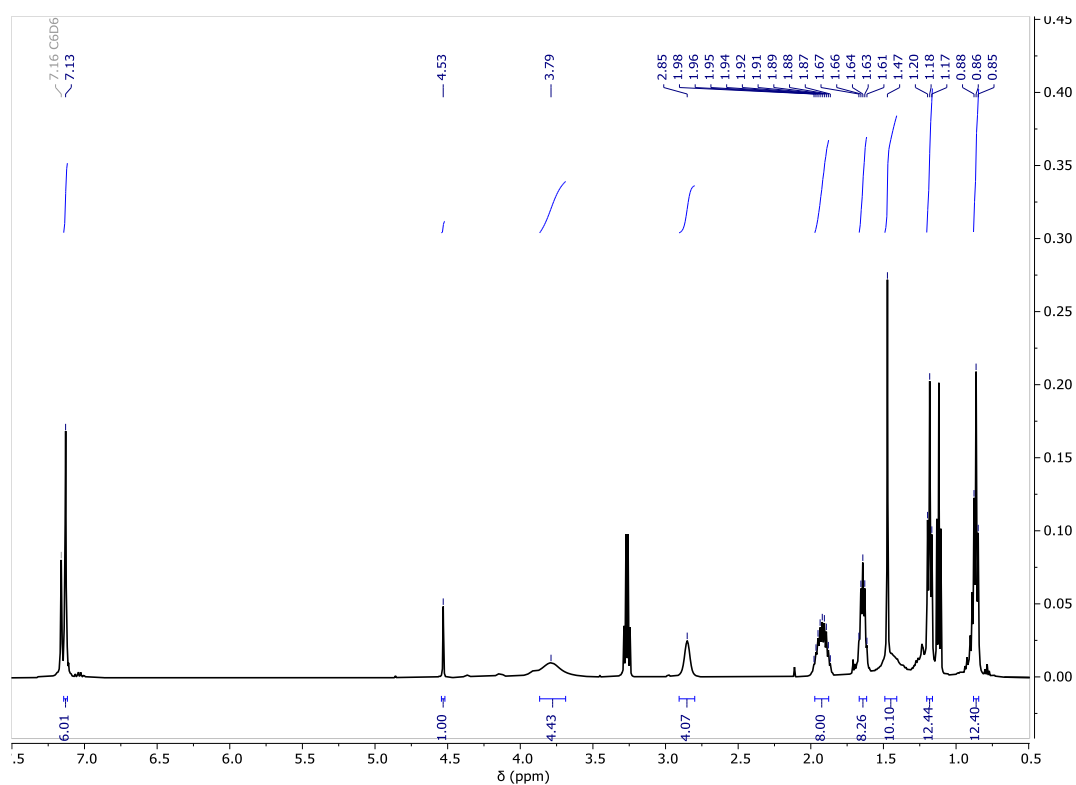
Supplementary Figure 2.54. Ortep representation (30% probability ellipsoids) of $[(\text{BDI}^{\text{Dipp}}\text{Yb})_3\text{P}_7]$ (**2.15**). Hydrogen atoms have been omitted for clarity.

[(BDI^{Dipep})Yb(THF)P₄Yb(THF)(BDI^{Dipep})] (2.16)

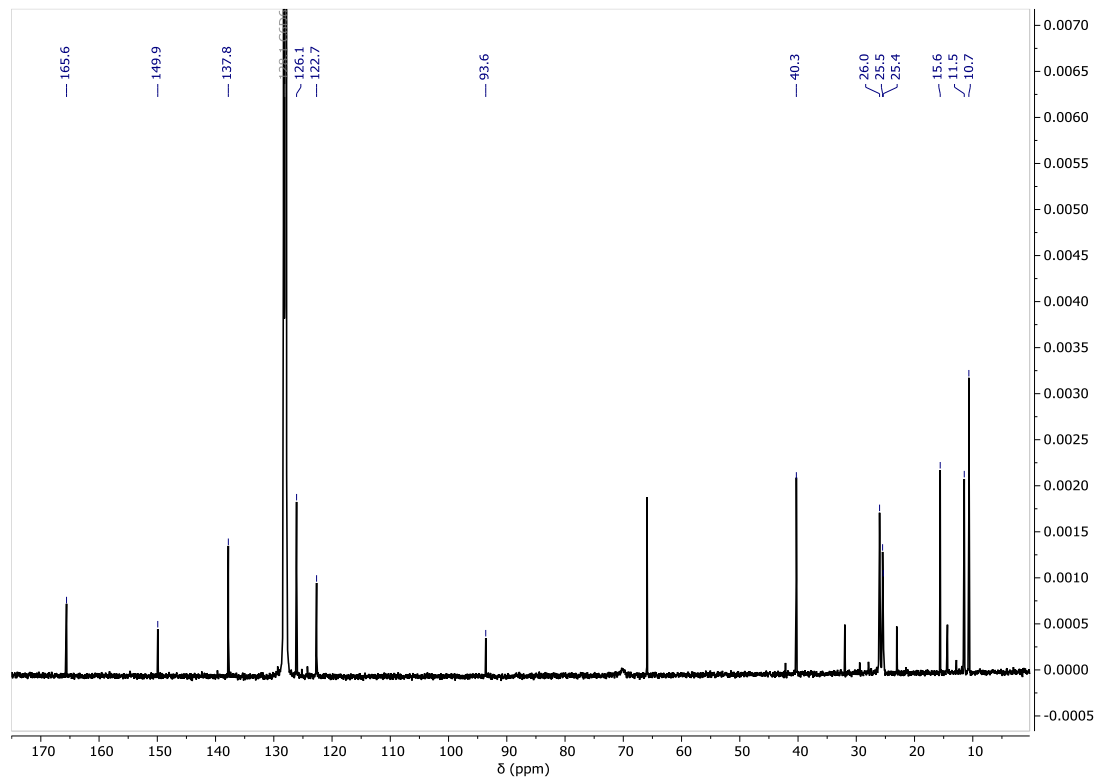
Addition of P₄ (6 mg, 0.05 mmol) to a J. Youngs tap NMR tube containing a brown C₆D₆ solution of [(BDI^{Dipep})YbH(THF)]₂ (78 mg, 0.05 mmol) resulted in a bright red solution. Complete consumption of the starting materials was achieved overnight at room temperature. The solvent was removed *in vacuo* and the crude product redissolved into hexane. The mixture was filtered, concentrated, and crystallised at room temperature to give red blocks suitable for X-ray diffraction analysis (Isolated yield: 20 mg, 47%).

¹H NMR (500 MHz, C₆D₆) δ 7.13 (s, 6H, ArH), 4.53 (s, 1H, NC(CH₃)CH), 3.79 (br, 4H, THF), 2.85 (br, 4H, CH(CH₂CH₃)₂), 1.92 (m, 8H, CH(CH₂CH₃)₂), 1.64 (m, 8H, CH(CH₂CH₃)₂), 1.47 (s, 10H, NC(CH₃)CH overlapping THF), 1.18 (t, *J* = 7.2 Hz, 12H, CH(CH₂CH₃)₂), 0.86 (t, *J* = 7.2 Hz, 12H, CH(CH₂CH₃)₂).

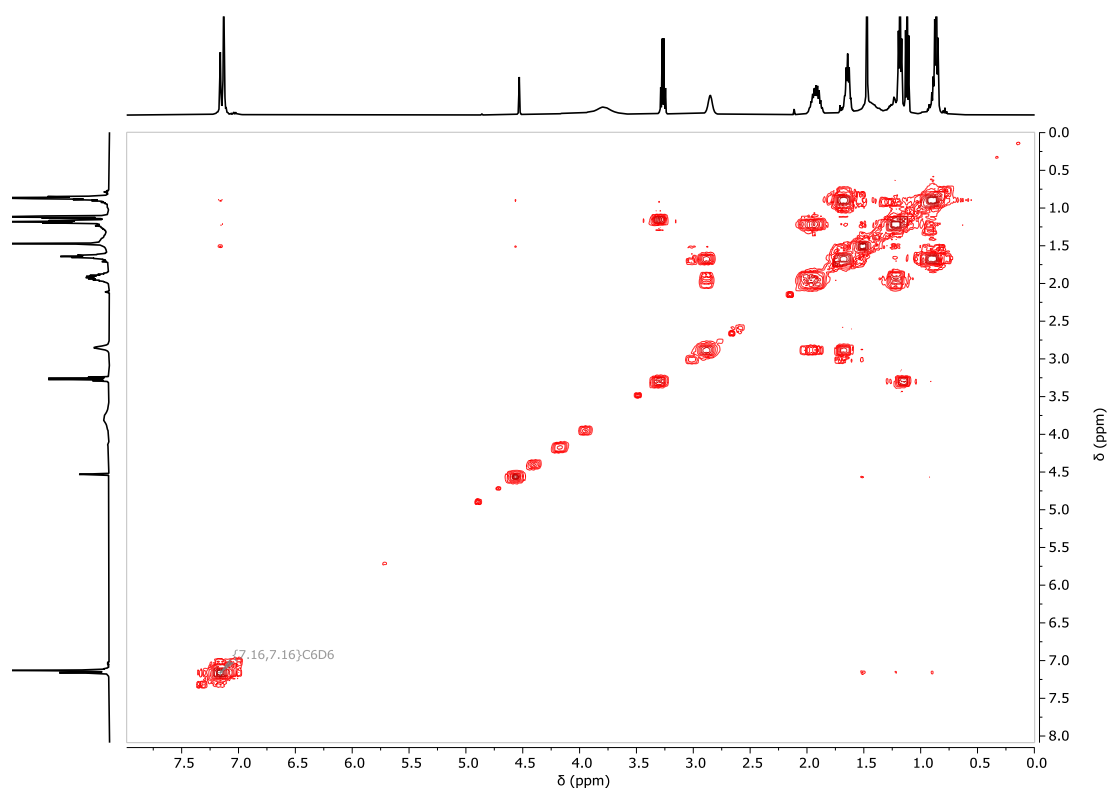
¹³C{¹H} NMR (126 MHz, C₆D₆) δ 165.6 (NC(CH₃)CH), 149.9 (C_{ipso}), 137.8 (C_{ortho}), 126.1 (C_{para}), 122.7 (C_{meta}), 93.6 (NC(CH₃)CH), 40.3 (CH(CH₂CH₃)₂), 26.0, 25.5 (CH(CH₂CH₃)₂), 25.4 NC(CH₃)CH, 11.5, 10.7 (CH(CH₂CH₃)₂).



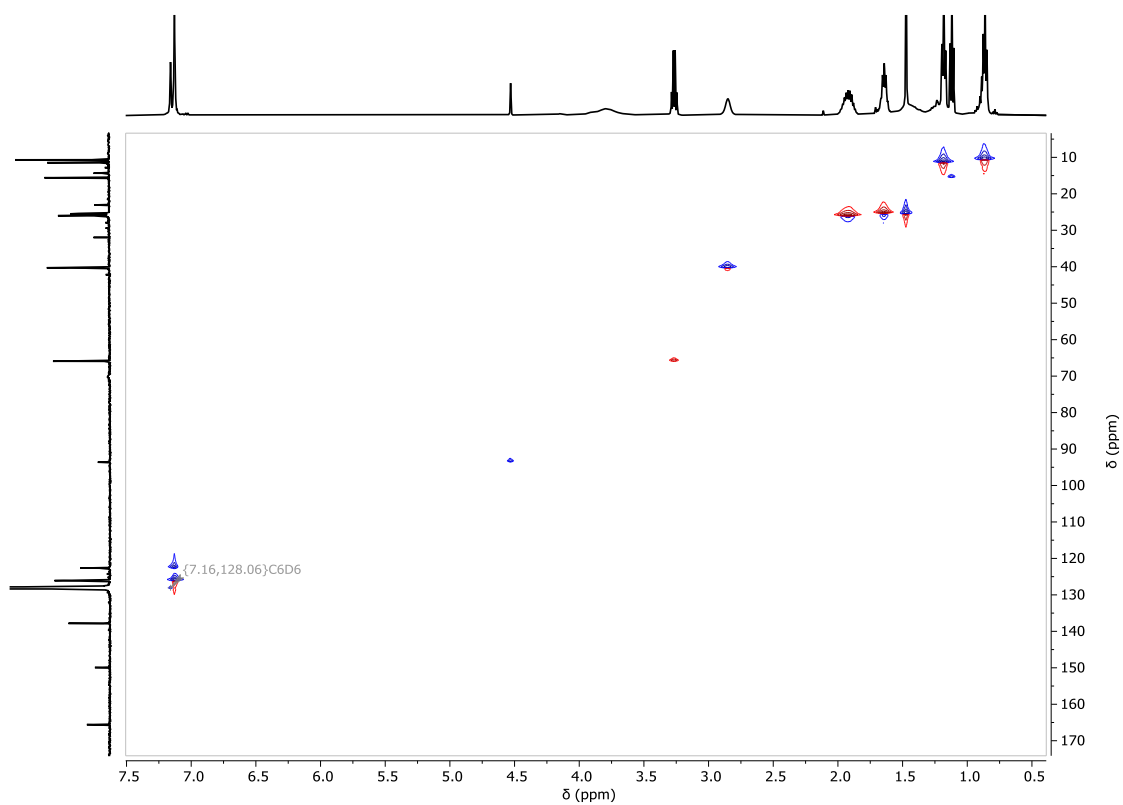
Supplementary Figure 2.55. ¹H NMR spectrum (500 MHz, C₆D₆) [(BDI^{Dipep})Yb(THF)P₄Yb(THF)(BDI^{Dipep})] (**2.16**).



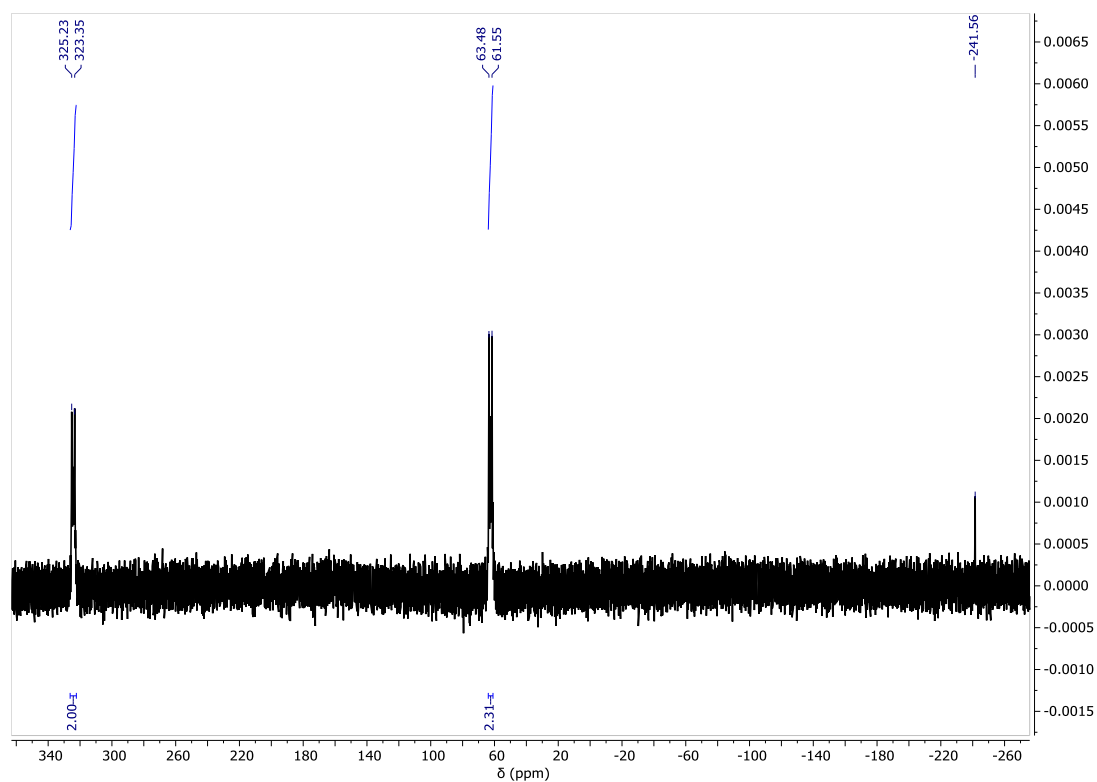
Supplementary Figure 2.56. ¹³C{¹H} NMR spectrum (126 MHz, C₆D₆) of [(BDI^{Dipep})Yb(THF)P₄Yb(THF)(BDI^{Dipep})] (**2.16**).



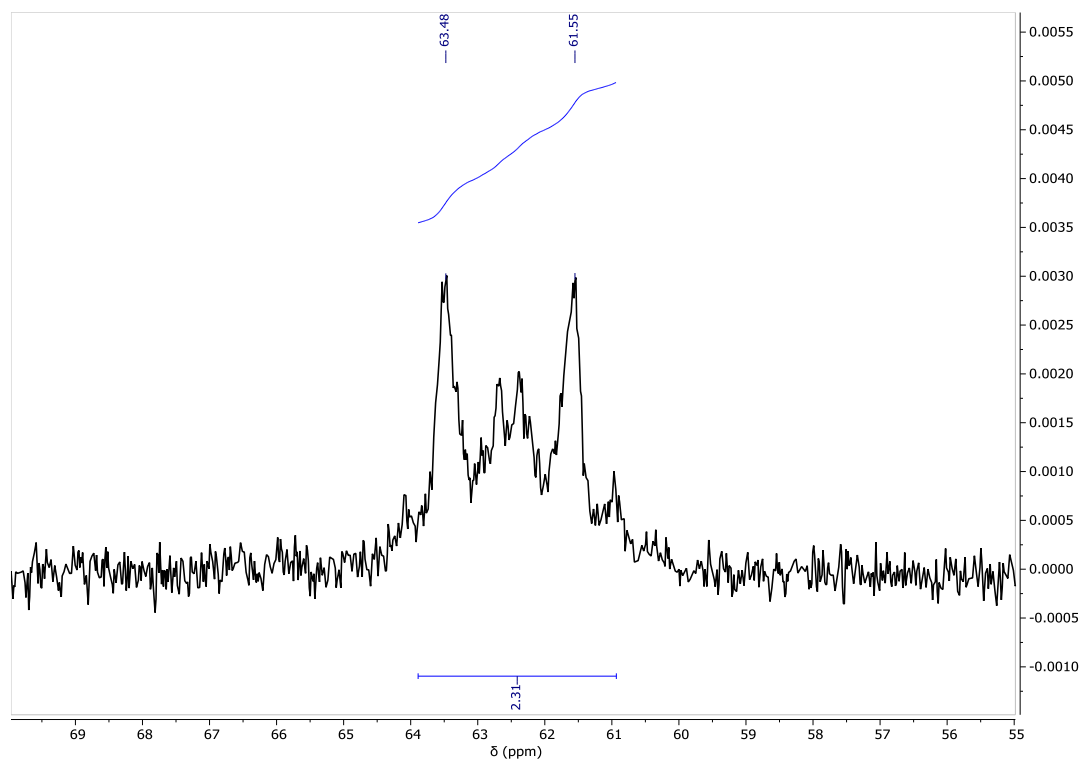
Supplementary Figure 2.57. ^1H – ^1H COSY NMR spectrum (500 MHz, C_6D_6) of $[(\text{BDI}^{\text{Dipep}})\text{Yb}(\text{THF})\text{P}_4\text{Yb}(\text{THF})(\text{BDI}^{\text{Dipep}})]$ (**2.16**).



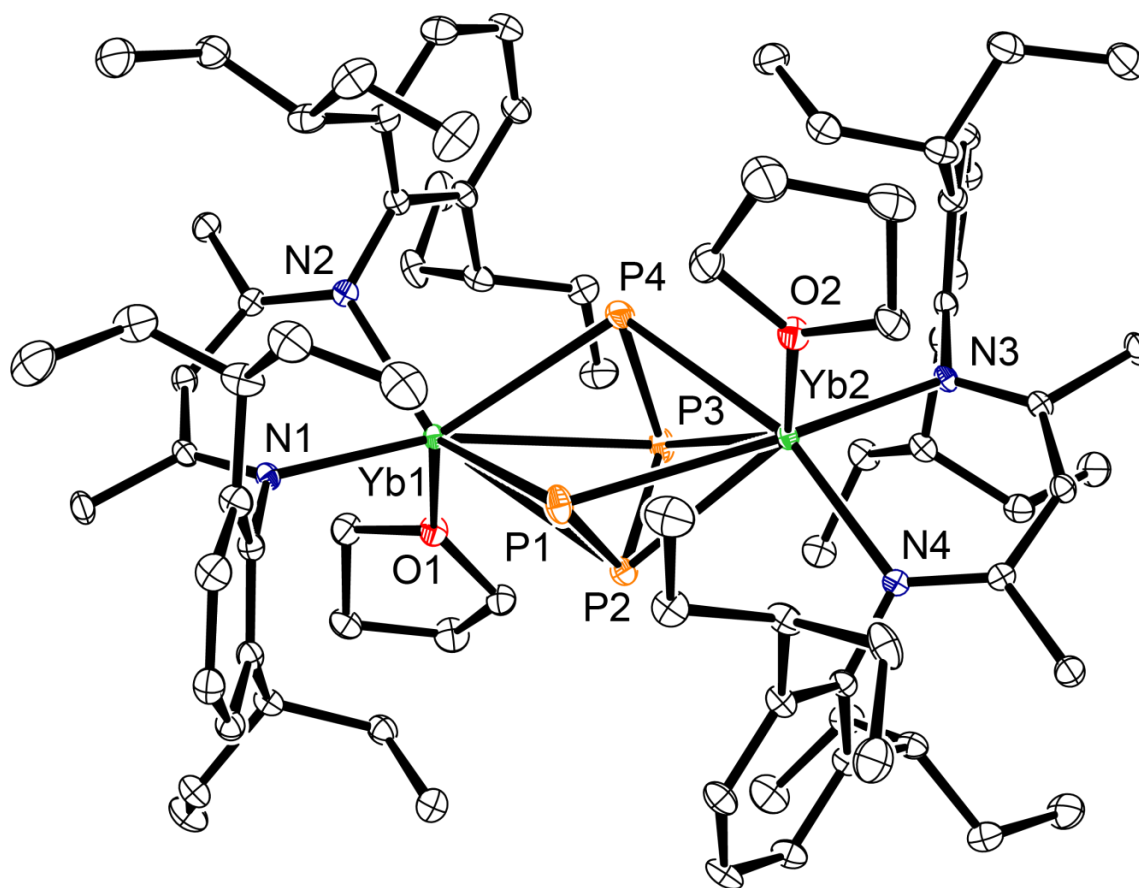
Supplementary Figure 2.58. ^1H – ^{13}C HSQC NMR spectrum (500 MHz, C_6D_6) of $[(\text{BDI}^{\text{Dipep}})\text{Yb}(\text{THF})\text{P}_4\text{Yb}(\text{THF})(\text{BDI}^{\text{Dipep}})]$ (**2.16**).



Supplementary Figure 2.59. ^{31}P NMR spectrum (202 MHz, C_6D_6) displaying the two phosphorus environments of $[(\text{BDI}^{\text{Dipep}})\text{Yb}(\text{THF})\text{P}_4\text{Yb}(\text{THF})(\text{BDI}^{\text{Dipep}})]$ (**2.16**) and the minor product peak at $\delta_{\text{P}} = -241$ ppm.



Supplementary Figure 2.60. Close up of the ^{31}P NMR spectrum (202 MHz, C_6D_6) of $[(\text{BDI}^{\text{Dipep}})\text{Yb}(\text{THF})\text{P}_4\text{Yb}(\text{THF})(\text{BDI}^{\text{Dipep}})]$ (**2.16**), showing the potential AA'XX' spin system.

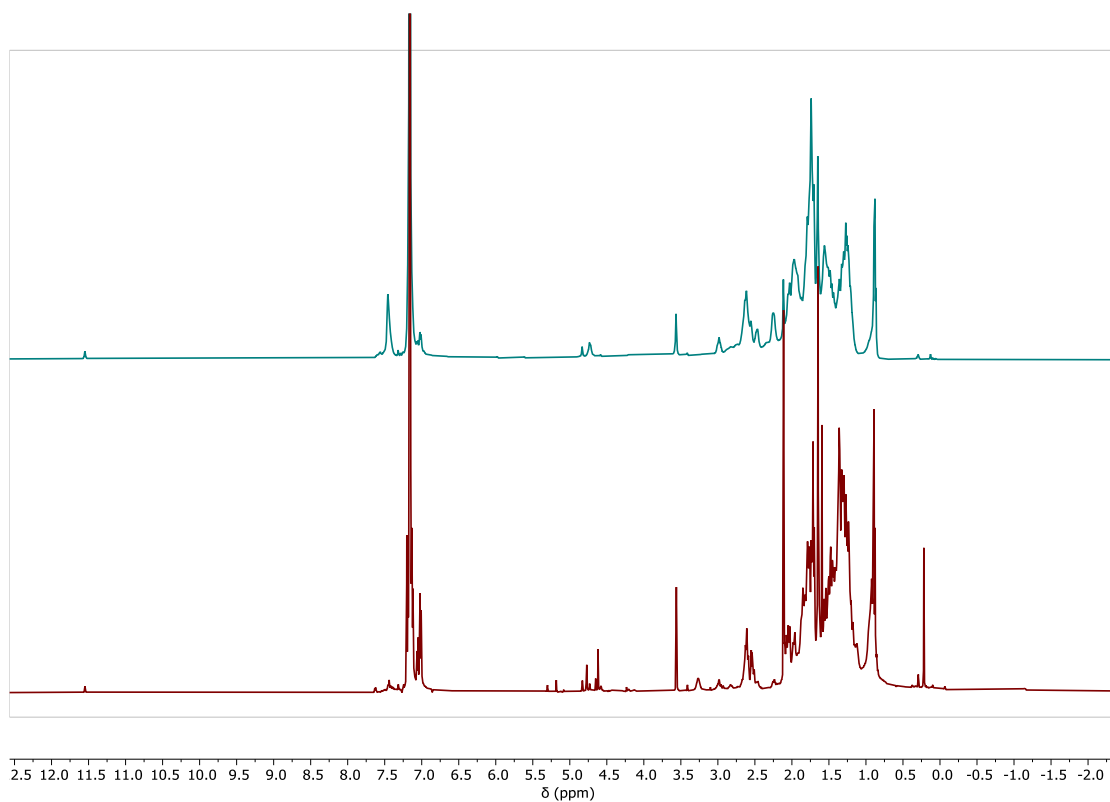


Supplementary Figure 2.61. Ortep representation (30% probability ellipsoids) of $[(\text{BDI}^{\text{Dipep}})\text{Yb}(\text{THF})\text{P}_4\text{Yb}(\text{THF})(\text{BDI}^{\text{Dipep}})]$ (**2.16**). Hydrogen atoms have been omitted for clarity.

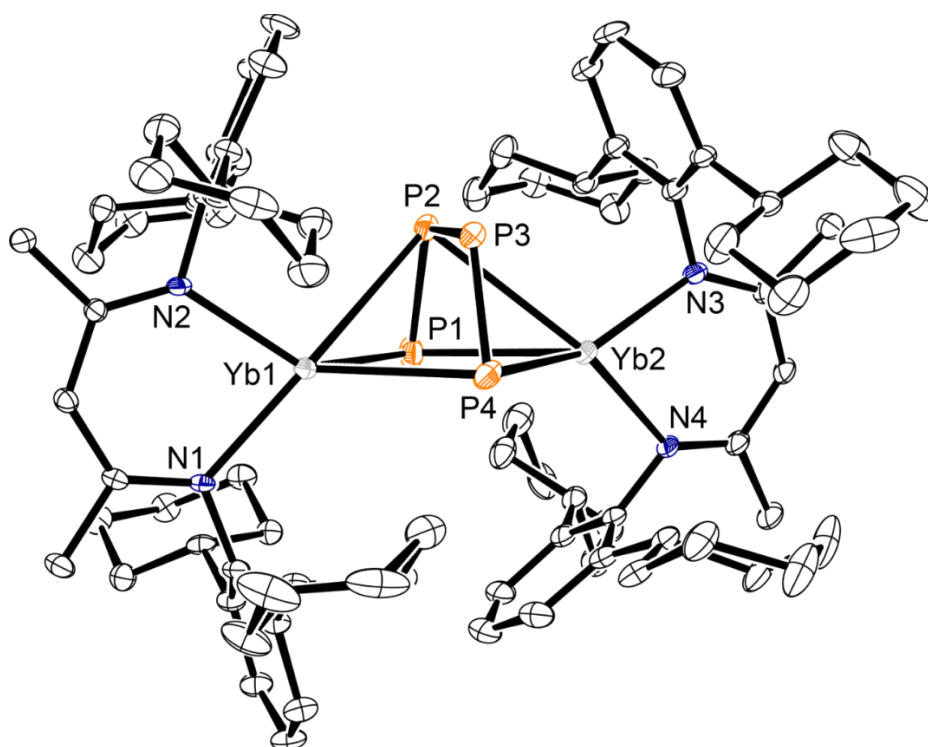
$[(\text{BDI}^{\text{DicyP}})\text{Yb}(\text{P}_4)\text{Yb}(\text{BDI}^{\text{DicyP}})]$ (2.17)

Addition of P_4 (9 mg, 0.08 mmol) to a scintillation vial containing a suspension of $[(\text{BDI}^{\text{DicyP}})\text{YbH}(\text{THF})]_2$ (116 mg, 0.08 mmol) in toluene resulted in a dark red solution and dark precipitate after ca. 2h at room temperature. The solvent was filtered through Celite, concentrated, and crystallised at room temperature to give red blocks suitable for X-ray diffraction analysis (Isolated yield: 25 mg, 39%).

The poor solubility of $[(\text{BDI}^{\text{DicyP}})\text{Yb}(\text{P}_4)\text{Yb}(\text{BDI}^{\text{DicyP}})]$ in aliphatic and aromatic solvents hampered characterisation by multinuclear NMR spectroscopic techniques.



Supplementary Figure 2.62. Stacked ^1H NMR spectrum (500 MHz, C_6D_6) of the crude reaction product of $[(\text{BDI}^{\text{Dicyclopentadienyl}})\text{Yb}(\text{P}_4)\text{Yb}(\text{BDI}^{\text{Dicyclopentadienyl}})]$ (**2.17**) (bottom) and $[(\text{BDI}^{\text{Dicyclopentadienyl}})\text{Yb}(\text{P}_4)\text{Yb}(\text{BDI}^{\text{Dicyclopentadienyl}})]$ (**2.17**) after attempted purification (top).



Supplementary Figure 2.63. Ortep representation (30% probability ellipsoids) of $[(\text{BDI}^{\text{Dicyclopentadienyl}})\text{Yb}(\text{P}_4)\text{Yb}(\text{BDI}^{\text{Dicyclopentadienyl}})]$ (**2.17**). Hydrogen atoms have been omitted for clarity.

[(BDI^{Dipp})Yb(μ -COT)Yb(BDI^{Dipp})] (2.18)

A pale yellow toluene solution of 1,3,5,7-cyclooctatetraene (9 mg, 0.09 mmol) was added to a scintillation vial containing a black toluene solution of [(BDI^{Dipp})YbH]₂ (100 mg, 0.09 mmol). The mixture was left to stir at room temperature for 16h to give a deep red solution. The solvent removed in vacuo to give the crude product as a thick red-purple oily residue. Deep red-purple crystals suitable for X-ray diffraction analysis were obtained from a saturated hexane solution at -30 °C.

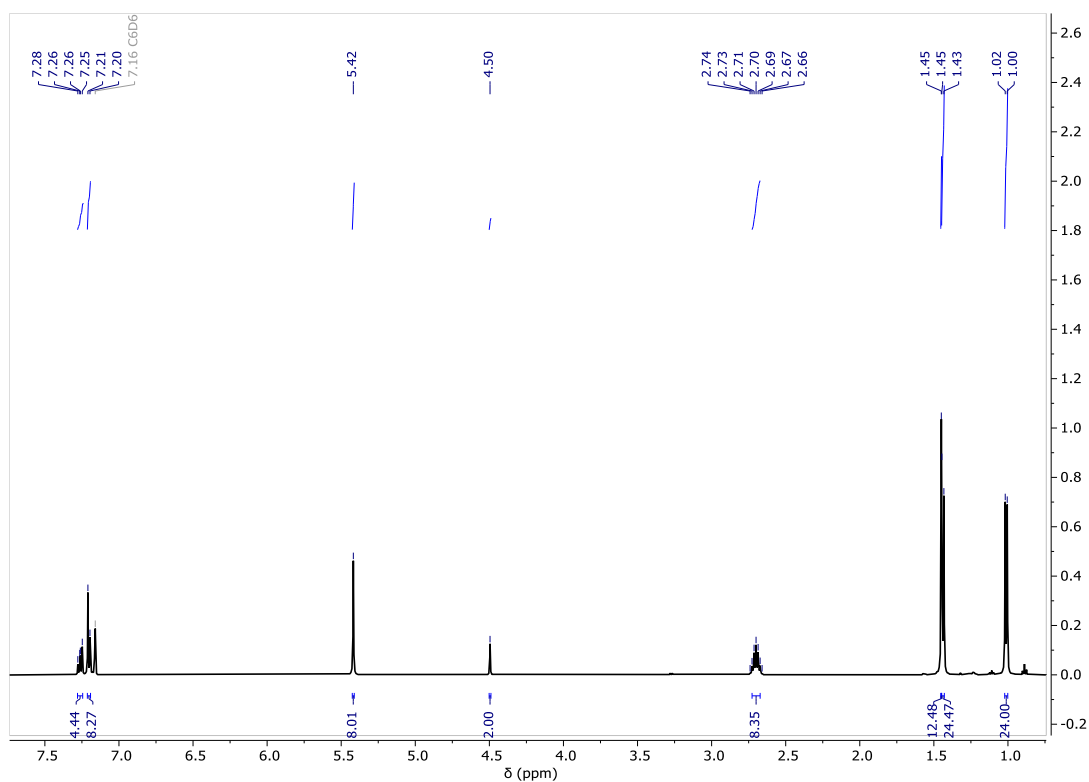
¹H NMR (500 MHz, C₆D₆) δ 7.26 (m, 2H, ArH), 7.21 (m, 4H, ArH), 5.42 (s, 4H, C₈H₈), 4.50 (s, 1H, NC(CH₃)CH), 2.70 (sept, J = 6.8 Hz, 4H, CH(CH₃)₂), 1.45 (s, 6H, NC(CH₃)CH), 1.44 (d, J = 6.8 Hz, 12H, CH(CH₃)₂), 1.01 (d, J = 6.8 Hz, 12H, CH(CH₃)₂).

¹³C{¹H} NMR (126 MHz, C₆D₆) δ 164.02 (NC(CH₃)CH), 146.30 (C_{ipso}), 141.89 (C_{ortho}), 124.54 (C_{para}), 123.70 (C_{meta}), 94.74 (NC(CH₃)CH), 90.82 (C₈H₈), 28.84 (CH(CH₃)₂), 24.57, 24.45 (CH(CH₃)₂), 24.23 (NC(CH₃)CH).

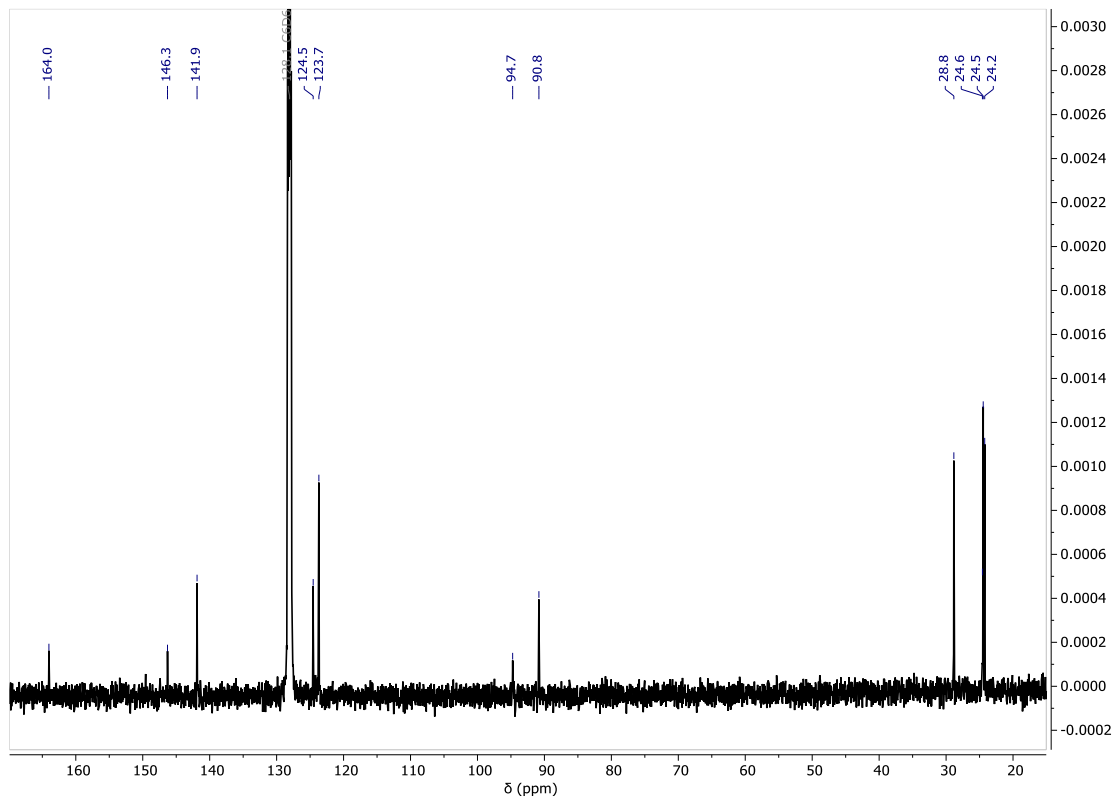
Elemental Analysis for [(BDI^{Dipp})Yb(μ -COT)Yb(BDI^{Dipp})] (1286.59 g mol⁻¹):

Calculated: C, 61.66; H, 7.06; N, 4.36 %.

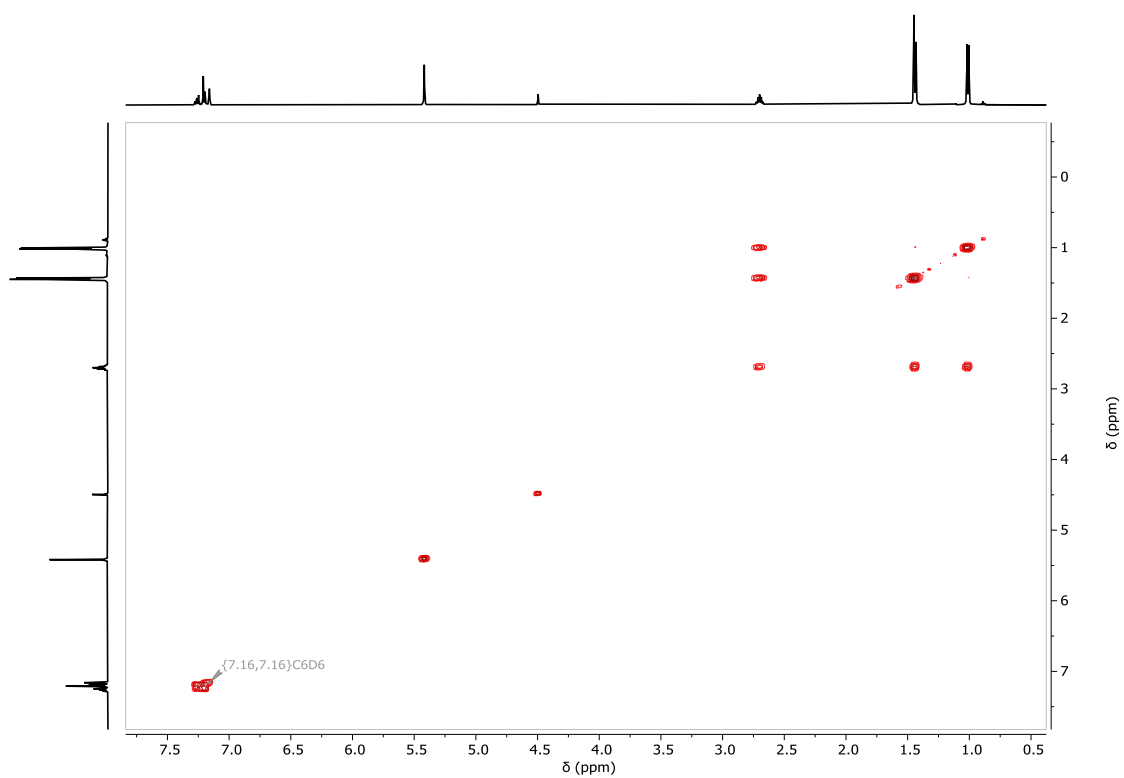
Found: C, 61.26; H, 7.06; N, 4.41 %



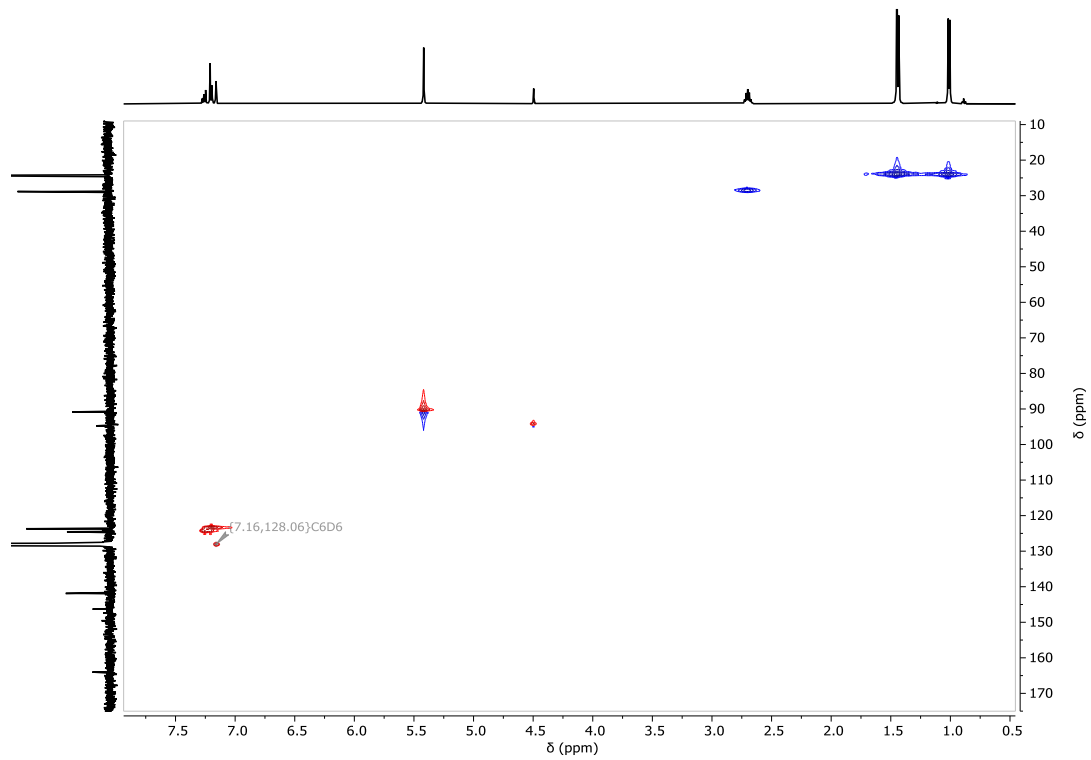
Supplementary Figure 2.64. ¹H NMR spectrum (500 MHz, C₆D₆) of [(BDI^{Dipp})Yb(μ-COT)Yb(BDI^{Dipp})] (2.18).



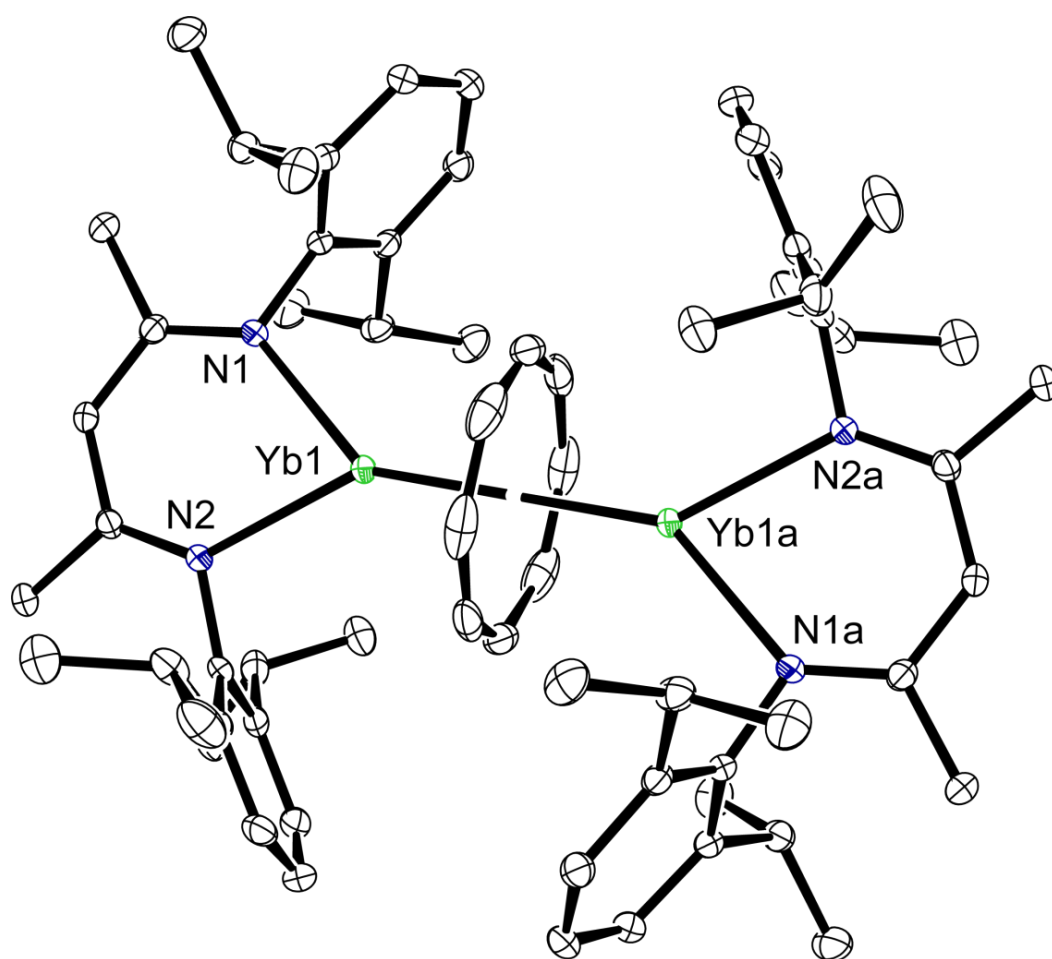
Supplementary Figure 2.65. ¹³C{¹H} NMR spectrum (126 MHz, C₆D₆) of [(BDI^{Dipp})Yb(μ-COT)Yb(BDI^{Dipp})] (2.18).



Supplementary Figure 2.66. ^1H - ^1H COSY NMR spectrum (500 MHz, C_6D_6) of $[(\text{BDI}^{\text{Dipp}})\text{Yb}(\mu\text{-COT})\text{Yb}(\text{BDI}^{\text{Dipp}})]$ (**2.18**).



Supplementary Figure 2.67. ^1H - ^{13}C HSQC NMR spectrum (500 MHz, C_6D_6) of $[(\text{BDI}^{\text{Dipp}})\text{Yb}(\mu\text{-COT})\text{Yb}(\text{BDI}^{\text{Dipp}})]$ (**2.18**).



Supplementary Figure 2.68. Ortep representation (30% probability ellipsoids) of $[(\text{BDI}^{\text{Dipp}})\text{Yb}(\mu\text{-COT})\text{Yb}(\text{BDI}^{\text{Dipp}})]$ (**2.18**). Hydrogen atoms have been omitted for clarity.

[(BDI^{Dipp})Yb(μ -COT)] (2.19)

Inside a glovebox a black toluene solution of [(BDI^{Dipp})YbH]₂ (71 mg, 0.06 mmol) was added dropwise to a scintillation vial containing a pale yellow toluene solution of 1,3,5,7-cyclooctatetraene (38 mg, 0.36 mmol) over half an hour. The mixture was stirred and left at room temperature for 16h to give a dark purple-red solution. The solvent was removed *in vacuo* to give the crude product as a thick purple-red paste. After fractional crystallisation, a small crop of deep purple crystals suitable for X-ray diffraction were obtained from a saturated hexane solution at -30 °C (Isolated yield: 10%).

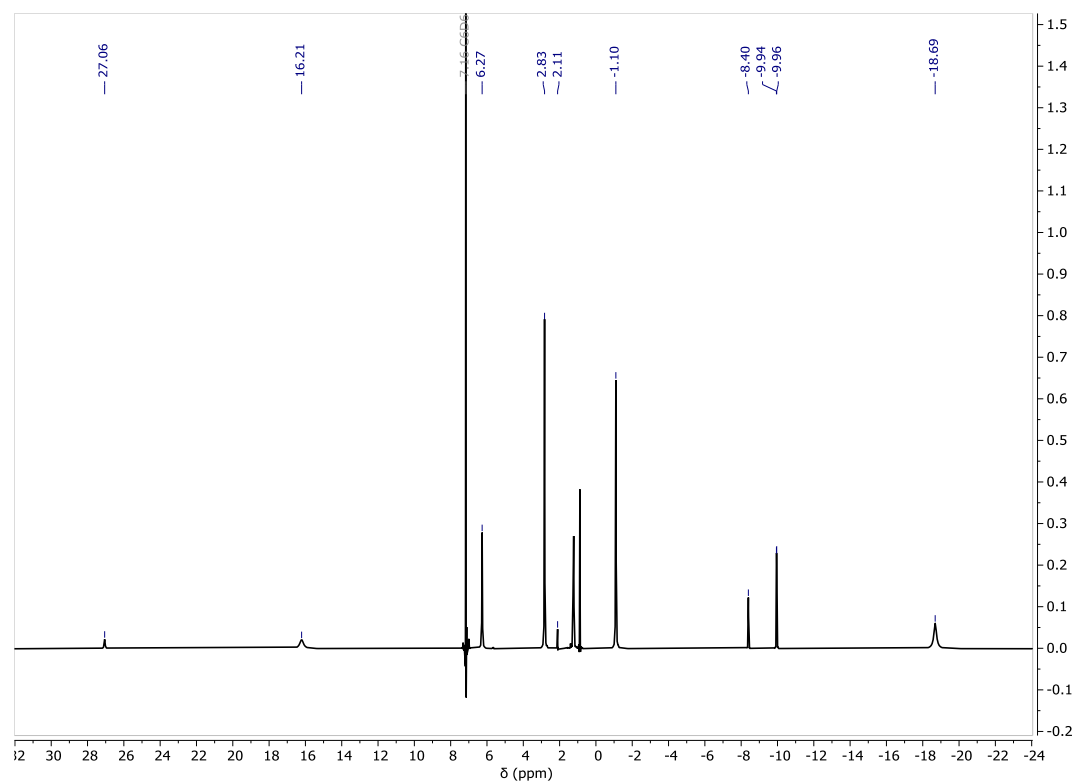
The paramagnetic nature of [(BDI^{Dipp})Yb(μ -COT)] hampered characterisation by multinuclear NMR spectroscopic techniques.

¹H NMR (500 MHz, C₆D₆) δ 27.06, 16.21, 6.27, 2.83, 2.11, -1.10, -8.40, -9.94, -9.96, -18.69.

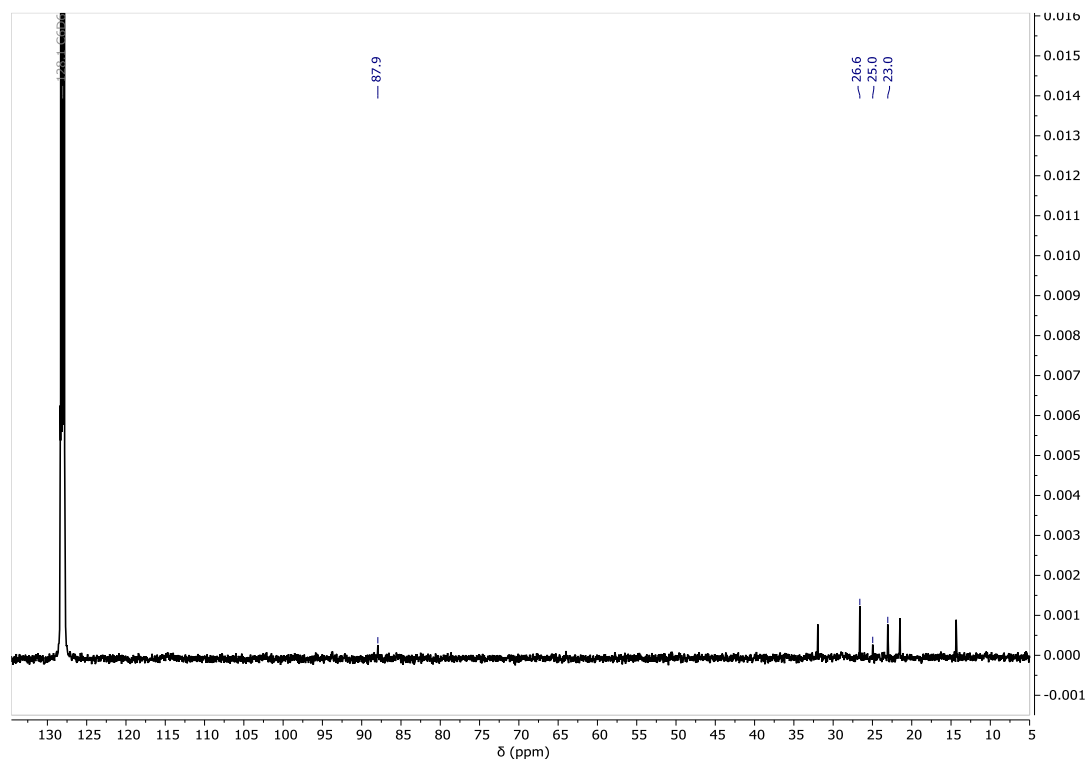
Elemental Analysis for [(BDI^{Dipp})Yb(μ -C₈H₈)] (695.33 g mol⁻¹):

Calculated: C, 63.96; H, 7.11; N, 4.03 %.

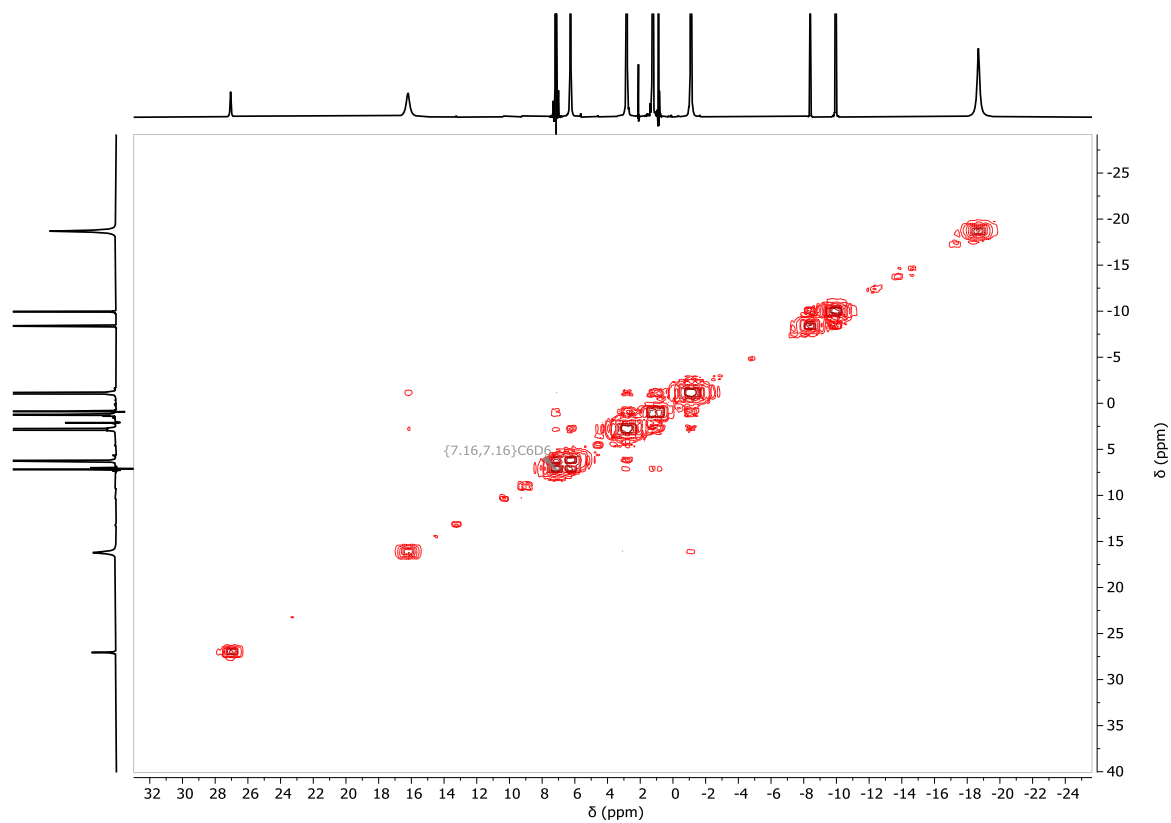
Found: C, 62.12; H, 7.28; N, 4.17 %



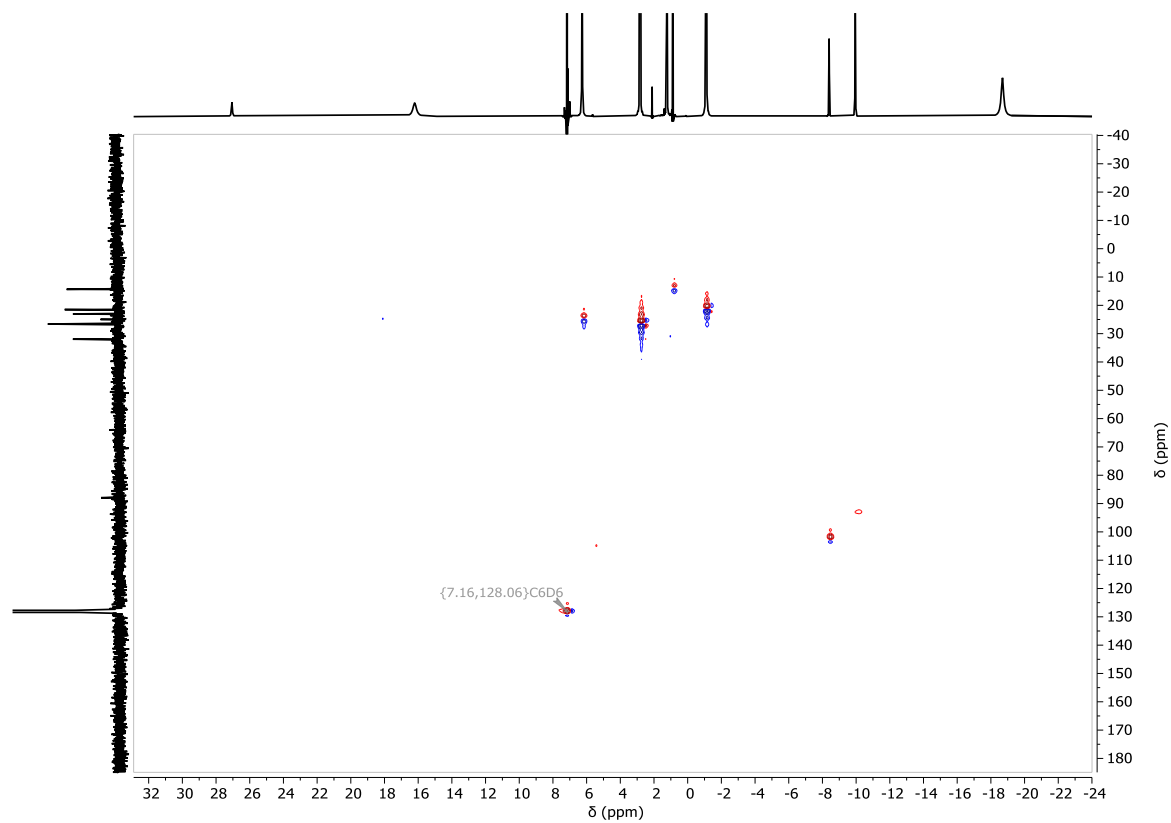
Supplementary Figure 2.69. ¹H NMR spectrum (500 MHz, C₆D₆) of [(BDI^{Dipp})Yb(μ-COT)] (2.19).



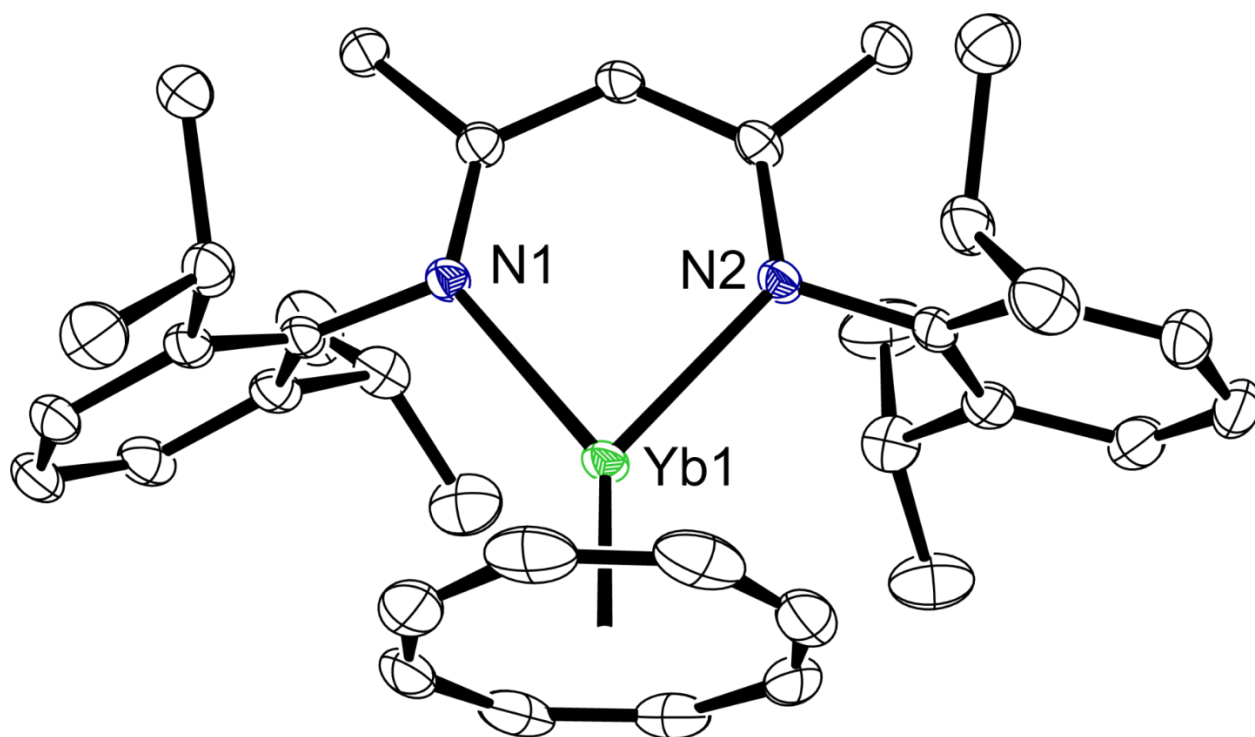
Supplementary Figure 2.70. ¹³C{¹H} NMR spectrum (126 MHz, C₆D₆) of [(BDI^{Dipp})Yb(μ-COT)] (2.19).



Supplementary Figure 2.71. ^1H - ^1H COSY NMR spectrum (500 MHz, C_6D_6) of $[(\text{BDI}^{\text{Dipp}})\text{Yb}(\mu\text{-COT})]$ (**2.19**).



Supplementary Figure 2.72. ^1H - ^{13}C HSQC NMR spectrum (500 MHz, C_6D_6) of $[(\text{BDI}^{\text{Dipp}})\text{Yb}(\mu\text{-COT})]$ (**2.19**).



Supplementary Figure 2.73. Ortep representation (30% probability ellipsoids) of $[(\text{BDI}^{\text{Dipp}})\text{Yb}(\mu\text{-COT})]$ (**2.19**). Hydrogen atoms have been omitted for clarity.

[(BDI^{Dipp})(Et₂O)Yb(μ-C₁₄H₁₀)Yb(OEt₂)(BDI^{Dipp})] (2.20)

A colourless toluene solution of anthracene (21 mg, 0.12 mmol) was added to a scintillation vial containing a black toluene solution of [(BDI^{Dipp})YbH]₂ (214 mg, 0.18 mmol) and left to stir for 48h at room temperature. The resultant deep blue solution was dried *in vacuo* and washed with hexane to give the crude product as a blue powder. Deep blue crystals suitable for X-ray diffraction analysis were obtained from a saturated diethyl ether solution at -30 °C.

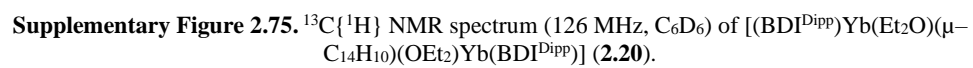
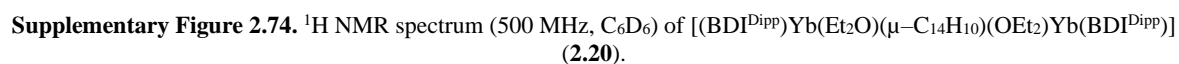
¹H NMR (500 MHz, C₆D₆, 333.15 K) δ 6.96 (m, 6H, ArH), 5.07 (s, 1H, NC(CH₃)CH), 4.14 (m, 2H, C₁₄H₁₀), 3.68 (br, 4H, Et₂O), 3.26 (sept, *J* = 6.8 Hz, 4H, CH(CH₃)₂), 2.78 (m, 2H, C₁₄H₁₀), 2.01 (s, 1H, C₁₄H₁₀), 1.82 (s, 6H, NC(CH₃)CH), 1.29 (d, *J* = 6.9 Hz, 12H, CH(CH₃)₂), 1.24 (d, *J* = 6.9 Hz, 12H, CH(CH₃)₂), 1.19 (t, *J* = 6.7 Hz, 4H, Et₂O).

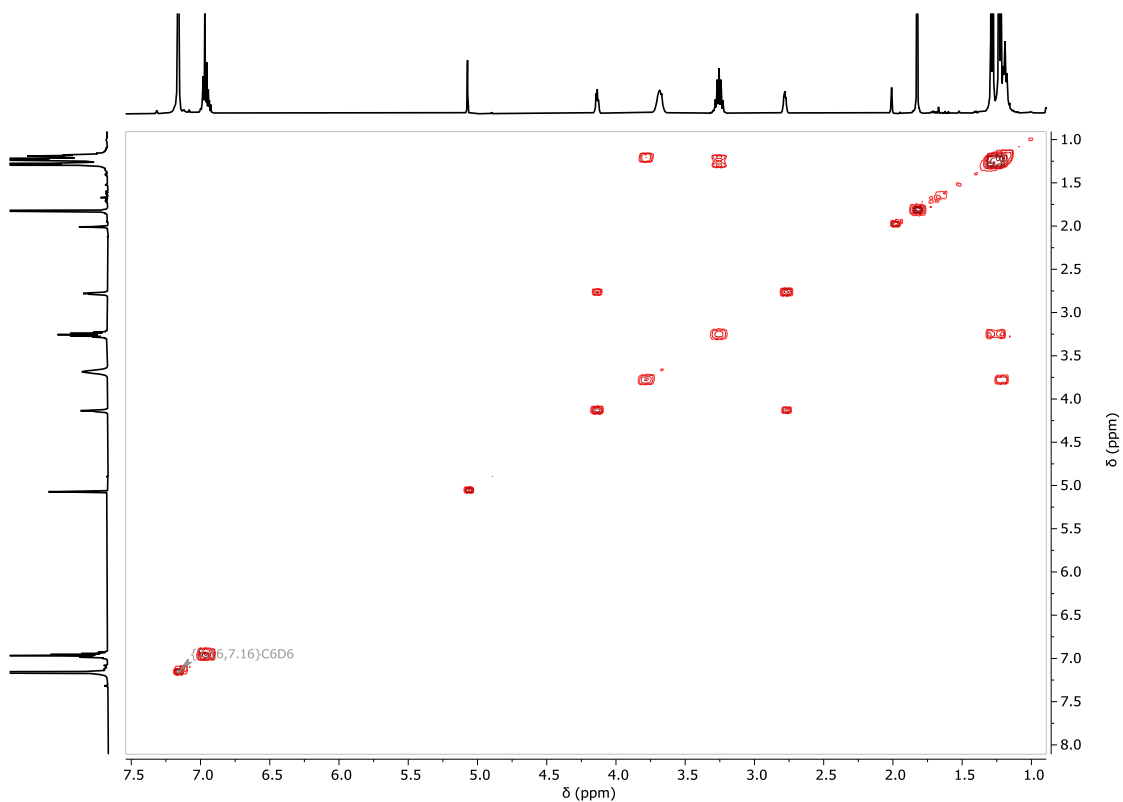
¹³C{¹H} NMR (126 MHz, C₆D₆, 333.15 K) δ 165.2 (NC(CH₃)CH), 145.8 (C_{ipso}), 143.6 (C₁₄H₁₀), 141.5 (C_{ortho}), 124.5 (C_{para}), 124.0 (C_{meta}), 117.2 (C₁₄H₁₀), 101.9 (C₁₄H₁₀), 95.2 (NC(CH₃)CH), 65.6 (Et₂O), 29.0 (CH(CH₃)₂), 24.7, 24.5 (CH(CH₃)₂), 24.4 (NC(CH₃)CH), 15.0 (Et₂O).

Elemental Analysis for [(BDI^{Dipp})Yb(Et₂O)(μ-C₁₄H₁₀)(OEt₂)Yb(BDI^{Dipp})] (1508.76 g mol⁻¹):

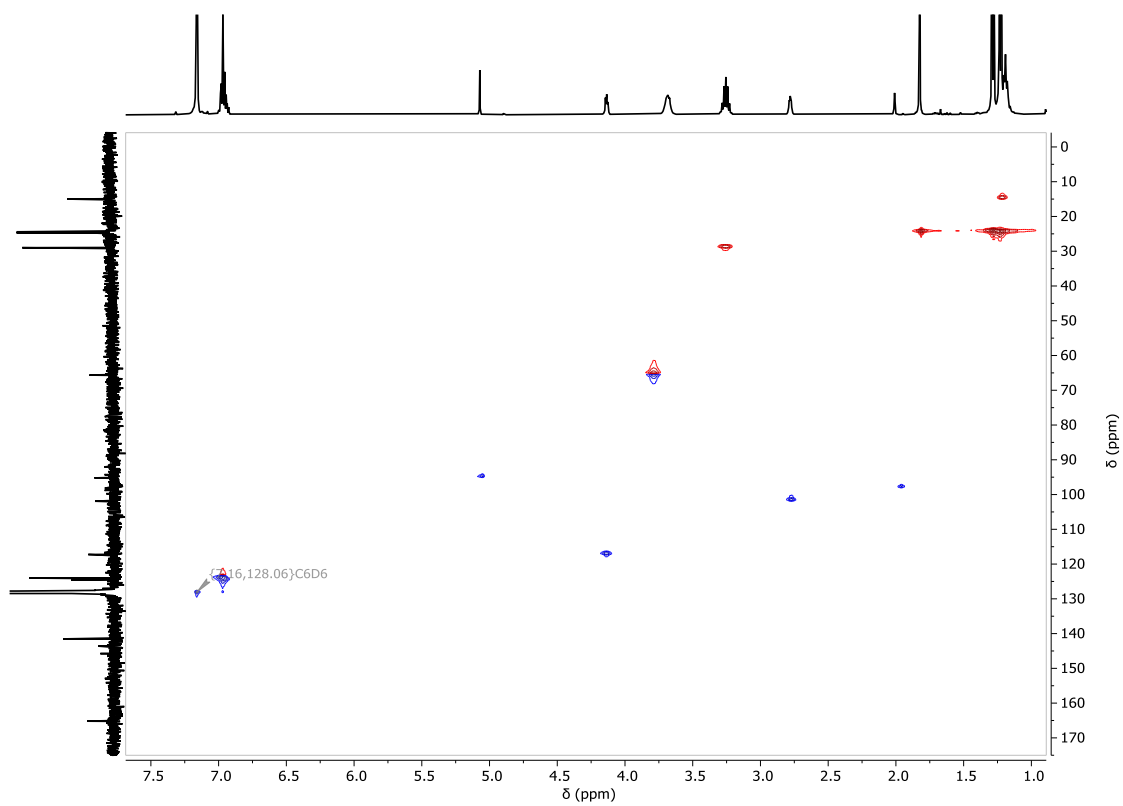
Calculated: C, 63.72; H, 7.49; N, 3.72 %.

Found: C, 62.70; H, 7.24; N, 3.88 %

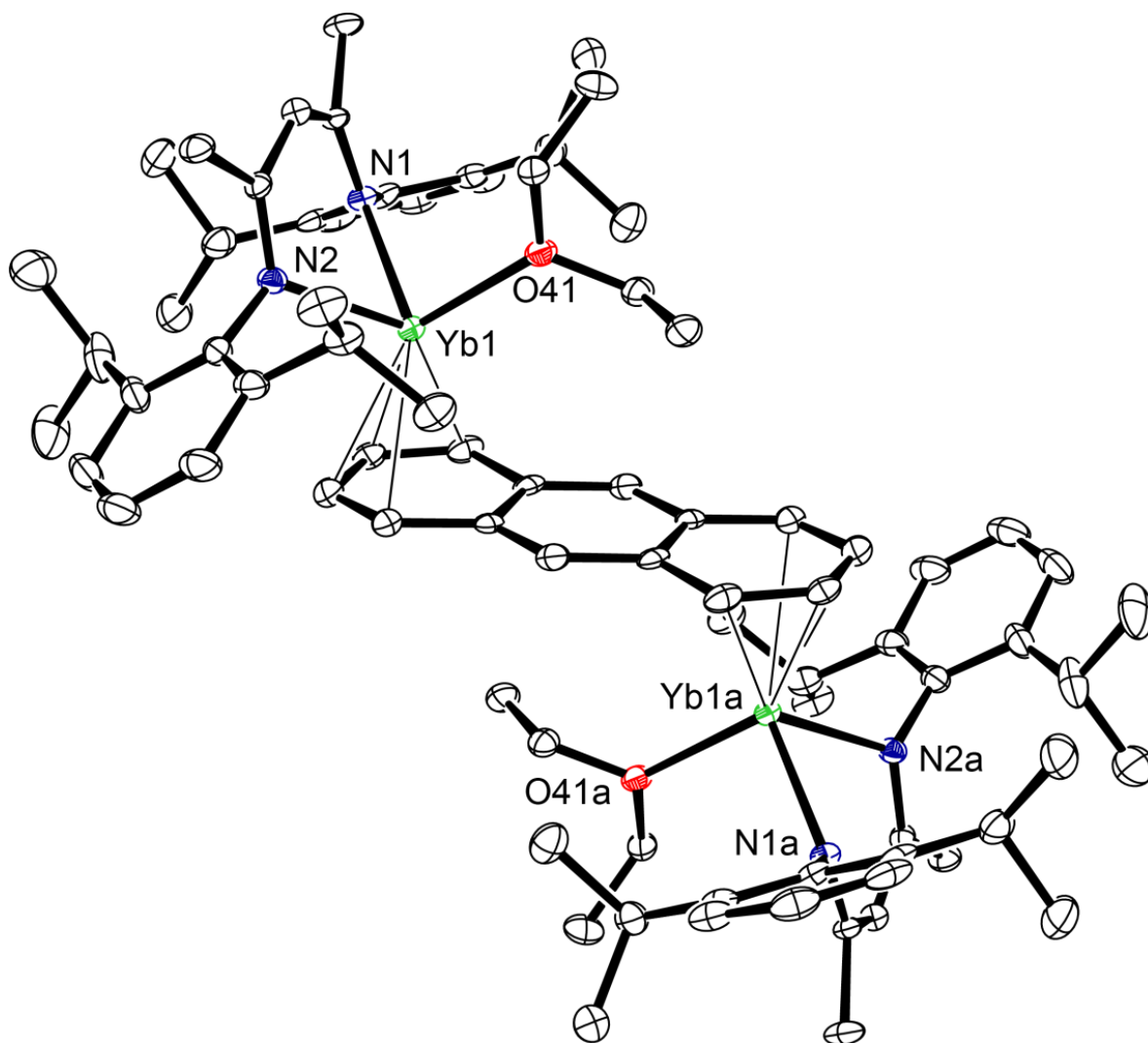




Supplementary Figure 2.76. ^1H - ^1H COSY NMR spectrum (500 MHz, C_6D_6) of $[(\text{BDI}^{\text{Dipp}})\text{Yb}(\text{Et}_2\text{O})(\mu\text{-C}_{14}\text{H}_{10})(\text{OEt}_2)\text{Yb}(\text{BDI}^{\text{Dipp}})]$ (**2.20**).



Supplementary Figure 2.77. ^1H - ^{13}C HSQC NMR spectrum (500 MHz, C_6D_6) of $[(\text{BDI}^{\text{Dipp}})\text{Yb}(\text{Et}_2\text{O})(\mu\text{-C}_{14}\text{H}_{10})(\text{OEt}_2)\text{Yb}(\text{BDI}^{\text{Dipp}})]$ (**2.20**).



Supplementary Figure 2.78. Ortep representation (30% probability ellipsoids) of $[(\text{BDI}^{\text{Dipp}})\text{Yb}(\text{Et}_2\text{O})(\mu\text{-C}_{14}\text{H}_{10})(\text{OEt}_2)\text{Yb}(\text{BDI}^{\text{Dipp}})]$ (**2.20**). Hydrogen atoms have been omitted for clarity.

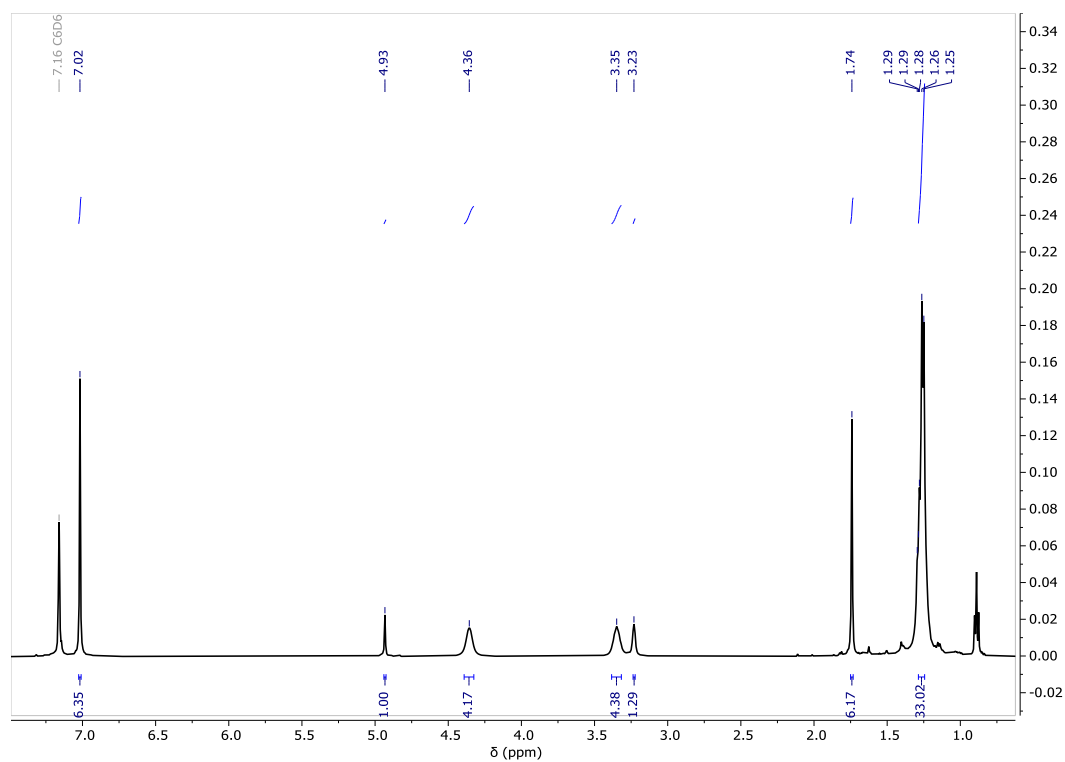
[(BDI^{Dipp})(Et₂O)Yb(μ-C₁₀H₈)Yb(OEt₂)(BDI^{Dipp})] (2.21)

Inside a glovebox a colourless toluene solution containing naphthalene (7 mg, 0.06 mmol) was added to a scintillation vial containing a black toluene solution [(BDI^{Dipp})YbH]₂ (102 mg, 0.09 mmol) and left to stir at room temperature for 16h, resulting in a grey-blue solution. Solvent was removed *in vacuo* and washing with hexane gave the crude product as a black-blue powder. Black-blue crystals suitable for X-ray diffraction were obtained from a saturated diethyl ether solution after two days at room temperature.

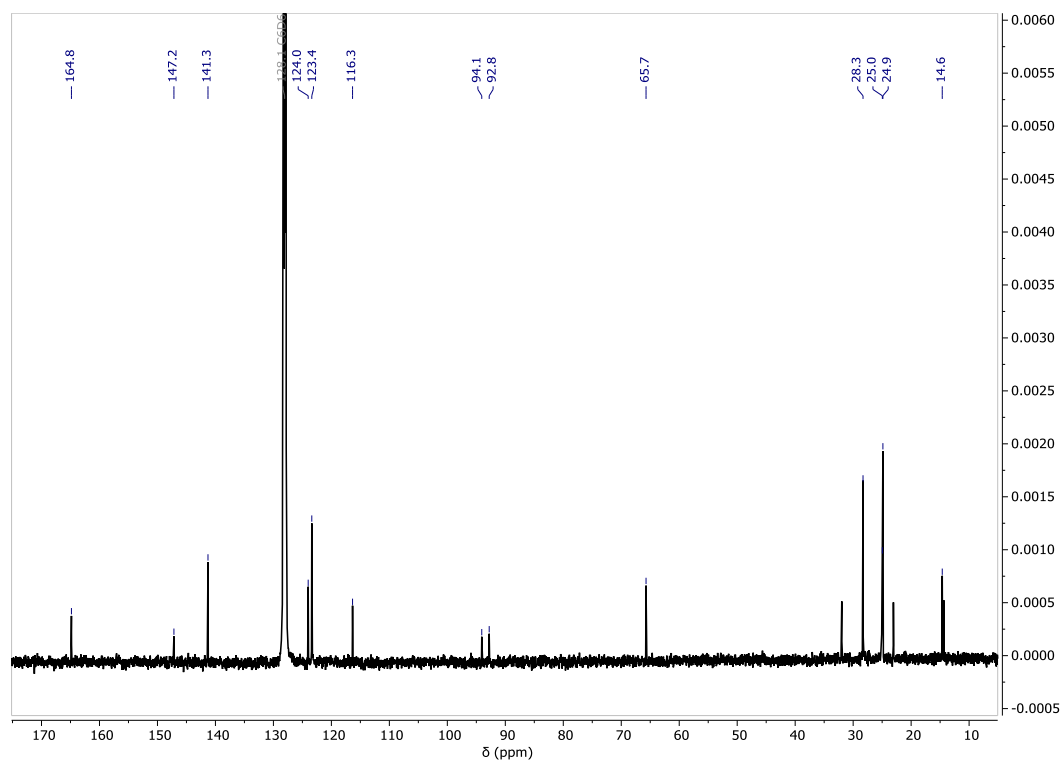
¹H NMR (500 MHz, C₆D₆) δ 7.02 (s, 6H, ArH), 4.93 (s, 1H, NC(CH₃)CH), 4.36 (br, 4H, Et₂O), 3.35 (br, 4H, CH(CH₃)₂), 3.23 (s, 1H, C₁₀H₈), 1.74 (s, 6H, NC(CH₃)CH), 1.27 (m, 33H, CH(CH₃)₂ overlapping Et₂O overlapping C₁₀H₈).

¹³C{¹H} NMR (126 MHz, C₆D₆) δ 164.8 (NC(CH₃)CH), 147.2 (C_{ipso}), 141.3 (C_{ortho}), 124.0 (C_{para}), 123.4 (C_{meta}), 116.3 (C₁₀H₈), 94.1 (NC(CH₃)CH), 92.8 (C₁₀H₈), 65.7 (Et₂O), 28.3 (CH(CH₃)₂), 25.0 (CH(CH₃)₂ overlapping CH(CH₃)₂), 24.9 (NC(CH₃)CH), 14.6 (Et₂O).

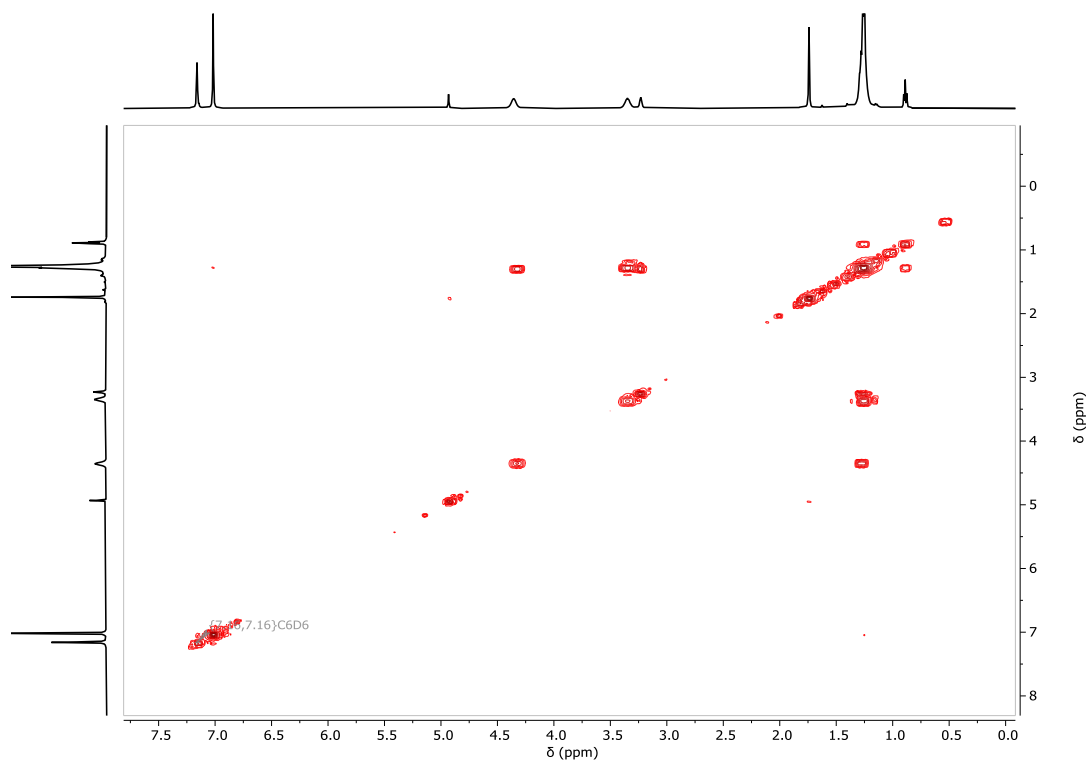
A satisfactory elemental analysis could not be obtained for compound **2.21** due to its extreme air and moisture sensitivity.



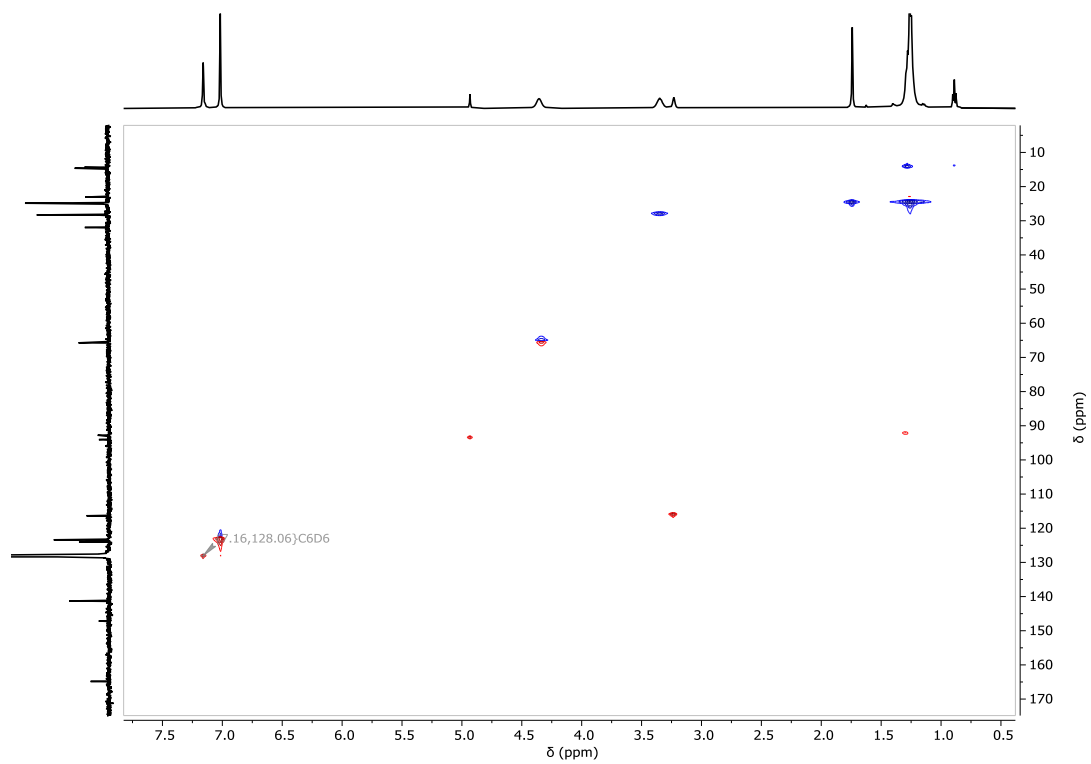
Supplementary Figure 2.79. ¹H NMR spectrum (500 MHz, C₆D₆) of [(BDI^{Dipp})Yb(Et₂O)(μ-C₁₀H₈)(OEt₂)Yb(BDI^{Dipp})] (**2.21**).



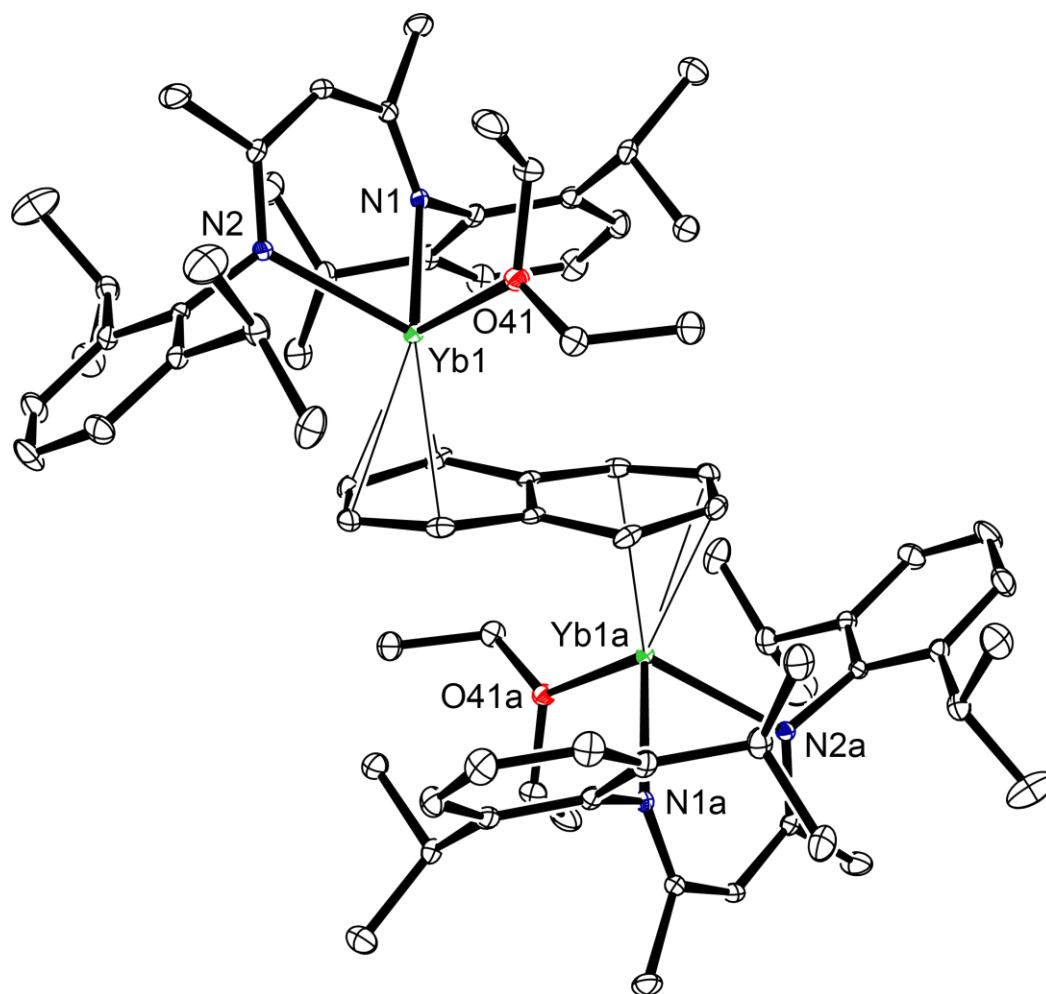
Supplementary Figure 2.80. ¹³C{¹H} NMR spectrum (126 MHz, C₆D₆) of [(BDI^{Dipp})Yb(Et₂O)(μ-C₁₀H₈)(OEt₂)Yb(BDI^{Dipp})] (**2.21**).



Supplementary Figure 2.81. ^1H - ^1H COSY NMR spectrum (500 MHz, C_6D_6) of $[(\text{BDI}^{\text{Dipp}})\text{Yb}(\text{Et}_2\text{O})(\mu\text{-C}_{10}\text{H}_8)(\text{OEt}_2)\text{Yb}(\text{BDI}^{\text{Dipp}})]$ (**2.21**).



Supplementary Figure 2.82. ^1H - ^{13}C HSQC NMR spectrum (500 MHz, C_6D_6) of $[(\text{BDI}^{\text{Dipp}})\text{Yb}(\text{Et}_2\text{O})(\mu\text{-C}_{10}\text{H}_8)(\text{OEt}_2)\text{Yb}(\text{BDI}^{\text{Dipp}})]$ (**2.21**).



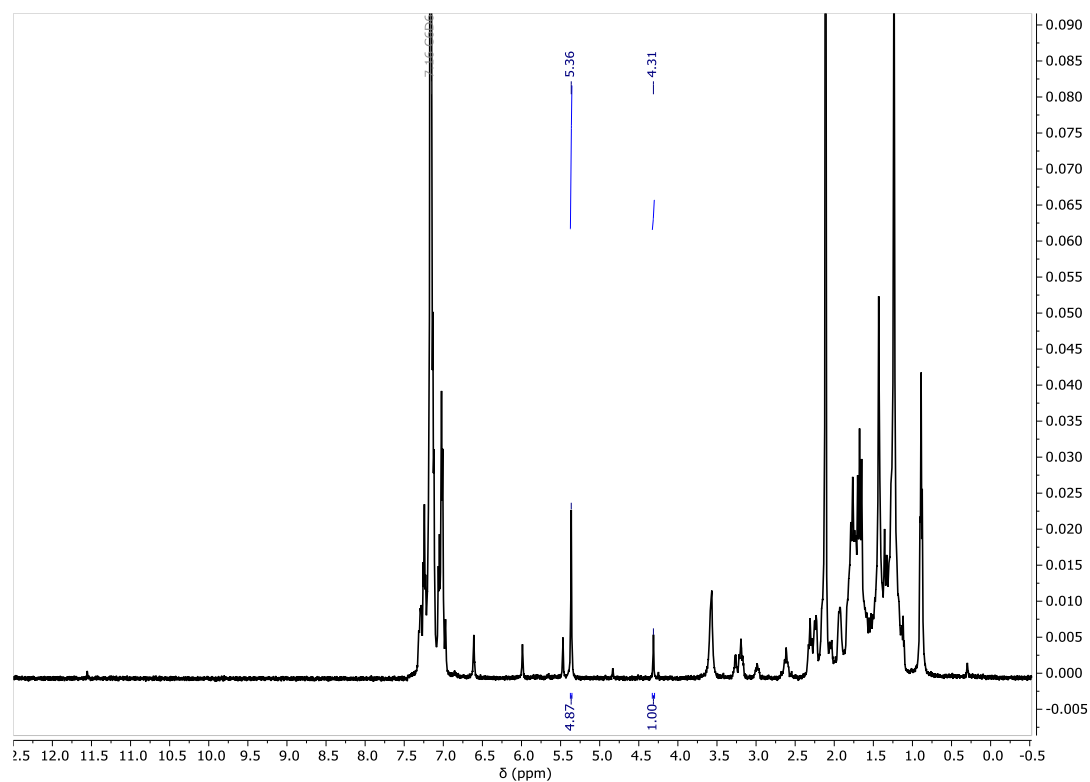
Supplementary Figure 2.83. Ortep representation (30% probability ellipsoids) of $[(BDI^{Dipp})Yb(Et_2O)(\mu-C_{10}H_8)(OEt_2)Yb(BDI^{Dipp})]$ (**2.21**). Hydrogen atoms have been omitted for clarity.

$[(\text{BDI}^{\text{DicyP}})\text{Yb}(\mu\text{-COT})\text{Yb}(\text{BDI}^{\text{DicyP}})]$ (2.22)

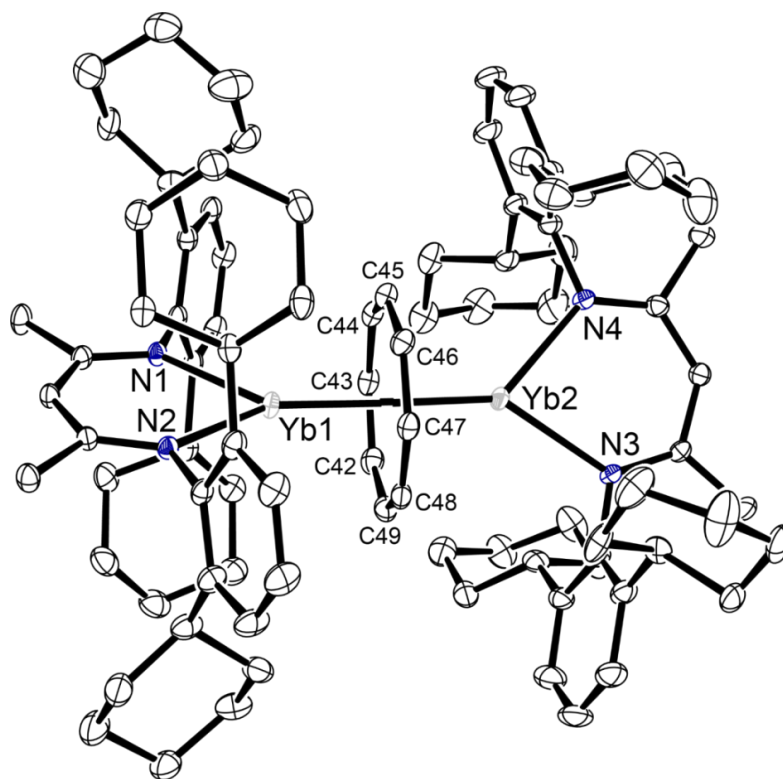
A pale yellow toluene solution of 1,3,5,7-cyclooctatetraene (10 mg, 0.09 mmol) was added to a scintillation vial containing a suspension of $[(\text{BDI}^{\text{DicyP}})\text{YbH}]_2$ (142 mg, 0.09 mmol) in toluene and the mixture was left to stir for 1 week at room temperature. The mixture was settled, and the pale pink solution was filtered into a new scintillation vial. After concentrating under vacuum, the solution was left to crystallise at room temperature, affording small dark crystals suitable for an X-ray diffraction experiment (Isolated yield: 20 mg, 26%).

The low yields of $[(\text{BDI}^{\text{DicyP}})\text{Yb}(\mu\text{-COT})\text{Yb}(\text{BDI}^{\text{DicyP}})]$ hampered characterisation by multinuclear NMR spectroscopic techniques.

^1H NMR (500 MHz, C_6D_6) δ 5.36 (s, 4H, C_8H_8), 4.31 (s, 1H, $\text{NC}(\text{CH}_3)\text{CH}$).



Supplementary Figure 2.84. ^1H NMR spectrum (500 MHz, C_6D_6) of $[(\text{BDI}^{\text{Dicyl}})\text{Yb}(\mu\text{-COT})\text{Yb}(\text{BDI}^{\text{Dicyl}})]$ (**2.22**).

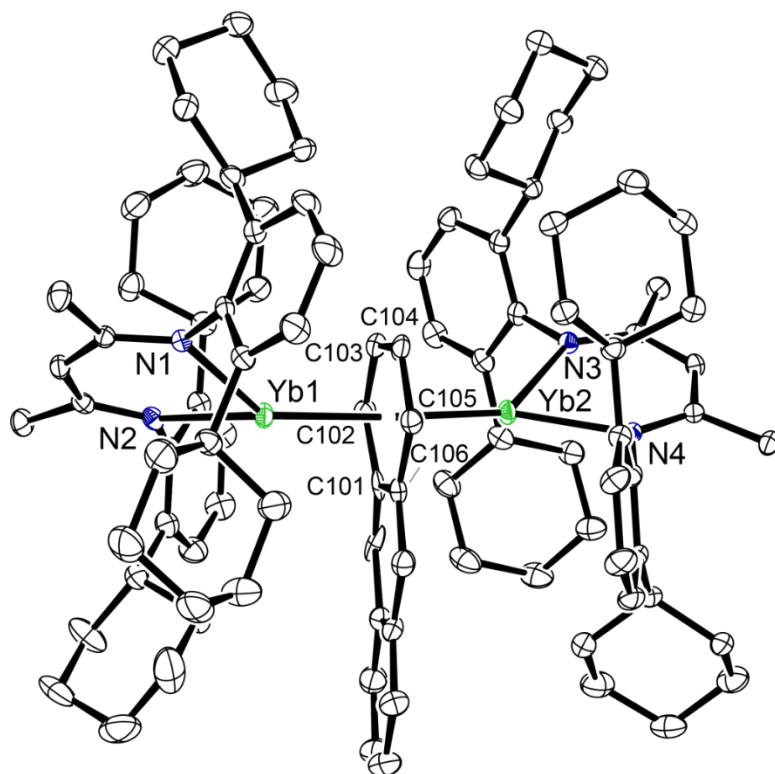


Supplementary Figure 2.85. Ortep representation (30% probability ellipsoids) of $[(\text{BDI}^{\text{Dicyl}})\text{Yb}(\mu\text{-COT})\text{Yb}(\text{BDI}^{\text{Dicyl}})]$ (**2.22**). Hydrogen atoms have been removed for clarity.

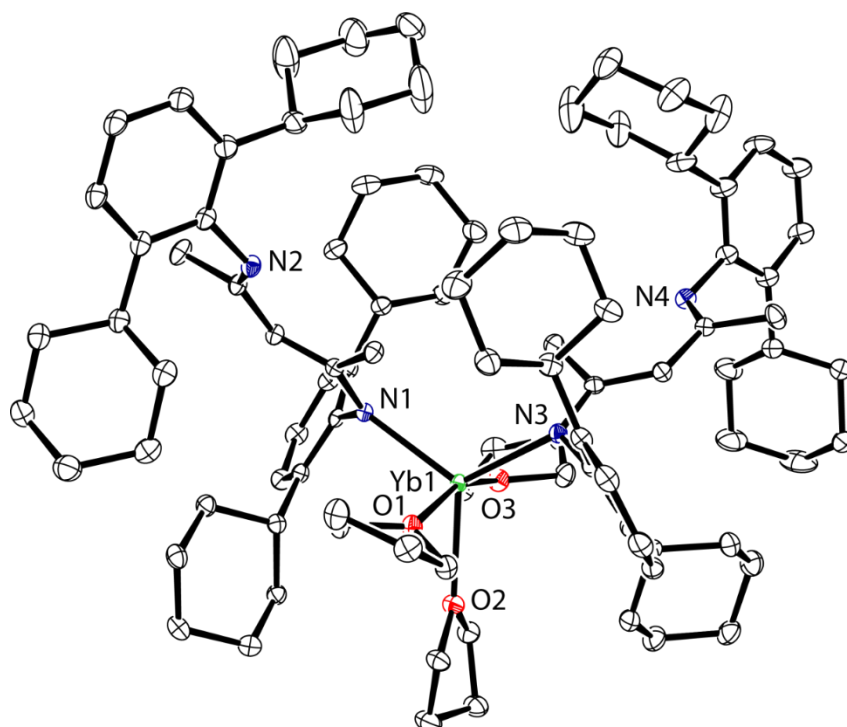
$[(\text{BDI}^{\text{DicyP}})\text{Yb}(\mu\text{-C}_{14}\text{H}_{10})\text{Yb}(\text{BDI}^{\text{DicyP}})]$ (2.23)

A THF solution of anthracene (33 mg, 0.19 mmol) to a scintillation vial containing a suspension of $[(\text{BDI}^{\text{DicyP}})\text{YbH}]_2$ (138 mg, 0.09 mmol) in THF and the mixture was left to stir overnight at room temperature to give a brown solution. The volatiles were removed *in vacuo* and the crude product dissolved into toluene to give a black-green solution. This was filtered and left to crystallise at room temperature, affording three set of crystals of multiple reaction products but all suitable for an X-ray diffraction experiment.

The impurity and solubility of the sample hindered purification attempts; hence no multinuclear NMR spectroscopic data was collected.



Supplementary Figure 2.86. Ortep representation (30% probability ellipsoids) of $[(\text{BDI}^{\text{Dicyclopentadienyl}})\text{Yb}(\mu\text{-C}_{14}\text{H}_{10})\text{Yb}(\text{BDI}^{\text{Dicyclopentadienyl}})]$ (**2.23**). Hydrogen atoms have been removed for clarity.



Supplementary Figure 2.87. Ortep representation (30% probability ellipsoids) of $[(\text{BDI}^{\text{Dicyclopentadienyl}})_2\text{Yb}(\text{THF})_3]$ (**2.24**), obtained alongside **2.23**. Hydrogen atoms have been removed for clarity.

2.2 Single Crystal X-ray Diffraction Analysis

2.2.1 Crystal Structure Data and Refinement Details

All non-hydrogen atoms were refined anisotropically, unless specified below. Hydrogen atoms were placed at calculated positions and refined using a riding model, unless otherwise specified.

[(BDI^{Dipep})YbI]₂ (2.1)

Monomer of [LYbI] in the asymmetric unit (ASU). Two independent iodine atoms present, both at 50% occupancy. One is on a special position with its symmetry equivalent situated close in space (i.e. a disorder situation). Two of the isopentyl chains were completely disordered: One of the components is near the disordered iodide atom, so these were modelled at a fixed 50% occupancy to ensure a logical physical scenario. One arm of another 3-pentyl side chain was also disordered, but with occupancy freely refined to 0.78:0.22. One of the atoms in the minor component (C131) needed to be refined isotropically. Both components were restrained to have geometry matching a well-behaved side chain (using SAME restraint).

[(BDI^{Dipep})YbN(SiMe₃)₂] (2.2)

One [LYbHMDS] molecule in ASU. No disorder. No solvent. Pseudo-polymeric structure formed via C43 – Yb interaction (2.93 Å) along c-axis.

[(BDI^{Dipep})₂Yb] (2.3)

Entire [L₂Yb] molecule in ASU. Disorder in two atoms of one isopentyl chain in a ligand. Occupancy freely refined to 0.75:0.25.

[(BDI^{Dipep})YbH(THF)]₂ (2.5)

There is half of [LYbH(THF)]₂ dimer + 2 half molecules of hexane in ASU. Both hexane molecules are disordered and present over symmetry sites. The first hexane molecule was modelled in full, but at 50% occupancy (PART -1 used). The second hexane molecule was refined as two parts with occupancy freely refined to 70%:30%; symmetry generates the other half of each of these molecules.

(BDI^{Dicyp})H (2.7)

The entire ligand and a toluene solvent molecule were present in the ASU. The amine hydrogen atom was freely refined (position and U_{iso}). The toluene molecule was disordered and was modelled as two components whose occupancies freely refined to 0.88:0.12. The geometry of the minor toluene component was restrained to be the same as the major component (SAME). The minor disorder component was modelled isotropically.

[2,6-di-cyclohexylaniline] (2.10)

There are two amine molecules in the ASU. Standard H-atom treatment, except hydrogen atoms on the nitrogen which were freely refined (position and Uiso).

(BDI^{Dicyp})K (2.11)

The ASU contains L_3K_3 as part of infinite 1D polymer along the c-axis (e.g. -L-K-L-K-L-K-). The packing arrangement in the polymer (with non-chiral ligand) results in non-centrosymmetric space group. Flack x parameter is non-zero, so structure was refined as having contribution from inversion twin (BASF refined to 0.20).

[(BDI^{Dicyp})YbI]₂ (2.12)

There is half of the [LYbI]₂ dimer in the ASU. Standard H-atom treatment. No solvent/disorder.

[(BDI^{Dicyp})YbCH(SiMe₃)₂]₂ (2.13)

There is an entire molecule of [LYbCH(SiMe₃)₂] in the ASU. Standard H-atom treatment.

[(BDI^{Dicyp})YbH]₂ (2.14)

There is half the [LYbH]₂ dimer in the ASU. Standard H-atom treatment, except for H1 (bridging hydride), which was allowed to freely refine (position and Uiso). No disorder or solvent present. This crystal simulates mmm symmetry, although the true space group is P 21/n. Initially, a C-centered lattice was identified with lengths of a=21.797, b=22.208 and c=14.821 (Rint=0.025). However, no solutions could be found. Reducing the symmetry to monoclinic, there are two options with Rint comparable to the orthorhombic crystal system: C-centered with the same cell constants as the orthorhombic cell (Rint=0.024) and a primitive cell with a=15.553, b=14.821, c=15.564, β =91.1 (Rint=0.021). Notably, the primitive cell had systematic absences consistent with P 21/n. The structure was solved as normal, but refined poorly (wR2=0.6014, R1=0.2368). The appropriate twin law was identified allowing routine refinement and excellent statistics. BASF refined to 0.492.

[(BDI^{Dipp})Yb]₃P₇] (2.15)

There is an entire molecule of [(LYb)₃P₇] and 0.6 of a hexane molecule in the ASU. Some atoms moderately prolate but not problematic enough to warrant modelling as being disordered. Hexane modelled as 0.6 occupancy.

[(BDI^{Dipep})Yb(THF)P₄Yb(THF)(BDI^{Dipep})] (2.16)

There is an entire molecule of [L(THF)Yb(P₄)Yb(THF)L] and two toluene molecules in the ASU. Standard H-atom treatment, no disorder.

[(BDI^{Dicyp})Yb(P₄)Yb(BDI^{Dicyp})] (2.17)

There is an entire molecule of [LYb(P₄)YbL] and two toluene molecules in the ASU. Standard H-atom treatment. One of the phenyl rings in the ligand was subjected to rigid-body restraint (RIGU). These toluene molecules were also subjected to the same restraint. The two toluene ring-methyl bond distances were restrained (DFIX). Additionally, the methyl to ortho-carbon atoms were restrained to be the same (SADI). Both toluene molecules were positioned over special sites, so the entire molecules were modelled at a fixed 50% occupancy and used with PART -1 to prevent bonding to the symmetry equivalent.

[(BDI^{Dipp})Yb(μ -COT)Yb(BDI^{Dipp})] (2.18)

No extra refinement details. Half of the [LYb(COT)YbL] sandwich complex is present in the ASU. Four of the central COT ligand atoms are in the ASU, with the remainder of the molecule generated by symmetry (inversion). No solvent molecules or disorder is present in the structure.

[(BDI^{Dipp})Yb(μ -COT)] (2.19)

No extra refinement details. The entire [LYb(COT)] complex is present in the ASU. No solvent molecules or disorder is present in the structure.

[(BDI^{Dipp})(Et₂O)Yb(μ -C₁₄H₁₀)Yb(OEt₂)(BDI^{Dipp})] (2.20)

No extra refinement details. Half of the [(Et₂O)LYb(anthracene)YbL(OEt₂)] sandwich complex is present in the ASU. Seven of the anthracene atoms are in the ASU, with the remainder of the molecule generated by symmetry (inversion). No additional solvent molecules or disorder is present in the structure.

[(BDI^{Dipp})(Et₂O)Yb(μ -C₁₀H₈)Yb(OEt₂)(BDI^{Dipp})] (2.21)

There were two unique halves of the [(Et₂O)LYb(naphthalene)YbL(OEt₂)] sandwich complex present in the asymmetric unit, with the other halves generated by symmetry (inversion). In the first, five of the naphthalene atoms are present, with symmetry generating the other half of the ligand. In the second dimer, the naphthalene is apparently rotationally disordered, thus all ten atoms of this ligand were modelled though with half occupancy. The symmetry mate of this naphthalene lies in close proximity, but with atom C81 at a special position and acting as a

pivot point for the apparent rotational motion. Treatment in this fashion required a negative PART number, equal occupancy, and the use of ISOR restraints for atoms C86, C89 and C90.

[(BDI^{DicyP})Yb(μ -COT)Yb(BDI^{DicyP})] (2.22)

There is an entire molecule of [LYb(COT)YbL] and 1.35 molecules of toluene in the ASU. One of the cyclohexyl groups was modelled as being disordered over two positions, with occupancies freely refined to 0.51:0.49. The ADPs of the tertiary carbon atoms in the disorder groups were constrained to be equal (EADP) and were restrained to be more spherical (ISOR) to prevent non-positive definite issues. Additionally, both disorder components were subjected to rigid body restraints (RIGU). One of the toluene molecules was present over a symmetry site, so a negative PART number was used, and the entire molecule modelled, requiring ring constraints (AFIX 66) to ensure correct geometry. This molecule was modelled at reduced occupancy (0.35 instead of 0.5). Additionally, the ring-methyl bond distance required restraining to achieve a realistic bond length (DFIX). Both toluene molecules were subjected to rigid body restraints (RIGU).

[(BDI^{DicyP})Yb(μ -C₁₄H₁₀)Yb(BDI^{DicyP})] (2.23)

There is an entire molecule of [LYb(anthracene)YbL] and half a molecule of toluene in the ASU. The toluene molecule is disordered, being present over a symmetry site. Consequently, this molecule was fixed at 50% occupancy. A ring constraint (AFIX 66) and ring-methyl bond restraints (SADI, for distances to ortho positions; and DFIX) were applied to ensure acceptable geometry. An additional EADP constraint was used for C123 and C127, whose atoms were almost coincident with the respective symmetry equivalents.

[(BDI^{DicyP})₂Yb(THF)₃] (2.24)

There are two [L₂Yb(THF)₃] complexes in ASU. Looks like collection didn't complete but is fine. Two rings are borderline disordered, but disorder refinement wasn't great so left with large ADPs.

Supplementary Table 2.1. Crystal data and refinement details for compounds **2.1** – **2.3**, **2.5** and **2.7**.

| | 2.1 | 2.2 | 2.3 | 2.5 | 2.7 |
|---|--|---|--|--|--|
| CCDC code | | | | | 2244289 |
| Empirical formula | C ₃₇ H ₅₇ IN ₂ Yb | C ₄₃ H ₇₅ N ₃ Si ₂ Yb | C ₇₄ H ₁₁₄ N ₄ Yb | C ₉₄ H ₁₆₀ N ₄ O ₂ Yb ₂ | C ₄₈ H ₆₆ N ₂ |
| Formula weight (g mol ⁻¹) | 829.78 | 863.28 | 1232.73 | 1724.33 | 671.02 |
| Temperature (K) | 120 | 150 | 150 | 120 | 150 |
| Crystal system | Monoclinic | Monoclinic | Triclinic | Triclinic | Triclinic |
| Space group | C 2/c | P 21/c | P -1 | P -1 | P -1 |
| a (Å) | 35.8419(10) | 22.02230(10) | 11.2709(5) | 12.4715(2) | 11.1346(4) |
| b (Å) | 16.48340(10) | 13.43250(10) | 16.8804(4) | 12.9837(2) | 14.2240(4) |
| c (Å) | 19.8280(5) | 14.83040(10) | 19.2021(4) | 15.9466(2) | 14.7362(5) |
| α (°) | 90 | 90 | 84.242(2) | 76.1130(10) | 106.359(2) |
| β (°) | 141.874(6) | 99.3660(10) | 74.092(3) | 77.4650(10) | 107.121(3) |
| γ (°) | 90 | 90 | 76.770(3) | 63.570(2) | 104.793(3) |
| Volume (Å ³) | 7232.3(7) | 4328.56(5) | 3417.4(2) | 2226.58(7) | 1989.25(12) |
| Z | 8 | 4 | 2 | 1 | 2 |
| Calculated density (Mg/ m ³) | 1.524 | 1.325 | 1.198 | 1.286 | 1.120 |
| Absorption coefficient (mm ⁻¹) | 11.660 | 4.747 | 2.834 | 4.125 | 0.473 |
| F(000) | 3328 | 1808 | 1312 | 908 | 736 |
| Crystal size (mm ³) | 0.187 x 0.073 x 0.062 | 0.133 x 0.073 x 0.054 | 0.097 x 0.071 x 0.046 | 0.189 x 0.078 x 0.042 | 0.292 x 0.104 x 0.100 |
| Theta range for data collection (°) | 3.587 to 73.358 ° | 3.869 to 73.501 ° | 3.531 to 73.515 ° | 3.854 to 73.593 ° | 3.484 to 73.335 ° |
| Index ranges | -44 ≤ h ≤ 43 -20 ≤ k ≤ 20 -24 ≤ l ≤ 23 | -27 ≤ h ≤ 17 -15 ≤ k ≤ 16 -17 ≤ l ≤ 18 | -14 ≤ h ≤ 13 -20 ≤ k ≤ 20 -23 ≤ l ≤ 22 | -15 ≤ h ≤ 9 -16 ≤ k ≤ 15 -19 ≤ l ≤ 19 | -12 ≤ h ≤ 13 -17 ≤ k ≤ 16 -18 ≤ l ≤ 14 |
| Reflections collected | 37249 | 31036 | 45392 | 43201 | 21886 |
| Independent reflections | 7247 R(int) = 0.0285 | 8669 R(int) = 0.0257 | 13609 R(int) = 0.0397 | 8892 R(int) = 0.0358 | 7955 R(int) = 0.0268 |
| Completeness to theta | 99.9% | 99.9% | 99.9 % | 99.4% | 100.0% |
| Data/ restraints/ parameters | 7247/ 9/ 494 | 8669/ 0/ 458 | 13609/ 9/ 752 | 8892/ 12/ 517 | 7955/ 15/ 488 |
| Goodness-of-fit on F ² | 1.214 | 1.026 | 1.049 | 1.024 | 1.046 |
| Final R indices [I>2sigma(I)] | R1 = 0.0325 wR2 = 0.0755 | R1 = 0.0223 wR2 = 0.0504 | R1 = 0.0399 wR2 = 0.0889 | R1 = 0.0308 wR2 = 0.0773 | R1 = 0.0460 wR2 = 0.1190 |
| R indices (all data) | R1 = 0.0330 wR2 = 0.0758 | R1 = 0.0247 wR2 = 0.0516 | R1 = 0.0485 wR2 = 0.0948 | R1 = 0.0322 wR2 = 0.0784 | R1 = 0.0509 wR2 = 0.1235 |
| Largest diff. peak and hole (e. Å ⁻³) | 1.285 and -0.883 | 0.985 and -0.438 | 0.974 and -2.276 | 0.0322 and -0.0784 | 0.265 and -0.277 |

Supplementary Table 2.2. Crystal data and refinement details for compounds **2.10** – **2.14**.

| | 2.10 | 2.11 | 2.12 | 2.13 | 2.14 |
|---|---|---|--|---|---|
| CCDC code | 2330106 | 2244290 | | | |
| Empirical formula | C ₁₈ H ₂₇ N | C ₄₁ H ₅₇ KN ₂ | C ₈₂ H ₁₁₄ I ₂ N ₄ Yb ₂ | C ₄₈ H ₇₆ N ₂ Si ₂ Yb | C ₈₂ H ₁₁₆ N ₄ Yb ₂ |
| Formula weight (g mol ⁻¹) | 257.40 | 559.53 | 1755.65 | 910.32 | 1503.86 |
| Temperature (K) | 120 | 120 | 150 | 120 | 120 |
| Crystal system | Monoclinic | Orthorhombic | Monoclinic | Monoclinic | Monoclinic |
| Space group | P 21/c | P 21 21 21 | I 2/a | P 21/c | P 21/n |
| a (Å) | 12.5844(5) | 14.6226(3) | 25.6617(6) | 15.80020(10) | 15.56390(10) |
| b (Å) | 10.2524(3) | 20.6506(2) | 15.6421(3) | 13.67620(10) | 14.80880(10) |
| c (Å) | 23.4693(10) | 35.8717(4) | 22.8493(6) | 21.88840(10) | 15.56750(10) |
| α (°) | 90 | 90 | 90 | 90 | 90 |
| β (°) | 99.565(4) | 90 | 122.663(4) | 91.8060(10) | 91.2030(10) |
| γ (°) | 90 | 90 | 90 | 90 | 90 |
| Volume (Å ³) | 2985.9(2) | 10832.0(3) | 7721.4(4) | 4727.44(5) | 3587.25(4) |
| Z | 8 | 12 | 4 | 4 | 2 |
| Calculated density (Mg/ m ³) | 1.145 | 1.029 | 1.510 | 1.279 | 1.392 |
| Absorption coefficient (mm ⁻¹) | 0.485 | 1.488 | 10.959 | 4.370 | 5.026 |
| F(000) | 1136 | 3348 | 3520 | 1904 | 1552 |
| Crystal size (mm ³) | 0.121 x 0.092 x 0.052 | 0.225 x 0.156 x 0.031 | 0.383 x 0.064 x 0.046 | 0.251 x 0.087 x 0.024 | 0.138 x 0.078 x 0.036 |
| Theta range for data collection (°) | 3.562 to 73.474 ° | 3.704 to 73.464 ° | 3.488 to 73.632 ° | 3.812 to 73.478 ° | 3.975 to 72.376 ° |
| Index ranges | -15 ≤ h ≤ 15 -8 ≤ k ≤ 12 -28 ≤ l ≤ 29 | -17 ≤ h ≤ 18 -25 ≤ k ≤ 23 -44 ≤ l ≤ 39 | -28 ≤ h ≤ 31 -19 ≤ k ≤ 19 -28 ≤ l ≤ 17 | -19 ≤ h ≤ 19 -14 ≤ k ≤ 16 -27 ≤ l ≤ 27 | -14 ≤ h ≤ 19 -18 ≤ k ≤ 17 -19 ≤ l ≤ 19 |
| Reflections collected | 18131 | 62067 | 41666 | 58053 | 46998 |
| Independent reflections | 5990 R(int) = 0.0286 | 21083 R(int) = 0.0335 | 7707 R(int) = 0.0324 | 9467 R(int) = 0.0406 | 7070 R(int) = 0.0215 |
| Completeness to theta | 100.0% | 100.0% | 99.9 % | 100.0% | 100.0% |
| Data/ restraints/ parameters | 5990/ 0/ 359 | 21083/ 0/ 1195 | 7707/ 0/ 408 | 9467/ 0/ 486 | 7070/ 0/ 404 |
| Goodness-of-fit on F ² | 1.039 | 1.037 | 1.046 | 1.034 | 1.079 |
| Final R indices [I>2sigma(I)] | R1 = 0.0407 wR2 = 0.1049 | R1 = 0.0476 wR2 = 0.1208 | R1 = 0.0382 wR2 = 0.1084 | R1 = 0.0308 wR2 = 0.0757 | R1 = 0.0165 wR2 = 0.0441 |
| R indices (all data) | R1 = 0.0494 wR2 = 0.1127 | R1 = 0.0542 wR2 = 0.1264 | R1 = 0.0402 wR2 = 0.1105 | R1 = 0.0346 wR2 = 0.0783 | R1 = 0.0175 wR2 = 0.0448 |
| Largest diff. peak and hole (e. Å ⁻³) | 0.242 and -0.213 | 0.370 and -0.306 | 1.226 and -2.385 | 0.876 and -1.234 | 0.608 and -1.056 |

Supplementary Table 2.3. Crystal data and refinement details for compounds **2.15** – **2.19**.

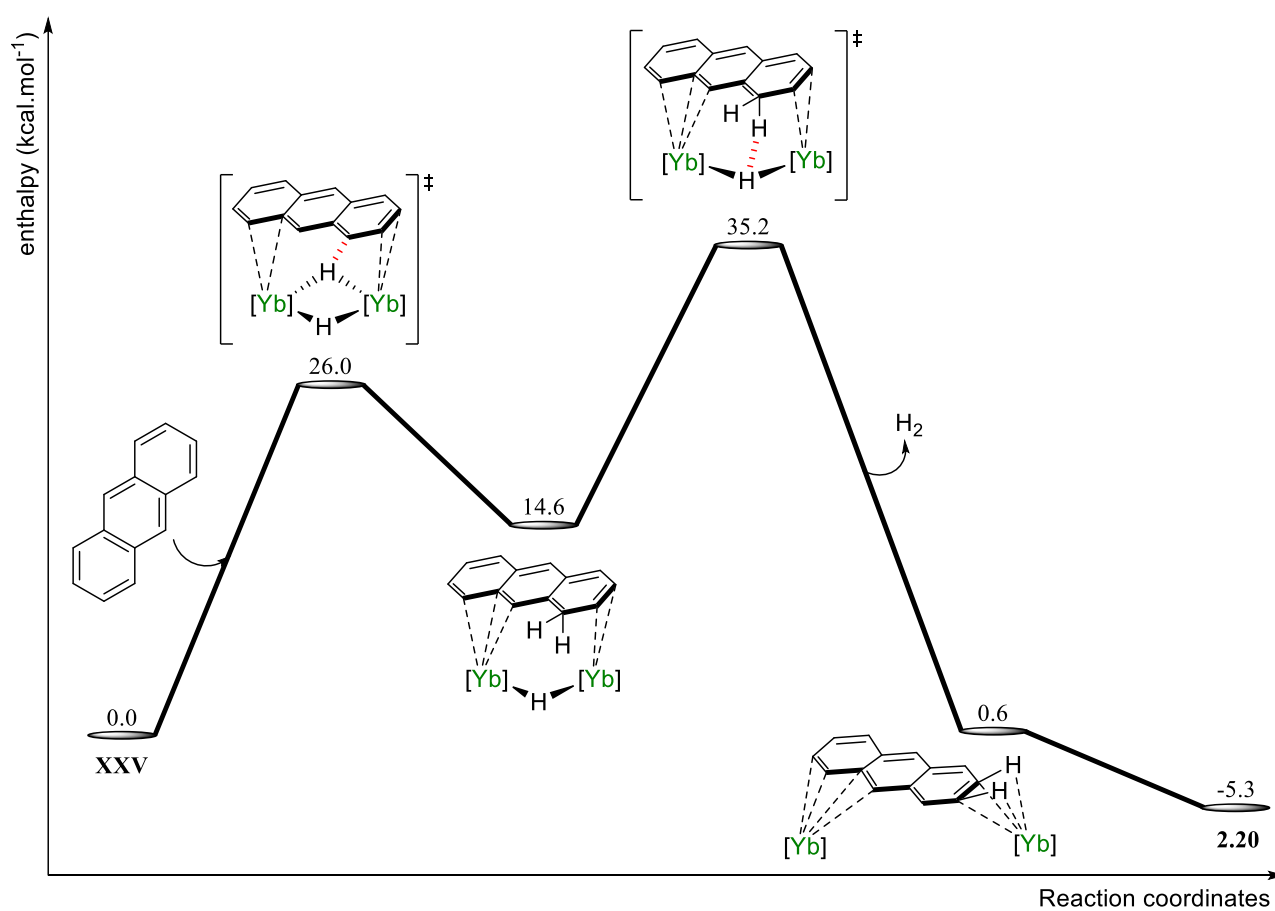
| | 2.15 | 2.16 | 2.17 | 2.18 | 2.19 |
|---|--|---|--|--|---|
| CCDC code | | | | 2083687 | 2083685 |
| Empirical formula | C ₉₀ H ₁₃₁ N ₆ P ₇ Yb ₃ | C ₉₆ H ₁₄₆ N ₄ O ₂ P ₄ Yb ₂ | C ₈₉ H ₁₂₂ N ₄ P ₄ Yb ₂ | C ₆₆ H ₉₀ N ₄ Yb ₂ | C ₃₇ H ₄₉ N ₂ Yb |
| Formula weight (g mol ⁻¹) | 2040.52 | 1858.12 | 1717.86 | 1285.49 | 694.82 |
| Temperature | 120 | 120 | 120 | 120 | 120 |
| Crystal system | Monoclinic | Triclinic | Monoclinic | Monoclinic | Triclinic |
| Space group | P 21/n | P -1 | P 21/c | P 21/n | P-1 |
| a (Å) | 12.18334(14) | 13.0026(4) | 29.9437(4) | 14.6924(2) | 9.6474(2) |
| b (Å) | 26.1588(3) | 18.5274(7) | 13.3681(2) | 10.2791(2) | 12.2607(3) |
| c (Å) | 29.9538(3) | 20.5125(6) | 21.6469(3) | 19.8571(3) | 13.8613(3) |
| α (°) | 90 | 78.915(3) | 90 | 90 | 100.436(2) |
| β (°) | 93.0389(10) | 74.797(2) | 108.7380(10) | 93.0540(10) | 94.475(2) |
| γ (°) | 90 | 78.064(3) | 90 | 90 | 95.724(2) |
| Volume (Å ³) | 9532.92(18) | 4615.4(3) | 8205.8(2) | 2994.65(8) | 1596.65(6) |
| Z | 4 | 2 | 4 | 2 | 2 |
| Calculated density (Mg/ m ³) | 1.422 | 1.337 | 1.391 | 1.426 | 1.445 |
| Absorption coefficient (mm ⁻¹) | 6.690 | 4.660 | 5.181 | 5.923 | 5.600 |
| F(000) | 4128 | 1932 | 3536 | 1308 | 710 |
| Crystal size (mm ³) | 0.115 x 0.041 x 0.039 | 0.108 x 0.082 x 0.028 | 0.120 x 0.080 x 0.030 | 0.123 × 0.065 × 0.030 | 0.290 × 0.209 × 0.092 |
| Theta range for data collection (°) | 3.688 to 73.402 ° | 3.572 to 73.859 ° | 3.655 to 68.251 ° | 3.842 to 73.586 ° | 3.691 to 73.536 ° |
| Index ranges | -15 ≤ h ≤ 14 -32 ≤ k ≤ 31 -37 ≤ l ≤ 36 | -16 ≤ h ≤ 14 -23 ≤ k ≤ 22 -25 ≤ l ≤ 25 | -36 ≤ h ≤ 35 -15 ≤ k ≤ 16 -25 ≤ l ≤ 26 | -17 ≤ h ≤ 18 -12 ≤ k ≤ 12 -24 ≤ l ≤ 20 | -11 ≤ h ≤ 11 -15 ≤ k ≤ 13 -15 ≤ l ≤ 17 |
| Reflections collected | 63384 | 60249 | 54809 | 18966 | 17734 |
| Independent reflections | 18962 R(int) = 0.0347 | 18422 R(int) = 0.0470 | 15007 R(int) = 0.0521 | 5995 R(int) = 0.0273 | 6372 R(int) = 0.0199 |
| Completeness to theta | 99.9% | 99.8% | 99.9 % | 99.9% | 99.9% |
| Data/ restraints/ parameters | 18962/ 0/ 1014 | 18422/ 0/ 995 | 15007/ 110/ 927 | 5995/ 0/ 335 | 6372 / 0 / 371 |
| Goodness-of-fit on F ² | 1.045 | 1.025 | 1.020 | 1.047 | 1.080 |
| Final R indices [I>2sigma(I)] | R1 = 0.0331 wR2 = 0.0842 | R1 = 0.0349 wR2 = 0.0867 | R1 = 0.0417 wR2 = 0.0871 | R1 = 0.0242 wR2 = 0.0556 | R1 = 0.0195 wR2 = 0.0505 |
| R indices (all data) | R1 = 0.0391 wR2 = 0.0879 | R1 = 0.0420 wR2 = 0.0917 | R1 = 0.0592 wR2 = 0.0940 | R1 = 0.0285 wR2 = 0.0575 | R1 = 0.0198 wR2 = 0.0507 |
| Largest diff. peak and hole (e. Å ⁻³) | 0.864 and -1.332 | 1.043 and -1.518 | 2.352 and -1.761 | 0.577 and 0.978 | 0.519 and 0.888 |

Supplementary Table 2.4. Crystal data and refinement details for compounds **2.20** – **2.24**.

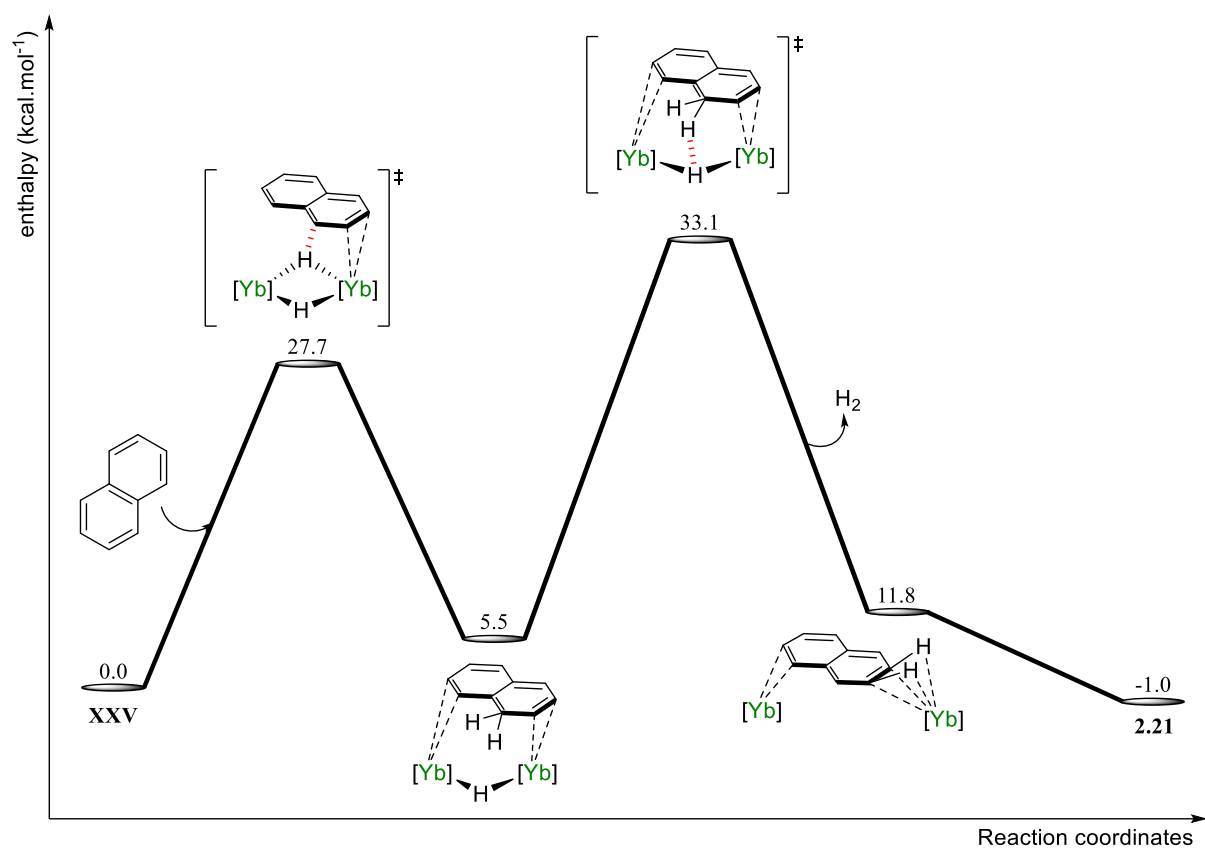
| | 2.20 | 2.21 | 2.22 | 2.23 | 2.24 |
|---|--|--|---|--|---|
| CCDC code | 2083686 | 2083688 | | | |
| Empirical formula | C ₈₀ H ₁₁₂ N ₄ O ₂ Yb ₂ | C ₇₆ H ₁₁₀ N ₄ O ₂ Yb ₂ | C ₉₉ H ₁₃₃ N ₄ Yb ₂ | C ₁₉₉ H ₂₅₆ N ₈ Yb ₄ | C ₉₄ H ₁₃₈ N ₄ O ₃ Yb |
| Formula weight (g mol ⁻¹) | 1507.81 | 1457.75 | 1730.37 | 3452.26 | 1545.12 |
| Temperature (K) | 120 | 120 | 120 | 120 | 120 |
| Crystal system | Monoclinic | Monoclinic | Monoclinic | Triclinic | Monoclinic |
| Space group | P 2/c | I 2/a | P 21/n | P -1 | P 2/c |
| a (Å) | 17.4217(4) | 31.4494(3) | 13.24688(10) | 14.2738(2) | 24.42960(10) |
| b (Å) | 9.6893(2) | 12.04970(10) | 28.76270(19) | 15.0292(2) | 13.77940(10) |
| c (Å) | 22.1250(5) | 39.0027(4) | 22.23286(16) | 21.7257(3) | 50.5155(2) |
| α (°) | 90 | 90 | 90 | 75.4220(10) | 90 |
| β (°) | 100.562(2) | 108.9840(10) | 92.6067(7) | 83.4940(10) | 94.68 |
| γ (°) | 90 | 90 | 90 | 68.5310(10) | 90 |
| Volume (Å ³) | 3671.53(15) | 13976.4(2) | 8462.31(11) | 4196.51(11) | 16948.00(16) |
| Z | 2 | 8 | 4 | 1 | 8 |
| Calculated density (Mg/ m ³) | 1.364 | 1.386 | 1.358 | 1.366 | 1.211 |
| Absorption coefficient (mm ⁻¹) | 4.933 | 2.707 | 4.335 | 4.371 | 2.414 |
| F(000) | 1552 | 6000 | 3590 | 1786 | 6592 |
| Crystal size (mm ³) | 0.105 × 0.091 × 0.038 | 0.139 × 0.065 × 0.061 | 0.097 × 0.078 × 0.026 | 0.176 × 0.057 × 0.022 | 0.195 × 0.142 × 0.039 |
| Theta range for data collection (°) | 4.065 to 73.500 ° | 3.187 to 29.472° | 3.662 to 72.410 ° | 3.442 to 72.419 ° | 3.511 to 72.590 ° |
| Index ranges | -20 ≤ h ≤ 21 -12 ≤ k ≤ 10 -27 ≤ l ≤ 25 | -42 ≤ h ≤ 43 -12 ≤ k ≤ 15 -53 ≤ l ≤ 51 | -16 ≤ h ≤ 16 -35 ≤ k ≤ 35 -24 ≤ l ≤ 27 | -17 ≤ h ≤ 17 -18 ≤ k ≤ 11 -26 ≤ l ≤ 26 | -26 ≤ h ≤ 30 -16 ≤ k ≤ 17 -59 ≤ l ≤ 62 |
| Reflections collected | 26316 | 61471 | 58235 | 54292 | 176617 |
| Independent reflections | 7339 R(int) = 0.0439 | 16881 R(int) = 0.0349 | 16654 R(int) = 0.0407 | 16481 R(int) = 0.0299 | 33357 R(int) = 0.0335 |
| Completeness to theta | 100.0% | 99.7% | 99.9 % | 99.9% | 100.0% |
| Data/ restraints/ parameters | 7339/ 0/ 409 | 16881/ 18/ 822 | 16654/ 205/ 1033 | 16481/ 2/ 969 | 33357 / 0/ 1845 |
| Goodness-of-fit on F ² | 1.334 | 1.029 | 1.023 | 1.026 | 1.013 |
| Final R indices [I>2sigma(I)] | R1 = 0.0674 wR2 = 0.1552 | R1 = 0.0267 wR2 = 0.0463 | R1 = 0.0336 wR2 = 0.0719 | R1 = 0.0257 wR2 = 0.0561 | R1 = 0.0285 wR2 = 0.0732 |
| R indices (all data) | R1 = 0.0713 wR2 = 0.1569 | R1 = 0.0377 wR2 = 0.0492 | R1 = 0.0440 wR2 = 0.0762 | R1 = 0.0313 wR2 = 0.0584 | R1 = 0.0347 wR2 = 0.0779 |
| Largest diff. peak and hole (e. Å ⁻³) | 2.719 and 2.171 | 0.903 and 0.527 | 1.648 and -1.133 | 1.236 and -0.924 | 0.950 and -0.815 |

2.3 Computational Details

All calculations were carried out by Prof. Laurent Maron and Iskander Douair at the DFT level of theory using the hybrid functional B3PW91¹⁰ with the Gaussian 09 suite of programs.¹¹ The Yb was represented with a small-core Stuttgart-Dresden relativistic effective core potential associated with the adapted basis set.¹²⁻¹⁴ All the other atoms C, N and H were described with a 6-31G (d,p), double ζ quality basis set.¹⁵ The nature of the extrema (minimum and transition states) was established with analytical frequencies calculations and geometry optimizations were computed without any symmetry constraints. The enthalpy energy was computed at T=298 k in the gas phase.



Supplementary Figure 2.88. Computed enthalpy profile for the two-electron reduction of anthracene by XXV to give 2.20.



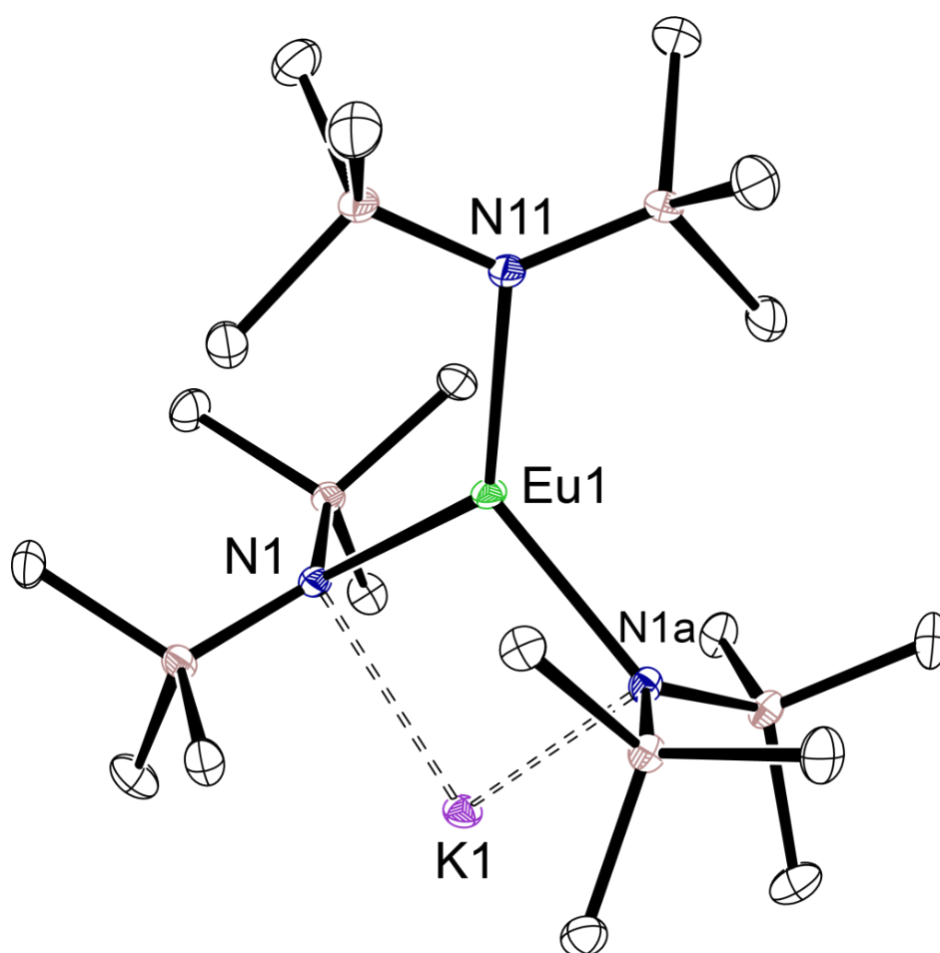
Supplementary Figure 2.89. Computed enthalpy profile for the two-electron reduction of naphthalene by **XXV** to give **2.21**.

3.0 Chapter Three Experimental

3.1 Synthetic, Spectroscopic and Analytical Data

K[Eu(HMDS)₃] (3.1)

A colourless C₆H₆ solution of KHMDS (211 mg, 1.06 mmol) was added to a suspension of EuI₂ (227 mg, 0.56 mmol) in C₆H₆ in a scintillation vial inside the glovebox. The mixture was left stir for 2 days at room temperature, affording an orange solution and a pale yellow precipitate. The solution was filtered through Celite, the volatiles removed under vacuum and the crude product re-dissolved into hexane. Yellow plates suitable for an X-ray diffraction experiment were obtained at –30 °C.

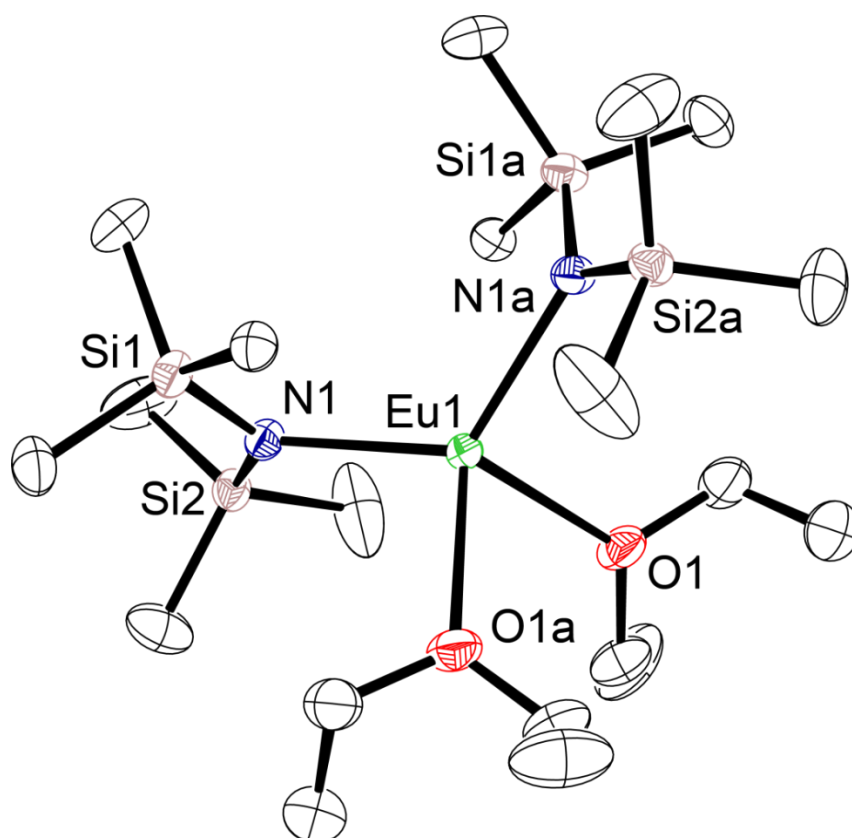


Supplementary Figure 3.1. Ortep representation (30% probability ellipsoids) of K[Eu(HMDS)₃] (3.1). Hydrogen atoms have been omitted for clarity.

[Eu(HMDS)₂(Et₂O)] (3.2)

A colourless Et₂O solution of KHMDS (759 mg, 3.80 mmol) was added to a suspension of EuI₂ (814 mg, 2.00 mmol) in Et₂O in a scintillation vial inside the glovebox. The mixture was left stir for 2 days at room temperature, affording an orange solution and a pale yellow precipitate. The solution was filtered through Celite, and the volatiles removed under vacuum. Yellow plates suitable for an X-ray diffraction experiment were obtained from a saturated hexane solution at −30 °C (Isolated yield: 1055 mg, 85%).

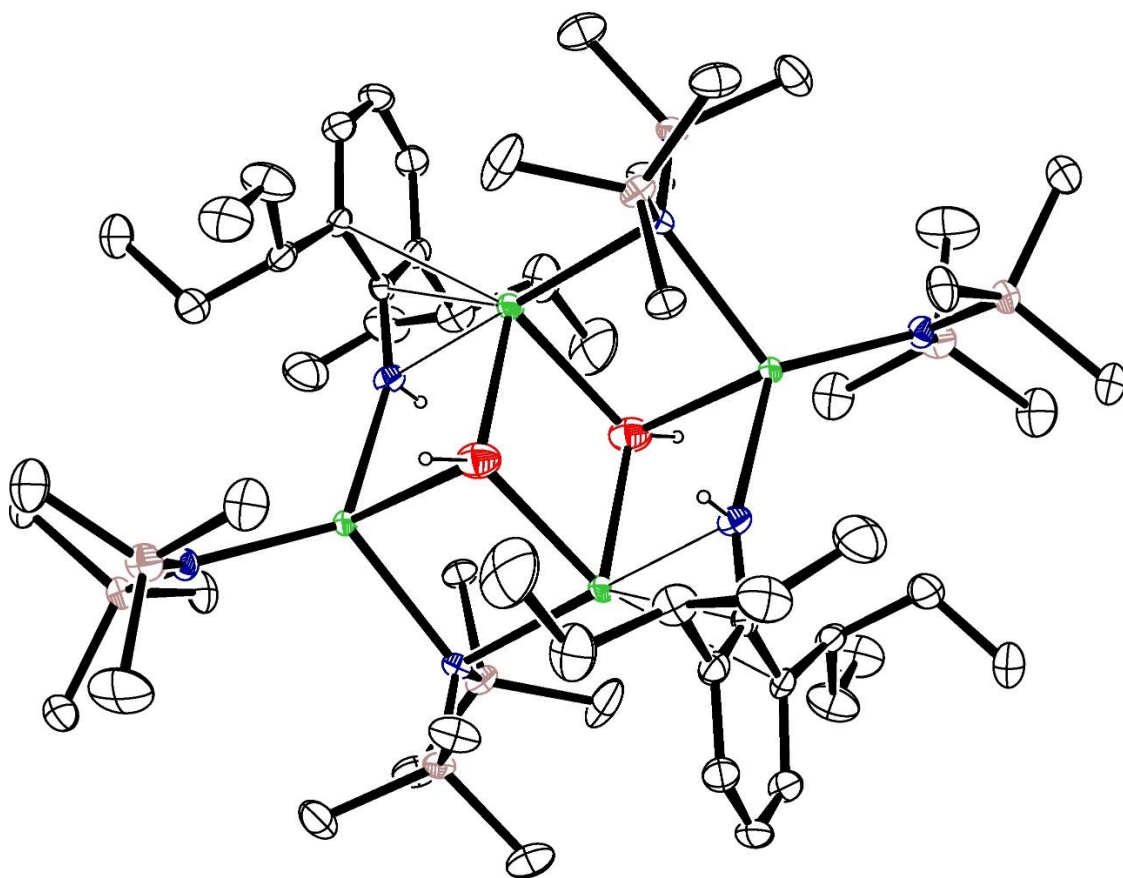
The paramagnetic nature of [Eu(HMDS)₂(Et₂O)] hampered characterisation by multinuclear NMR spectroscopic techniques.



Supplementary Figure 3.2. Ortep representation (30% probability ellipsoids) of [Eu(HMDS)₂(Et₂O)₂] (3.1). Hydrogen atoms have been omitted for clarity.

Attempted Synthesis of $[(\text{BDI}^{\text{Dipep}})\text{EuN}(\text{SiMe}_3)_2]$

Both $[\text{Eu}(\text{HMDS})_2(\text{Et}_2\text{O})_2]$ (490 mg, 0.79 mmol) and $(\text{BDI}^{\text{Dipep}})\text{H}$ (377 mg, 0.71 mmol) were added to an ampoule in toluene solvent and stirred for 1 week at 80 °C. The resultant orange solution was dried under vacuum and the ampoule transferred into the glovebox. The crude orange solid was recrystallised from hexane at room temperature, yielding yellow crystals suitable for an X-ray diffraction experiment.



Supplementary Figure 3.3. Ortep representation (30% probability ellipsoids) of compound **3.3**, isolated from the attempted synthesis of $[(\text{BDI}^{\text{Dipep}})\text{EuN}(\text{SiMe}_3)_2]$. Hydrogen atoms (except those on the oxygen atoms and nitrogen atoms of the Dipec substituents) have been omitted for clarity.

[(BDI^{Dipep})EuI]₂ (3.4)

A colourless Et₂O solution of (BDI^{Dipep})K (300 mg, 0.53 mmol) was added to a pale green-yellow suspension of EuI₂ (214 mg, 0.53 mmol) in Et₂O and the resulting orange-yellow mixture was left to react for 2 days at room temperature. The solvent was removed *in vacuo*, the crude product extracted with hexane and filtered through celite. Yellow crystals suitable for an X-ray diffraction experiment were obtained from a saturated hexane solution at room temperature (324 mg, 75%).

The paramagnetic nature of [(BDI^{Dipep})EuI]₂ hampered characterisation by multinuclear NMR spectroscopic techniques.

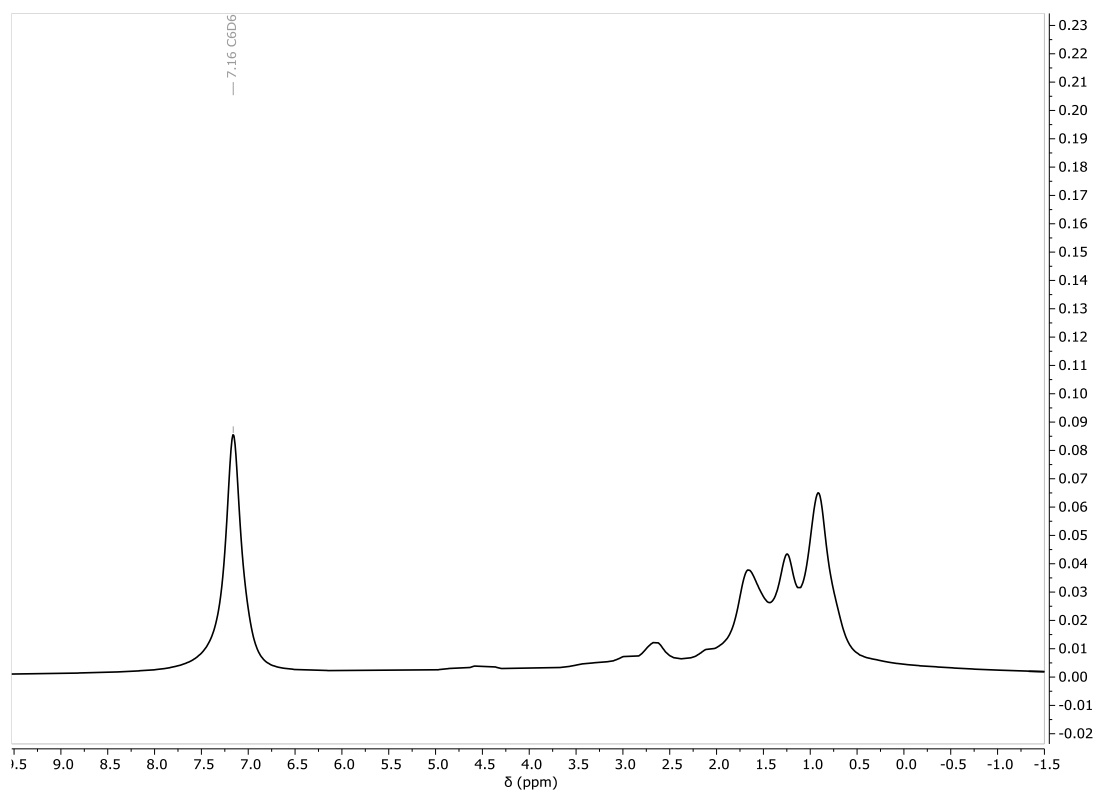
M.p: 251–260 °C (dec.).

IR (cm⁻¹): 3054 (w), 2958 (s), 2922 (s), 2870 (s), 2851 (s), 1621 (s), 1550 (s), 1524 (m), 1447 (s), 1395 (s), 1337 (s), 1361 (s), 1343 (s), 1267 (s), 1212 (w), 1165 (s), 1142 (w), 1099 (m), 1019 (m), 925 (s), 861 (w), 828 (m), 782 (s), 751 (s), 703 (w).

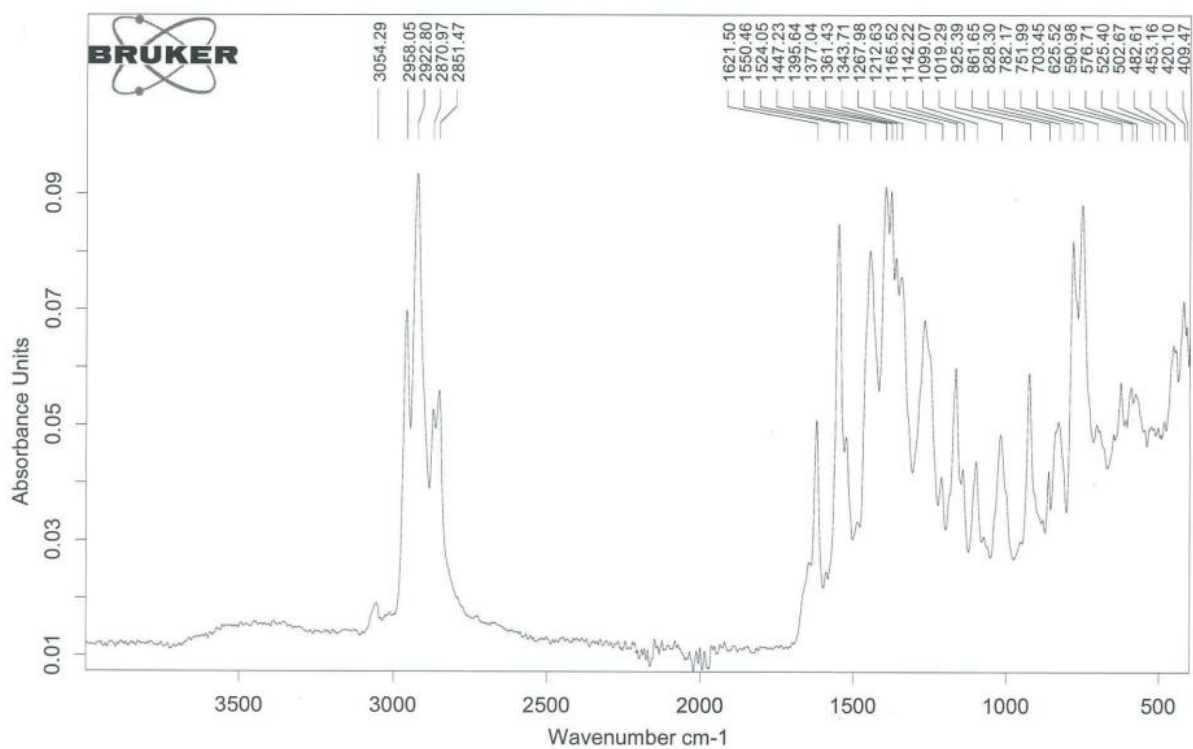
Elemental analysis for [(BDI^{Dipep})EuI]₂ (1617.5 g mol⁻¹):

Calculated: C: 54.95, H: 7.10, N: 3.46 %.

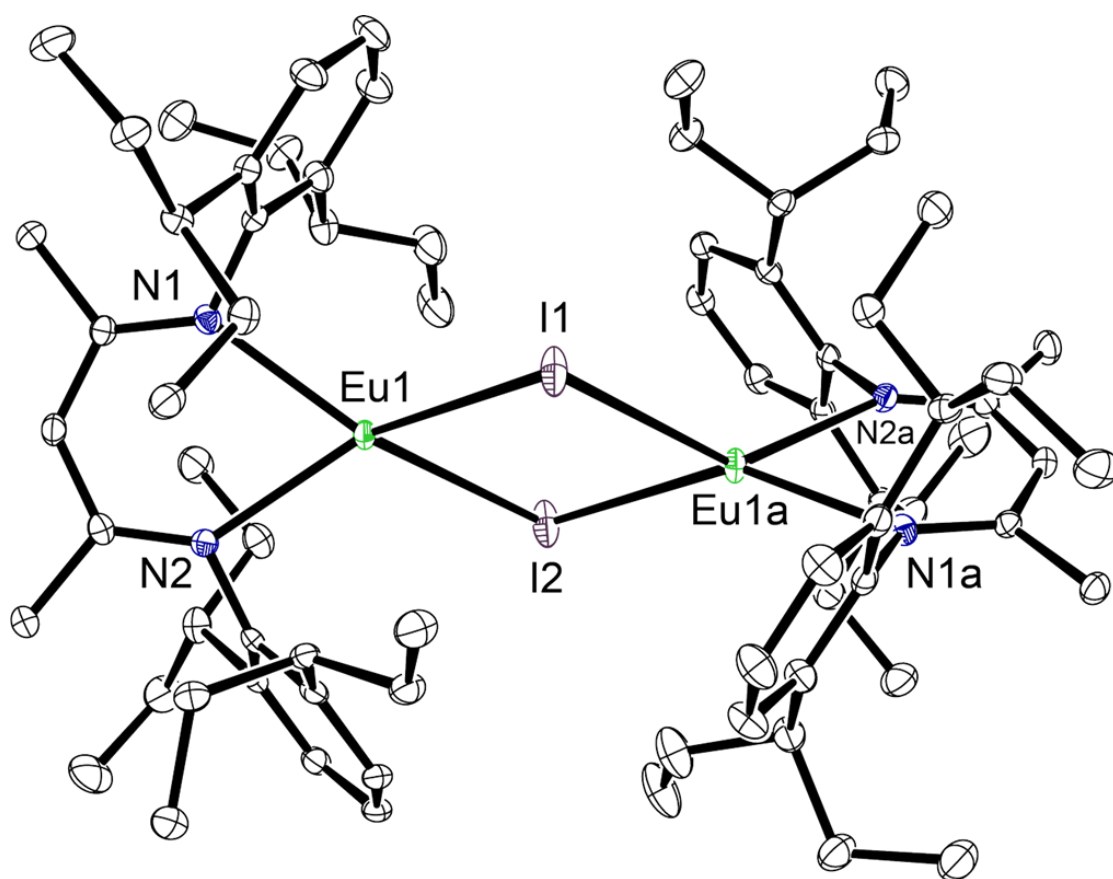
Found: C: 56.91, H: 7.49, N: 3.76 %.



Supplementary Figure 3.4. ^1H NMR spectrum (500 MHz, C_6D_6) of $[(\text{BDI}^{\text{Dipep}})\text{EuI}]_2$ (**3.4**).



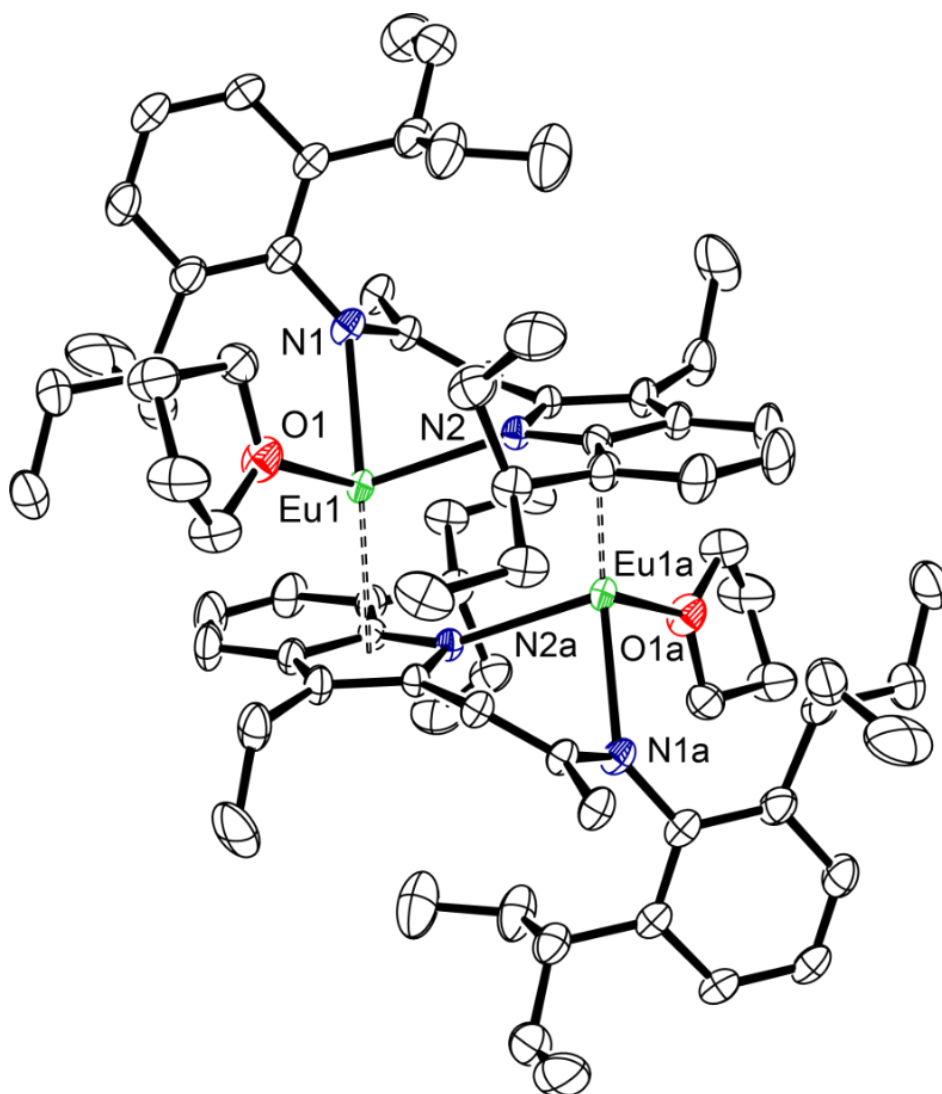
Supplementary Figure 3.5. Infrared spectrum of $[(\text{BDI}^{\text{Dipep}})\text{EuI}]_2$ (**3.4**).



Supplementary Figure 3.6. Ortep representation (30% probability ellipsoids) of $[(\text{BDI}^{\text{Dipep}})\text{EuI}]_2$ (**3.4**). Hydrogen atoms have been omitted for clarity.

Attempted Synthesis of $[(\text{BDI}^{\text{Dipep}})\text{EuN}(\text{SiMe}_3)_2]$

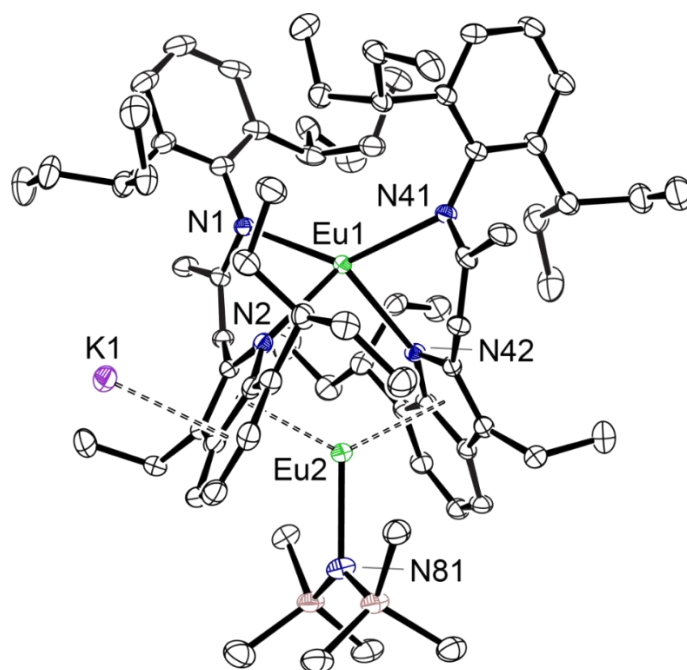
Both $[(\text{BDI}^{\text{Dipep}})\text{EuI}]_2$ (246 mg, 0.15 mmol) and KHMDS (58 mg, 0.30 mmol) were added to a scintillation vial in Et_2O and left to stir for overnight at room temperature, to give a yellow solution with a pale precipitate. The volatiles were removed *in vacuo*, the crude mixture was extracted with hexane and filtered through celite. Yellow crystals suitable for an X-ray diffraction experiment were obtained from a saturated hexane solution at $-30\text{ }^\circ\text{C}$.



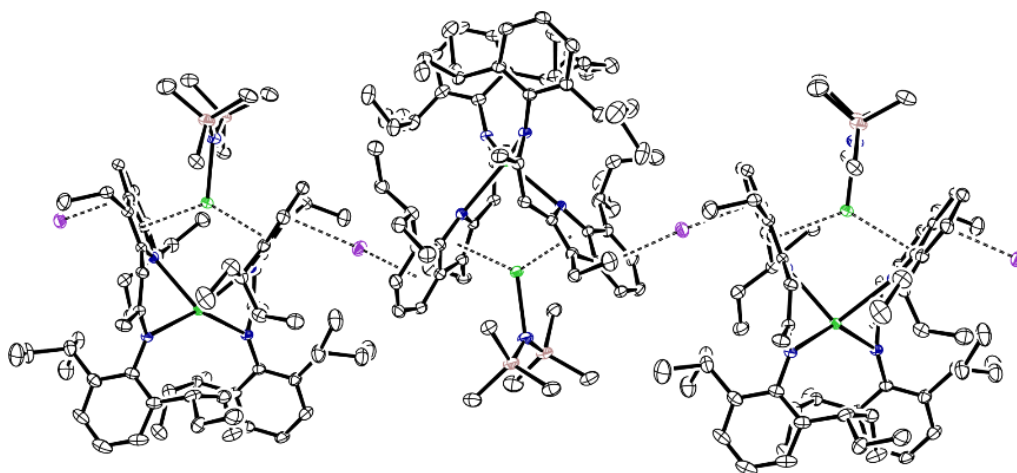
Supplementary Figure 3.7. Ortep representation (30% probability ellipsoids) of compound **3.5**, isolated from the attempted synthesis of $[(\text{BDI}^{\text{Dipep}})\text{EuN}(\text{SiMe}_3)_2]$. Hydrogen atoms have been omitted for clarity.

Attempted Synthesis of $[(\text{BDI}^{\text{Dipep}})\text{EuN}(\text{SiMe}_3)_2]$

Both $[(\text{BDI}^{\text{Dipep}})\text{EuI}]_2$ (118 mg, 0.07 mmol) and KHMDS (29 mg, 0.14 mmol) were added to a scintillation vial in toluene and left to stir overnight at room temperature, to give a yellow solution with a pale precipitate. The volatiles were removed *in vacuo*, the crude mixture was extracted with hexane and filtered through celite. Yellow crystals suitable for an X-ray diffraction experiment were obtained from a saturated hexane solution at $-30\text{ }^\circ\text{C}$.



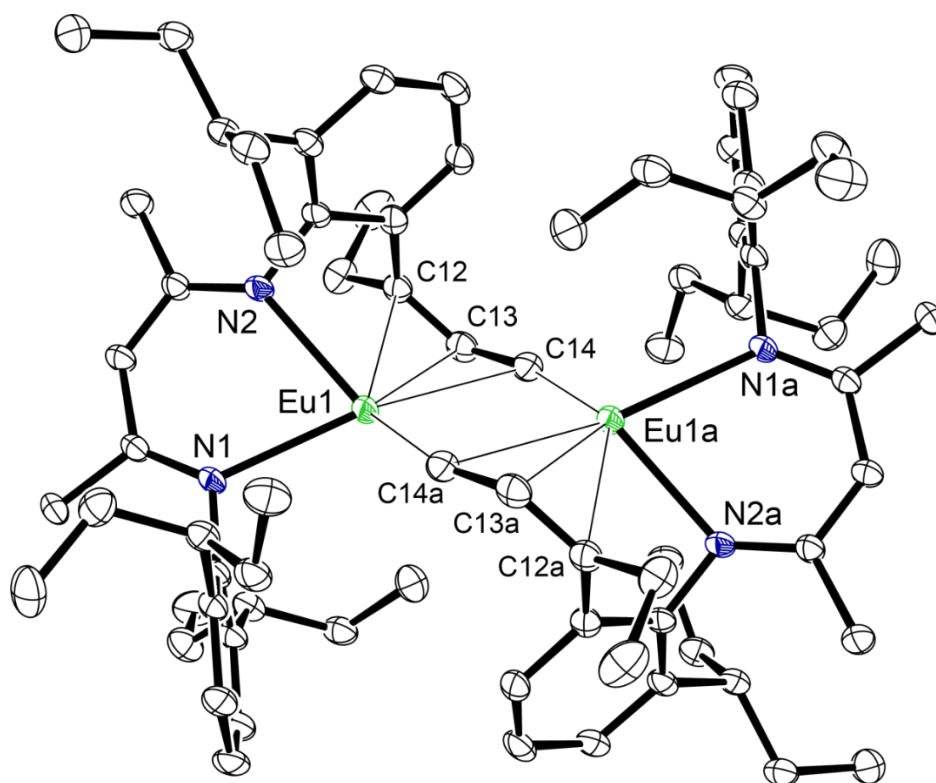
Supplementary Figure 3.8. Ortep representation (30% probability ellipsoids) of compound **3.6**, isolated from the attempted synthesis of $[(\text{BDI}^{\text{Dipep}})\text{EuN}(\text{SiMe}_3)_2]$. Hydrogen atoms have been omitted for clarity.



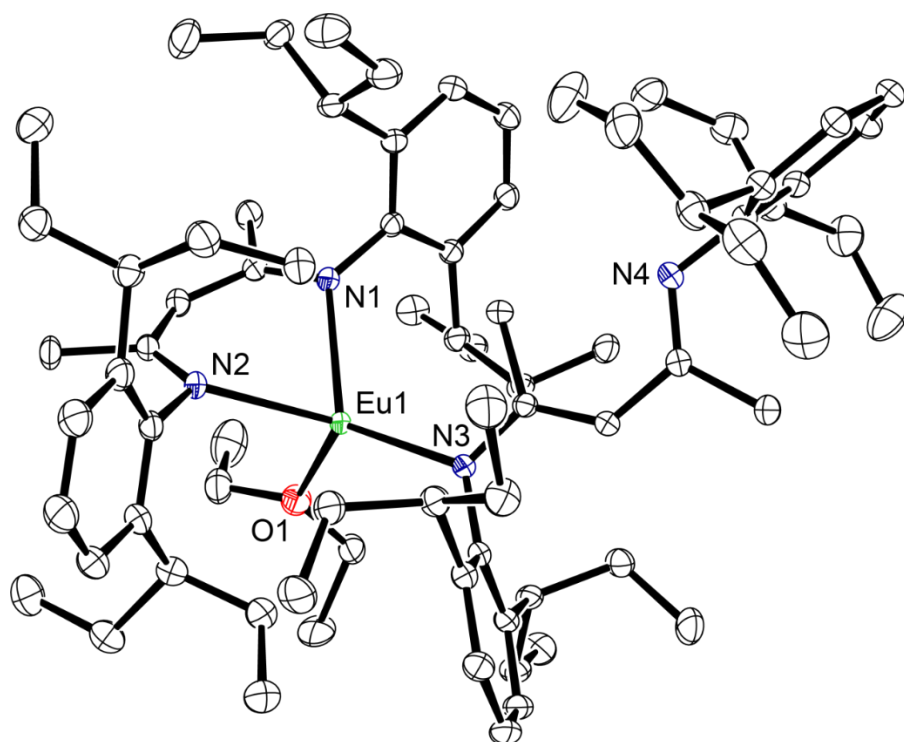
Supplementary Figure 3.9. Ortep representation (30% probability ellipsoids) of the pseudo polymer of compound **3.6**, isolated from the attempted synthesis of $[(\text{BDI}^{\text{Dipep}})\text{EuN}(\text{SiMe}_3)_2]$. Hydrogen atoms have been omitted for clarity.

Attempted Synthesis of $[(\text{BDI}^{\text{Dipep}})\text{EuCH}(\text{SiMe}_3)_2]$

The $[(\text{BDI}^{\text{Dipep}})\text{EuI}]_2$ (1395 mg, 0.86 mmol) was added to a Schlenk flask in Et_2O solvent, while the $\text{KCH}(\text{SiMe}_3)_2$ (325 mg, 1.63 mmol) was added to a separate Schlenk flask in Et_2O solvent. Both Schlenk flasks were transferred out of the glovebox and hooked up to a Schlenk line and cooled to $-78\text{ }^\circ\text{C}$ in a dry ice bath. The red Et_2O solution containing the $\text{KCH}(\text{SiMe}_3)_2$ was added dropwise *via* cannula transfer to the flask containing $[(\text{BDI}^{\text{Dipep}})\text{EuI}]_2$ and the resultant mixture was left to slowly warm up to room temperature. The volatiles were removed under vacuum and the crude product redissolved into a pentane/toluene mix and left to crystallise at room temperature, affording yellow crystals suitable for an X-ray diffraction experiment.



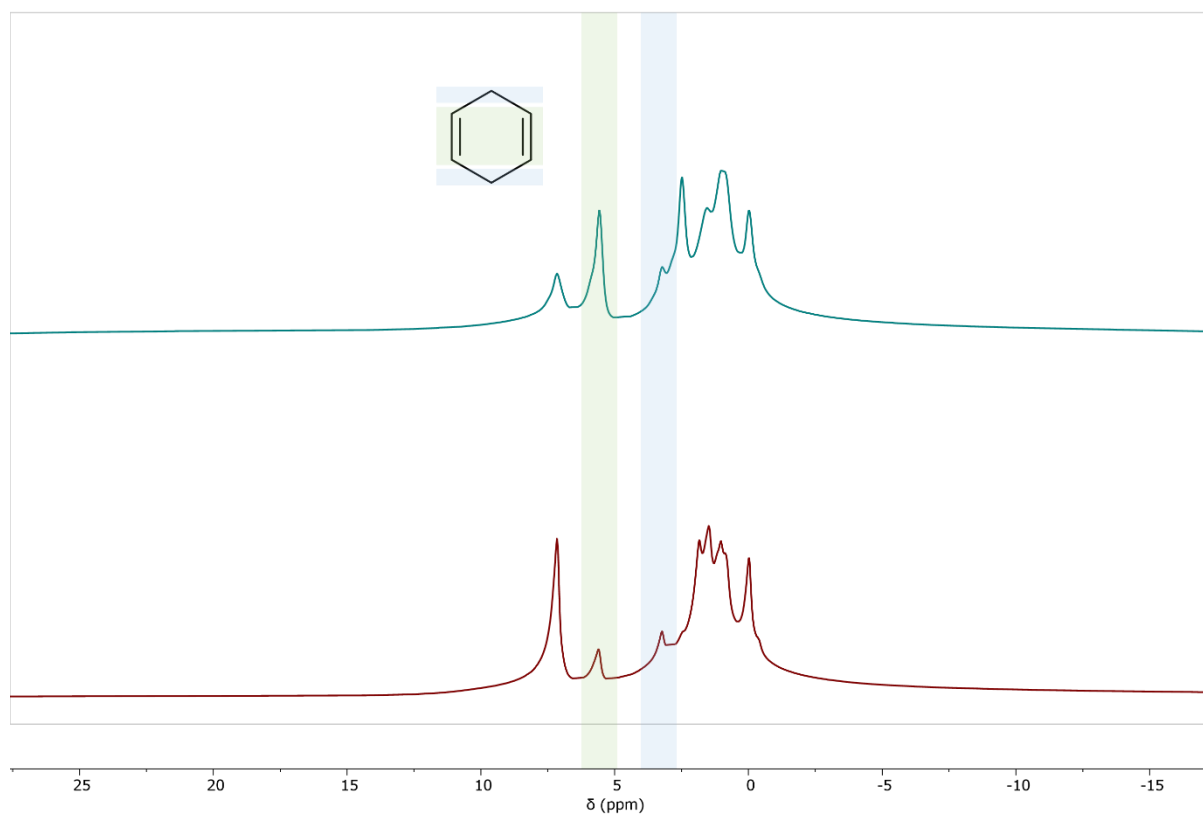
Supplementary Figure 3. 10. Ortep representation (30% probability ellipsoids) of compound **3.7**, isolated from the attempted synthesis of $[(\text{BDI}^{\text{Dipep}})\text{EuCH}(\text{SiMe}_3)_2]$. Hydrogen atoms have been omitted for clarity.



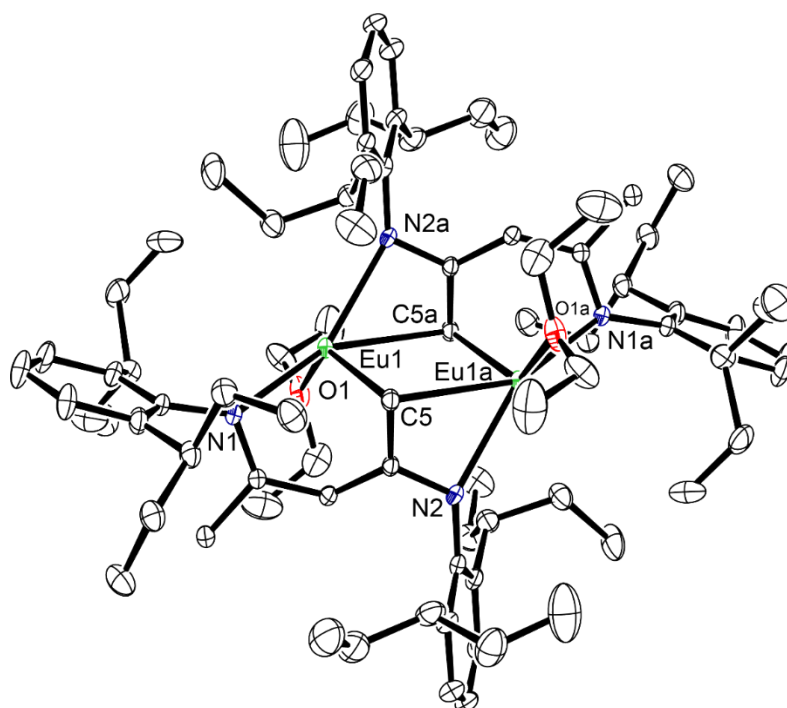
Supplementary Figure 3.11. Ortep representation (30% probability ellipsoids) of $[(\text{BDI}^{\text{Dipep}})_2\text{Eu}(\text{Et}_2\text{O})]$ (**3.8**), isolated from the attempted recrystallisation of compound **3.7**. Hydrogen atoms have been omitted for clarity.

Attempted synthesis of [(BDI^{Dipep})EuH]₂

Both [(BDI^{Dipep})₂Eu₂] (**3.7**) (159 mg, 0.12 mmol) and 1,4-CHD (9 mg, 0.12 mmol) were added to an NMR tube fitted with a J. Youngs tap in C₆D₆ solvent and monitored the reaction progress *via* ¹H NMR analysis. After heating for 4 days at 60 °C, the starting material peaks had decreased in the ¹H NMR spectrum, so the NMR tube was transferred to the glovebox. The volatiles were removed *in vacuo*, the product dissolved into Et₂O, filtered through Celite and left to crystallise at room temperature, affording yellow crystals suitable for an X-ray diffraction experiment.



Supplementary Figure 3.12. Stacked ^1H NMR spectra (500 MHz, C_6D_6) of **3.7** immediately after the addition of 1,4-CHD (top) and after 4 days at 60 °C (bottom), highlighting the proton environments for the 1,4-CHD reagent.



Supplementary Figure 3.13. Ortep representation (30% probability ellipsoids) of compound **3.9**, isolated from the attempted synthesis of $[(\text{BDI}^{\text{Dipep}})\text{EuH}]_2$. Hydrogen atoms have been omitted for clarity.

[(BDI^{Dicyp})Eu(I)₂Eu(THF)(BDI^{Dicyp})] (3.10)

A colourless THF solution of (BDI^{Dicyp})K (291 mg, 0.47 mmol) was added to a pale green-yellow suspension of EuI₂ (191 mg, 0.47 mmol) in THF and the resulting orange-yellow mixture was left to react for 4 hours at room temperature. The solvent was removed *in vacuo*, the crude product extracted with toluene and filtered through celite. Yellow crystals suitable for an X-ray diffraction experiment were obtained from a saturated toluene solution at room temperature (363 mg, 90%).

The paramagnetic nature of [(BDI^{Dicyp})EuI]₂ hampered characterisation by multinuclear NMR spectroscopic techniques.

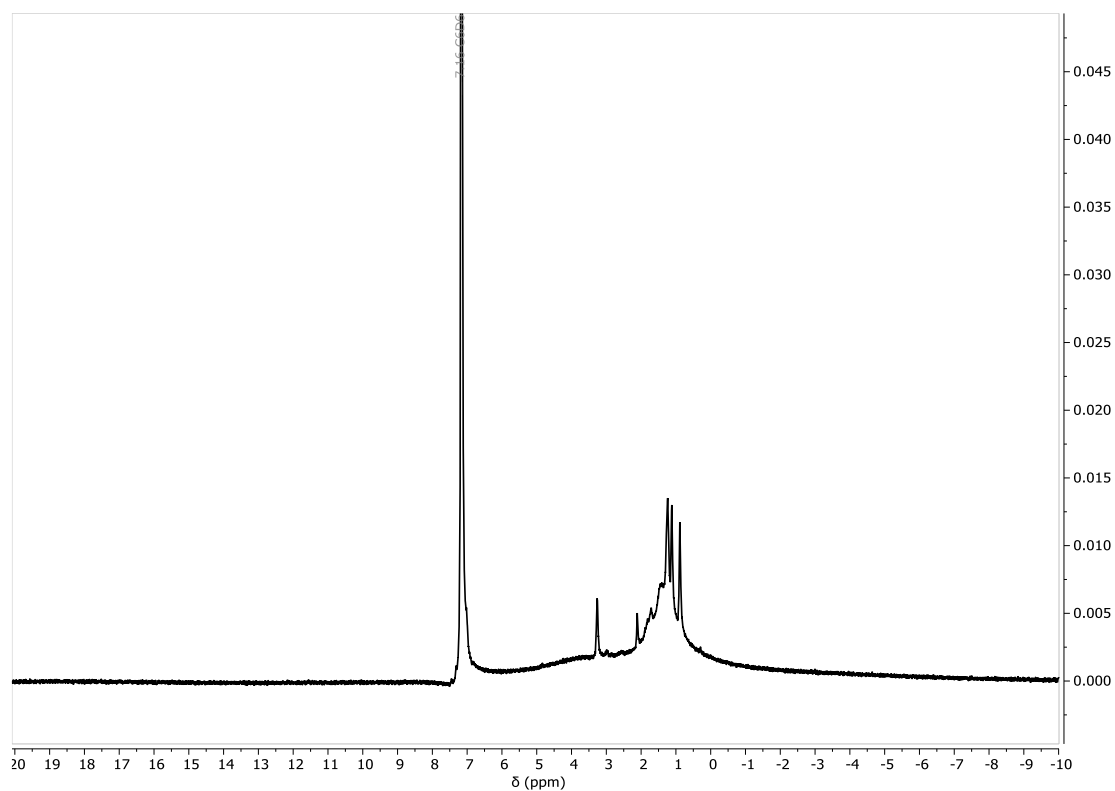
M.p: >260 °C (dec.).

IR (cm⁻¹): 3057 (w), 2920 (s), 2848 (s), 2666 (w), 1621 (m), 1551 (s), 1525 (w), 1494 (w), 1445 (m), 1394 (s), 1351 (m), 1302 (m), 1270 (m), 1210 (w), 1163 (m), 1130 (w), 1080 (w), 1018 (m), 997 (w), 926 (m), 889 (m), 841 (w), 785 (w), 775 (m), 763 (s).

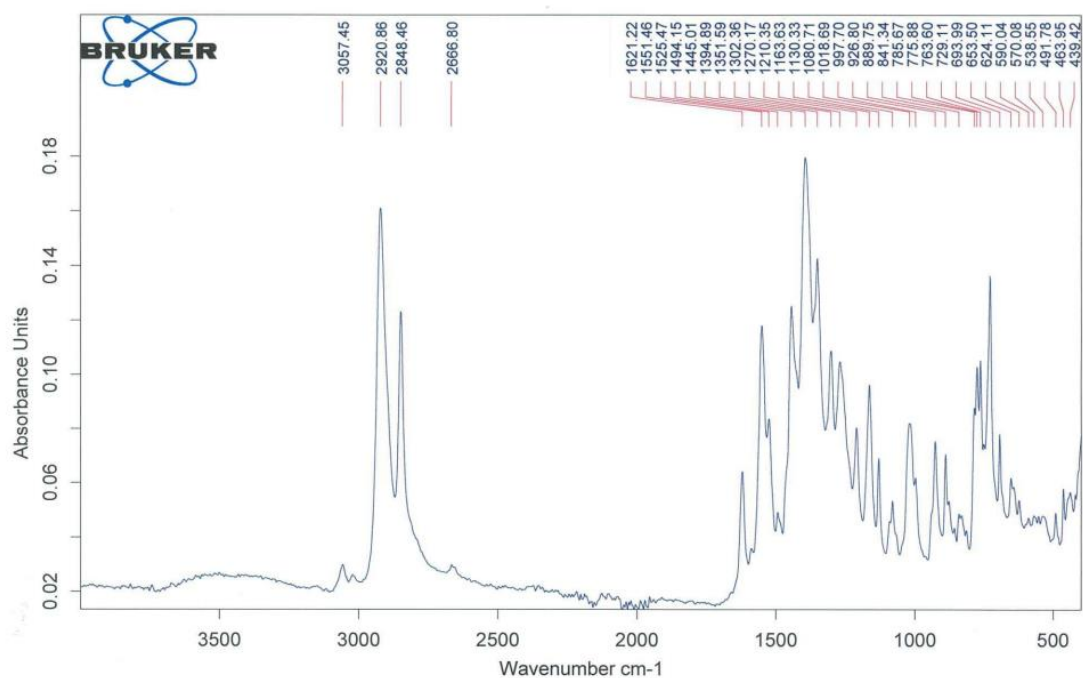
Elemental analysis for [(BDI^{Dicyp})EuI]₂ (1713.6 g mol⁻¹):

Calculated: C: 57.48, H: 6.71, N: 3.27 %.

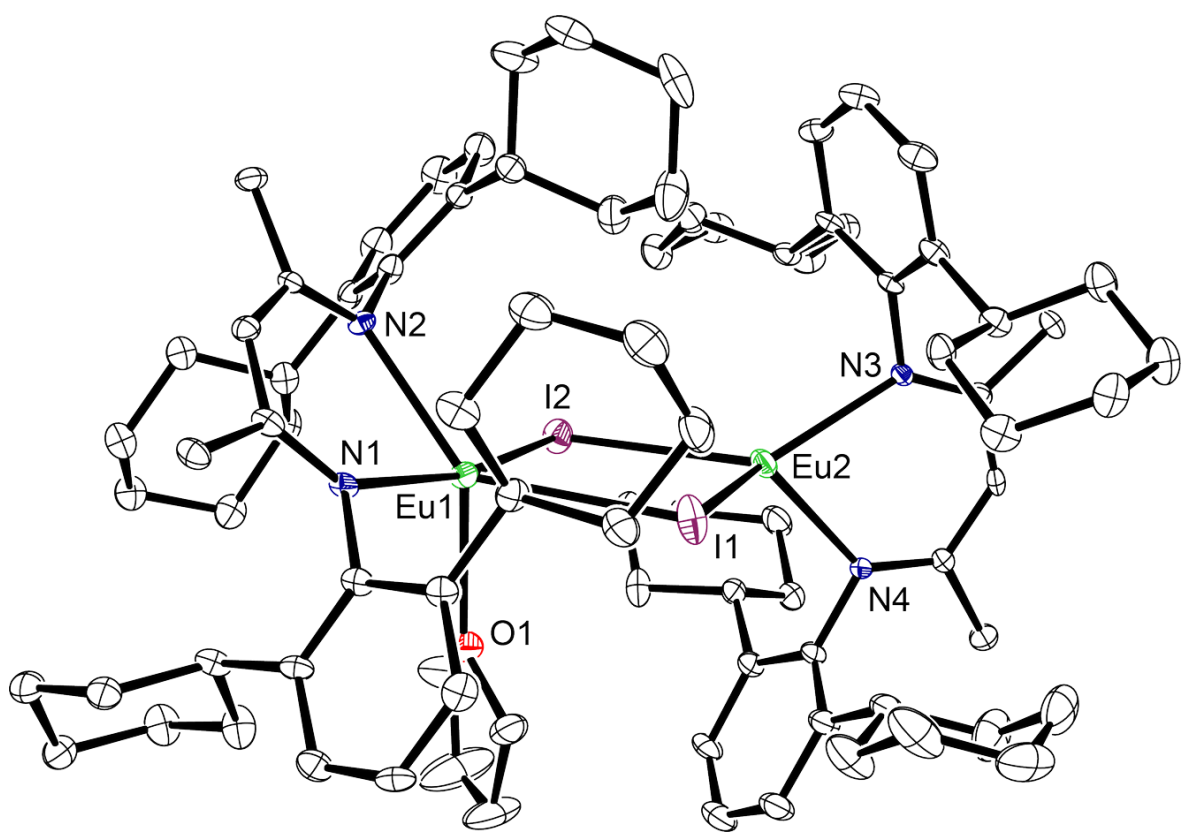
Found: C: 56.22, H: 6.70, N: 3.19 %.



Supplementary Figure 3.14. ^1H NMR spectrum (500 MHz, C_6D_6) of $[(\text{BDI}^{\text{Dicyl}})\text{Eu}(\text{I})_2\text{Eu}(\text{THF})(\text{BDI}^{\text{Dicyl}})]$ (**3.10**).



Supplementary Figure 3.15. Infrared spectrum $[(\text{BDI}^{\text{Dicyl}})\text{Eu}(\text{I})_2\text{Eu}(\text{THF})(\text{BDI}^{\text{Dicyl}})]$ (**3.10**).



Supplementary Figure 3.16. Ortep representation (30% probability ellipsoids) of $[(\text{BDI}^{\text{Dicyl}})\text{Eu}(\text{I})_2\text{Eu}(\text{THF})(\text{BDI}^{\text{Dicyl}})]$ (**3.10**). Hydrogen atoms have been omitted for clarity.

$[(\text{BDI}^{\text{DicyP}})\text{EuCH}(\text{SiMe}_3)_2]$ (3.11)

A red THF solution of $\text{KCH}(\text{SiMe}_3)_2$ (55.5 mg, 0.28 mmol) was added to an orange THF solution of $[(\text{BDI}^{\text{DicyP}})\text{EuI}]_2$ (239.6 mg, 0.14 mmol) while stirring and left to react for 15 minutes at room temperature. The orange mixture was dried *in vacuo*, the residue extracted with hexane and filtered through Celite. Yellow crystals suitable for an X-ray diffraction experiment was obtained from a saturated hexane solution at $-30\text{ }^\circ\text{C}$ (80.5 mg, 32%).

The paramagnetic nature of $[(\text{BDI}^{\text{DicyP}})\text{EuCH}(\text{SiMe}_3)_2]$ hampered characterisation by multinuclear NMR spectroscopic techniques.

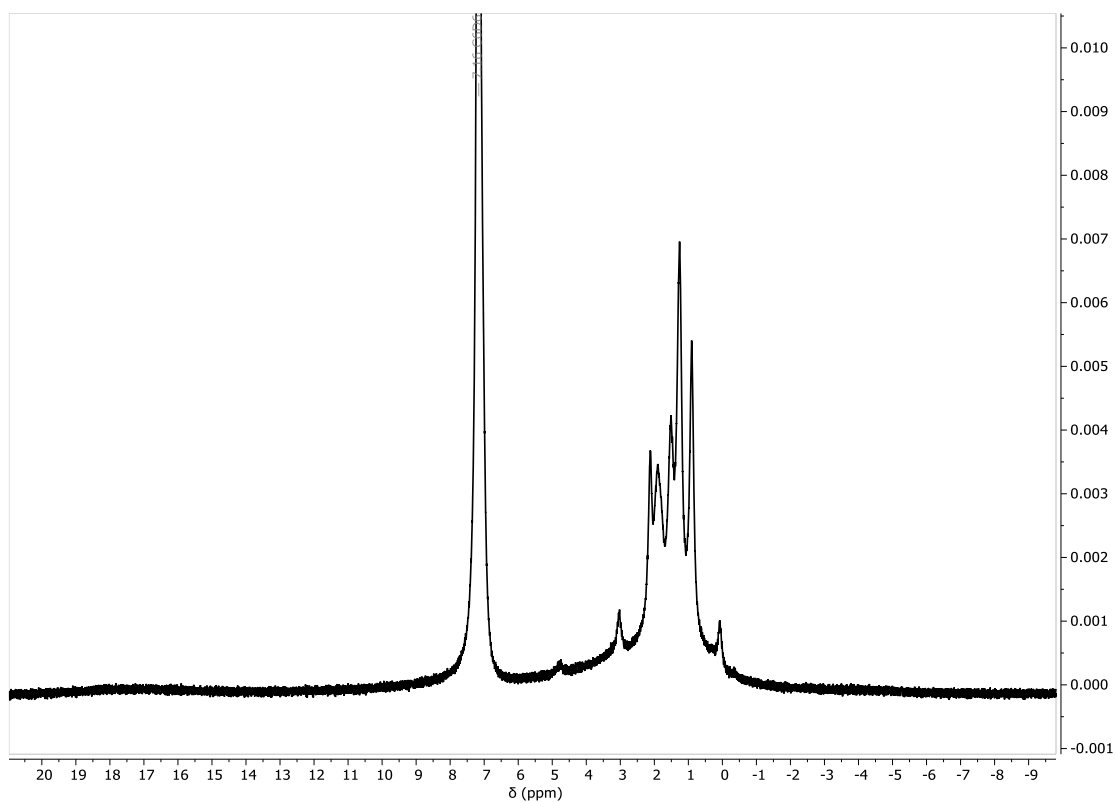
M.p: $168\text{--}176\text{ }^\circ\text{C}$ (dec.).

IR (cm^{-1}): 3061 (w), 2992 (s), 2849 (s), 1622 (m), 1551 (s), 1445 (s), 1398 (m), 1351 (m), 1304 (w), 1249 (m), 1211 (w), 1165 (w), 1131 (w), 1081 (w), 1050 (w), 1021 (w), 927 (w), 890 (w), 839 (s).

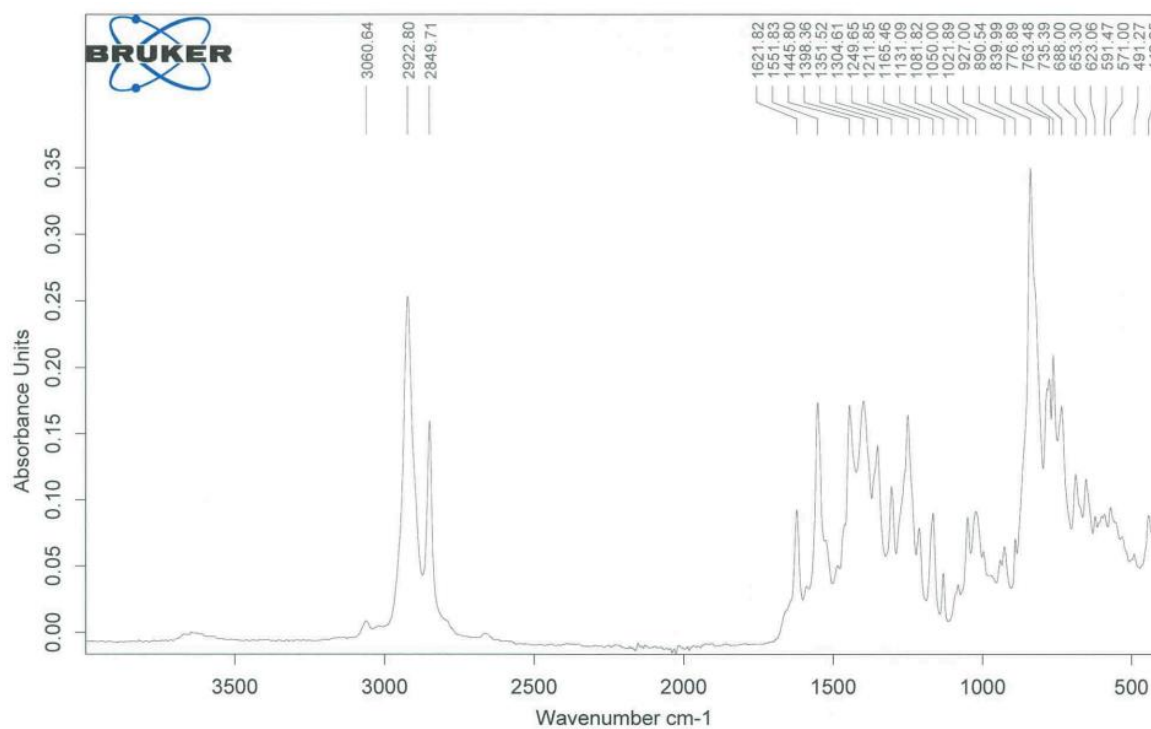
Elemental Analysis for $[(\text{BDI}^{\text{DicyP}})\text{EuCH}(\text{SiMe}_3)_2]$ (889.3 g mol^{-1}):

Calculated: C: 64.83, H: 8.61, N: 3.15 %.

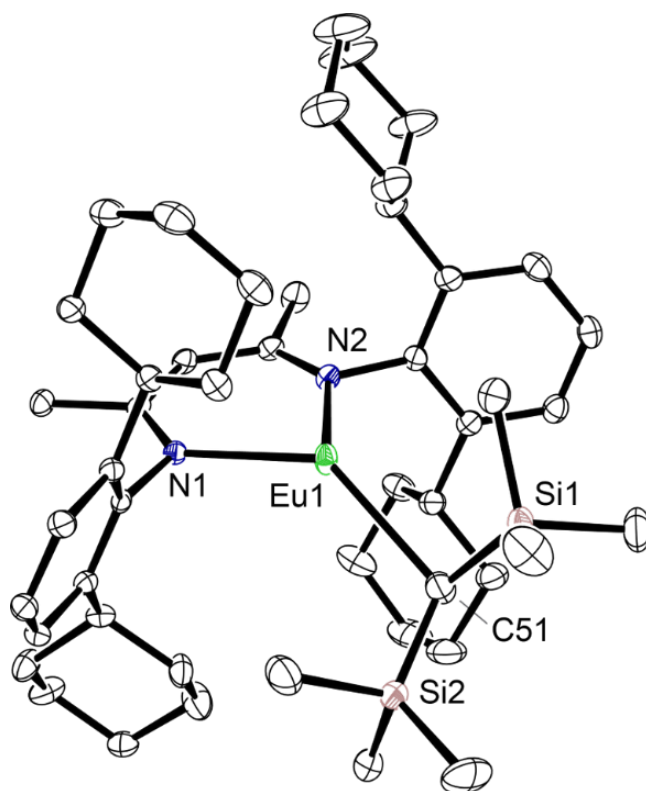
Found: C: 64.19, H: 8.09, N: 3.29 %.



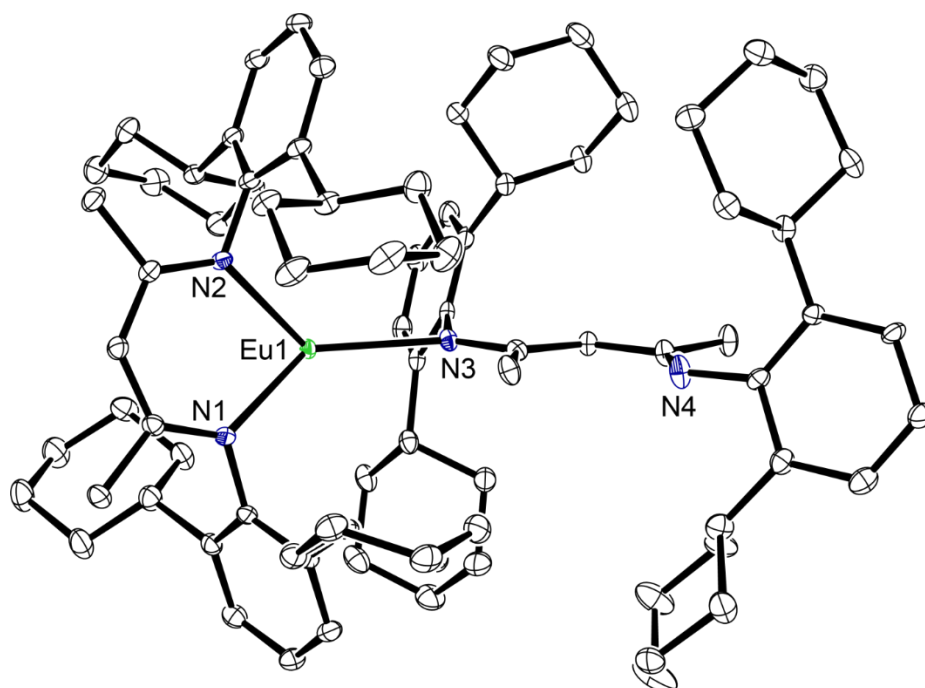
Supplementary Figure 3.17. ^1H NMR spectrum (500 MHz, C_6D_6) of $[(\text{BDI}^{\text{Dicyl}})\text{EuCH}(\text{SiMe}_3)]$ (**3.11**).



Supplementary Figure 3.18. Infrared spectrum of $[(\text{BDI}^{\text{Dicyl}})\text{EuCH}(\text{SiMe}_3)]$ (**3.11**).



Supplementary Figure 3.19. Ortep representation (ellipsoid 30% probability) of $[(\text{BDI}^{\text{Dicyp}})\text{EuCH}(\text{SiMe}_3)]$ (**3.11**). Hydrogen atoms have been omitted for clarity.



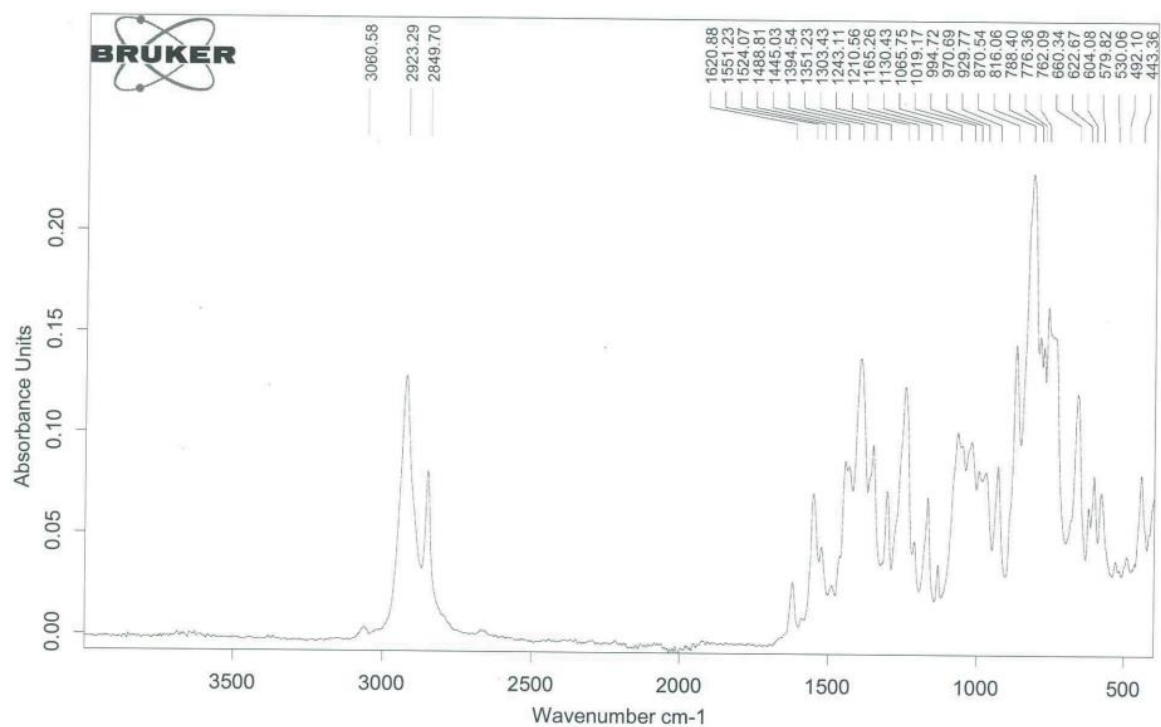
Supplementary Figure 3. 20. Ortep representation (ellipsoid 30% probability) of $[(\text{BDI}^{\text{Dicyp}})_2\text{Eu}]$ (**3.12**), isolated during the synthesis of compound **3.11**. Hydrogen atoms have been omitted for clarity.

$[(\text{BDI}^{\text{DicyP}})\text{EuN}(\text{SiMe}_3)_2]$ (3.13)

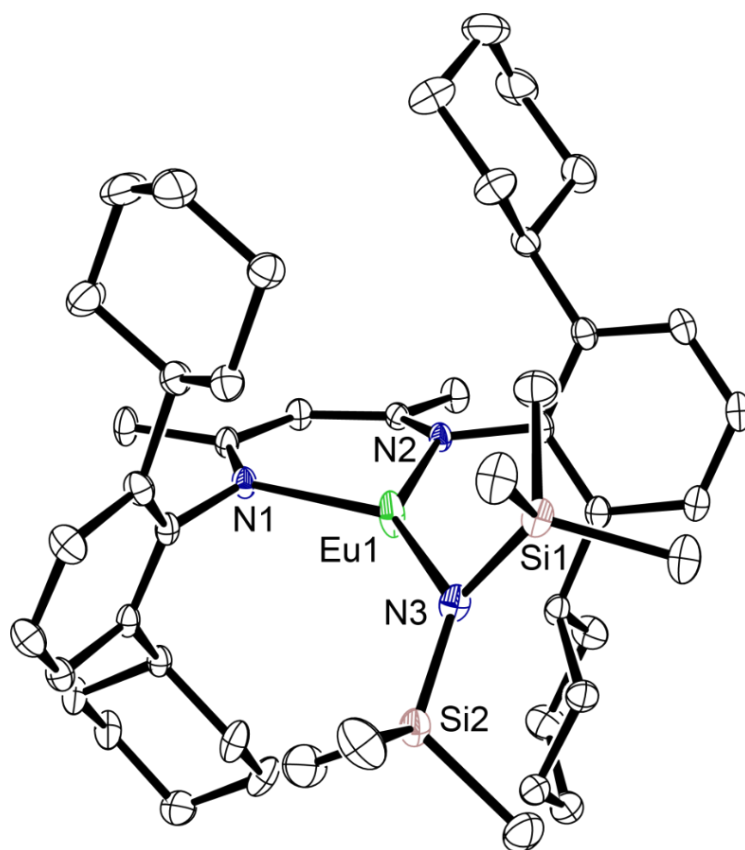
A red THF solution of $\text{KN}(\text{SiMe}_3)_2$ (136 mg, 0.68 mmol) was added to an orange THF solution of $[(\text{BDI}^{\text{DicyP}})\text{EuI}]_2$ (585 mg, 0.34 mmol) while stirring and left to react for 15 minutes at room temperature. The orange mixture was dried *in vacuo*, the residue extracted with hexane and filtered through Celite. Yellow crystals suitable for an X-ray diffraction experiment was obtained from a saturated hexane solution at room temperature (363 mg, 60%).

The paramagnetic nature of $[(\text{BDI}^{\text{DicyP}})\text{EuN}(\text{SiMe}_3)_2]$ hampered characterisation by multinuclear NMR spectroscopic techniques.

IR (cm⁻¹): 3060 (w), 2923 (s), 2849 (m), 1620 (w), 1551 (m), 1524 (w), 1488 (w), 1445 (w), 1394 (s), 1351 (w), 1303 (m), 1243 (s), 1210 (w), 1165 (m), 1130 (w), 1065 (w), 1019 (w), 994 (w), 970 (w), 929 (m), 870 (m), 816 (s), 788 (w), 776 (w), 762 (w), 660 (s).



Supplementary Figure 3.21. Infrared spectrum of [(BDI^{Dicyl})EuN(SiMe₃)] (**3.13**).



Supplementary Figure 3.22. Ortep representation (ellipsoid 30% probability) of [(BDI^{Dicyl})EuN(SiMe₃)] (**3.13**). Hydrogen atoms have been omitted for clarity.

[(BDI^{Dicyp})EuH]₂ (3.14)

A buffer toluene solution was gently layered on top of an orange toluene solution containing [(BDI^{Dicyp})EuCH(SiMe₃)₂] (523.0 mg, 0.59 mmol). A concentrated toluene containing 1,4-cyclohexadiene (94.2 mg, 1.18 mmol) was then gently layered on top of the buffer solution and the vial was left unmoved at room temperature with the vial lid cracked open. Small orange crystals suitable for a single crystal X-ray diffraction experiment were obtained over the course of 2 days (322.0 mg, 74.9%)

The paramagnetic nature and solubility of [(BDI^{Dicyp})EuH]₂ hampered characterisation by NMR spectroscopic techniques.

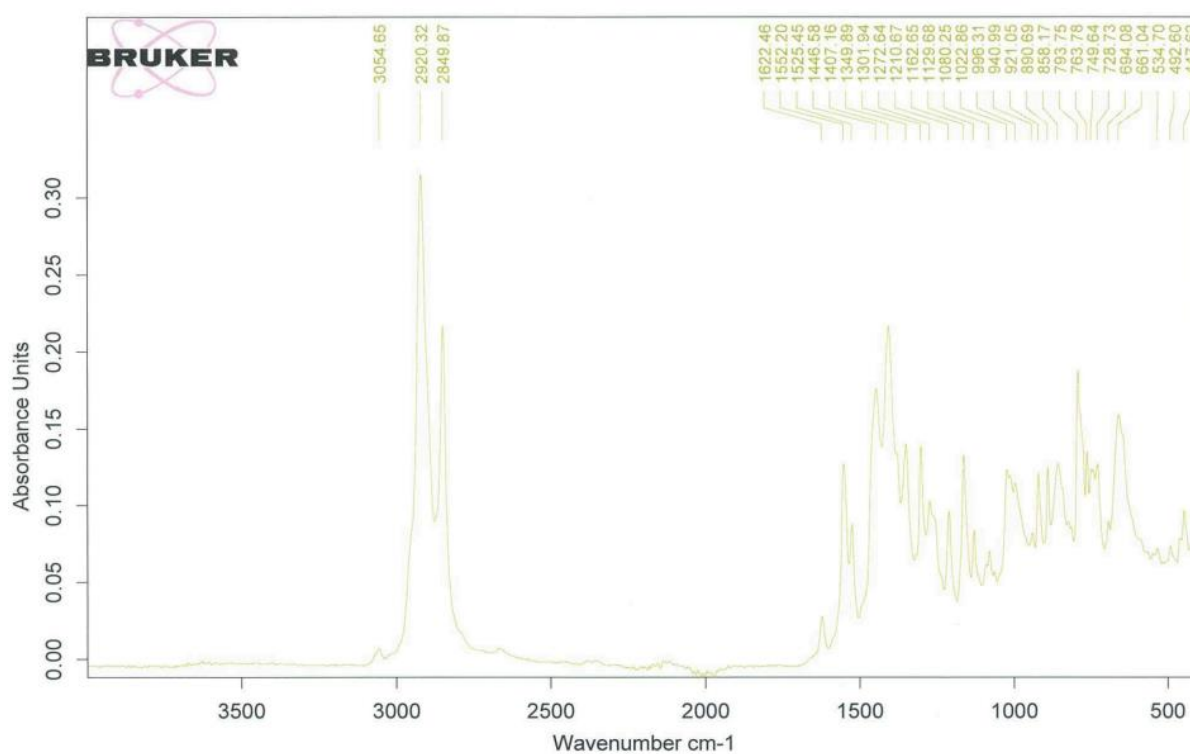
M.p: >260 °C (dec.).

IR (cm⁻¹): 3054 (w), 2920 (s), 2849 (s), 1622 (w), 1552 (m), 1525 (w), 1446 (m), 1407 (s), 1349 (w), 1301 (m), 1272 (w), 1210 (w), 1162 (m), 1129 (w), 1080 (w), 1022 (m), 996 (w), 940 (w), 921 (w), 890 (w), 858 (w), 793 (m), 763 (w), 749 (w), 728 (w), 694 (w), 661 (m).

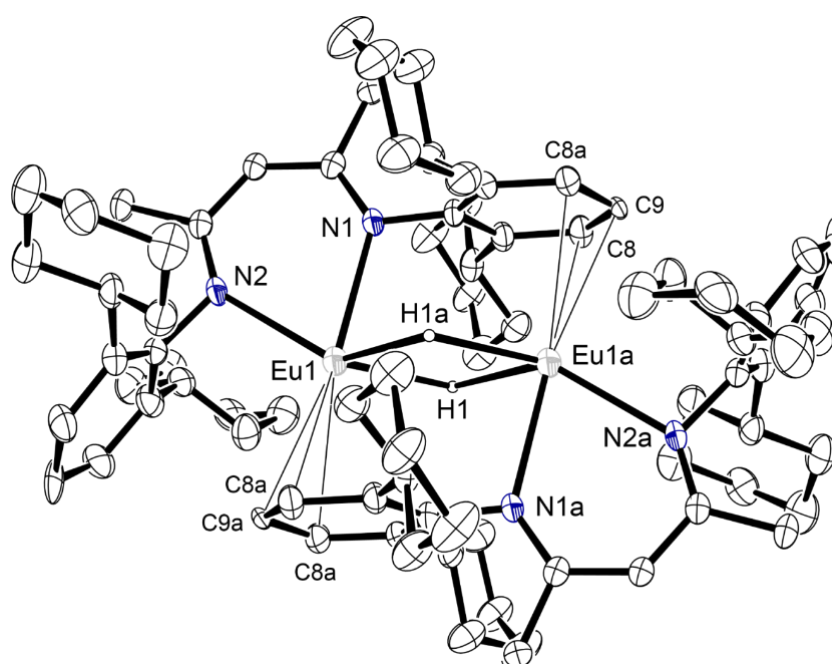
Elemental Analysis for [(BDI^{Dicyp})EuH]₂ (1461.79 g mol⁻¹):

Calculated: C: 67.38, H: 8.00, N: 3.83 %.

Found: C: 66.24, H: 7.93, N: 3.73 %.



Supplementary Figure 3.23. Infrared spectrum of $[(\text{BDI}^{\text{Dicyclopentadienyl}})\text{EuH}]_2$ (**3.14**).



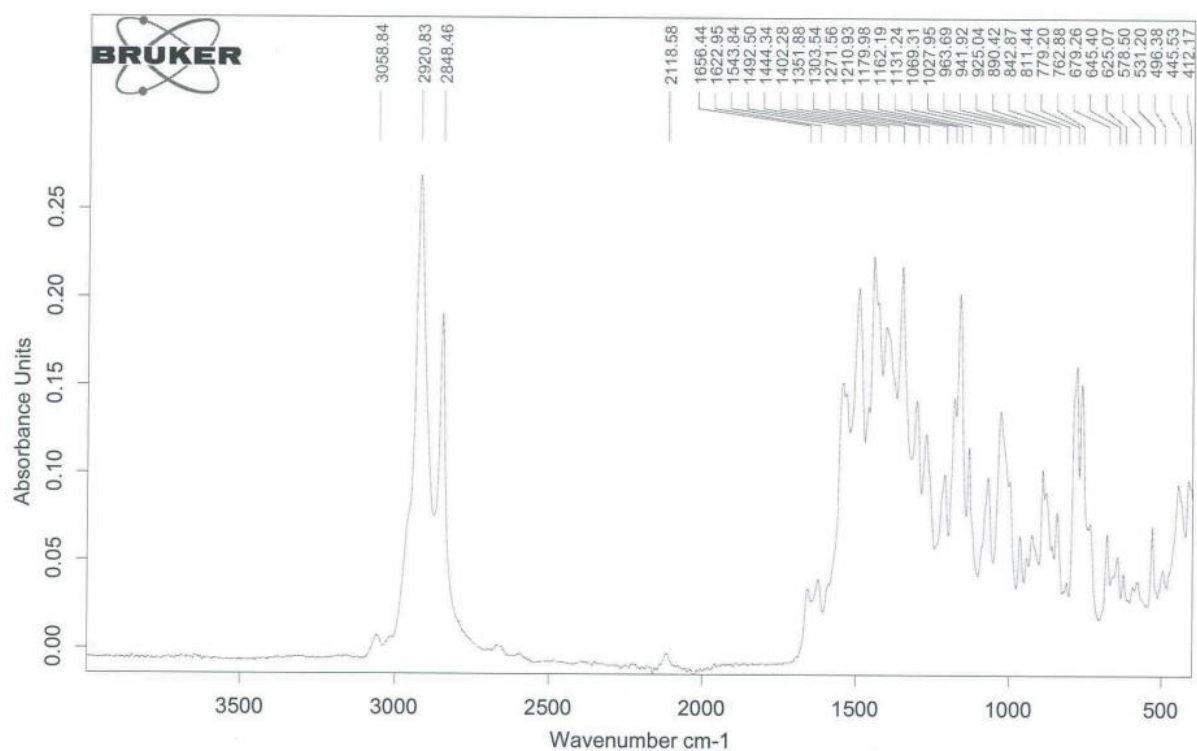
Supplementary Figure 3.24. Ortep representation (ellipsoid 30% probability) of $[(\text{BDI}^{\text{Dicyclopentadienyl}})\text{EuH}]_2$ (**3.14**). Hydrogen atoms (except the bridging H1 and H1a) have been omitted for clarity.

[(BDI^{Dicyp})Eu(DIC)] (3.15)

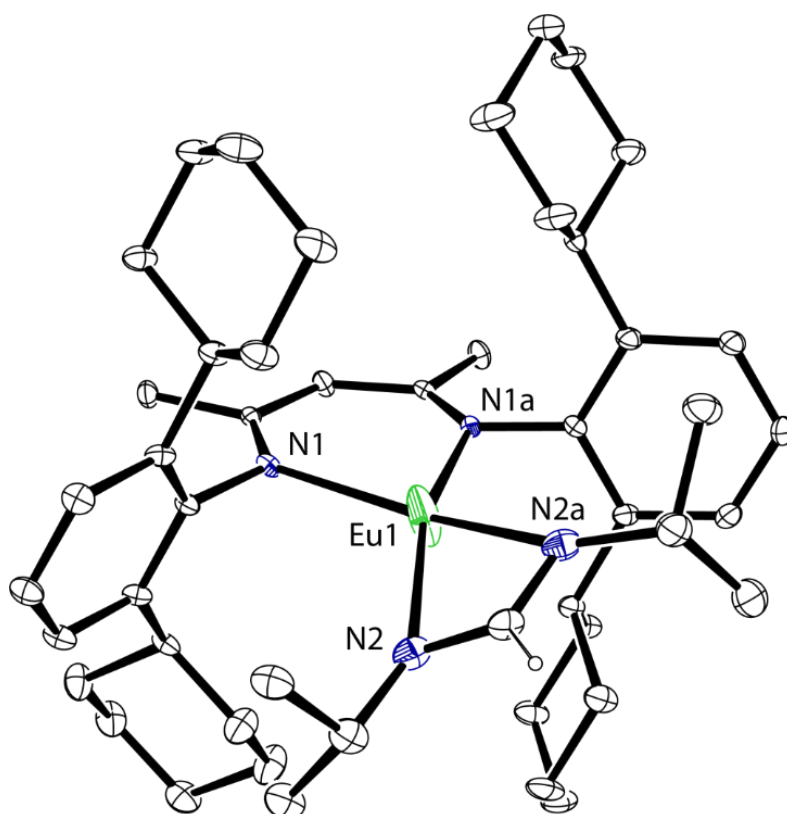
A colourless THF solution containing *N,N*-di-isopropylcarbodiimide (41 mg, 0.33 mmol) was added to a scintillation vial containing a red suspension of [(BDI^{Dicyp})EuH]₂ (239 mg, 0.16 mmol) in THF. The suspension was left to stir at room temperature for 3h, affording a yellow solution which was then dried under vacuum. Orange blocks suitable for an X-ray diffraction experiment were obtained from a saturated toluene solution at –30 °C (Isolated yield: 256 mg, 78%).

The paramagnetic nature of [(BDI^{Dicyp})Eu(DIC)] hampered characterisation by multinuclear NMR spectroscopic techniques.

IR (cm⁻¹): 3058 (w), 2920 (s), 2848 (s), 2118 (w), 1656 (w), 1622 (w), 1543 (w), 1492 (m), 1444 (m), 1402 (w), 1351 (m), 1303 (w), 1271 (w), 1210(w), 1179 (w), 1162 (s), 1131 (w), 1069 (m), 1027 (m), 963 (w), 941 (w), 925 (w), 890 (m), 842 (w), 811 (w), 779 (s), 762 (s).



Supplementary Figure 3.25. Infrared spectrum of $[(\text{BDI}^{\text{Dicyl}})\text{Eu}(\text{DIC})]$ (**3.15**).



Supplementary Figure 3.26. Ortep representation (ellipsoid 30% probability) of $[(\text{BDI}^{\text{Dicyl}})\text{Eu}(\text{DIC})]$ (**3.15**). Hydrogen atoms (except on the C atom of the DIC ligand) have been omitted for clarity.

(BDI^{Dipp,Dicyp})H (3.16)

Acetylacetone (2139 mg, 21.36 mmol), *p*-toluenesulfonic acid monohydrate (169 mg, 0.89 mmol) and one molar equivalent of 2,6-diisopropylaniline (3788 mg, 21.36 mmol) were dissolved in toluene and refluxed with a Dean Stark condenser for 24h. The solution was cooled, one molar equivalent of 2,6-dicyclohexylaniline (5500 mg, 21.36 mmol) and *p*-toluenesulfonic acid monohydrate (4064 mg, 21.36 mmol) were added and the mixture refluxed with a Dean Stark condenser for an additional 16h. After the resultant brown solution was cooled to room temperature, triethylamine (2160 mg, 21.36 mmol) was added, and the mixture stirred for 1h. The organic phase was washed twice with water, dried over MgSO₄ and the solvent was removed under vacuum. The resultant brown oil was stirred with methanol until crude product precipitated out as a white powder. Recrystallisation from a boiling ethanol/ethylacetate solution first afforded colourless blocks identified as (BDI^{Dicyp})H, with a second crop yielding colourless needles suitable for an X-ray diffraction experiment, identified as (BDI^{Dipp,Dicyp})H (4461 mg, 41.9%).

¹H NMR (500 MHz, C₆D₆) δ 12.27 (br, 1H, NH), 7.18 (m, 6H, ArH), 4.88 (s, 1H, NC(CH₃)CH), 3.34 (m, 2H, CH(CH₃)₂), 2.94 (m, 2H, Cy-CH), 1.84 (m, 10H, Cy-CH₂), 1.72, 1.67 (s, 3H, NC(CH₃)CH), 1.45 (m, 10H, Cy-CH₂), 1.27, 1.21 (d, *J* = 6.8 Hz, 6H, CH(CH₃)₂).

¹³C{¹H} NMR (126 MHz, C₆D₆) δ 162.2, 161.0 (NC(CH₃)CH), 142.4, 142.3 (C_{ipso}), 142.1, 141.0 (C_{ortho}), 125.9, 125.6 (C_{para}), 124.6, 123.6 (C_{meta}), 94.3 (NC(CH₃)CH), 39.4 (Cy-CH), 34.4 (Cy-CH₂ overlapping Cy-CH₂), 28.6 (CH(CH₃)₂), 27.6, 27.6, 26.7 (Cy-CH₂ overlapping Cy-CH₂), 24.4, 23.7 (CH(CH₃)₂), 21.1, 20.9 (NC(CH₃)CH).

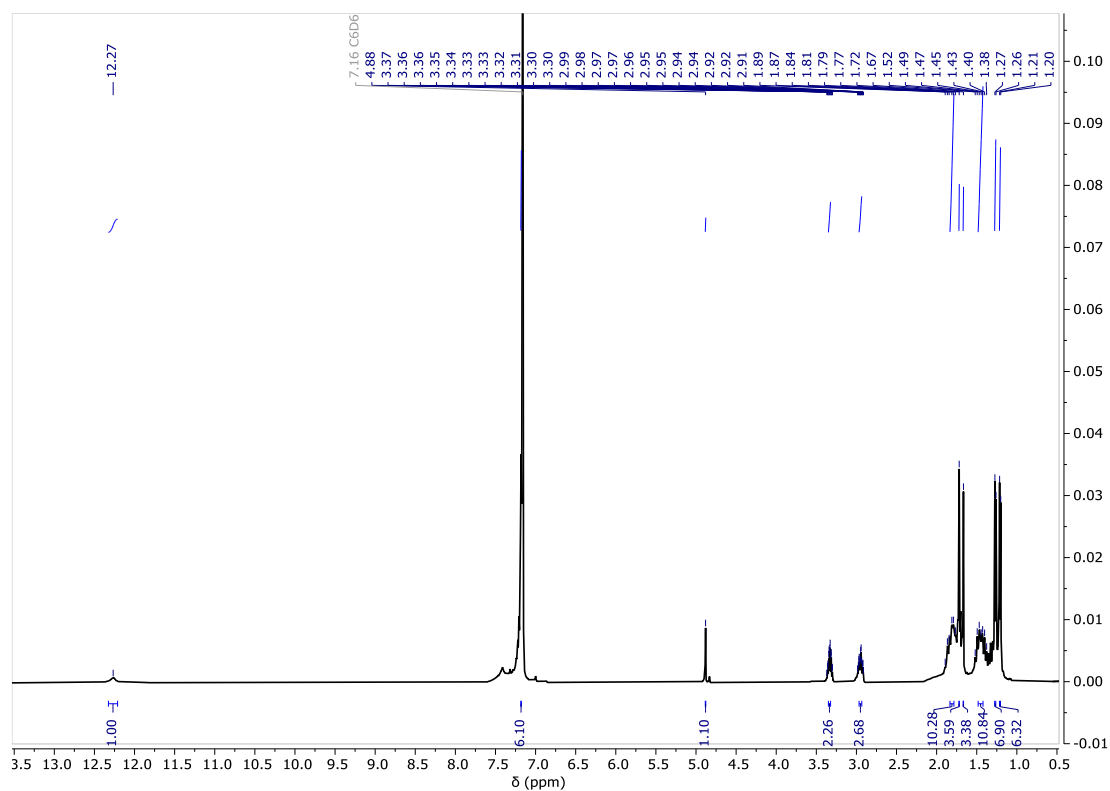
M.p: 135–142 °C (dec.).

IR (cm⁻¹): 3059 (w), 2957 (w), 2921 (s), 2848 (s), 1619 (s), 1544 (s), 1482 (w), 1460 (w), 1438 (s), 1377 (w), 1358 (m), 1320 (w), 1307 (w), 1258 (s), 1212 (m), 1172 (s), 1131 (w), 1097 (w), 1056 (w), 1024 (m), 995 (w), 923 (w), 891 (m), 834 (w), 822 (w), 784 (m), 763 (s), 736 (m).

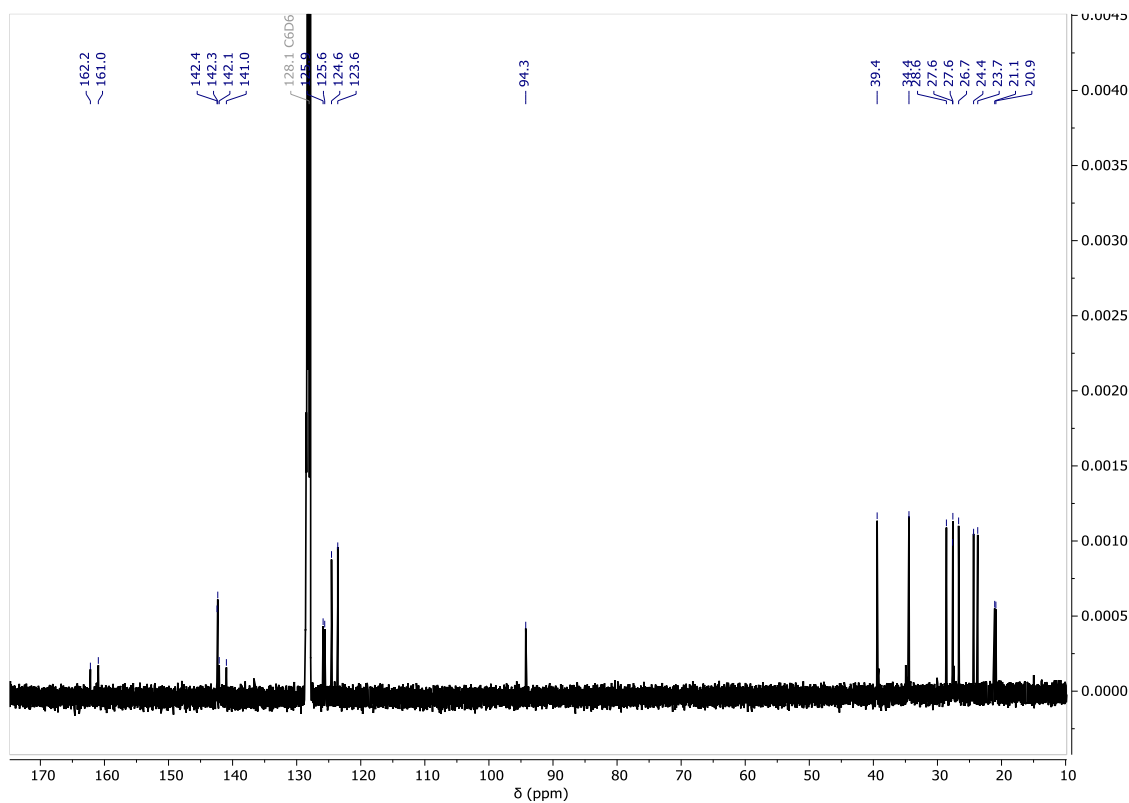
Elemental Analysis for (BDI^{Dipp,Dicyp})H (498.8 g mol⁻¹):

Calculated: C: 84.28, H: 10.10, N: 5.62 %.

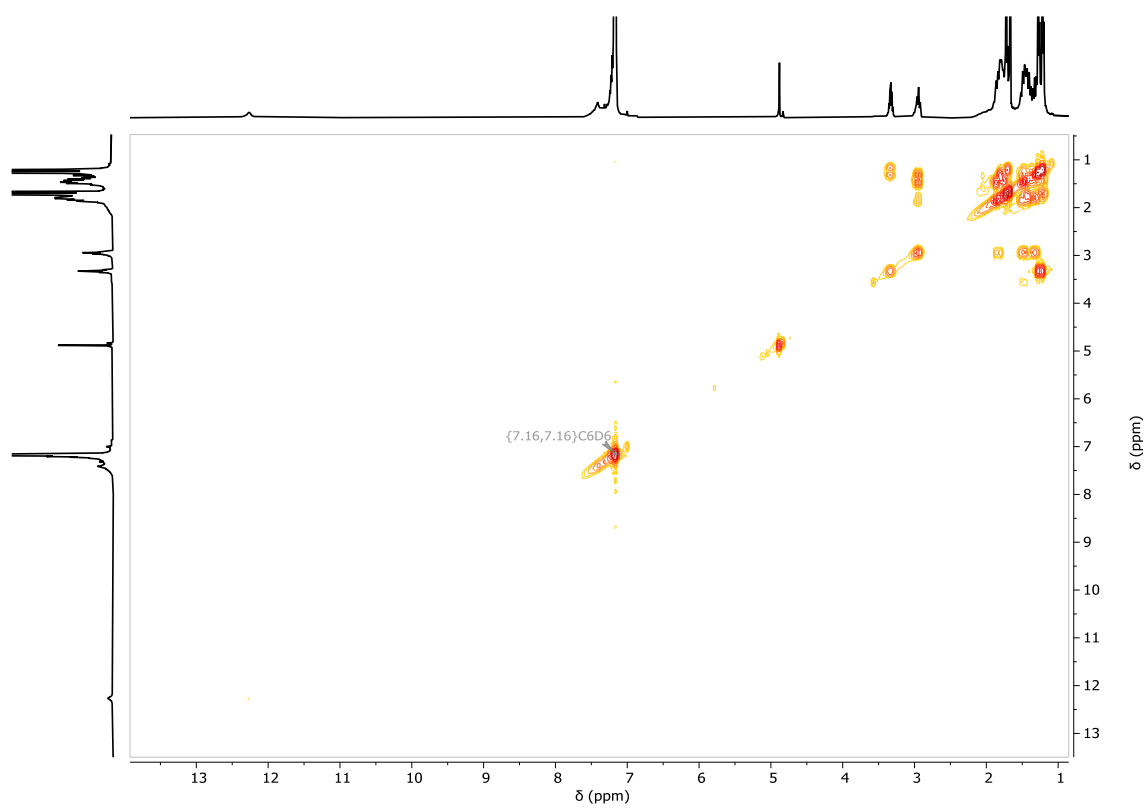
Found: C: 84.08, H: 10.18, N: 5.55 %.



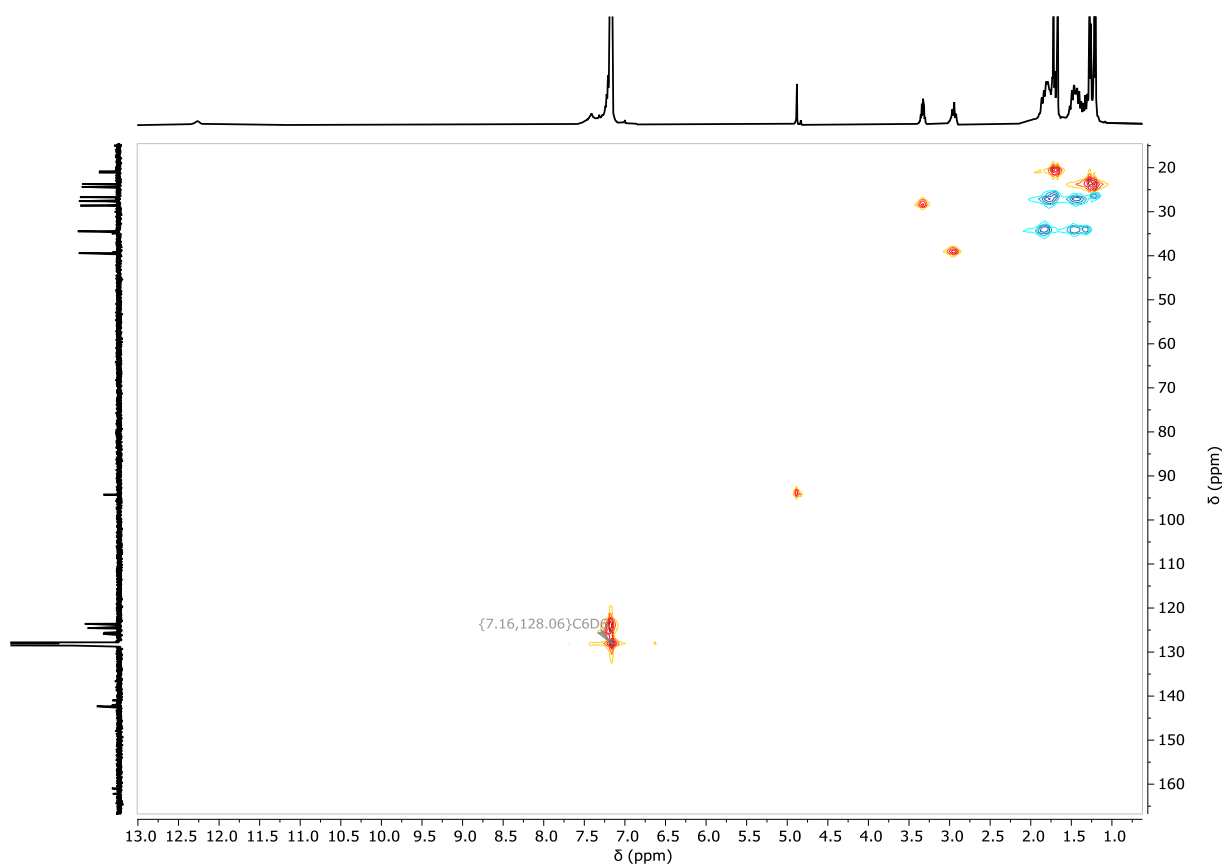
Supplementary Figure 3.27. ¹H NMR spectrum (500 MHz, C₆D₆) of (BDI^{Dipp,Dicyp})H (3.16).



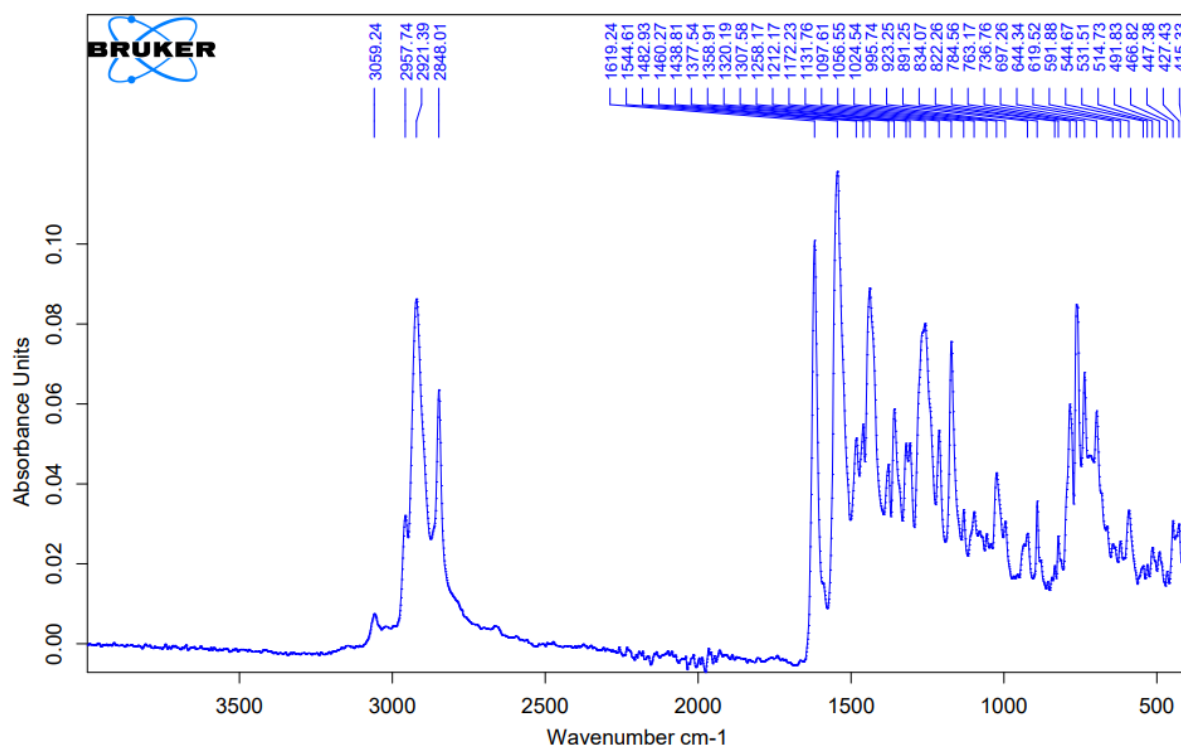
Supplementary Figure 3.28. ¹³C{¹H} NMR spectrum (126 MHz, C₆D₆) of (BDI^{Dipp,Dicyp})H (3.16).



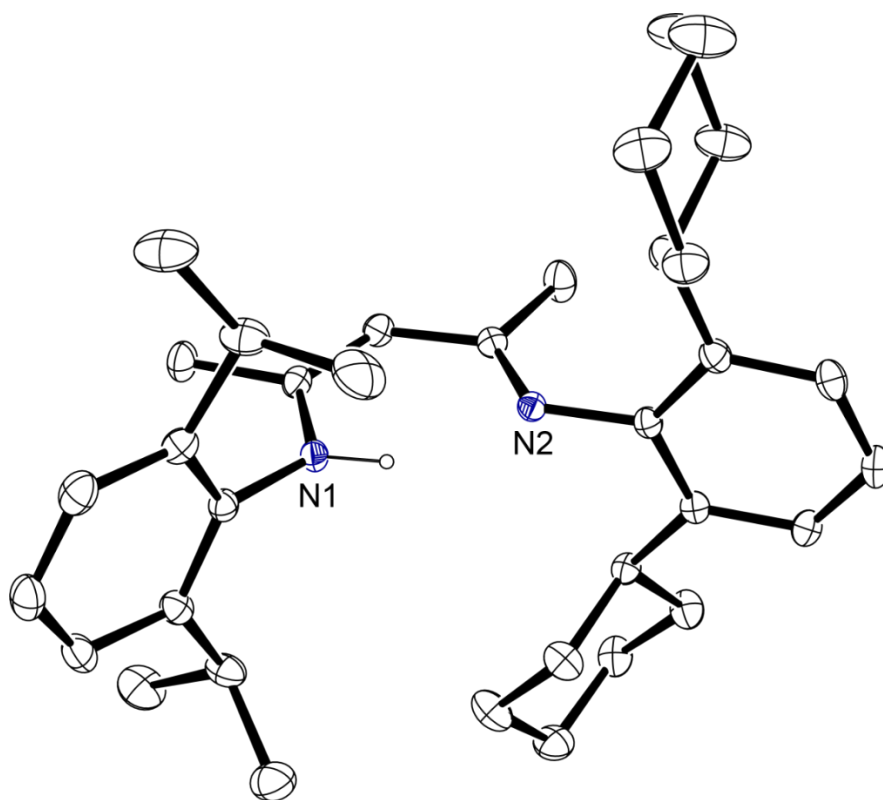
Supplementary Figure 3. 29. ^1H - ^1H COSY NMR spectrum (500 MHz, C_6D_6) of $(\text{BDI}^{\text{Dipp,Dicyp}})\text{H}$ (**3.16**).



Supplementary Figure 3.30. ^1H - ^{13}C HSQC NMR spectrum (500 MHz, C_6D_6) of $(\text{BDI}^{\text{Dipp,Dicyp}})\text{H}$ (**3.16**).



Supplementary Figure 3.31. Infrared spectrum of $(\text{BDI}^{\text{Dipp,Dicyp}})\text{H}$ (**3.16**).



Supplementary Figure 3.32. Ortep representation (30% probability ellipsoids) of (BDI^{Dipp,Dicyp})H (**3.16**). Hydrogen atoms (except N1–H) have been omitted for clarity.

(BDI^{Dipp,Dicyp})K (3.17)

A colourless toluene solution containing KHMDS (1454.4 mg, 7.31 mmol) was added to a Schlenk flask containing a stirring solution of (BDI^{Dipp,Dicyp})H (3646 mg, 7.31 mmol) inside the glovebox and left to stir overnight at room temperature, resulting in the precipitation of a beige solid. The solution was filtered away and the solid washed once more with toluene before drying the crude solid under vacuum (3079.5 mg, 78.5%).

¹H NMR (500 MHz, C₆D₆) δ 7.18 (m, 4H, ArH), 7.05 (t, *J* = 7.6 Hz, 2H, ArH), 4.81 (s, 1H, NC(CH₃)CH), 3.37 (m, 2H, CH(CH₃)₂), 2.98 (m, 2H, Cy-CH), 1.93, 1.89 (s, 3H, NC(CH₃)CH), 1.85 (m, 4H, Cy-CH₂), 1.76 (m, 4H, Cy-CH₂), 1.50 (m, 8H, Cy-CH₂), 1.33 (d, *J* = 6.4 Hz, 6H, CH(CH₃)₂), 1.27 (m, 4H, Cy-CH₂), 1.15 (d, *J* = 6.9 Hz, 6H, CH(CH₃)₂).

¹³C{¹H} NMR (126 MHz, C₆D₆) δ 160.4, 160.2 (NC(CH₃)CH), 151.2, 151.0 (C_{ipso}), 139.5, 138.8 (C_{ortho}), 124.5, 123.7 (C_{para}), 121.2, 121.0 (C_{meta}), 91.2 (NC(CH₃)CH), 38.8 (Cy-CH), 35.7 (Cy-CH₂), 34.3 (Cy-CH₂ overlapping Cy-CH₂), 27.9 (CH(CH₃)₂), 27.5, 26.8 (Cy-CH₂ overlapping Cy-CH₂), 24.3, 24.0 (CH(CH₃)₂), 23.7, 23.5 (NC(CH₃)CH).

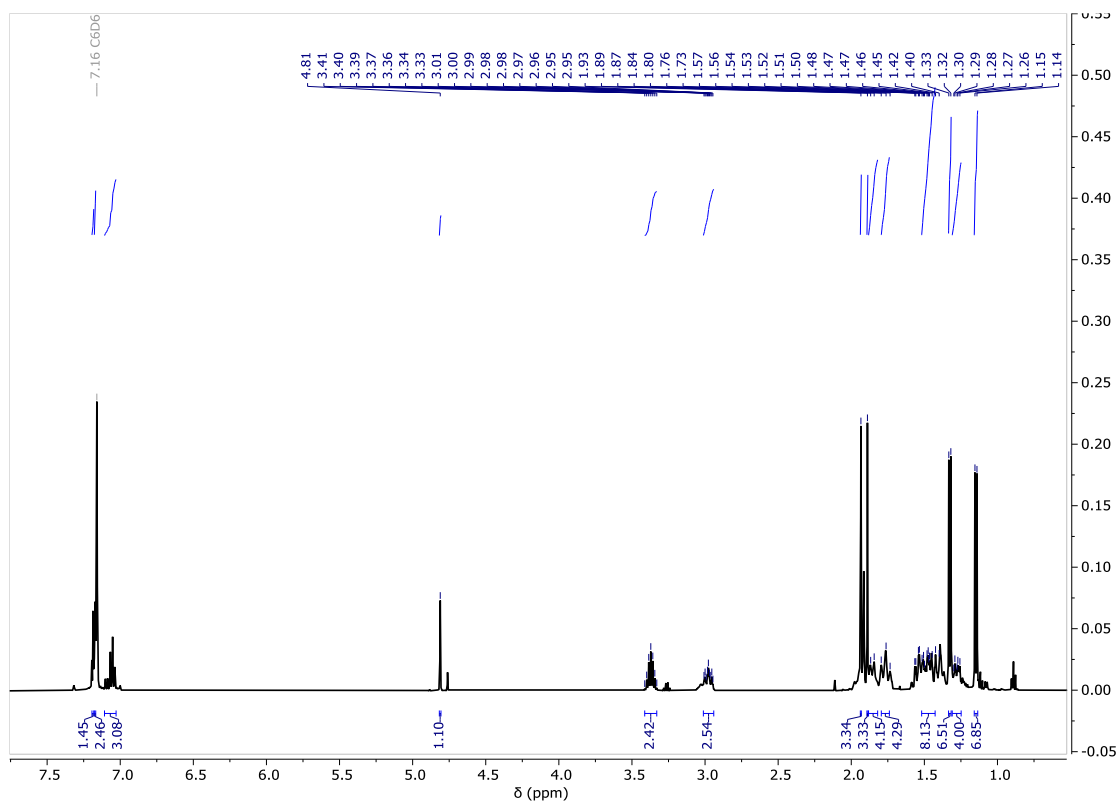
M.p: >260 °C (dec.).

IR (cm⁻¹): 2922 (m), 2850 (m), 1620 (w), 1566 (m), 1517 (w), 1464 (m), 1414 (s), 1352 (w), 1319 (w), 1306 (w), 1254 (w), 1212 (w), 1163 (s), 1130 (w), 1095 (w), 1014 (m), 921 (w), 891 (w), 842 (w), 782 (m), 760 (m), 728 (w).

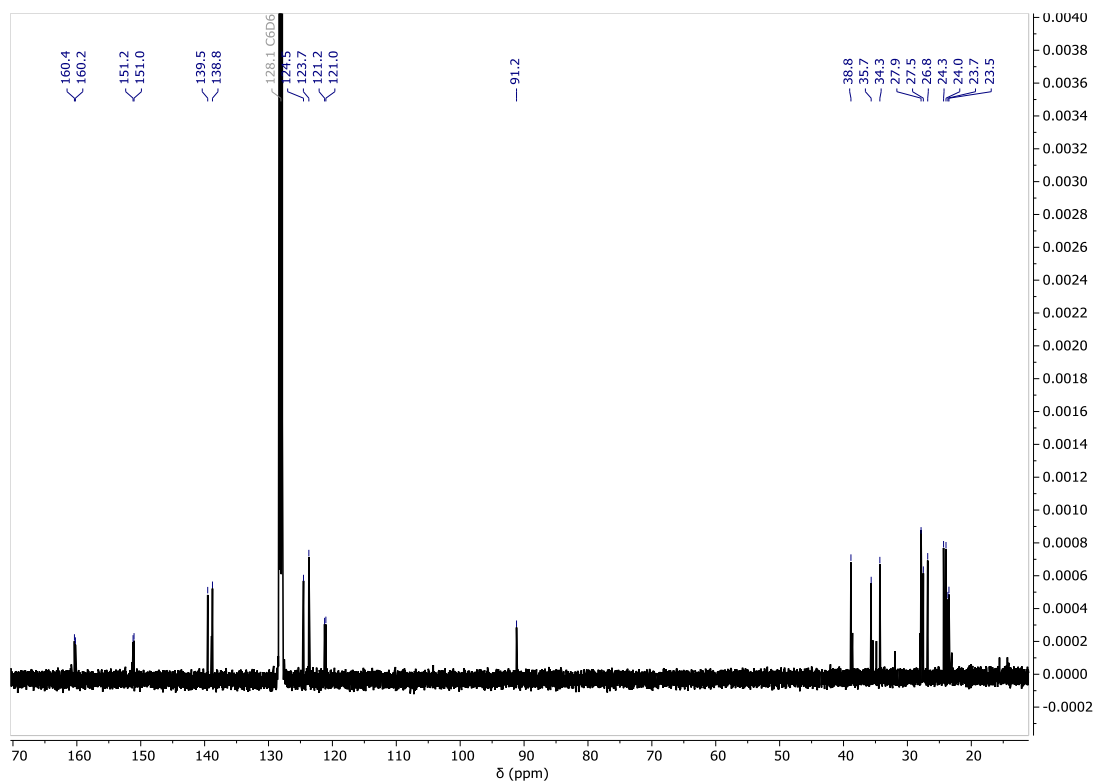
Elemental Analysis for (BDI^{Dipp,Dicyp})K (536.9 g mol⁻¹):

Calculated: C: 78.3, H: 9.20, N: 5.22 %.

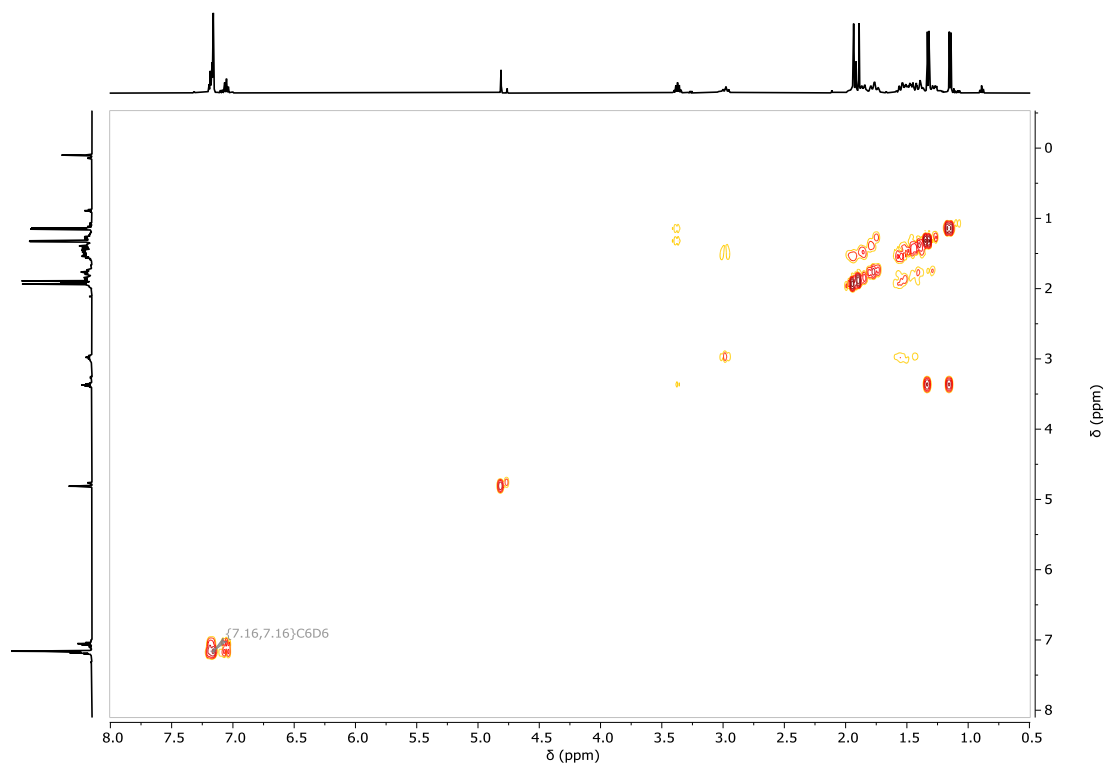
Found: C: 72.66, H: 8.96, N: 4.85 %.



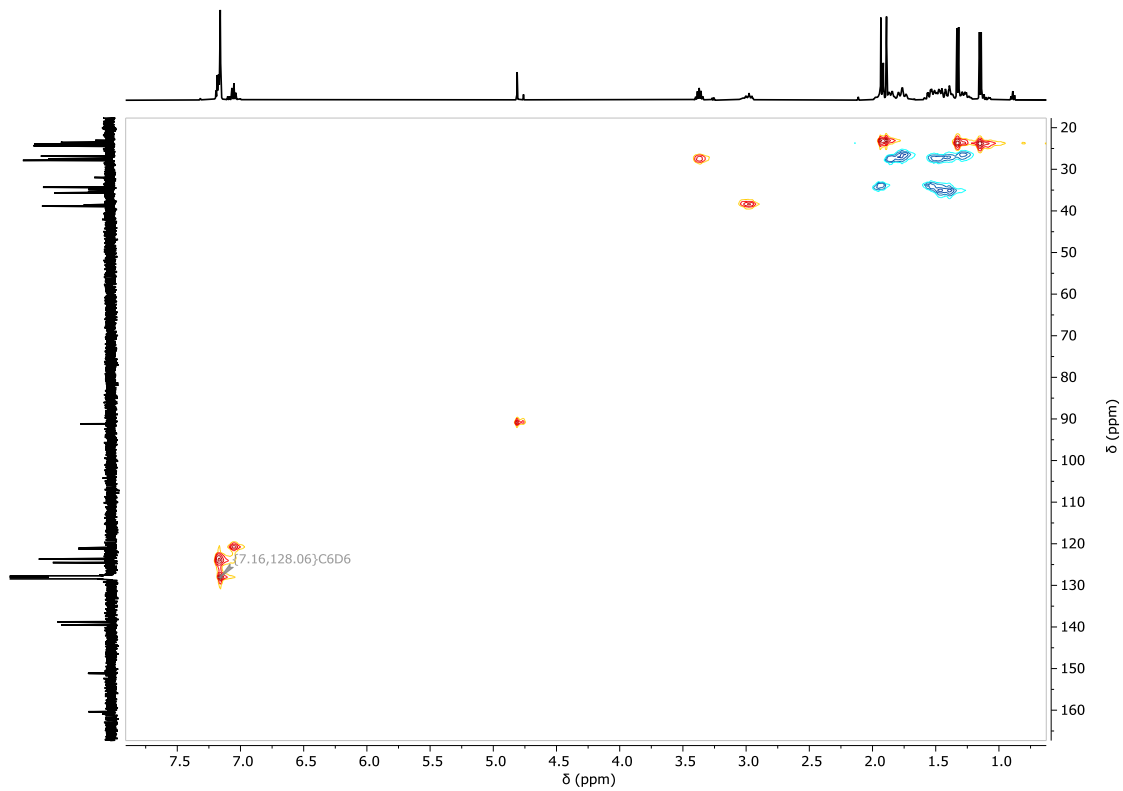
Supplementary Figure 3.33. ^1H NMR spectrum (500 MHz, C_6D_6) of $(\text{BDI}^{\text{Dipp,Dicyp}})\text{K}$ (3.17).



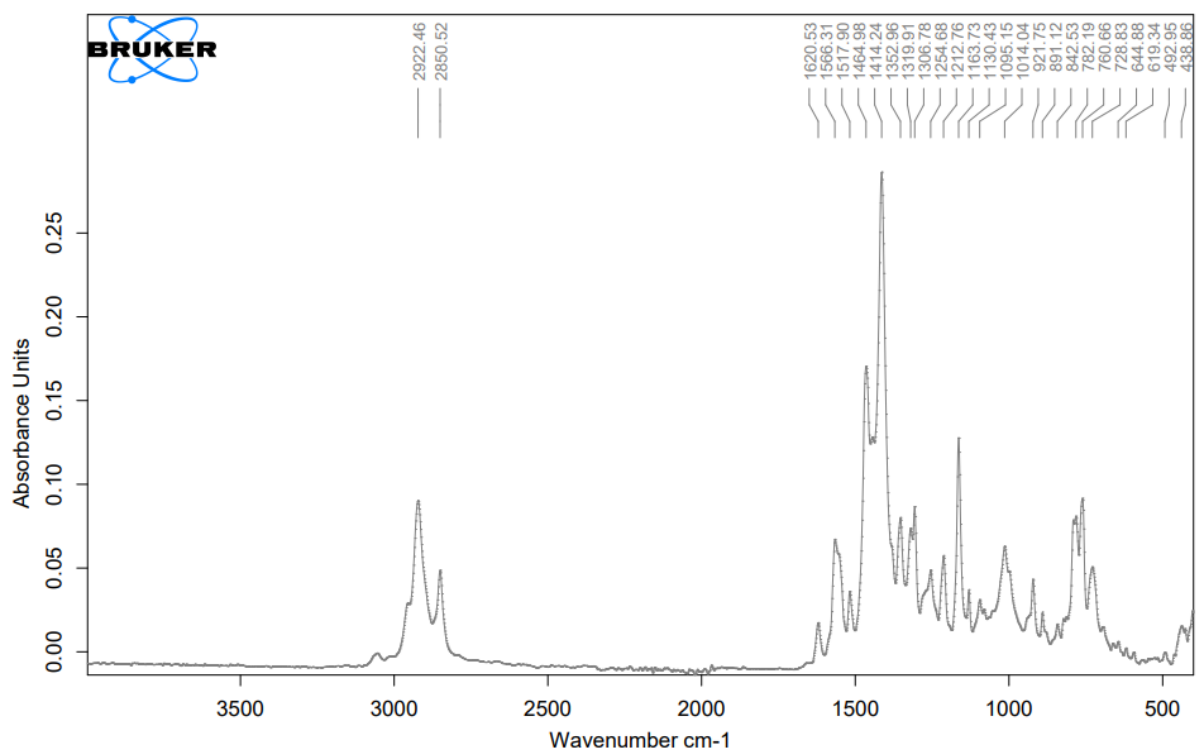
Supplementary Figure 3.34. $^{13}\text{C}\{^1\text{H}\}$ NMR spectrum (126 MHz, C_6D_6) of $(\text{BDI}^{\text{Dipp,Dicyp}})\text{K}$ (3.17).



Supplementary Figure 3.35. ^1H - ^1H COSY NMR spectrum (500 MHz, C_6D_6) of $(\text{BDI}^{\text{Dipp,Dicyp}})\text{K}$ (**3.17**).



Supplementary Figure 3.36. ^1H - ^{13}C HSQC NMR spectrum (500 MHz, C_6D_6) of $(\text{BDI}^{\text{Dipp,Dicyp}})\text{K}$ (**3.17**).



Supplementary Figure 3.37. Infrared spectrum of (BDI^{Dipp,Dicyp})K (3.17).

$[(\text{BDI}^{\text{Dipp,Dicyp}})\text{EuI}]_2$ (3.18)

A colourless THF solution of $(\text{BDI}^{\text{Dipp,Dicyp}})\text{K}$ (1150 mg, 2.14 mmol) was added to a pale green-yellow suspension of EuI_2 (1176 mg, 2.14 mmol) in THF and the resulting orange-yellow mixture was left to react for 4 hours at room temperature. The solvent was removed in vacuo, the crude product extracted with toluene and filtered through celite, yielding a yellow powder (947 mg, 57%).

The paramagnetic nature and solubility of $[(\text{BDI}^{\text{Dipp,Dicyp}})\text{EuI}]_2$ hampered characterisation by NMR spectroscopic techniques and single crystal X-ray diffraction analysis.

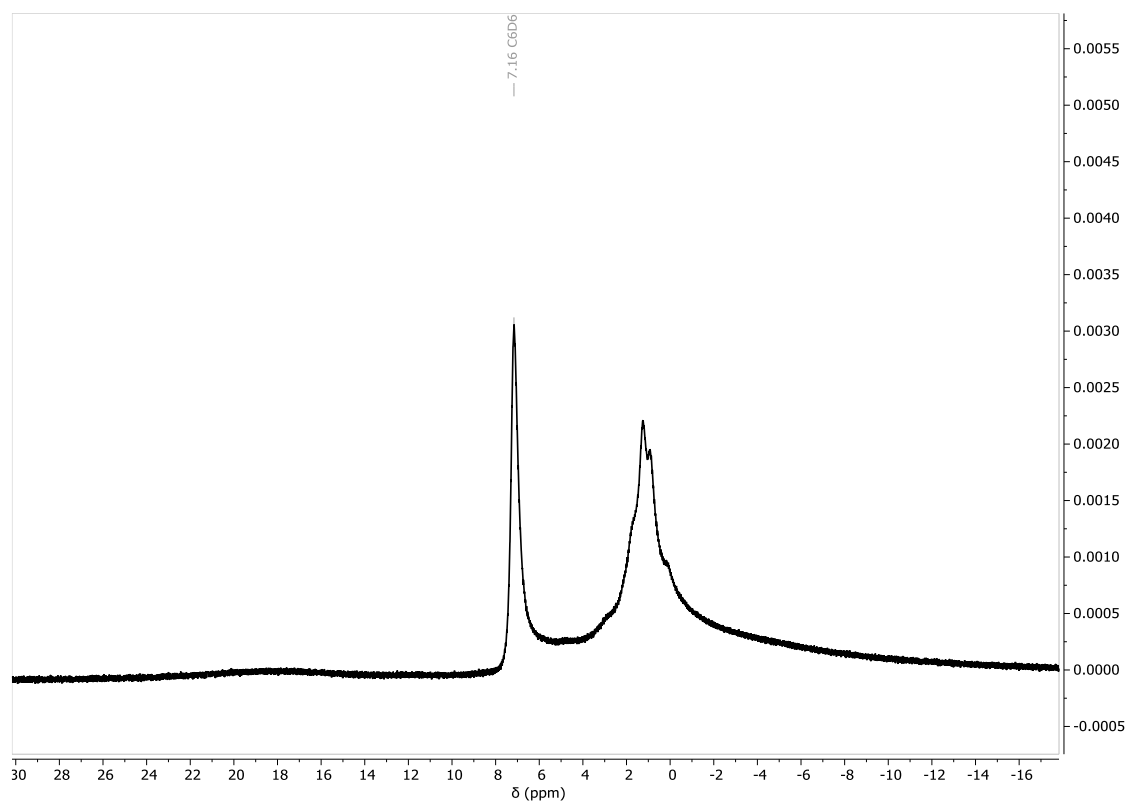
M.p: >260 °C (dec.).

IR (cm⁻¹): 3058 (w), 2921 (s), 2849 (s), 1620 (w), 1550 (m), 1523 (m), 1445 (m), 1398 (s), 1352 (w), 1303 (w), 1258 (w), 1212 (w), 1164 (m), 1130 (w), 1081 (w), 1017 (m), 928 (m), 889 (w), 876 (w), 832 (w), 786 (m).

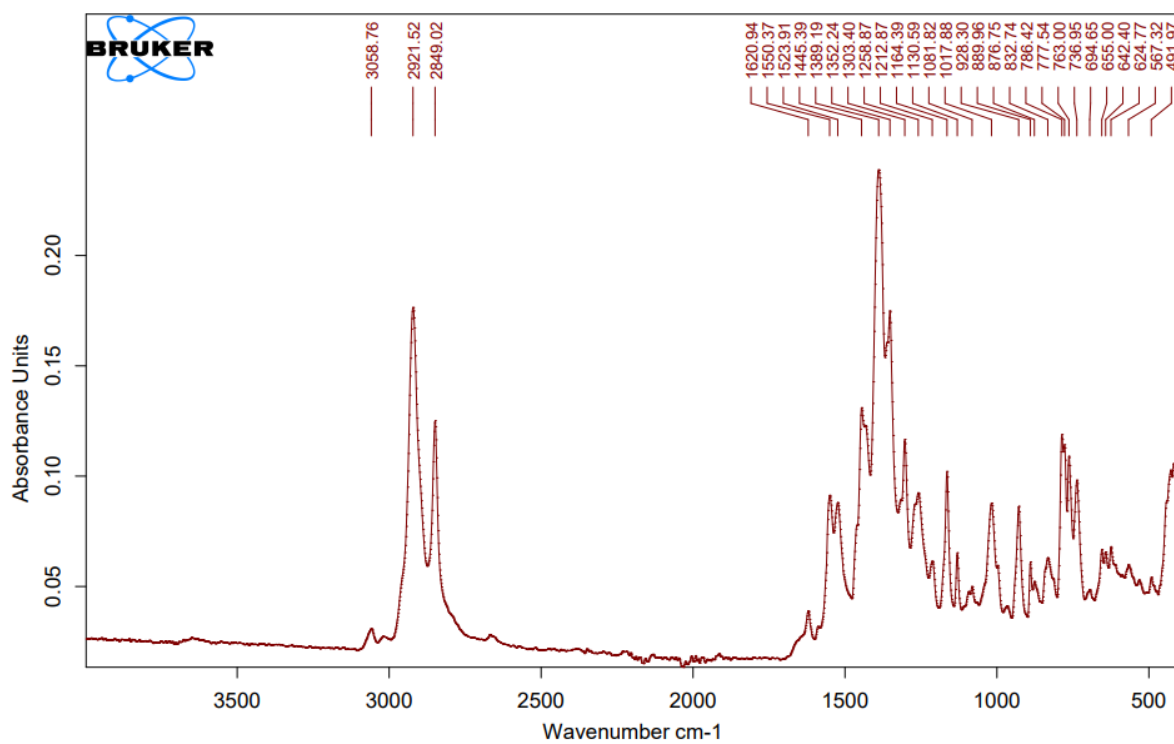
Elemental analysis for $[(\text{BDI}^{\text{Dipp,Dicyp}})\text{EuI}]_2$ (1553.32 g mol⁻¹):

Calculated: C: 54.13, H: 6.36, N: 3.61 %.

Found: C: 56.27, H: 6.79, N: 3.38 %.



Supplementary Figure 3.38. ^1H NMR spectrum (500 MHz, C_6D_6) of $[(\text{BDI}^{\text{Dipp,Dicyp}})\text{EuI}]_2$ (**3.18**).



Supplementary Figure 3.39. Infrared spectrum of $[(\text{BDI}^{\text{Dipp,Dicyp}})\text{EuI}]_2$ (**3.18**).

[(BDI^{Dipp,Dicyp})EuCH(SiMe₃)₂] (3.19)

A red THF solution of KCH(SiMe₃)₂ (180 mg, 0.91 mmol) was added to an orange THF solution of [(BDI^{Dipp,Dicyp})EuI]₂ (706 mg, 0.45 mmol) while stirring and left to react for 15 minutes at room temperature. The orange mixture was dried *in vacuo*, the residue extracted with hexane and filtered through celite. Yellow crystals suitable for an X-ray diffraction experiment was obtained from a saturated hexane solution at – 30 °C (393 mg, 53.4%).

The paramagnetic nature of [(BDI^{Dipp,Dicyp})EuCH(SiMe₃)₂] hampered characterisation by multinuclear NMR spectroscopic techniques.

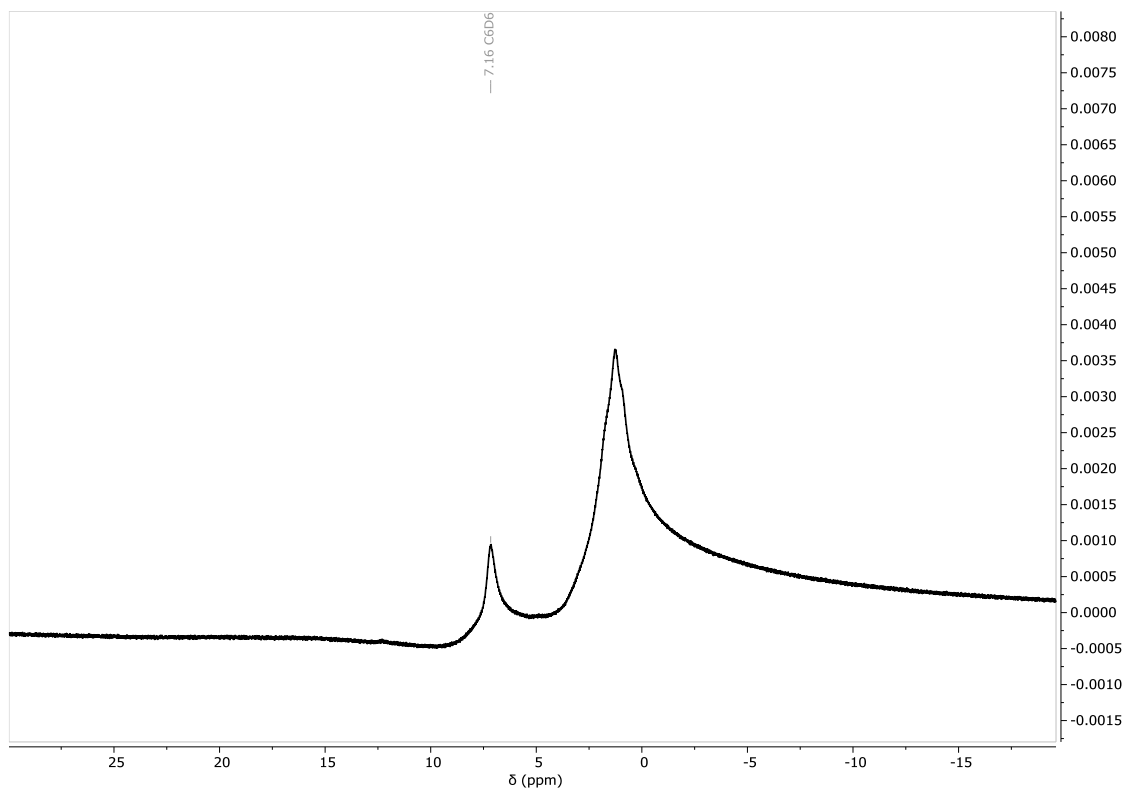
M.p: 160–178 °C (dec.).

IR (cm⁻¹): 3051 (w), 2924 (s), 2850 (m), 1619 (w), 1601 (w), 1588 (w), 1540 (m), 1523 (w), 1474 (w), 1459 (w), 1443 (m), 1426 (w), 1406 (s), 1354 (m), 1249 (w), 1216 (w), 1191 (w), 1164 (w), 1132 (w), 1096 (m), 1050 (m), 1021 (w), 994 (w), 919 (w), 889 (w), 836 (s), 783 (m), 757 (s), 735 (m).

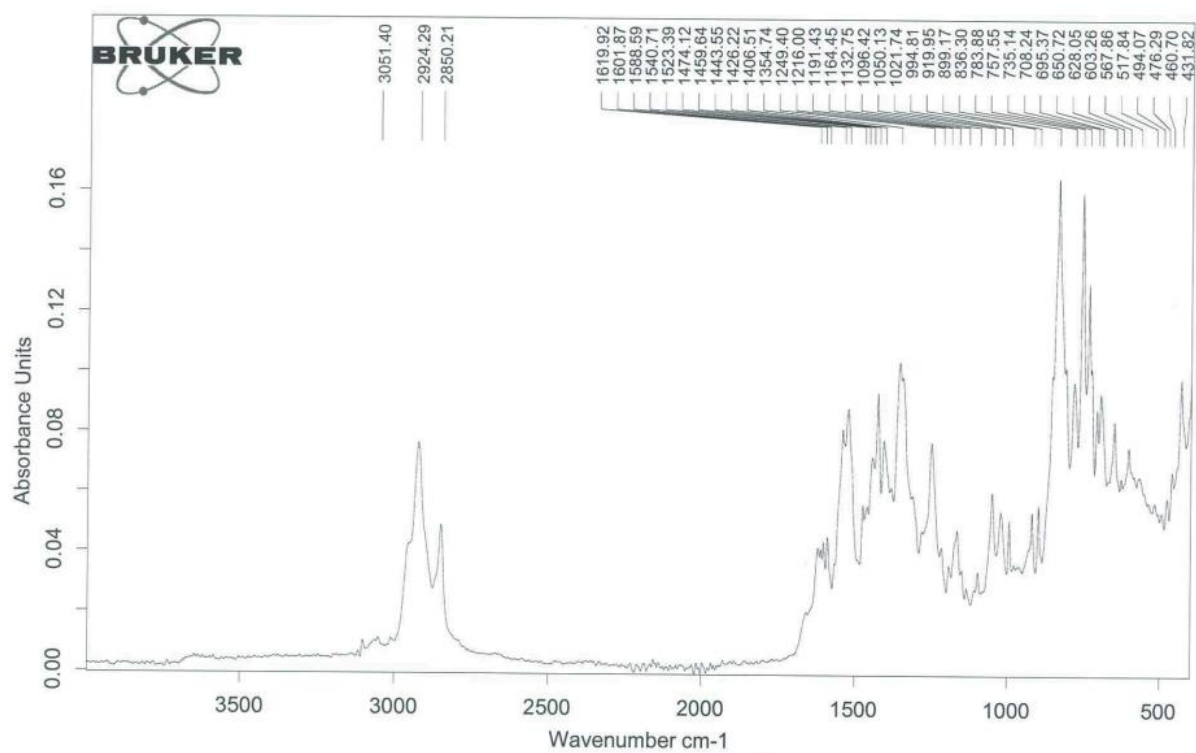
Elemental Analysis for [(BDI^{Dipp,Dicyp})EuCH(SiMe₃)₂] (809.15 g mol⁻¹):

Calculated: C: 62.34, H: 8.47, N: 3.46 %.

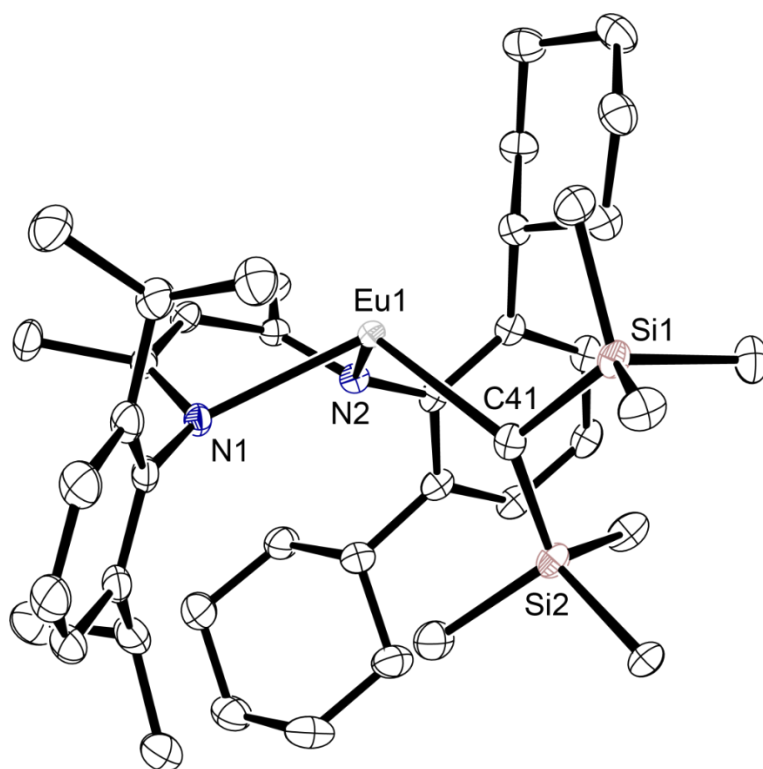
Found: C: 62.17, H: 8.63, N: 3.20 %.



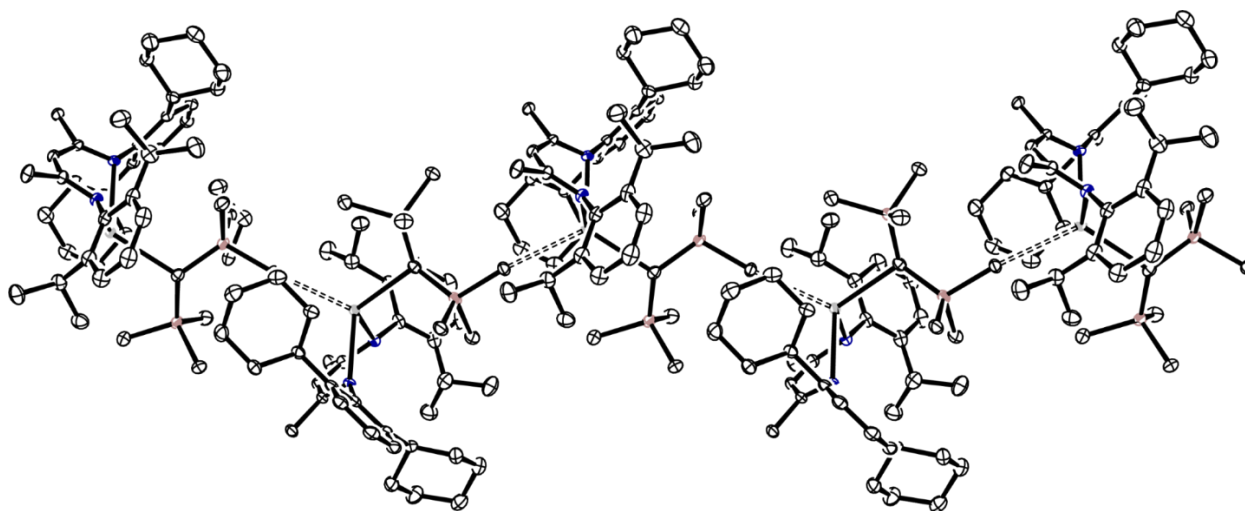
Supplementary Figure 3.40. ^1H NMR spectrum (500 MHz, C_6D_6) of $[(\text{BDI}^{\text{Dipp,Dicyp}})\text{EuCH}(\text{SiMe}_3)_2]$ (**3.19**).



Supplementary Figure 3.41. Infrared spectrum of $[(\text{BDI}^{\text{Dipp,Dicyp}})\text{EuCH}(\text{SiMe}_3)_2]$ (**3.19**).



Supplementary Figure 3.42. Ortep representation (30% probability ellipsoids) of $[(\text{BDI}^{\text{Dipp,Dicyp}})\text{EuCH}(\text{SiMe}_3)_2]$ (**3.19**). Hydrogen atoms have been omitted for clarity.



Supplementary Figure 3.43. Ortep representation (30% probability ellipsoids) of the pseudo polymer of $[(\text{BDI}^{\text{Dipp,Dicyp}})\text{EuCH}(\text{SiMe}_3)_2]$ (**3.19**). Hydrogen atoms have been omitted for clarity.

[(BDI^{Dipp,Dicyp})EuH] (3.20)

A concentrated toluene solution containing 1,4-cyclohexadiene (78 mg, 0.98 mmol) was then gently layered on top of an orange toluene solution containing [(BDI^{Dipp,Dicyp})EuCH(SiMe₃)₂] (393 mg, 0.49 mmol) and the vial was left unmoved at room temperature with the vial lid cracked open. Small orange crystals suitable for a single crystal X-ray experiment were obtained over the course of 2 days (191 mg, 60%)

The paramagnetic nature and solubility of [(BDI^{Dipp,Dicyp})EuH]₂ hampered characterisation by multinuclear NMR spectroscopic techniques.

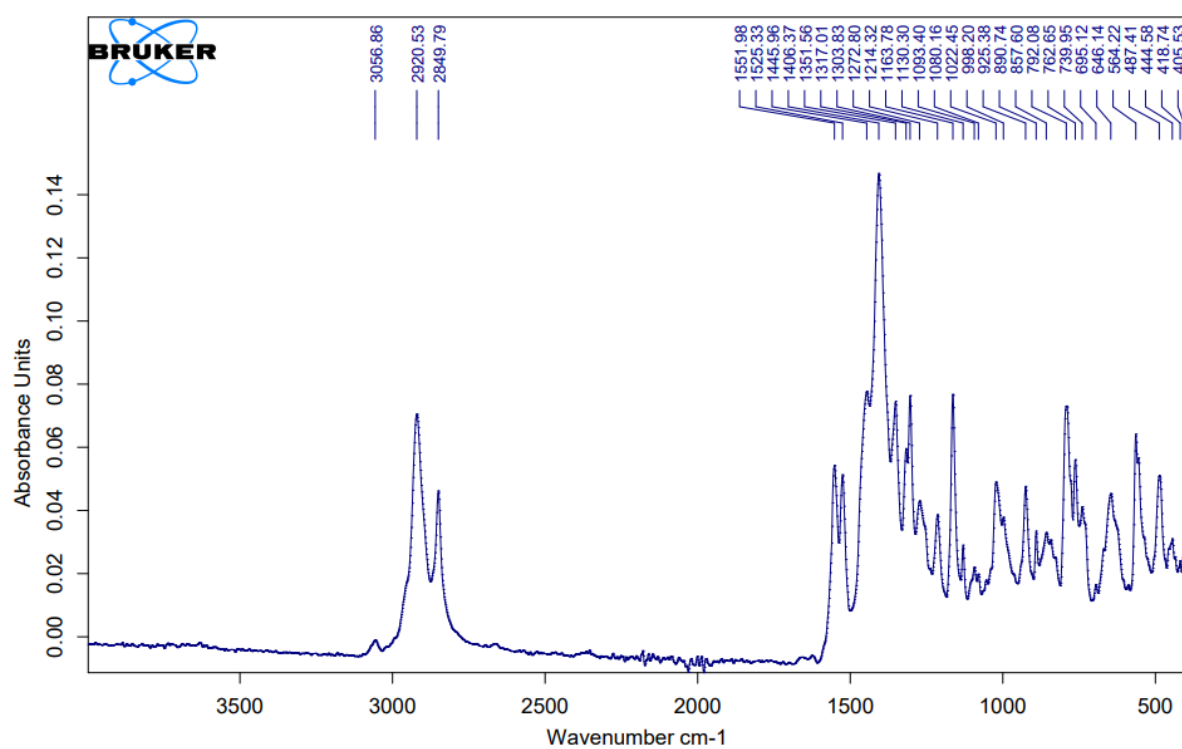
M.p: 220–233 °C (dec.).

IR (cm⁻¹): 3056 (w), 2920 (s), 2849 (m), 1551 (m), 1525 (m), 1445 (w), 1406 (s), 1351 (w), 1317 (w), 1303 (m), 1272 (w), 1214 (w), 1163 (s), 1130 (w), 1093 (w), 1080 (w), 1022 (m), 998 (w), 925 (m), 890 (w), 857 (w), 792 (s), 762 (m), 739 (w), 695 (w), 646 (m), 564 (s).

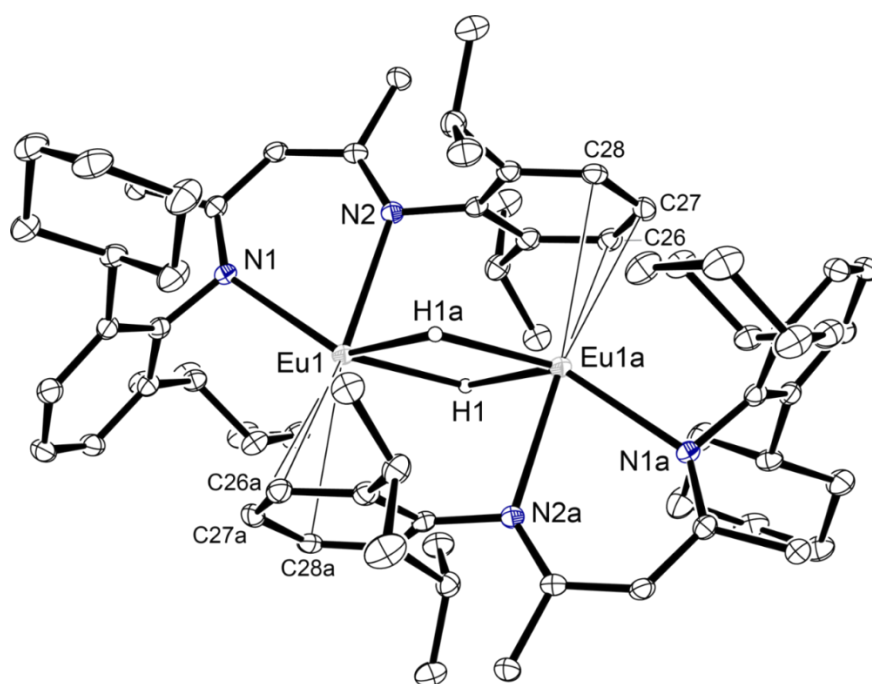
Elemental Analysis for [(BDI^{Dipp,Dicyp})EuH]₂ (1301.5 g mol⁻¹):

Calculated: C: 64.6, H: 7.74, N: 4.30 %.

Found: C: 66.24, H: 7.97, N: 3.80 %.



Supplementary Figure 3.44. Infrared spectrum of $[(\text{BDI}^{\text{Dipp,Dicyp}})\text{EuH}]_2$ (**3.20**).



Supplementary Figure 3.45. Ortep representation (30% probability ellipsoids) of $[(\text{BDI}^{\text{Dipp,Dicyp}})\text{EuH}]_2$ (**3.20**). Hydrogen atoms (except the bridging H1 and H1a) have been omitted for clarity.

[(BDI^{Dipp,TCHP})EuI]₂ (3.21)

A colourless THF solution of (BDI^{Dipp,TCHP})K (684 mg, 1.1 mmol) was added to a pale green-yellow suspension of EuI₂ (607 mg, 1.1 mmol) in THF and the resulting orange-yellow mixture was left to react for 4 hours at room temperature. The solvent was removed *in vacuo*, the crude product extracted with toluene and filtered through Celite. Yellow crystals suitable for X-ray diffraction analysis were obtained from a saturated toluene solution at room temperature (692 mg, 73%).

The paramagnetic nature of [(BDI^{Dipp,TCHP})EuI]₂ hampered characterisation by multinuclear NMR spectroscopic techniques.

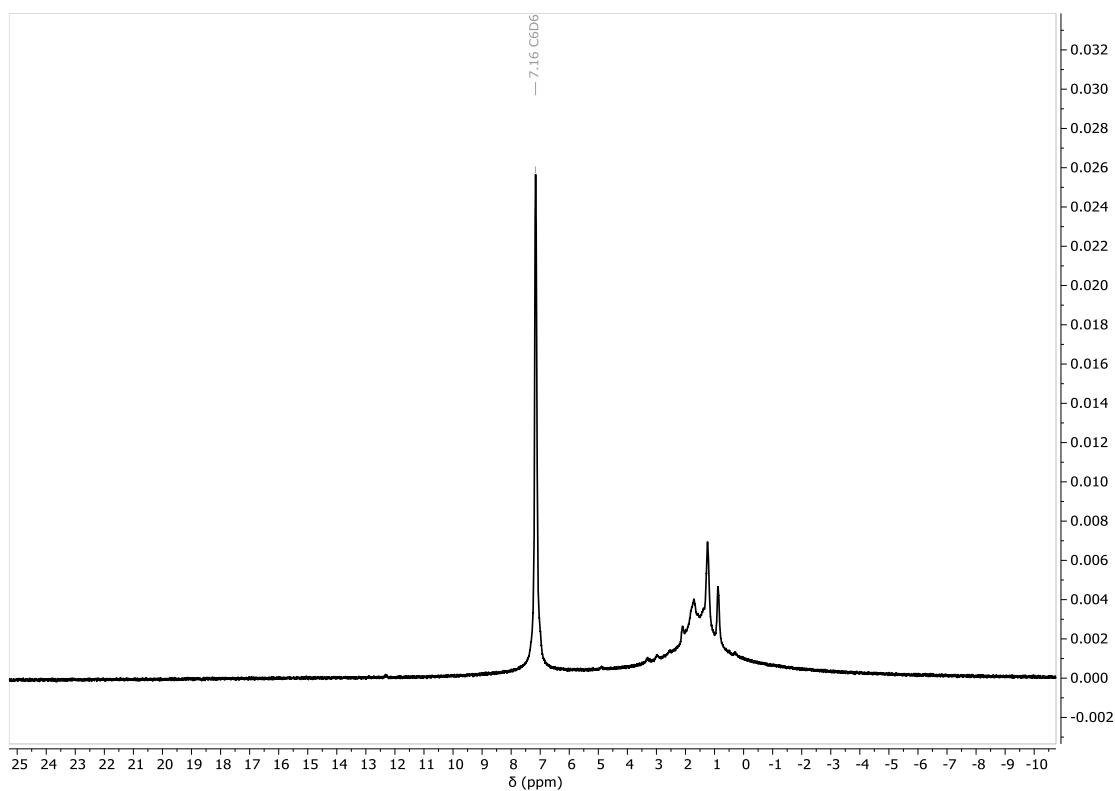
M.p: >260 °C (dec.).

IR (cm⁻¹): 3062 (w), 2922 (s), 2848 (s), 1620 (m), 1550 (s), 1521 (w), 1493 (w), 1445 (s), 1389 (s), 1362 (w), 1309 (m), 1271 (w), 1197 (w), 1172 (m), 1142 (w), 1100 (w), 1018 (m), 997 (w), 950 (w), 926 (w), 888 (w), 861 (m), 821 (w), 805 (w), 785 (m), 757 (m), 728 (s), 693 (m), 670 (w).

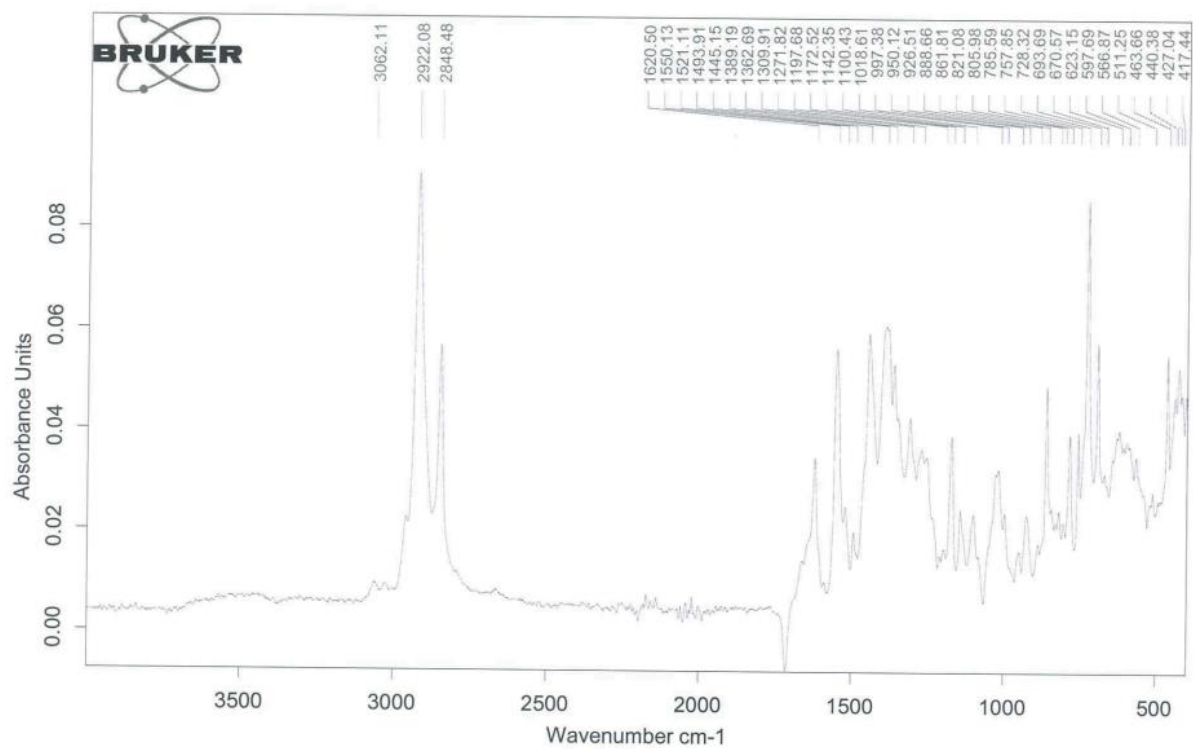
Elemental analysis for [(BDI^{Dipp,TCHP})EuI]₂ (1717.62 g mol⁻¹):

Calculated: C: 57.34, H: 6.92, N: 3.26 %.

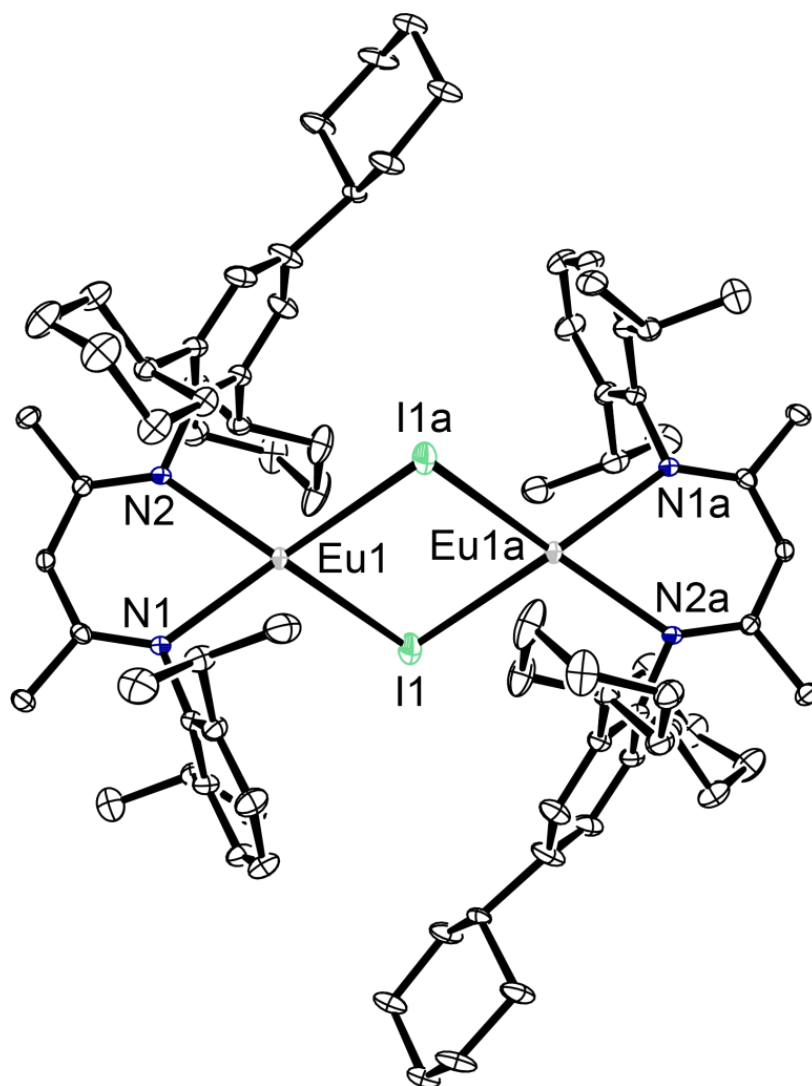
Found: C: 60.08, H: 7.43, N: 3.08 %.



Supplementary Figure 3.46. ^1H NMR spectrum (500 MHz, C_6D_6) of $[(\text{BDI}^{\text{Dipp,TCHP}})\text{EuI}]_2$ (**3.21**).



Supplementary Figure 3.47. Infrared spectrum of $[(\text{BDI}^{\text{Dipp,TCHP}})\text{EuI}]_2$ (**3.21**).



Supplementary Figure 3.48. Ortep representation (30% probability ellipsoids) of $[(\text{BDI}^{\text{Dipp,TCHP}})\text{EuI}]_2$ (**3.21**). Hydrogen atoms have been omitted for clarity.

$[(\text{BDI}^{\text{Dipp,TCHP}})\text{EuCH}(\text{SiMe}_3)_2(\text{THF})]$ (3.22)

A red THF solution of $\text{KCH}(\text{SiMe}_3)_2$ (125 mg, 0.63 mmol) was added to an orange THF solution of $[(\text{BDI}^{\text{Dipp,TCHP}})\text{EuI}]_2$ (541 mg, 0.31 mmol) while stirring and left to react for 15 minutes at room temperature. The orange mixture was dried *in vacuo*, the residue extracted with hexane and filtered through celite. Yellow crystals suitable for an X-ray diffraction experiment was obtained from a saturated hexane solution at $-30\text{ }^\circ\text{C}$ (195 mg, 32%).

The paramagnetic nature of $[(\text{BDI}^{\text{Dipp,TCHP}})\text{EuCH}(\text{SiMe}_3)_2(\text{THF})]$ hampered characterisation by multinuclear NMR spectroscopic techniques.

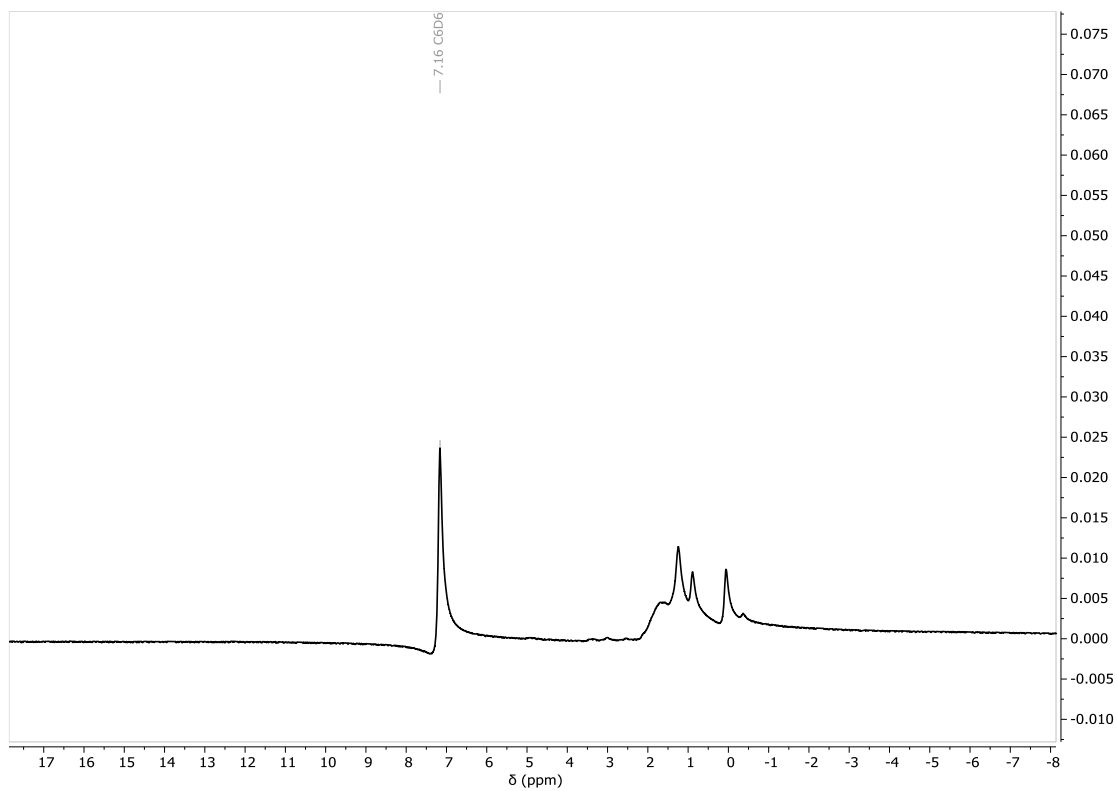
M.p: $132\text{--}142\text{ }^\circ\text{C}$ (dec.).

IR (cm⁻¹): 2923 (s), 2850 (s), 1621 (w), 1589 (w), 1550 (m), 1446 (m), 1398 (m), 1362 (m), 1313 (w), 1248 (s), 1175 (m), 1144 (w), 1107 (w), 1049 (w), 1025 (w), 954 (w), 923 (w), 860 (w), 839 (s), 785 (w), 758 (m).

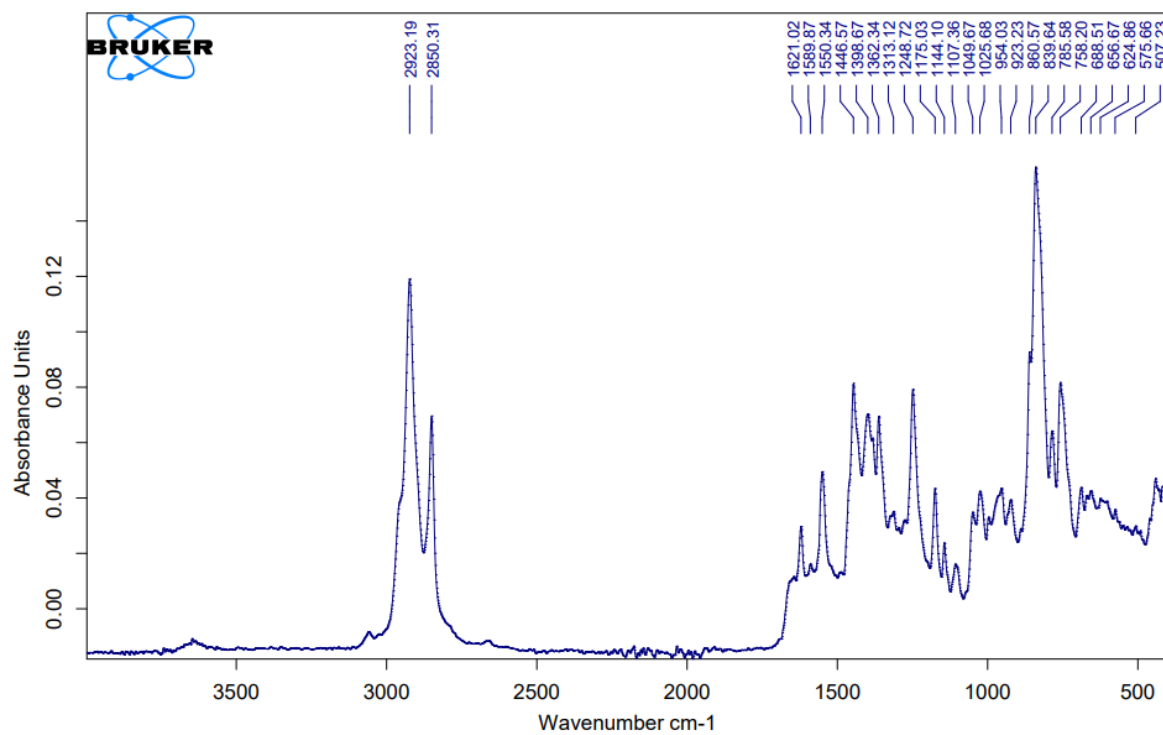
Elemental Analysis for $[(\text{BDI}^{\text{Dipp,TCHP}})\text{EuCH}(\text{SiMe}_3)_2(\text{THF})]$ (963.4 g mol^{-1}):

Calculated: C: 64.82, H: 9.00, N: 2.91 %.

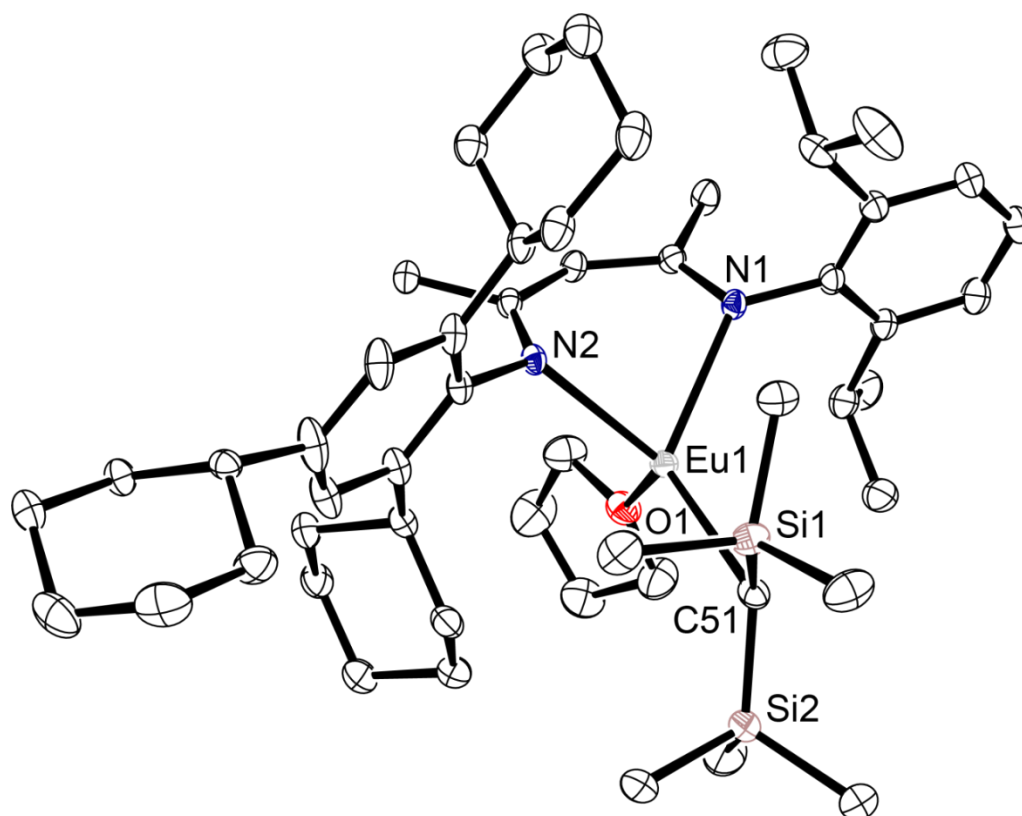
Found: C: 64.63, H: 8.81, N: 2.99 %.



Supplementary Figure 3.49. ^1H NMR spectrum (500 MHz, C_6D_6) of $[(\text{BDI}^{\text{Dipp,TCHP}})\text{EuCH}(\text{SiMe}_3)_2(\text{THF})]$ (**3.22**).



Supplementary Figure 3.50. Infrared spectrum of $[(\text{BDI}^{\text{Dipp,TCHP}})\text{EuCH}(\text{SiMe}_3)_2(\text{THF})]$ (**3.22**).



Supplementary Figure 3.51. Ortep representation (30% probability ellipsoids) of $[(\text{BDI}^{\text{Dipp,TCHP}})\text{EuCH}(\text{SiMe}_3)_2(\text{THF})]$ (**3.22**). Hydrogen atoms have been omitted for clarity.

[(BDI^{Dipp,TCHP})EuH] (3.23)

A concentrated toluene solution containing 1,4-cyclohexadiene (35 mg, 0.44 mmol) was then gently layered on top of an orange toluene solution containing [(BDI^{Dipp,TCHP})EuCH(SiMe₃)₂] (195 mg, 0.22 mmol) and the vial was left unmoved at room temperature with the vial lid cracked open. Small orange crystals suitable for a single crystal X-ray experiment were obtained over the course of 2 days (109 mg, 67%).

The paramagnetic nature and solubility of [(BDI^{Dipp,TCHP})EuH]₂ hampered characterisation by multinuclear NMR spectroscopic techniques.

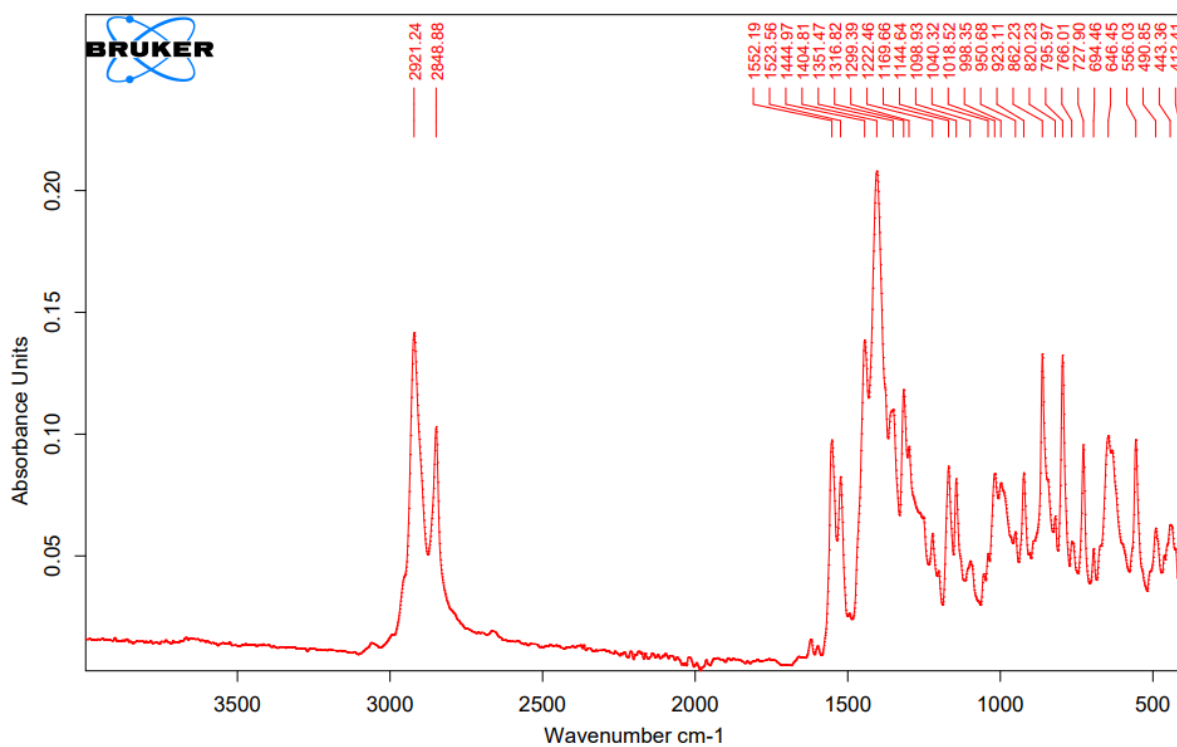
M.p: 230–239 °C (dec.).

IR (cm⁻¹): 2921 (s), 2848 (s), 1552 (m), 1523 (m), 144 (m), 1040 (s), 1351 (w), 1316 (m), 1299 (w), 1222 (w), 1169 (m), 1144 (m), 1098 (w), 1040 (w), 1018 (w), 998 (w), 950 (w), 923 (m), 862 (s), 820 (w), 795 (s), 766 (w), 727 (m), 694 (w), 646 (m), 556 (m).

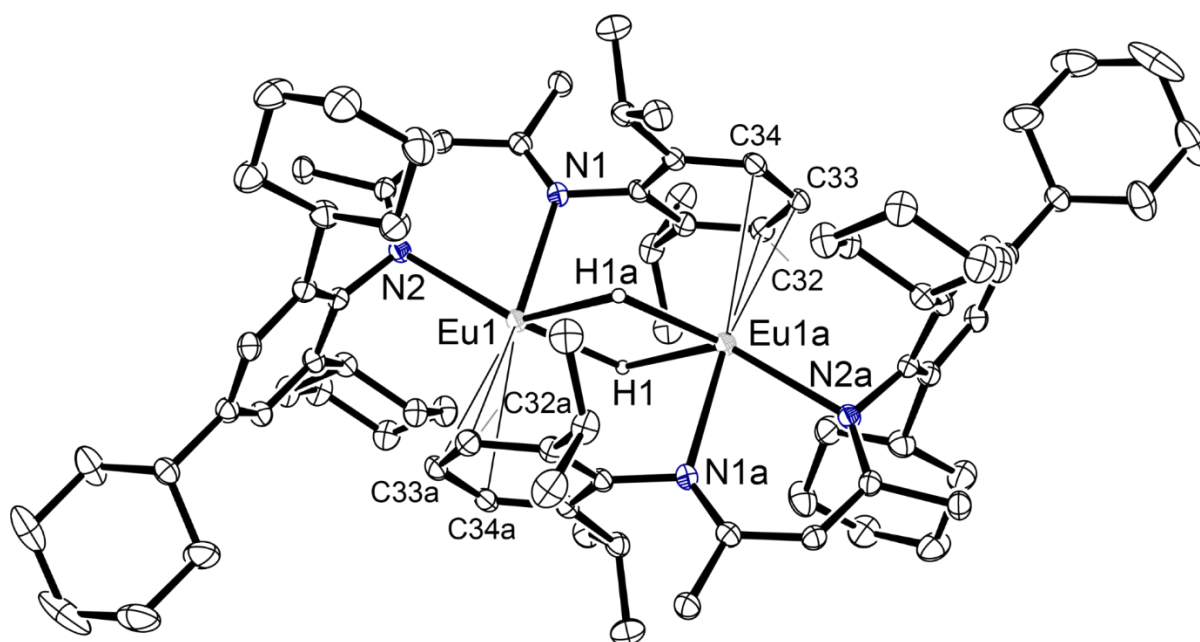
Elemental Analysis for [(BDI^{Dipp,TCHP})EuH]₂ (1465.8 g mol⁻¹):

Calculated: C: 67.19, H: 8.25, N: 3.82 %.

Found: C: 66.88, H: 8.31, N: 3.66 %.



Supplementary Figure 3.52. Infrared spectrum of $[(\text{BDI}^{\text{Dipp,TCHP}})\text{EuH}]_2$ (**3.23**).



Supplementary Figure 3.53. Ortep representation (30% probability ellipsoids) of $[(\text{BDI}^{\text{Dipp,TCHP}})\text{EuH}]_2$ (**3.23**). Hydrogen atoms (except the bridging H1 and H1a) have been omitted for clarity.

$[(\text{BDI}^{\text{DicyP}})\text{Eu}(\mu\text{-COT})\text{Eu}(\text{BDI}^{\text{DicyP}})]$ (3.24)

A pale yellow THF solution containing COT (8 mg, 0.08 mmol) was added to a scintillation vial containing a red suspension of $[(\text{BDI}^{\text{DicyP}})\text{EuH}]_2$ (113 mg, 0.08 mmol) in THF, the mixture left to stir overnight at room temperature to give a yellow solution. Volatiles were removed *in vacuo* to obtain the crude product as a bright orange solid. Orange crystals suitable for a single crystal X-ray diffraction experiment were grown from a saturated toluene solution at room temperature (51 mg, 81%).

The paramagnetic nature of $[(\text{BDI}^{\text{DicyP}})\text{Eu}(\mu\text{-COT})\text{Eu}(\text{BDI}^{\text{DicyP}})]$ hampered characterisation by multinuclear NMR spectroscopic techniques.

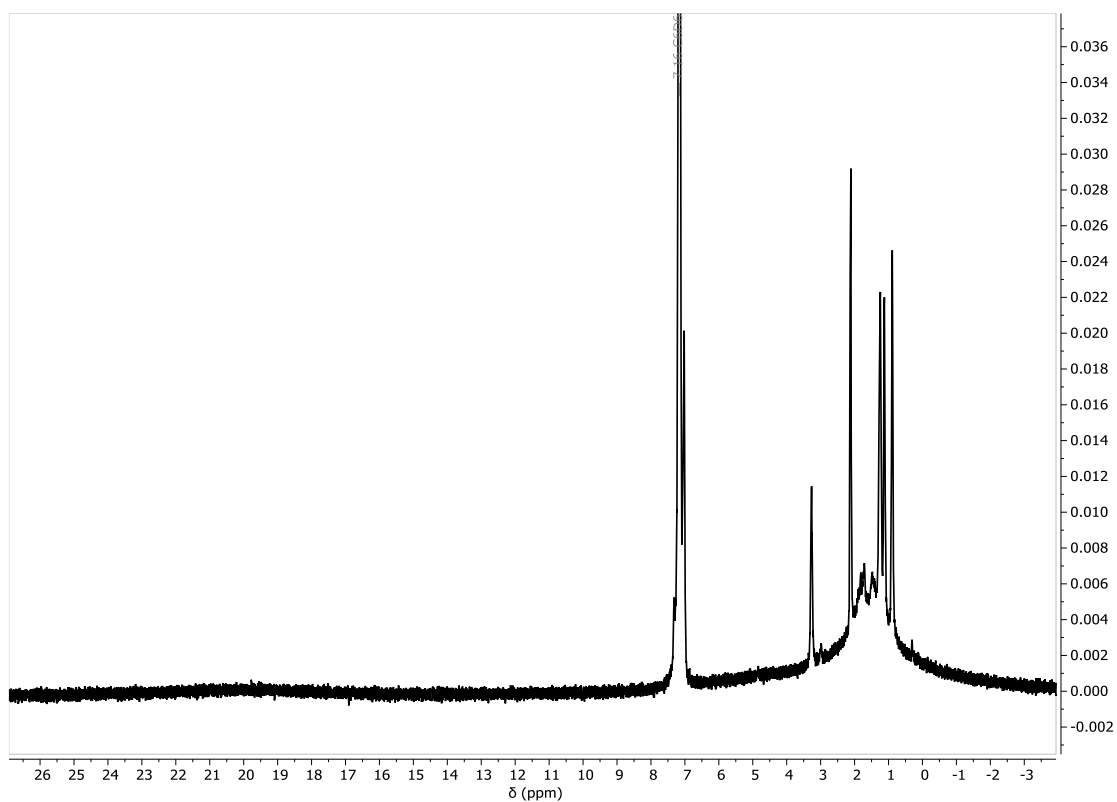
M.p: >260 °C (dec.).

IR (cm⁻¹): 3058 (w), 3001 (w), 2921 (s), 2848 (s), 1619 (s), 1590 (w), 1549 (s), 1486 (w), 1443 (s), 1377 (w), 1354 (m), 1306 (w), 1266 (m), 1211 (m), 1170 (m), 1130 (w), 1081 (w), 1018 (w), 997 (w), 941 (w), 923 (m), 890 (w), 842 (w), 822 (w), 799 (w), 775 (s), 764 (s), 728 (m)

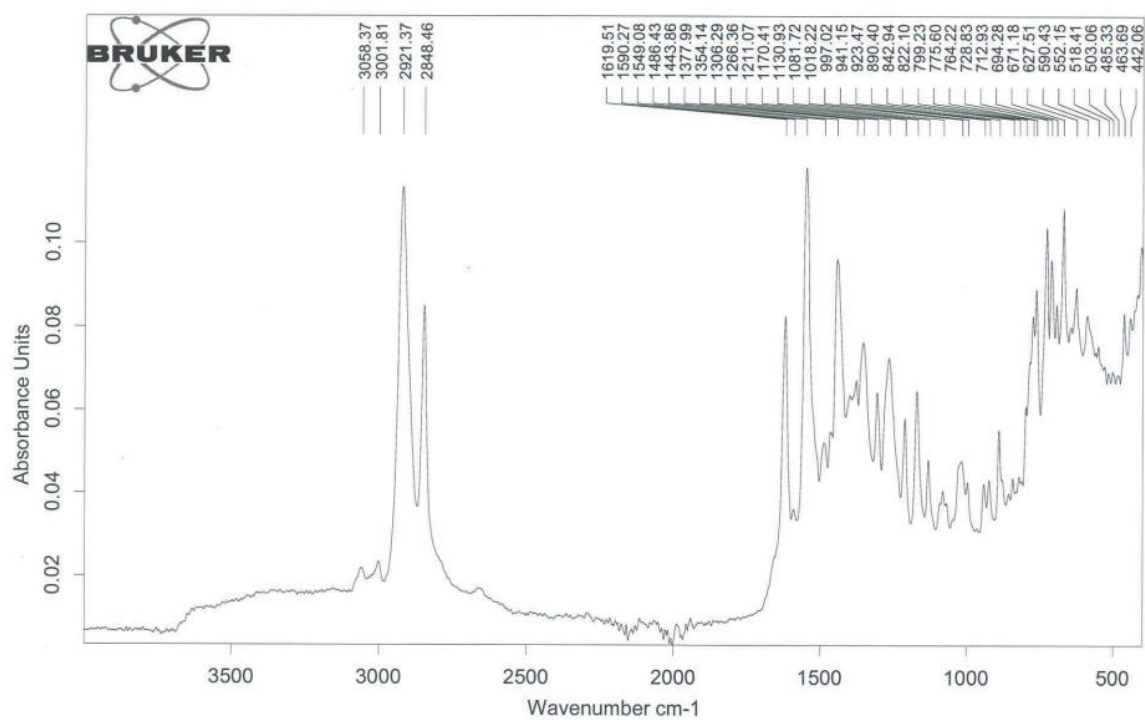
Elemental Analysis for $[(\text{BDI}^{\text{DicyP}})\text{Eu}(\mu\text{-COT})\text{Eu}(\text{BDI}^{\text{DicyP}})]$ (1563.9 g mol⁻¹):

Calculated: C: 69.08, H: 7.92, N: 3.58 %.

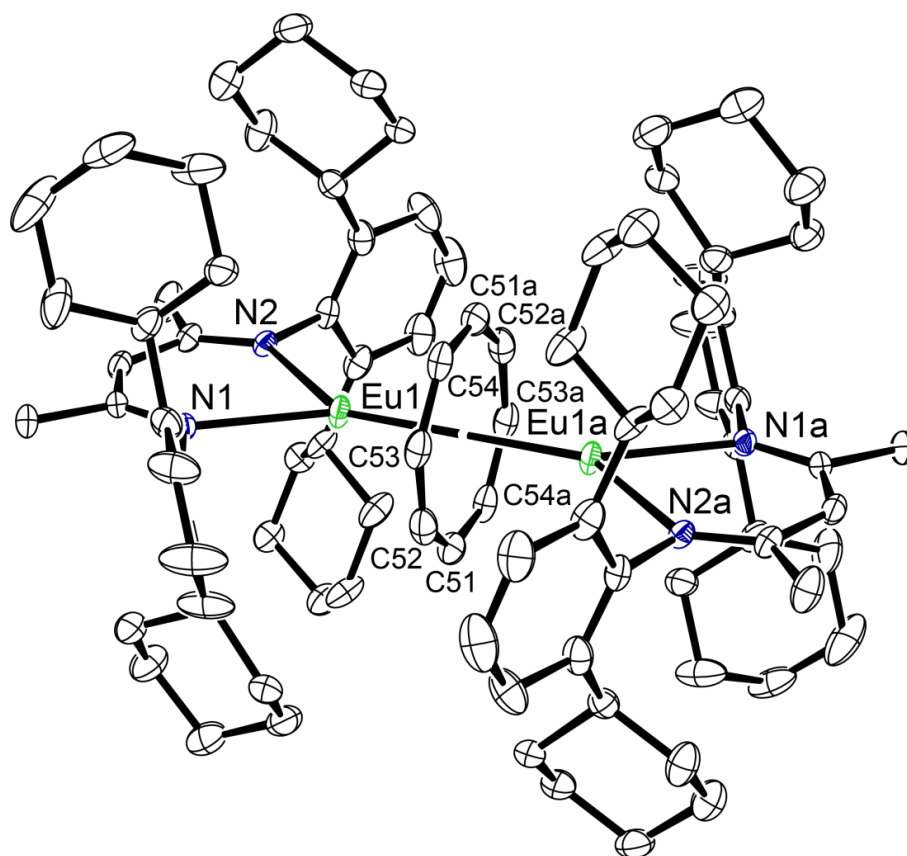
Found: C: 69.85, H: 7.88, N: 3.37 %.



Supplementary Figure 3.54. ¹H NMR spectrum (500 MHz, C₆D₆) of [(BDI^{Dicyl})Eu(μ-COT)Eu(BDI^{Dicyl})] (**3.24**).



Supplementary Figure 3.55. Infrared spectrum of [(BDI^{Dicyl})Eu(μ-COT)Eu(BDI^{Dicyl})] (**3.24**).



Supplementary Figure 3.56. Ortep representation (30% probability ellipsoids) of $[(\text{BDI}^{\text{DicyP}})\text{Eu}(\mu\text{-COT})\text{Eu}(\text{BDI}^{\text{DicyP}})]$ (**3.24**). Hydrogen atoms have been omitted for clarity.

$[(\text{BDI}^{\text{Dipp,DicyP}})\text{Eu}(\mu\text{-COT})\text{Eu}(\text{BDI}^{\text{Dipp,DicyP}})]$ (3.25)

A pale yellow toluene solution containing COT (13 mg, 0.13 mmol) was added to a scintillation vial containing a red suspension of $[(\text{BDI}^{\text{Dipp,DicyP}})\text{EuH}]_2$ (166 mg, 0.13 mmol) in toluene, the mixture was left to stir overnight at room temperature to give a yellow solution. The reaction solution was concentrated under vacuum and left to crystallise at room temperature, affording yellow crystals suitable for a single crystal X-ray diffraction experiment (63 mg, 69%).

The paramagnetic nature of $[(\text{BDI}^{\text{Dipp,DicyP}})\text{Eu}(\mu\text{-COT})\text{Eu}(\text{BDI}^{\text{Dipp,DicyP}})]$ hampered characterisation by multinuclear NMR spectroscopic techniques.

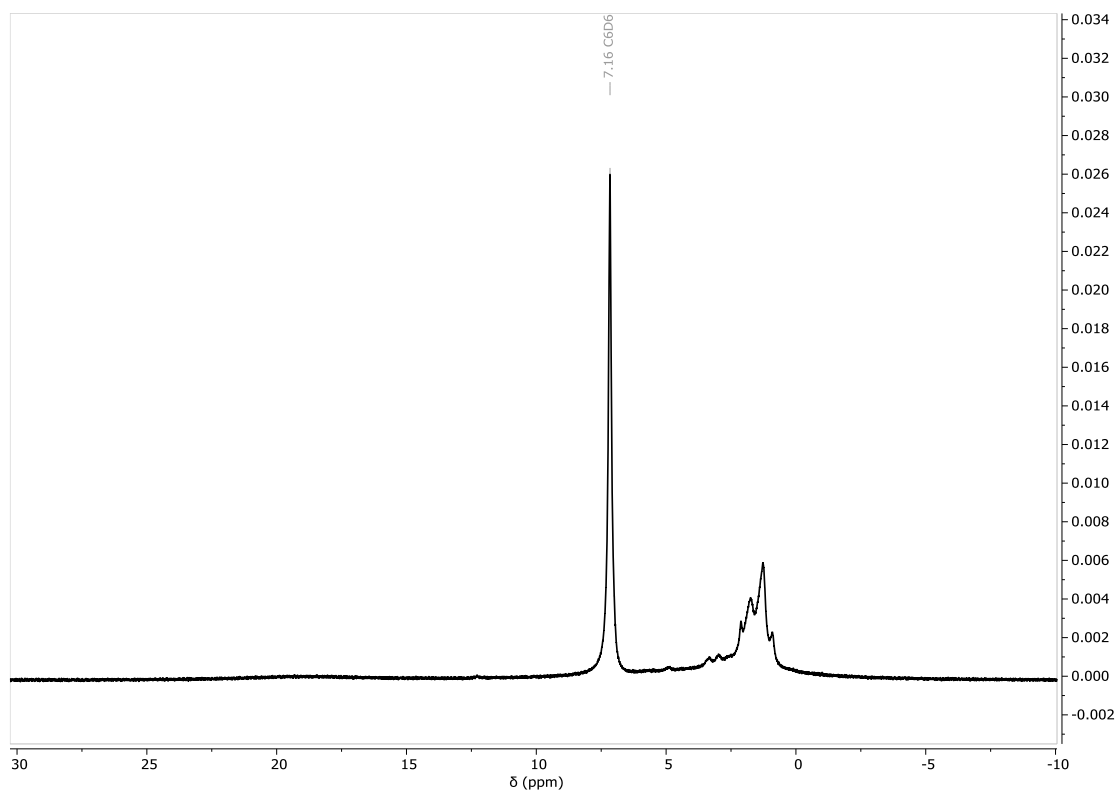
M.p: 110–125 °C (dec.).

IR (cm⁻¹): 3056 (w), 2920 (s), 2848 (m), 1619 (w), 1551 (m), 1522 (m), 1446 (w), 1399 (s), 1354 (w), 1030 (m), 1270 (w), 1216 (w), 1164 (s), 1130 (w), 1094 (w), 1019 (m), 925 (m), 890 (w), 839 (w), 786 (s), 761 (w), 729 (m), 713 (s).

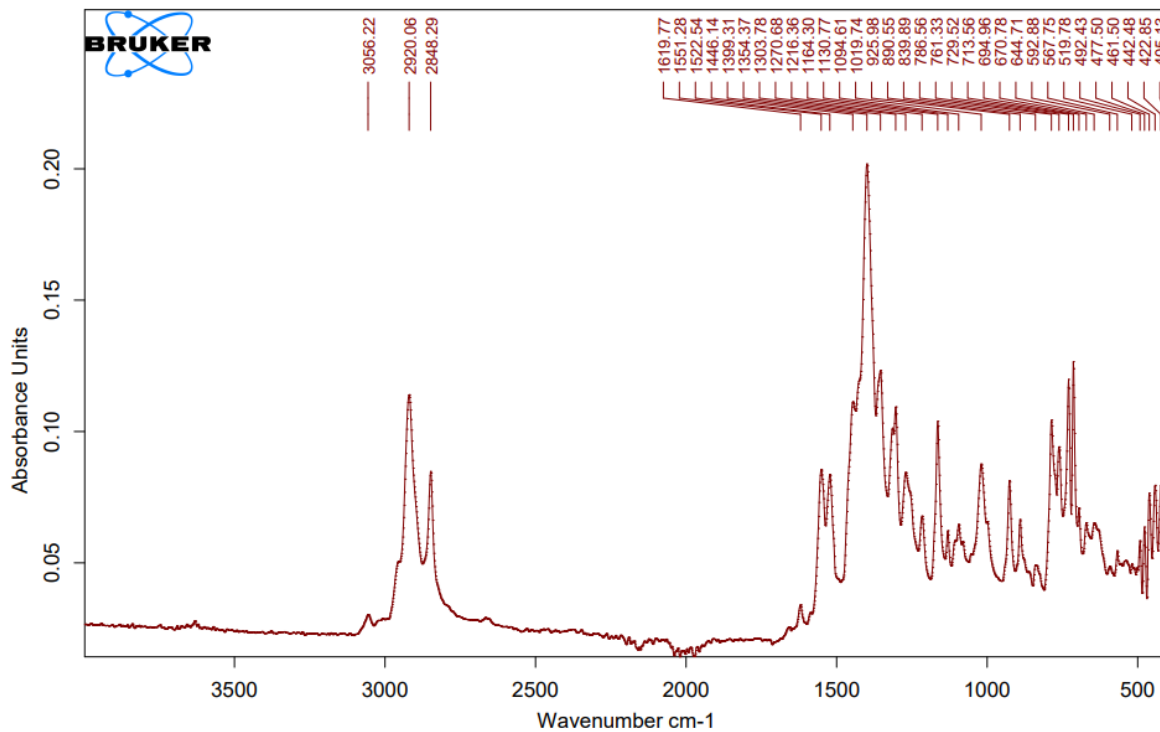
Elemental Analysis for $[(\text{BDI}^{\text{Dipp,DicyP}})\text{Eu}(\mu\text{-COT})\text{Eu}(\text{BDI}^{\text{Dipp,DicyP}})]$ (1403.7 g mol⁻¹):

Calculated: C: 66.74, H: 7.61, N: 3.99 %.

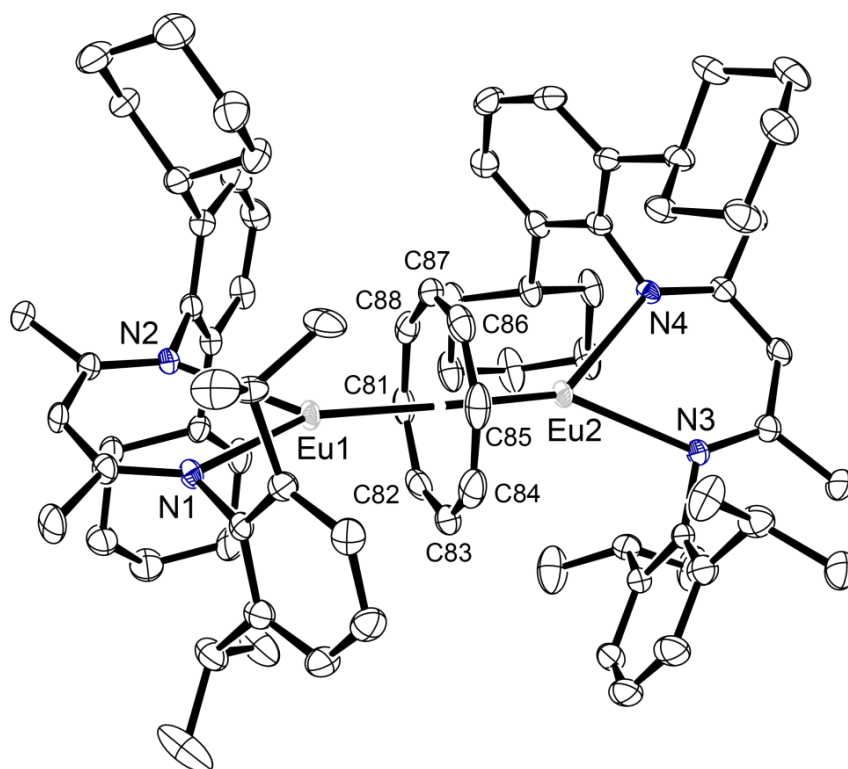
Found: C: 67.26, H: 7.79, N: 3.75 %.



Supplementary Figure 3.57. ^1H NMR spectrum (500 MHz, C_6D_6) of $[(\text{BDI}^{\text{Dipp,Dicyp}})\text{Eu}(\mu\text{-COT})\text{Eu}(\text{BDI}^{\text{Dipp,Dicyp}})]$ (**3.25**).



Supplementary Figure 3.58. Infrared spectrum of $[(\text{BDI}^{\text{Dipp,Dicyp}})\text{Eu}(\mu\text{-COT})\text{Eu}(\text{BDI}^{\text{Dipp,Dicyp}})]$ (**3.25**).



Supplementary Figure 3.59. Ortep representation (30% probability ellipsoids) of $[(\text{BDI}^{\text{Dipp,Dicyp}})\text{Eu}(\mu\text{-COT})\text{Eu}(\text{BDI}^{\text{Dipp,Dicyp}})]$ (**3.25**). Hydrogen atoms have been omitted for clarity.

$[(\text{BDI}^{\text{Dipp,TCHP}})(\text{THF})\text{Eu}(\mu\text{-COT})\text{Eu}(\text{THF})(\text{BDI}^{\text{Dipp,TCHP}})]$ (3.26)

A pale yellow THF solution containing COT (22 mg, 0.20 mmol) was added to a scintillation vial containing a red suspension of $[(\text{BDI}^{\text{Dipp,TCHP}})\text{EuH}]_2$ (304 mg, 0.20 mmol) in THF, the mixture was left to stir for 30 minutes at room temperature to give a yellow solution. The volatiles were removed *in vacuo* and the crude solid redissolved into toluene. Yellow crystals suitable for a single crystal X-ray diffraction experiment were obtained from a closed vial at room temperature (158 mg, 92 %).

The paramagnetic nature of $[(\text{BDI}^{\text{Dipp,TCHP}})(\text{THF})\text{Eu}(\mu\text{-COT})\text{Eu}(\text{THF})(\text{BDI}^{\text{Dipp,TCHP}})]$ hampered characterisation by multinuclear NMR spectroscopic techniques.

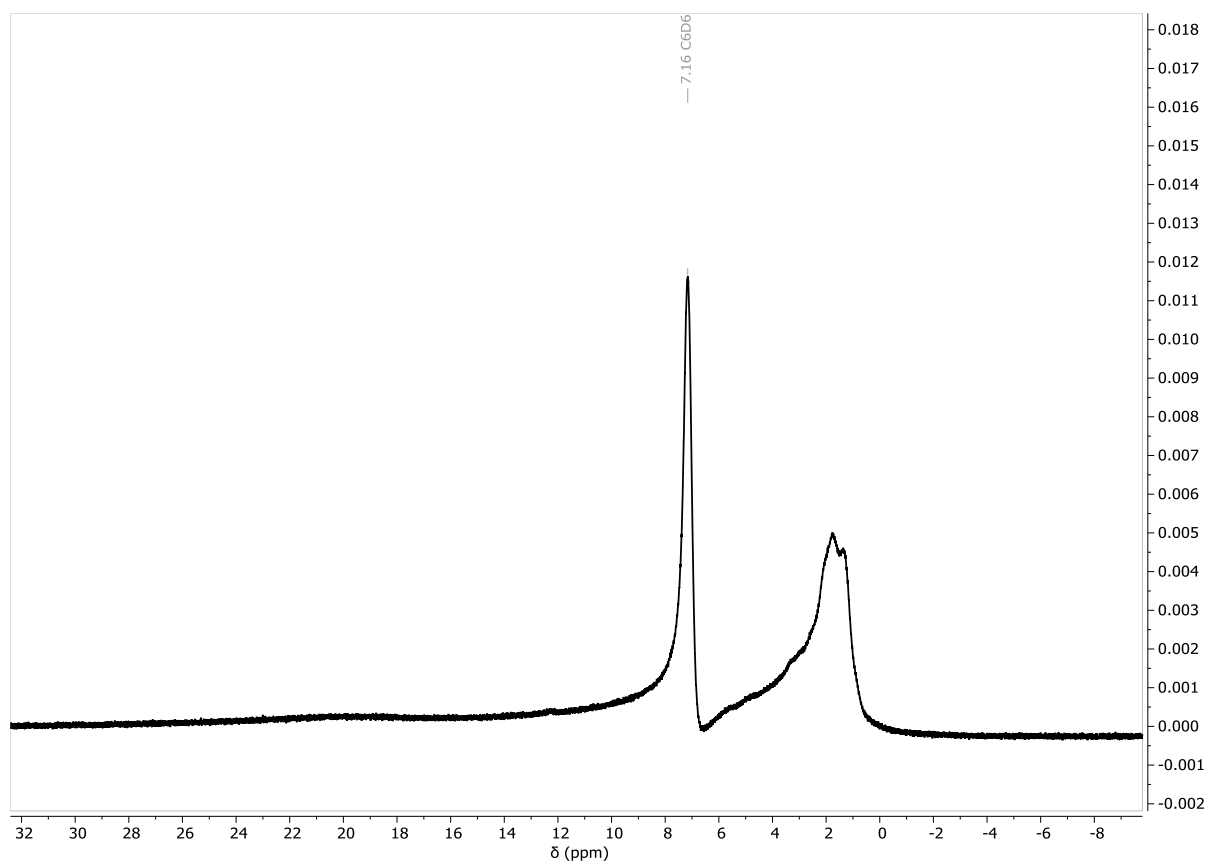
M.p: 100–119 °C (dec.).

IR (cm⁻¹): 2920 (s), 2848 (s), 1620 (w), 1550 (m), 1520 (w), 1444 (w), 1400 (s), 1359 (w), 1313 (w), 1277 (w), 1224 (w), 1172 (m), 1143 (m), 1108 (w), 1019 (m), 998 (w), 951 (w), 924 (m), 889 (w), 861 (m), 844 (w), 819 (w), 784 (m), 758 (m), 728 (m), 711 (s)

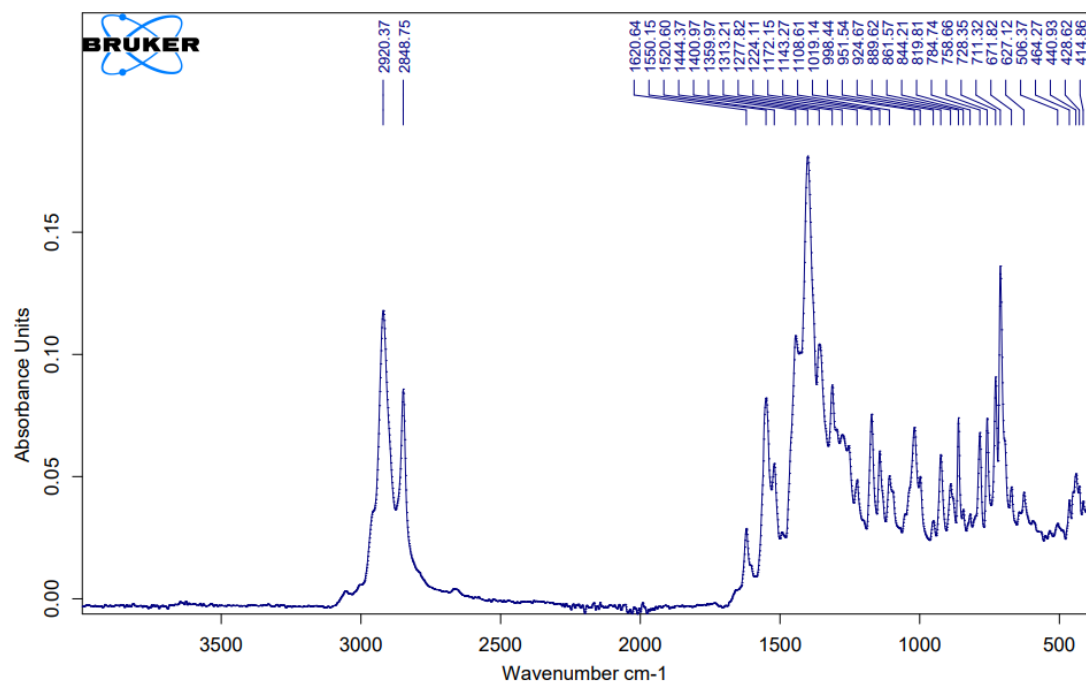
Elemental Analysis for $[(\text{BDI}^{\text{Dipp,TCHP}})(\text{THF})\text{Eu}(\mu\text{-COT})\text{Eu}(\text{THF})(\text{BDI}^{\text{Dipp,TCHP}})]$ (1712.2 g mol⁻¹):

Calculated: C: 68.75, H: 8.36, N: 3.27 %.

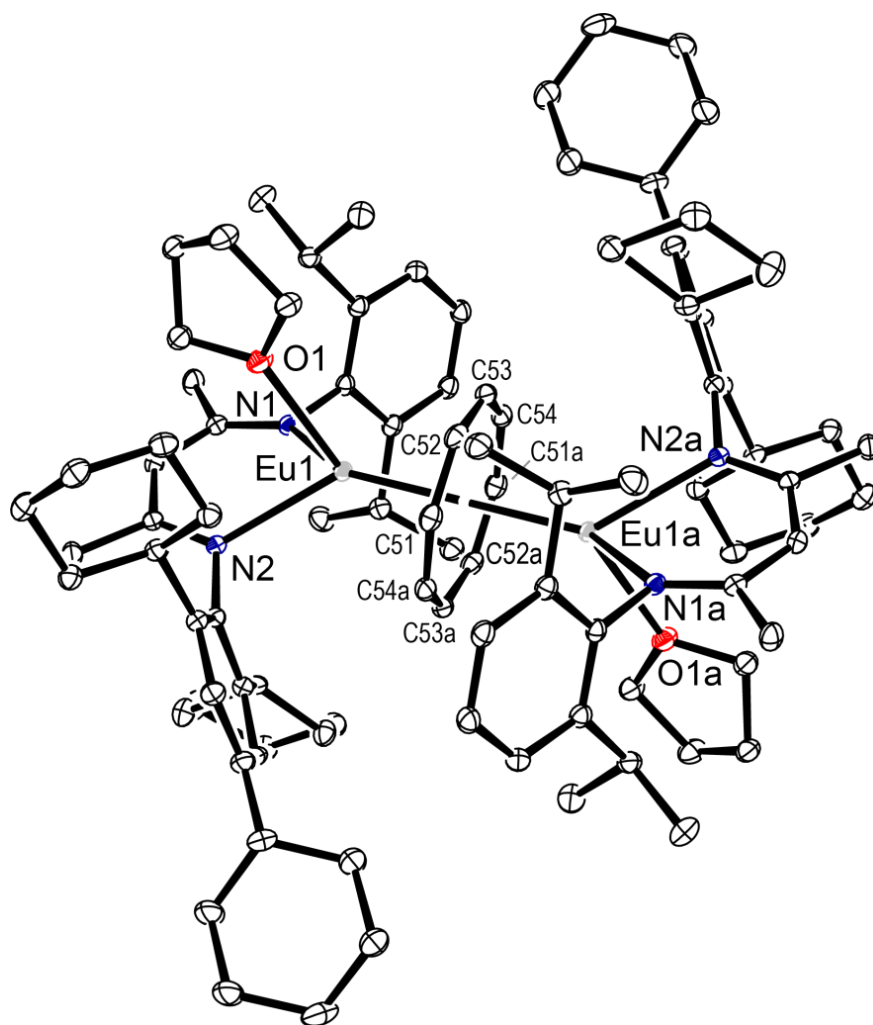
Found: C: 68.37, H: 8.41, N: 3.29 %.



Supplementary Figure 3.60. ^1H NMR spectrum (500 MHz, C_6D_6) of $[(\text{BDI}^{\text{Dipp,TCHP}})(\text{THF})\text{Eu}(\mu\text{-COT})\text{Eu}(\text{THF})(\text{BDI}^{\text{Dipp,TCHP}})]$ (**3.26**).



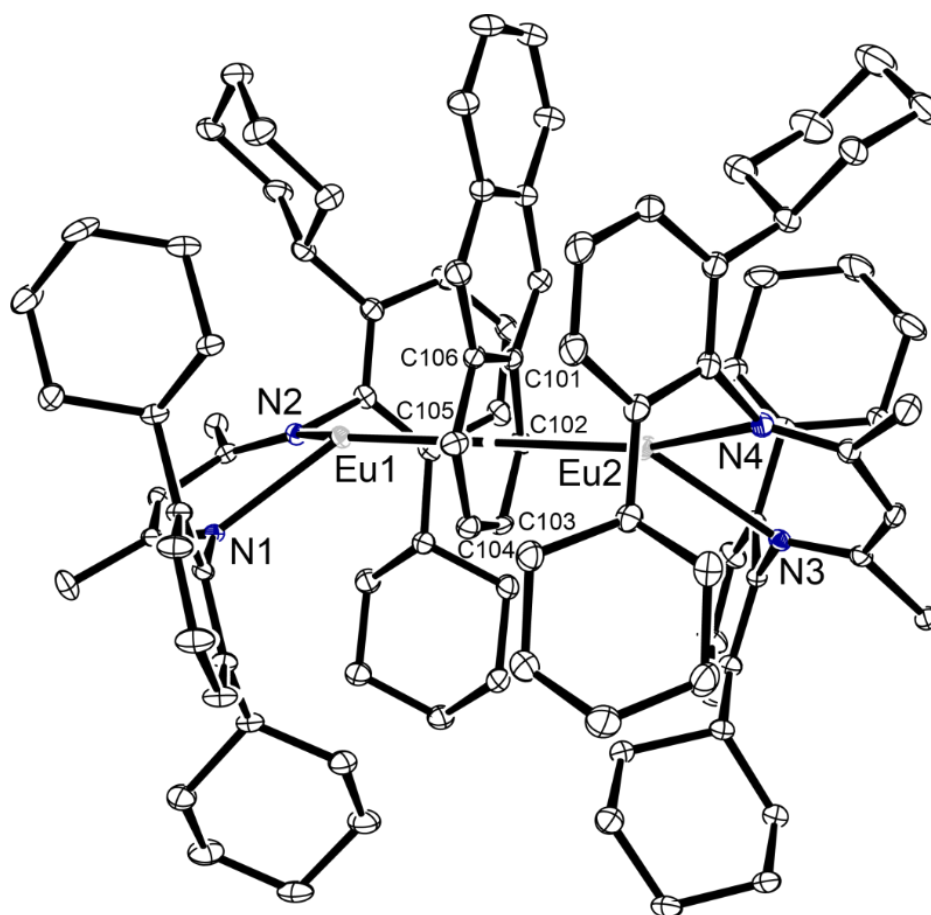
Supplementary Figure 3.61. Infrared spectrum of $[(\text{BDI}^{\text{Dipp,TCHP}})(\text{THF})\text{Eu}(\mu\text{-COT})\text{Eu}(\text{THF})(\text{BDI}^{\text{Dipp,TCHP}})]$ (**3.26**).



Supplementary Figure 3.62. Ortep representation (30% probability ellipsoids) of $[(\text{BDI}^{\text{Dipp,TCHP}})(\text{THF})\text{Eu}(\mu\text{-COT})\text{Eu}(\text{THF})(\text{BDI}^{\text{Dipp,TCHP}})]$ (**3.26**). Hydrogen atoms have been omitted for clarity.

$[(\text{BDI}^{\text{DicyP}})\text{Eu}(\mu\text{-C}_{14}\text{H}_{10})\text{Eu}(\text{BDI}^{\text{DicyP}})]$ (3.27)

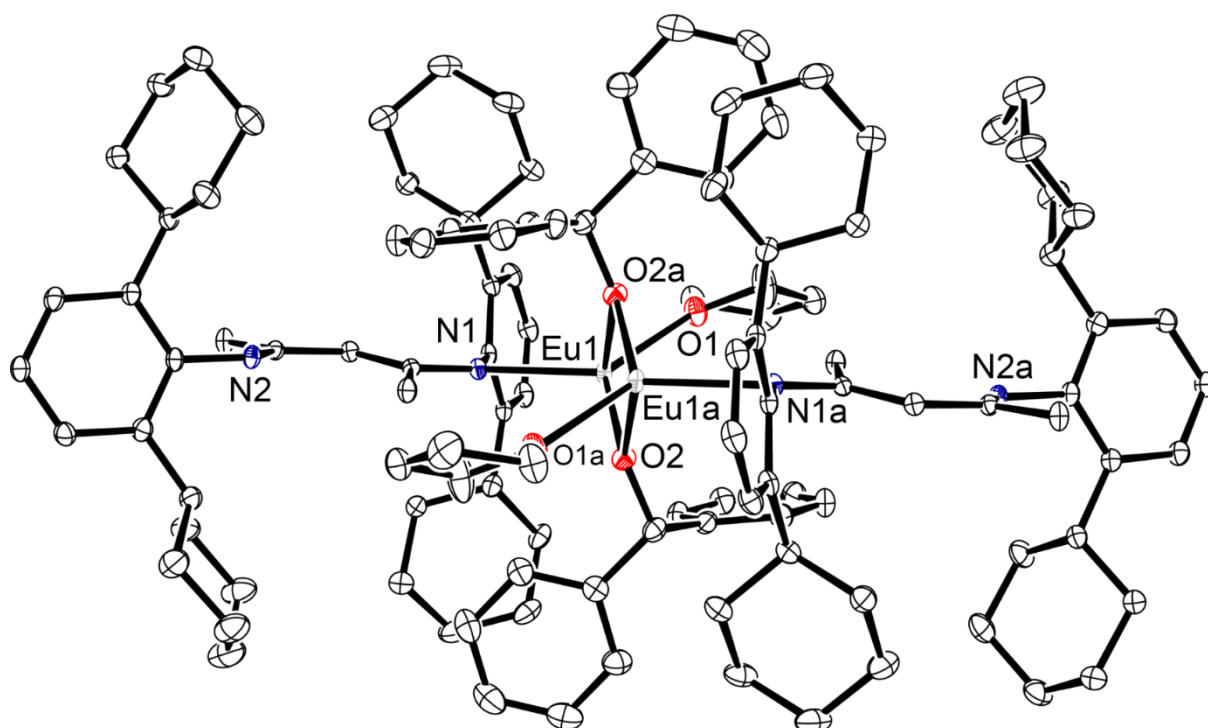
A THF solution of anthracene (22 mg, 0.13 mmol) was added to a scintillation vial containing a suspension of $[(\text{BDI}^{\text{DicyP}})\text{EuH}]_2$ (183 mg, 0.13 mmol) in THF. The mixture was left to stir at room temperature, resulting in a dark blue solution. The volatiles were removed under vacuum, the crude product dissolved into toluene and filtered through Celite. Brown crystals suitable for an X-ray diffraction experiment were afforded after slow evaporation at room temperature (Isolated yield: 90 mg, 84%).



Supplementary Figure 3.63. Ortep representation (30% probability ellipsoids) of $[(\text{BDI}^{\text{DicyP}})\text{Eu}(\mu\text{-C}_{14}\text{H}_{10})\text{Eu}(\text{BDI}^{\text{DicyP}})]$ (3.27). Hydrogen atoms have been omitted for clarity.

$[(\text{BDI}^{\text{DicyP}})\text{Eu}(\text{OCHPh}_2)(\text{THF})]_2$ (3.28)

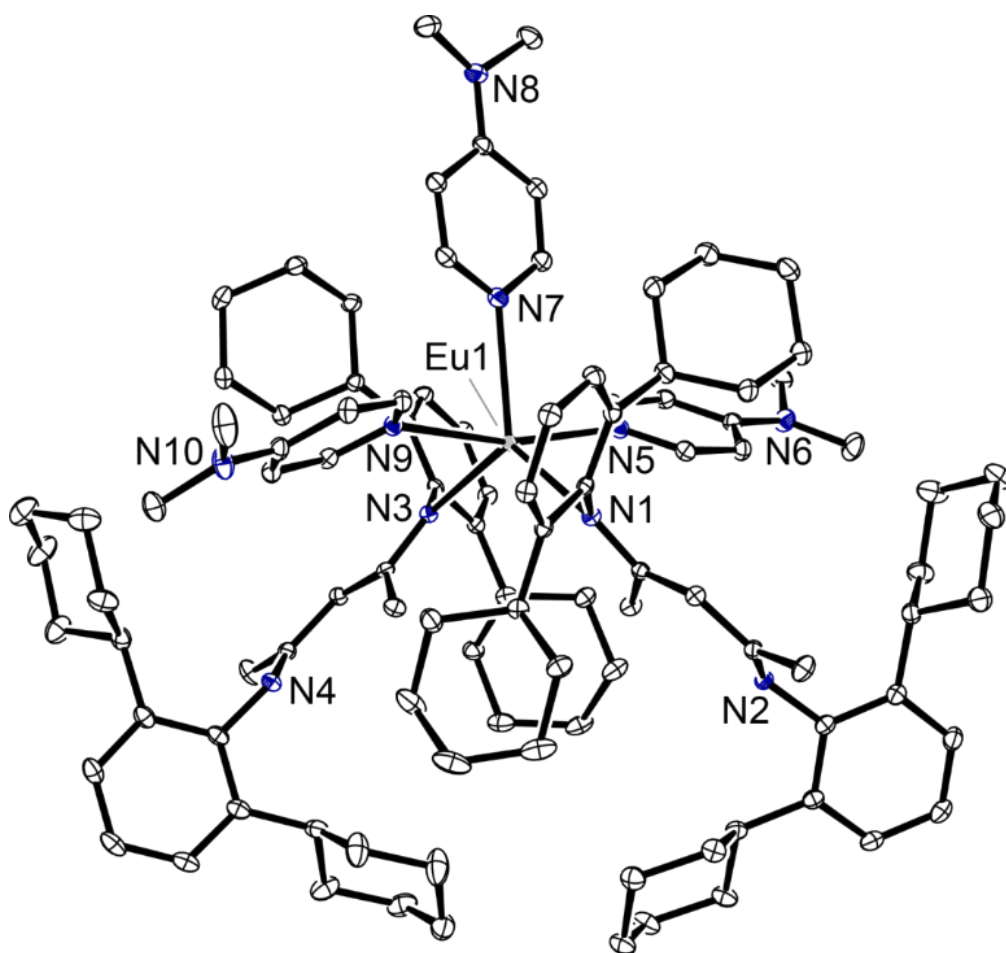
A colourless THF solution of benzophenone (39 mg, 0.21 mmol) was added to a scintillation vial containing a suspension of $[(\text{BDI}^{\text{DicyP}})\text{EuH}_2]$ (155 mg, 0.11 mmol) in THF and the mixture was left to stir at room temperature. After 1h, the solution was a blue-green colour, so the volatiles were removed under vacuum and the crude product dissolved into toluene. The solution was filtered through Celite and left to crystallise at room temperature affording yellow blocks suitable for an X-ray diffraction experiment.



Supplementary Figure 3.64. Ortep representation (30% probability ellipsoids) of $[(\text{BDI}^{\text{DicyP}})\text{Eu}(\mu\text{-OC(H)Ph}_2)(\text{THF})]_2$ (3.28). Hydrogen atoms have been omitted for clarity.

$[(\text{BDI}^{\text{Dicyp}})_2\text{Eu}(\text{DMAP})_3]$ (3.29)

A colourless THF solution of DMAP (25 mg, 0.20 mmol) was added to a scintillation vial containing a suspension of $[(\text{BDI}^{\text{Dicyp}})\text{EuH}_2]$ (150 mg, 0.10 mmol) in THF and the mixture was left to stir at room temperature. After 24h, the solution was dark orange-brown colour, so the volatiles were removed under vacuum and the crude product dissolved into the minimum volume of toluene. The crude product precipitated out within a few hours at room temperature, so the product was dissolved in $\frac{3}{4}$ of a vial of toluene solvent and left to slowly evaporate at room temperature, affording brown crystals suitable for an X-ray diffraction experiment.



Supplementary Figure 3.65. Ortep representation (30% probability ellipsoids) of $[(\text{BDI}^{\text{Dicyp}})_2\text{Eu}(\text{DMAP})_3]$ (3.29). Hydrogen atoms have been omitted for clarity.

[(2,6-di-^tBu-4-MePhO)₂Eu(THF)₃] (3.30)

A colourless THF solution of 2,6-di-^tBu-4-MePhOH (46 mg, 0.21 mmol) was added to a scintillation vial containing a suspension of [(BDI^{Dicyp})EuH₂] (150 mg, 0.10 mmol) in THF. The solution began turning yellow almost instantaneously and was gently bubbling. Within 1h, minimal residual [(BDI^{Dicyp})EuH₂] was left in the vial, so the solution was filtered through Celite and dried under vacuum. The crude product was redissolved into toluene, with formation of big yellow blocks suitable for an X-ray diffraction experiment after slow evaporation at room temperature.

This structure has been previously reported within the literature.^{16, 17}

3.2 Single Crystal X-ray Diffraction Analysis

3.2.1 Crystal Structure Data and Refinement Details

All non-hydrogen atoms were refined anisotropically, unless specified below. Hydrogen atoms were placed at calculated positions and refined using a riding model, unless otherwise specified.

K[Eu(HMDS)₃] (3.1)

There is half of the K[Eu(HMDS)₃] molecule in the asymmetric unit (ASU). No solvent. No disorder.

[Eu(HMDS)₂(Et₂O)] (3.2)

There is half of the [Eu(HMDS)₂] molecule in the ASU. Note the chiral space group. Standard H-atom treatment.

[(BDI^{Dipep})EuI]₂ (3.4)

There is half of the [LEuI]₂ dimer and half of a hexane molecule in the asymmetric unit (ASU). The remainder of the molecule is generated by an inversion operator. All non-H atoms were refined anisotropically, except for the atoms in the minor component of the isopentyl disorder (C129 and C130). Atom C28 was also modelled as two parts to model the attached proton position more correctly, and so was constrained to have the same position (EXYZ) and Uij components (EADP). The bond length between the ordered C28 and the disordered C29 and C129 was restrained to be the same length (SADI).

[(BDI^{Dipep})₂Eu(THF)₂] (3.5)

There is half of the [(L)₂Eu(THF)₂] dimer in the ASU. All non-H were refined anisotropically, except for second disorder component of "isopentyl" side chain. Standard H-atom treatment. No non-coordinated solvent. One of the "isopentyl" side chains is 50:50 disordered. The second orientation occupies space nearby the coordinated THF molecule (i.e. the THF molecule is only present at 50% occupancy). No THF was used in prep.

K[(BDI^{Dipep})₂Eu₂(HMDS)] (3.6)

There is one molecule of [L₂Eu₂.KHMS] in the ASU but grows to a polymeric structure. Just one minor disorder (C33/C34), which required bond length restraint. Electron density present in voids surrounding polymeric chain was too diffuse to be modelled. Squeeze was used to account for this unmodelled density, yielding 78 electrons/428 ang³ void.

[(BDI^{Dipep})₂Eu₂] (3.7)

There is half of the [(L)₂Eu₂] dimer in the ASU. Standard H-atom treatment, except for bridging methylene hydrogen atoms (H14B, H14B), whose coordinates were freely refined, though restrained to be the same length (SADI). Uiso for these hydrogen atoms were fixed to be 1.2x parent atom (C14). Still some high Q-peaks around Eu centre. Possibly seeing localised orbitals.

[(BDI^{Dipep})₂Eu(Et₂O)] (3.8)

There is an entire molecule of [(L)₂Eu(Et₂O)] and one molecule of Et₂O in the ASU. All non-H were refined anisotropically, except for minor component of disordered coordinated ether (occupancy 70:30).

[(BDI^{Dicyp})Eu(I)₂Eu(THF)(BDI^{Dicyp})] (3.10)

There is an entire molecule of [(L)Eu(I)₂Eu(THF)(L)] and one toluene molecule in the ASU. Some areas slightly more mobile (e.g. THF, cyclohexyl ring) but not obviously discrete components, so left with higher ADPs

[(BDI^{Dicyp})EuCH(SiMe₃)₂] (3.11)

There is an entire molecule of [(L)EuCH(TMS)₂] and 1.5 molecules of toluene in the ASU. Two toluene solvent molecules. One is full occupancy. The other sits on an inversion centre, so the entire molecule was modelled. PART -1 used alongside a fixed occupancy of 0.5. This molecule required ring constraints (AFIX 66), methyl-ring bond distance restraint (DFIX, SADI) and ADP restraints (SIMU) to ensure acceptable bonding and ADPs.

[(BDI^{Dicyp})₂Eu] (3.12)

There is an entire molecule of [(L)₂Eu] and 1.5 molecules of toluene in the ASU. Entire non-coordinated end of second ligand is disordered over two positions. Freely refined to occupancies of 0.57:0.43. All atoms in this disorder modelled anisotropically, but SIMU restraints were separately applied to benzene and cyclohexyl rings to achieve reasonable/sensible ADPs. One toluene molecule present on inversion centre, so entire molecule modelled (PART -1 used) and occupancy fixed to 0.5. The second toluene molecule is disordered over two sites; these disorder components were freely refined to occupancies of 0.51:0.49. All toluene solvent molecules were refined isotropically. Ring constraints (AFIX 66) were also applied to these molecules to ensure sensible bond lengths/angles.

[(BDI^{Dicyp})EuN(SiMe₃)₂] (3.13)

There are two [LEuHMDS] molecules and two half molecules of hexane (both at half occupancy) in the ASU. One of the cyclohexyl substituents in one of the ligands was disordered and modelled as two parts. The occupancy was freely refined to 0.51:0.49. The methine carbon atom in these disorder parts were very close so an EADP restraint was necessary. Both cyclohexyl disorder parts were restrained to be like a well-behaved cyclohexyl substituent (SAME restraint). One of the Eu atoms and the attached HMDS ligand was disordered and modelled as two parts. The occupancy was freely refined to 0.53:0.47. The geometry of both HMDS disorder parts were restrained to be like the well-behaved HMDS ligand (SAME restraint). Both half molecules of hexane are transformed into full hexane molecules by symmetry (inversion centre). However, both were also modelled at half occupancy, since higher occupancies gave unacceptably large ADPs. One of these molecules required a rigid bond restraint (DELU), with one atom (C113) also requiring an ISOR restraint to make the ADP of the atom less oblate. In the other hexane molecule, the non-terminal bond distances were restrained to be the same (SADI).

[(BDI^{Dicyp})EuH]₂ (3.14)

One quarter of [LEuH]₂ dimer in the ASU. Standard H-atom treatment, except H1. Without a DFIX restraint, this hydrogen atom refines acceptably, but results in a bond length that was considered too high (2.60 Å), so the bond length was restrained to 2.3 Å to be consistent with our other europium hydride structures with highly similar ligands and metal-ligand conformations. No solvent. Several rigid body restraints (DELU and/or RIGU) were required for the cyclohexyl and phenyl rings to achieve more sensible ADPs. One of the cyclohexyl rings was modelled as being disordered over two positions, with occupancies freely refined to 0.60:0.40. The bond length between the phenyl and disordered cyclohexyl ring was restrained (DFIX).

[(BDI^{Dicyp})Eu(DIC)] (3.15)

There is half of a [LEu(DIC)] molecule in the ASU. No solvent or disorder.

(BDI^{Dipp,Dicyp})H (3.16)

There are two LH molecules in the ASU. Standard H-atom treatment, except H1 and H41 (attached to one of the nitrogen atoms in each molecule), which were allowed to freely refine (Uiso and position). No solvent. Some of the atoms in the cyclohexyl rings had larger ADPs,

however, this was not considered problematic enough to warrant modelling as being disordered.

[(BDI^{Dipp,Dicyp})EuCH(SiMe₃)₂] (3.19)

There is an entire molecule of [LEuCH(SiMe₃)₂] and half a hexane molecule in the ASU. Standard H-atom treatment.

[(BDI^{Dipp,Dicyp})EuH]₂ (3.20)

There is half of the [LEuH]₂ dimer and two toluene molecules in the ASU. Standard H-atom treatment, except H1 (bridging hydride), which was allowed to freely refine (position and Uiso).

[(BDI^{Dipp,TCHP})EuI]₂ (3.21)

There is half of the [LEuI]₂ dimer and two toluene molecules in the ASU. One of the cyclohexyl rings on the ligand was modelled as a three-part disorder, with occupancies freely refined to 0.27:0.39:0.33. The geometry of these rings was restrained to be like another well-behaved cyclohexyl ring (SAME). Rigid bond restraints (DELU) were also applied to the atoms in these disordered rings. One of the isopropyl substituents was modelled as a two-part disorder, with occupancies freely refined to 0.59:41. The geometry of this group was restrained to be like another well-behaved isopropyl group (SAME).

[(BDI^{Dipp,TCHP})EuCH(SiMe₃)₂(THF)] (3.22)

There is an entire molecule of [LEuCH(SiMe₃)₂(THF)] in the ASU. One of the cyclohexyl groups on the ligand was modelled as a two-part disorder, with occupancies freely refined to 0.66:0.34. The geometries of both components were restrained to be like a well behaved cyclohexyl group (SAME). One of the methylene carbon atoms in the coordinated THF was modelled as a two-part disorder, with occupancies freely refined to 0.56:0.44. The toluene molecule was rather disordered, but despite large ADPs was modelled instead of using SQUEEZE (or equivalent). This toluene molecule was modelled as a two-part disorder, with occupancies freely refined to 0.65:0.35. The ring geometries of these toluene disorder components were constrained to ideal values (AFIX 66). Additionally, the methyl groups were constrained to have the same ADPs (EADP).

[(BDI^{Dipp,TCHP})EuH]₂ (3.23)

There is half of the [LEuH]₂ dimer and 3 molecules of benzene in the ASU. Standard H-atom treatment, except H1, which was allowed to refine freely (position and Uiso).

[(BDI^{Dicyp})Eu(μ -COT)Eu(BDI^{Dicyp})] (3.24)

There is half of the [LEu(COT)EuL] sandwich complex in the ASU. All non-H were refined anisotropically, except disordered toluene solvent molecule. One of the cyclohexyl side chains was disordered. Modelled as two disorder parts and occupancies freely refined to 0.71:0.29. The methine-aryl bond lengths in this disorder component were restrained to be the same (SADI). The geometry of both disorder parts was restrained to be like a well behaved cyclohexyl side chain (SAME). The methine atoms (C12/C12B) and one of the methylene atom pairs (C15/C15B) occupied similar coordinates, so were constrained to have the same ADPs (EADP). A rigid bond restraint (DELU) was applied to one of the other cyclohexyl side chains. The toluene solvent molecule was disordered over a symmetry site. The entire molecule was modelled at 0.4 occupancy and required use of a negative PART to prevent bonding to itself. Additionally, ring constraints (AFIX 66) were applied to this molecule to maintain appropriate geometry.

[(BDI^{Dipp,Dicyp})Eu(μ -COT)Eu(BDI^{Dipp,Dicyp})] (3.25)

There is the entire molecule of [LEu(COT)EuL] and half a toluene molecule in the ASU. One of the isopropyl side chains was modelled as being disordered over two sites, with occupancies freely refined to 0.63:0.37. The geometries of both components were restrained to be like a well-behaved isopropyl group (SAME). The toluene solvent molecule was present over a symmetry site, so the entire molecule was modelled at half occupancy. A negative PART instruction was required to prevent the symmetry mate bonding to itself. The benzene ring geometry was constrained (AFIX 66) and the ring-methyl bond was restrained (DFIX). Finally, the symmetry equivalent pairs were constrained to have the same ADPs (EADP).

[(BDI^{Dipp,TCHP})(THF)Eu(μ -COT)Eu(THF)(BDI^{Dipp,TCHP})] (3.26)

There is half of the [L(THF)Eu(COT)Eu(THF)L] dimer in the ASU. No solvent or disorder. Somewhat large, apparently empty, voids present, but no evidence of residual electron density.

[(BDI^{Dicyp})Eu(μ -C₁₄H₁₀)Eu(BDI^{Dicyp})] (3.27)

The entire [LEu(anthracene)EuL] molecule and half a molecule of toluene are in the ASU. All non-H atoms were refined anisotropically, except toluene carbon atoms. Toluene molecule was present at a symmetry site and was modelled as the entire molecule in a negative part to prevent improper molecule construction. The ring geometry was constrained (AFIX 66).

$[(\text{BDI}^{\text{DicyP}})\text{Eu}(\text{OC}\{\text{H}\}\text{Ph}_2)(\text{THF})]_2$ (3.28)

There is half of the $[(\text{L})\text{Eu}(\text{OCHPh}_2)(\text{THF})]_2$ dimer and two toluene molecules in the ASU. All non-H atoms were refined anisotropically except minor solvent disorder component. Both toluene molecules required ring constraints (AFIX 66) to impose correct ring geometry. One of these molecules was modelled as being disordered over two positions, with occupancies freely refined to 0.80:0.20.

$[(\text{BDI}^{\text{DicyP}})_2\text{Eu}(\text{DMAP})_3]$ (3.29)

The entire $[(\text{L})_2\text{Eu}(\text{DMAP})_3]$ molecule and three toluene molecules in the ASU. All non-H atoms were refined anisotropically, except for minor component of toluene disorder. One of the toluenes was modelled as being disordered over two positions, with occupancies freely refined to 0.83:0.17. The geometry of the minor component was restrained to be like that of one of the well-behaved toluene molecules.

Supplementary Table 3. 1. Crystal data and refinement for compounds **3.1**, **3.2** and **3.4 – 3.7**.

| | 3.1 | 3.2 | 3.4 | 3.5 | 3.6 | 3.7 |
|---|---|---|--|---|--|---|
| CCDC code | | | 2330119 | 2330117 | 2330118 | |
| Empirical formula | C ₁₈ H ₃₄ EuKN ₃ Si ₆ | C ₂₀ H ₅₆ EuN ₂ O ₂ Si ₄ | C ₈₀ H ₁₂₈ Eu ₂ I ₂ N ₄ | C ₇₂ H ₁₀₄ Eu ₂ N ₄ O | C ₇₄ H ₁₁₄ Eu ₂ KN ₅ Si ₂ | C ₇₄ H ₁₀₈ Eu ₂ N ₄ |
| Formula weight (g mol ⁻¹) | 672.24 | 620.98 | 1703.58 | 1345.51 | 1472.90 | 1357.56 |
| Temperature (K) | 120 | 120 | 150 | 150 | 120 | 120 |
| Crystal system | Monoclinic | Orthorhombic | Monoclinic | Monoclinic | Monoclinic | Triclinic |
| Space group | C 2/c | A b a 2 | C 2/c | P 21/n | C 21/n | P -1 |
| a (Å) | 8.5973(2) | 12.00948(15) | 22.1838(4) | 12.3651(4) | 12.7959(3) | 10.6524(3) |
| b (Å) | 21.1796(4) | 16.5780(2) | 12.5905(2) | 16.0430(4) | 23.2679(6) | 12.2194(5) |
| c (Å) | 19.2043(4) | 17.0067(2) | 30.0993(3) | 16.9974(6) | 26.5898(6) | 13.9477(4) |
| α (°) | 90 | 90 | 90 | 90 | 90 | 106.809(3) |
| β (°) | 90.818(2) | 90 | 108.611(2) | 102.825(4) | 100.001(2) | 90.043(2) |
| γ (°) | 90 | 90 | 90 | 90 | 90 | 104.839(3) |
| Volume (Å ³) | 3496.50(13)) | 3385.92(7) | 1989.25(12) | 3287.71(18) | 7796.4(3) | 1674.48(10) |
| Z | 4 | 4 | 4 | 2 | 4 | 1 |
| Calculated density (Mg/ m ³) | 1.277 | 1.218 | 1.420 | 1.359 | 1.255 | 1.346 |
| Absorption coefficient (mm ⁻¹) | 15.947 | 14.728 | 17.540 | 13.842 | 12.464 | 13.581 |
| F(000) | 1396 | 1300 | 3472 | 1396 | 3064 | 706 |
| Crystal size (mm ³) | 0.207 x 0.112 x 0.084 | 0.231 x 0.106 x 0.090 | 0.257 x 0.183 x 0.056 | 0.135 x 0.052 x 0.035 | 0.193 x 0.101 x 0.051 | 0.149 x 0.090 x 0.067 |
| Theta range for data collection (°) | 4.175 to 73.491 ° | 5.202 to 73.176 ° | 4.093 to 73.461 ° | 3.835 to 73.434 ° | 3.619 to 73.188 ° | 3.922 to 73.550 ° |
| Index ranges | -9 ≤ h ≤ 10 -21 ≤ k ≤ 26 -22 ≤ l ≤ 23 | -14 ≤ h ≤ 14 -20 ≤ k ≤ 19 -21 ≤ l ≤ 20 | -26 ≤ h ≤ 27 -15 ≤ k ≤ 15 -37 ≤ l ≤ 24 | -15 ≤ h ≤ 11 -16 ≤ k ≤ 19 -20 ≤ l ≤ 21 | -15 ≤ h ≤ 11 -28 ≤ k ≤ 28 -32 ≤ l ≤ 31 | -9 ≤ h ≤ 13 -15 ≤ k ≤ 15 -17 ≤ l ≤ 17 |
| Reflections collected | 9130 | 9209 | 23175 | 22949 | 54209 | 18500 |
| Independent reflections | 3501 R(int) = 0.0298 | 3248 R(int) = 0.0231 | 7925 R(int) = 0.0434 | 555 R(int) = 0.0466 | 15484 R(int) = 0.0492 | 6701 R(int) = 0.0593 |
| Completeness to theta | 99.9% | 100.0 % | 99.7% | 100.0% | 99.9 % | 99.9% |
| Data/ restraints/ parameters | 3501/ 0/ 142 | 3248/ 1/ 140 | 7925/ 1/ 419 | 6555/ 21/ 409 | 15484/ 2/ 789 | 6701/ 1/ 376 |
| Goodness-of-fit on F ² | 1.067 | 1.056 | 1.021 | 1.027 | 1.035 | 1.019 |
| Final R indices [I>2sigma(I)] | R1 = 0.0318 wR2 = 0.0748 | R1 = 0.0315 wR2 = 0.0862 | R1 = 0.0487 wR2 = 0.1156 | R1 = 0.0395 wR2 = 0.0920 | R1 = 0.0498 wR2 = 0.1340 | R1 = 0.0623 wR2 = 0.1609 |
| R indices (all data) | R1 = 0.0330 wR2 = 0.0754 | R1 = 0.0351 wR2 = 0.0903 | R1 = 0.0643 wR2 = 0.1248 | R1 = 0.0536 wR2 = 0.0993 | R1 = 0.0657 wR2 = 0.1437 | R1 = 0.0677 wR2 = 0.1675 |
| Largest diff. peak and hole (e. Å ⁻³) | 0.973 and -1.134 | 0.686 and -0.830 | 1.576 and -1.416 | 0.759 and -1.105 | 1.851 and -1.828 | 4.535 and -1.324 |

Supplementary Table 3.2. Crystal data and refinement details for compounds **3.8** and **3.10 – 3.14**.

| | 3.8 | 3.10 | 3.11 | 3.12 | 3.13 | 3.14 |
|---|--|--|--|--|---|---|
| CCDC code | 2330120 | 2330122 | 2330109 | 2330110 | | 2330105 |
| Empirical formula | C ₈₂ H ₁₃₄ EuN ₄ O ₂ | C ₉₃ H ₁₃₀ Eu ₂ I ₂ N ₄ O | C ₁₁₇ H ₁₇₆ Eu ₂ N ₄ Si ₄ | C ₁₈₅ H ₂₅₂ Eu ₂ N ₈ | C ₉₇ H ₁₅₇ Eu ₂ N ₆ Si ₄ | C ₈₂ H ₁₁₆ Eu ₂ N ₄ |
| Formula weight (g mol ⁻¹) | 1359.88 | 1877.72 | 2054.89 | 2891.85 | 1823.59 | 1461.70 |
| Temperature (K) | 150 | 120 | 120 | 120 | | |
| Crystal system | Triclinic | Monoclinic | Triclinic | Triclinic | Triclinic | Monoclinic |
| Space group | P -1 | P 21/c | P -1 | P -1 | P -1 | C 2/m |
| a (Å) | 13.5181(4) | 21.6702(2) | 13.4434(2) | 13.6155(2) | 12.4240(2) | 21.977(4) |
| b (Å) | 14.9144(4) | 13.0961(2) | 13.8071(2) | 14.5166(2) | 19.1187(3) | 14.914(3) |
| c (Å) | 21.6471(6) | 31.6904(4) | 15.9610(3) | 21.7762(3) | 22.7172(4) | 15.389(3) |
| α (°) | 75.840(2) | 90 | 95.2500(10) | 97.0580(10) | 105.471(2) | 90 |
| β (°) | 77.247(2) | 106.5980(10) | 95.0380(10) | 106.2130(10) | 100.418(2) | 134.18(3) |
| γ (°) | 67.707(3) | 90 | 109.735(2) | 102.0020(10) | 94.569(1) | 90 |
| Volume (Å ³) | 3875.4(2) | 8618.84(19) | 2754.52(8) | 3966.85(10) | 5068.01(16) | 3617.5(18) |
| Z | 2 | 4 | 1 | 1 | 2 | 2 |
| Calculated density (Mg/ m ³) | 1.165 | 1.447 | 1.239 | 1.211 | 1.195 | 1.342 |
| Absorption coefficient (mm ⁻¹) | 6.129 | 16.283 | 8.829 | 6.004 | 9.540 | 1.763 |
| F(000) | 1466 | 3824 | 1088 | 1544 | 1926.0 | 1524 |
| Crystal size (mm ³) | 0.234 x 0.115 x 0.050 | 0.111 x 0.079 x 0.034 | 0.146 x 0.085 x 0.039 | 0.132 x 0.100 x 0.049 | 0.209 x 0.103 x 0.036 | 0.010 x 0.005 x 0.003 |
| Theta range for data collection (°) | 3.557 to 73.467 ° | 3.676 to 73.508 ° | 3.430 to 73.568 ° | 3.474 to 73.548 ° | 3.651 to 72.426 ° | 1.845 to 25.681 ° |
| Index ranges | -16 ≤ h ≤ 11 | -20 ≤ h ≤ 26 | -16 ≤ h ≤ 15 | -16 ≤ h ≤ 16 | -15 ≤ h ≤ 15 | -26 ≤ h ≤ 26 |
| | -18 ≤ k ≤ 17 | -15 ≤ k ≤ 16 | -17 ≤ k ≤ 16 | -17 ≤ k ≤ 14 | -23 ≤ k ≤ 22 | -18 ≤ k ≤ 18 |
| | -26 ≤ l ≤ 26 | -39 ≤ l ≤ 38 | -19 ≤ l ≤ 19 | -27 ≤ l ≤ 27 | -24 ≤ l ≤ 28 | -18 ≤ l ≤ 17 |
| Reflections collected | 51898 | 60939 | 35970 | 53391 | 69026 | 11674 |
| Independent reflections | 15481 | 17243 | 11038 | 15843 | 19894 | 3492 |
| | R(int) = 0.0416 | R(int) = 0.0782 | R(int) = 0.0479 | R(int) = 0.0393 | R(int) = 0.0454 | R(int) = 0.0687 |
| Completeness to theta | 100.0 % | 100.0% | 100.0 % | 100.0% | 99.1% | 97.5 % |
| Data/ restraints/ parameters | 15481/ 0/ 844 | 17243/ 0/ 924 | 11038/ 44/ 602 | 15843/ 469/ 1003 | 19894/ 67/ 1134 | 3492/ 75/ 275 |
| Goodness-of-fit on F ² | 1.028 | 1.023 | 1.024 | 1.016 | 1.023 | 0.999 |
| Final R indices [I>2sigma(I)] | R1 = 0.0329 | R1 = 0.0577 | R1 = 0.0372 | R1 = 0.0323 | R1 = 0.0393 | R1 = 0.0631 |
| | wR2 = 0.0795 | wR2 = 0.1309 | wR2 = 0.0918 | wR2 = 0.0784 | wR2 = 0.1031 | wR2 = 0.1616 |
| R indices (all data) | R1 = 0.0364 | R1 = 0.0861 | R1 = 0.0416 | R1 = 0.0342 | R1 = 0.0477 | R1 = 0.0749 |
| | wR2 = 0.0818 | wR2 = 0.1456 | wR2 = 0.0950 | wR2 = 0.0796 | wR2 = 0.1085 | wR2 = 0.1707 |
| Largest diff. peak and hole (e. Å ⁻³) | 0.955 and -1.141 | 3.428 and -1.835 | 0.536 and -0.802 | 0.650 and -0.957 | 0.870 and -0.890 | 1.838 and -1.688 |

Supplementary Table 3.3. Crystal data and refinement data for compounds **3.15**, **3.16** and **3.19 – 3.22**.

| | 3.15 | 3.16 | 3.19 | 3.20 | 3.21 | 3.22 |
|---|--|--|--|---|--|---|
| CCDC code | | 2330116 | 2330108 | 2330115 | 2330121 | 2330111 |
| Empirical formula | C ₄₈ H ₇₂ EuN ₄ | C ₃₅ H ₅₀ N ₂ | C ₄₅ H ₇₅ EuN ₂ Si ₂ | C ₈₄ H ₁₁₆ Eu ₂ N ₂ | C ₉₆ H ₁₃₄ Eu ₂ I ₂ N ₄ | C ₅₉ H ₉₄ EuN ₂ OSi ₂ |
| Formula weight (g mol ⁻¹) | 857.05 | 498.77 | 852.21 | 1485.72 | 1901.78 | 1055.50 |
| Temperature (K) | 120 | 120 | 120 | 120 | 120 | 120 |
| Crystal system | Monoclinic | Monoclinic | Monoclinic | Monoclinic | Monoclinic | Orthorhombic |
| Space group | C 2/c | P 21/c | P 21/n | C 2/c | P 21/n | P b c a |
| a (Å) | 17.4348(3) | 23.3557(6) | 12.36550(10) | 20.5874(3) | 13.86930(10) | 13.91550(10) |
| b (Å) | 11.78636(15) | 10.31370(10) | 15.75300(10) | 17.83133(18) | 20.9262(2) | 22.5503(2) |
| c (Å) | 21.2730(3) | 28.0251(6) | 23.6871(2) | 21.5918(3) | 15.7801(2) | 36.3105(3) |
| α (°) | 90 | 90 | 90 | 90 | 90 | 90 |
| β (°) | 95.9680(15) | 113.911(3) | 96.6860(10) | 110.3114(15) | 103.6180(10) | 90 |
| γ (°) | 90 | 90 | 90 | 90 | 90 | 90 |
| Volume (Å ³) | 4347.76(11) | 6171.4(3) | 4582.72(6) | 7433.50(17) | 4451.13(8) | 11394.19(16) |
| Z | 4 | 8 | 4 | 4 | 2 | 8 |
| Calculated density (Mg/ m ³) | 1.309 | 1.074 | 1.235 | 1.328 | 1.419 | 1.231 |
| Absorption coefficient (mm ⁻¹) | 10.585 | 0.457 | 10.507 | 12.286 | 15.763 | 8.563 |
| F(000) | 1804 | 2192 | 1800 | 3096 | 1940 | 4488 |
| Crystal size (mm ³) | 0.205 x 0.099 x 0.040 | 0.346 x 0.089 x 0.031 | 0.199 x 0.111 x 0.040 | 0.104 x 0.051 x 0.032 | 0.146 x 0.113 x 0.046 | 0.204 x 0.196 x 0.034 |
| Theta range for data collection (°) | 4.179 to 73.460 ° | 4.141 to 72.451 ° | 3.758 to 72.364 ° | 3.561 to 72.276 ° | 3.573 to 73.053 ° | 3.921 to 72.333 ° |
| Index ranges | -21 ≤ h ≤ 21 -9 ≤ k ≤ 14 -26 ≤ l ≤ 26 | -28 ≤ h ≤ 28 -12 ≤ k ≤ 12 -34 ≤ l ≤ 28 | -10 ≤ h ≤ 15 -19 ≤ k ≤ 19 -28 ≤ l ≤ 29 | -25 ≤ h ≤ 24 -18 ≤ k ≤ 21 -22 ≤ l ≤ 26 | -16 ≤ h ≤ 17 -25 ≤ k ≤ 25 -18 ≤ l ≤ 19 | -16 ≤ h ≤ 17 -18 ≤ k ≤ 27 -44 ≤ l ≤ 44 |
| Reflections collected | 13288 | 43453 | 32279 | 32364 | 45331 | 72993 |
| Independent reflections | 4327 R(int) = 0.0313 | 12110 R(int) = 0.0412 | 8988 R(int) = 0.0360 | 7301 R(int) = 0.0535 | 8786 R(int) = 0.0348 | 11190 R(int) = 0.0364 |
| Completeness to theta | 99.8 % | 99.8% | 99.8% | 99.9% | 100.0 % | 100.0% |
| Data/ restraints/ parameters | 4327/ 0/ 244 | 12110/ 0/ 687 | 8988/ 0/ 464 | 7301/ / 417 | 8786/ 118/ 617 | 11190/ 36/ 699 |
| Goodness-of-fit on F ² | 1.161 | 1.037 | 1.032 | 1.046 | 1.023 | 1.030 |
| Final R indices [I>2sigma(I)] | R1 = 0.0884 wR2 = 0.2215 | R1 = 0.0634 wR2 = 0.1585 | R1 = 0.0290 wR2 = 0.051 | R1 = 0.0351 wR2 = 0.0763 | R1 = 0.0371 wR2 = 0.0873 | R1 = 0.0280 wR2 = 0.0643 |
| R indices (all data) | R1 = 0.0943 wR2 = 0.2266 | R1 = 0.0792 wR2 = 0.1691 | R1 = 0.0348 wR2 = 0.0676 | R1 = 0.0457 wR2 = 0.0808 | R1 = 0.0414 wR2 = 0.0903 | R1 = 0.0360 wR2 = 0.0680 |
| Largest diff. peak and hole (e. Å ⁻³) | 0.568 and -3.468 | 0.431 and -0.335 | 0.782 and -0.728 | 0.788 and -0.789 | 2.589 and -1.253 | 0.414 and -0.458 |

Supplementary Table 3.4. Crystal data and refinement data for compounds **3.23** – **3.29**.

| | 3.23 | 3.24 | 3.25 | 3.26 | 3.27 | 3.28 | 2.29 |
|---|--|---|--|---|--|---|---|
| CCDC code | 2330112 | 2330107 | 2330114 | 2330113 | | | |
| Empirical formula | C ₁₀₀ H ₁₃₈ Eu ₂ N ₄ | C _{95.60} H _{128.40} Eu ₂ N ₄ | C ₁₆₃ H ₂₂₀ Eu ₂ N ₈ | C ₉₈ H ₁₄₂ Eu ₂ N ₄ O | C ₁₉₉ H ₂₅₆ Eu ₄ N ₈ | C ₁₄₄ H ₁₈₂ Eu ₂ N ₄ O ₄ | C ₁₂₄ H ₁₆₈ EuN ₁₀ |
| Formula weight (g mol ⁻¹) | 1700.06 | 1637.54 | 2899.30 | 1712.07 | 3367.94 | 2336.85 | 1950.63 |
| Crystal system | Triclinic | Monoclinic | Monoclinic | Triclinic | Triclinic | Triclinic | Monoclinic |
| Space group | P -1 | P 21/n | P 21/n | P -1 | P -1 | P-1 | I 2/a |
| a (Å) | 12.45300(10) | 15.7815(4) | 17.7433(3) | 12.7581(2) | 14.1444(2) | 14.2684(4) | 28.0027(2) |
| b (Å) | 14.6303(2) | 13.3072(5) | 18.0873(3) | 12.9495(3) | 15.4167(3) | 15.9299(6) | 18.6157(2) |
| c (Å) | 14.70390(10) | 21.1484(6) | 23.5099(3) | 15.2308(3) | 21.6746(4) | 16.1987(5) | 42.5741(3) |
| α (°) | 106.9100(10) | 90 | 90 | 114.877(2) | 73.4860(15) | 63.414(3) | 90 |
| β (°) | 101.8580(10) | 108.409(3) | 107.231(2) | 104.398(2) | 79.0923(13) | 78.669(3) | 97.8620(10) |
| γ (°) | 113.2500(10) | 90 | 90 | 90.451(2) | 70.5141(14) | 68.178(3) | 90 |
| Volume (Å ³) | 2193.05(4) | 1989.25(12) | 7206.4(2) | 2192.93(8) | 4248.50(13) | 3054.6(2) | 21984.8(3) |
| Z | 1 | 2 | 2 | 1 | 1 | 1 | 8 |
| Calculated density (Mg/ m ³) | 1.287 | 1.291 | 1.336 | 1.296 | 1.316 | 1.270 | 1.179 |
| Absorption coefficient (mm ⁻¹) | 10.477 | 10.886 | 12.661 | 10.498 | 10.814 | 7.692 | 4.475 |
| F(000) | 892 | 1712 | 3012 | 900 | 1758 | 1232 | 8360 |
| Crystal size (mm ³) | 0.359 x 0.263 x 0.115 | 0.228 x 0.069 x 0.033 | 0.117 x 0.078 x 0.036 | 0.128 x 0.075 x 0.035 | 0.197 x 0.145 x 0.044 | 0.266 x 0.258 x 0.054 | 0.440 x 0.190 x 0.10 |
| Theta range for data collection (°) | 3.612 to 72.389 ° | 3.986 to 72.322 ° | 3.574 to 68.247 ° | 3.606 to 72.355 ° | 3.768 to 72.407 ° | 3.849 to 72.569 ° | 3.672 to 72.583 ° |
| Index ranges | -15 ≤ h ≤ 15 -18 ≤ k ≤ 18 -15 ≤ l ≤ 18 | -10 ≤ h ≤ 19 -15 ≤ k ≤ 16 -25 ≤ l ≤ 26 | -21 ≤ h ≤ 19 -21 ≤ k ≤ 21 -28 ≤ l ≤ 28 | -15 ≤ h ≤ 12 -15 ≤ k ≤ 16 -18 ≤ l ≤ 18 | -17 ≤ h ≤ 16 -18 ≤ k ≤ 18 -26 ≤ l ≤ 26 | -16 ≤ h ≤ 17 -19 ≤ k ≤ 19 -19 ≤ l ≤ 20 | -32 ≤ h ≤ 34 -22 ≤ k ≤ 22 -51 ≤ l ≤ 52 |
| Reflections collected | 69364 | 26954 | 48399 | 25087 | 54745 | 36683 | 63373 |
| Independent reflections | 8656 R(int) = 0.0448 | 8263 R(int) = 0.0610 | 13177 R(int) = 0.0613 | 8603 R(int) = 0.0292 | 16601 R(int) = 0.0464 | 11998 R(int) = 0.0368 | 21555 R(int) = 0.0195 |
| Completeness to theta | 100.0% | 100.0% | 99.9% | 99.9% | 99.8 % | 99.9% | 99.8% |
| Data/ restraints/ parameters | 8656/ 0/ 488 | 8263/ 46/ 496 | 13177/ 10/ 839 | 8603/ 0/ 484 | 16601/ 0/ 945 | 11998/ 0/ 692 | 21555/ 15/ 1259 |
| Goodness-of-fit on F ² | 1.084 | 1.027 | 1.051 | 1.029 | 1.039 | 1.039 | 1.036 |
| Final R indices [I>2sigma(I)] | R1 = 0.0403 wR2 = 0.1046 | R1 = 0.0600 wR2 = 0.1518 | R1 = 0.0422 wR2 = 0.0895 | R1 = 0.0247 wR2 = 0.0574 | R1 = 0.0353 wR2 = 0.0817 | R1 = 0.0354 wR2 = 0.0897 | R1 = 0.0243 wR2 = 0.0589 |
| R indices (all data) | R1 = 0.0406 wR2 = 0.1049 | R1 = 0.0749 wR2 = 0.1636 | R1 = 0.0582 wR2 = 0.0958 | R1 = 0.0261 wR2 = 0.0582 | R1 = 0.0444 wR2 = 0.0861 | R1 = 0.0369 wR2 = 0.0910 | R1 = 0.0255 wR2 = 0.0596 |
| Largest diff. peak and hole (e. Å ⁻³) | 1.864 and -1.440 | 1.618 and -1.303 | 0.631 and -1.001 | 0.664 and -0.705 | 0.996 and -1.192 | 0.765 and -0.914 | 0.268 and -0.491 |

4.0 Chapter Four Experimental

4.1 Synthetic, Spectroscopic and Analytic Data

[(BDI^{Dicyp})SmI]₂ (4.1)

A colourless THF solution of diiodoethane (217.9 mg, 0.77 mmol) was added to a scintillation vial containing a suspension of Sm_(m) (119.7 mg, 0.80 mmol) in THF and was left to stir overnight at room temperature. A brown THF solution of (BDI^{Dicyp})K (477.0 mg, 0.77 mmol) was added dropwise to the resultant turquoise solution and left to stir for an additional 4 hr at room temperature to give a dark army green solution with grey precipitates. The solvent was removed *in vacuo* and the residue extracted with toluene. The solution was filtered through celite, concentrated, and left to crystallise at room temperature, giving dark green blocks suitable for an X-ray diffraction experiment (602.0 mg, 91%).

¹H NMR (500 MHz, C₆D₆) δ 29.05 (s, 2H, Cy-CH₂), 26.87 (s, 2H, Cy-CH₂), 22.80 (s, 4H, Cy-CH₂), 13.83 (s, 4H, Cy-CH₂), 13.09 (s, 4H, Cy-CH₂), 8.18 (s, 4H, Cy-CH₂), 7.97 (s, 4H, Cy-CH₂), 7.44 (m, 4H, Cy-CH₂), 7.13 (br, 4H, Cy-CH₂), 6.14 (s, 4H, Cy-CH₂), 3.89 (m, 4H, Cy-CH₂), 2.05 (s, 4H, Cy-CH₂), -0.39 (s, 4H, Cy-CH₂), -2.54 (s, 6H, NC(CH₃)CH), -12.61 (s, 1H, NC(CH₃)CH).

¹³C{¹H} NMR (126 MHz, C₆D₆) δ 209.4 (NC(CH₃)CH), 133.0 (C_{ortho}), 127.1 (C_{meta}), 123.2 (C_{para}), 45.4 (Cy-CH₂ overlapping Cy-CH₂), 35.4 (Cy-CH₂ overlapping Cy-CH₂), 34.0 (Cy-CH₂ overlapping Cy-CH₂).

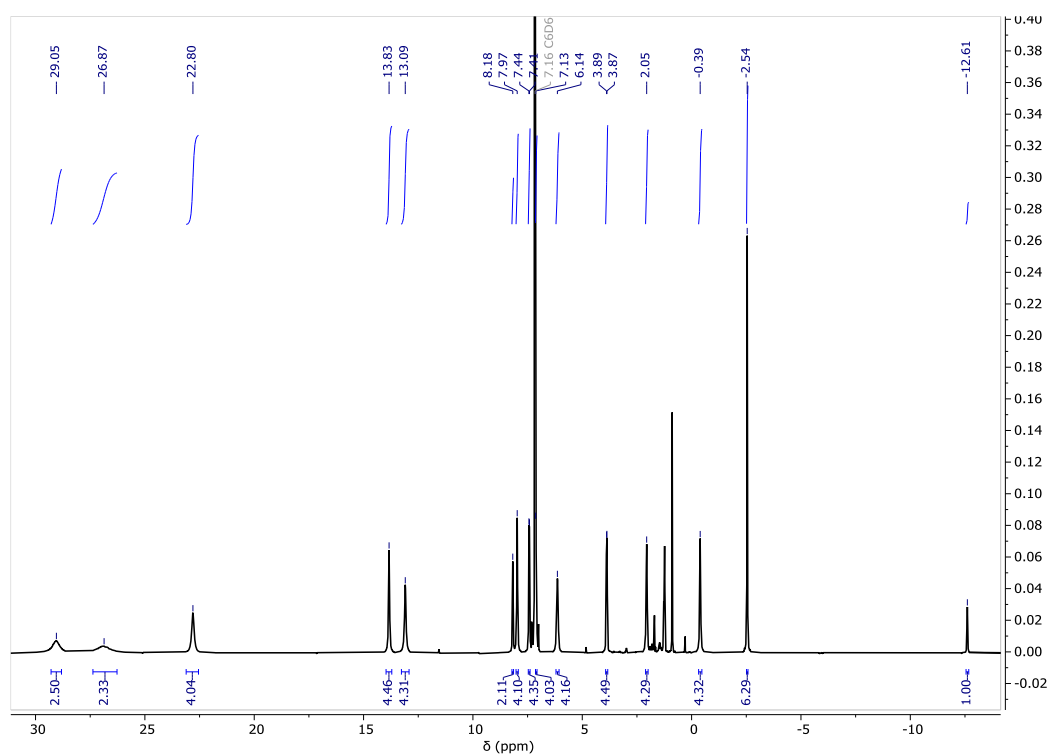
IR (cm⁻¹): 3058 (w), 2921 (s), 2848 (s), 1623 (m), 1554 (w), 1522 (m), 1445 (s), 1396 (s), 1352 (s), 1304 (s), 1271 (w), 1209 (w), 1161 (m), 1130 (m), 1082 (w), 1014 (m), 997 (m), 928 (m), 890 (m), 842 (w), 812 (w), 776 (m), 763 (s), 728 (s), 694 (w).

$\mu_{\text{eff}} = 3.74 \mu_{\text{B}}$ (C₆D₆, 22 °C).

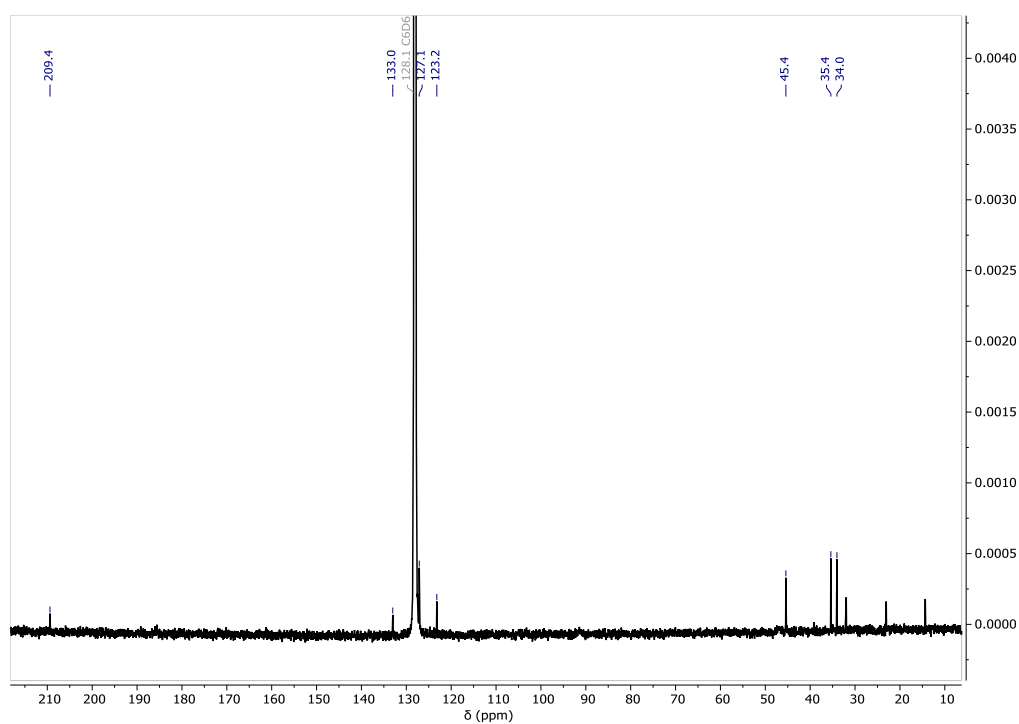
Elemental Analysis for [(BDI^{Dicyp})SmI]₂ (1710.37 g mol⁻¹):

Calculated: C, 57.58; H, 6.72; N, 3.28%.

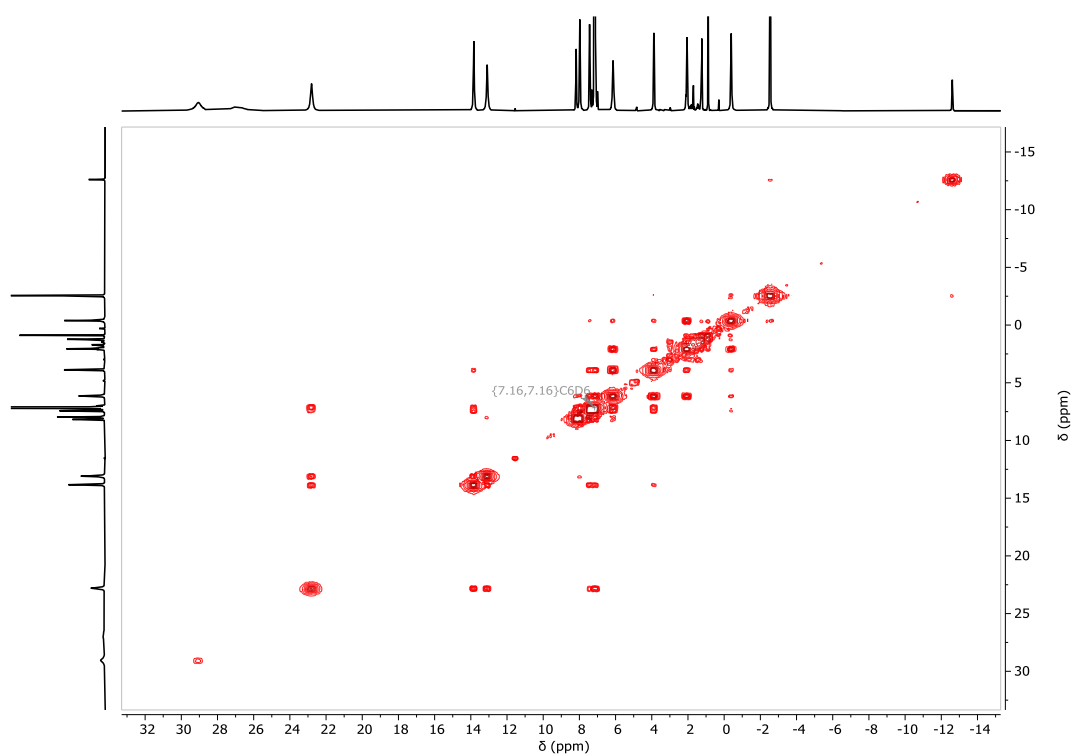
Found: C, 52.54; H, 6.32; N, 2.89%.



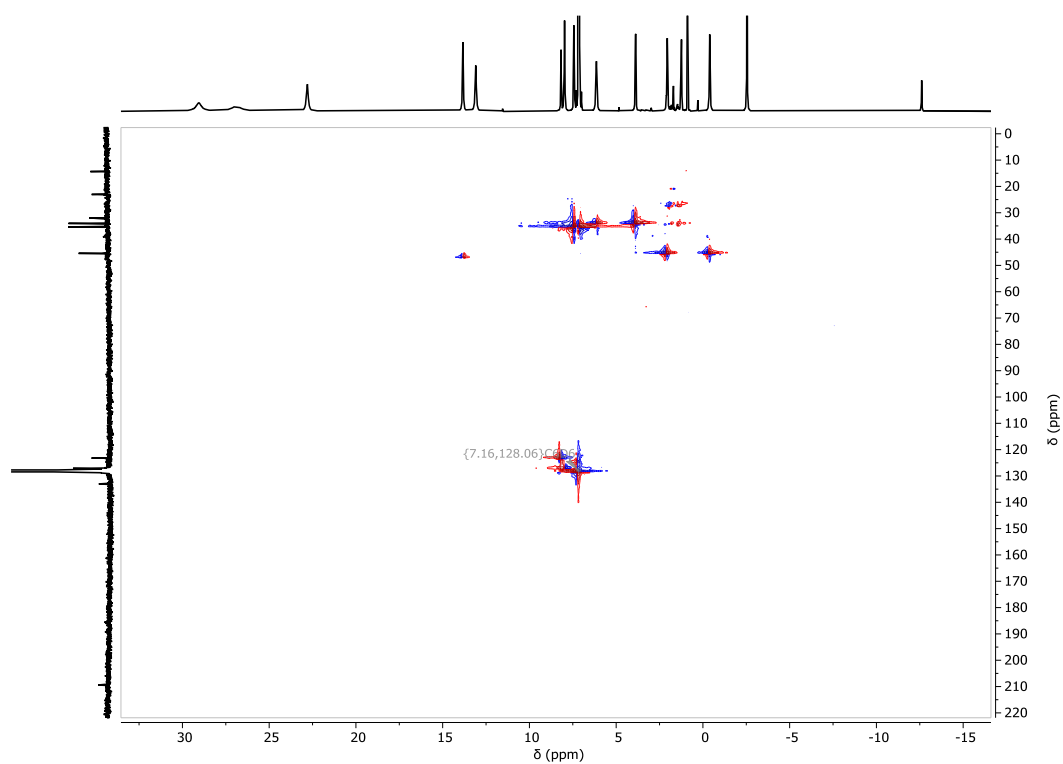
Supplementary Figure 4.1. ¹H NMR spectrum (500 MHz, C₆D₆) of [(BDI^{Dicyl})SmI]₂ (4.1).



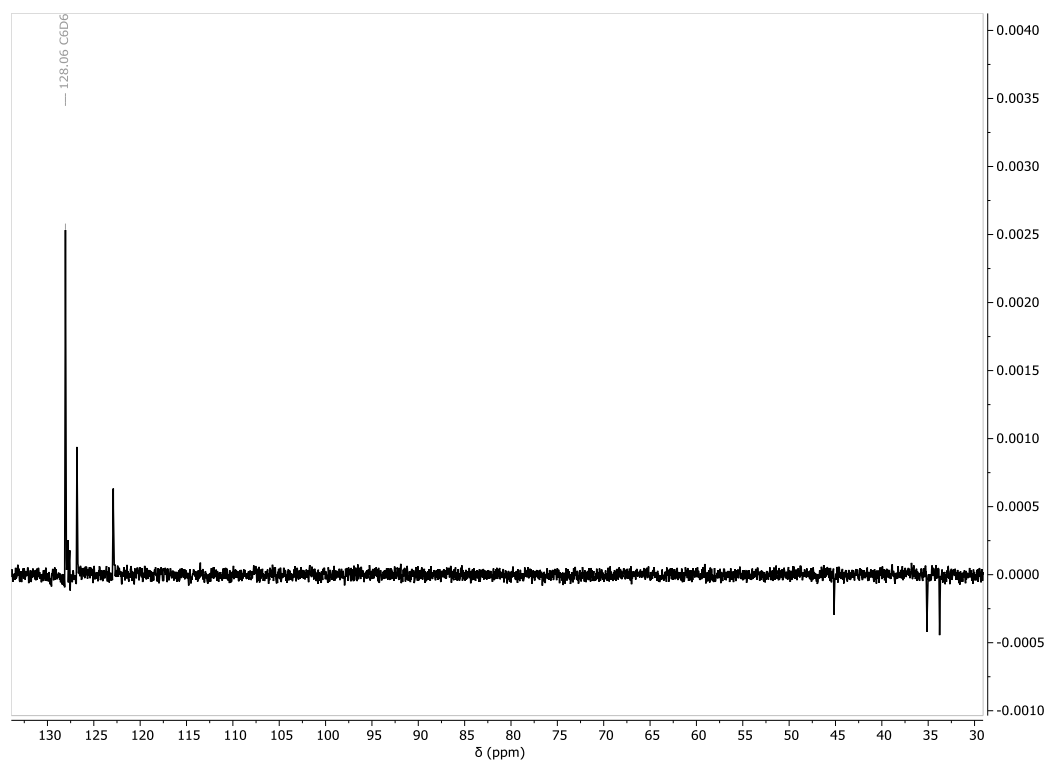
Supplementary Figure 4.2. ¹³C{¹H} NMR spectrum (126 MHz, C₆D₆) of [(BDI^{Dicyl})SmI]₂ (4.1).



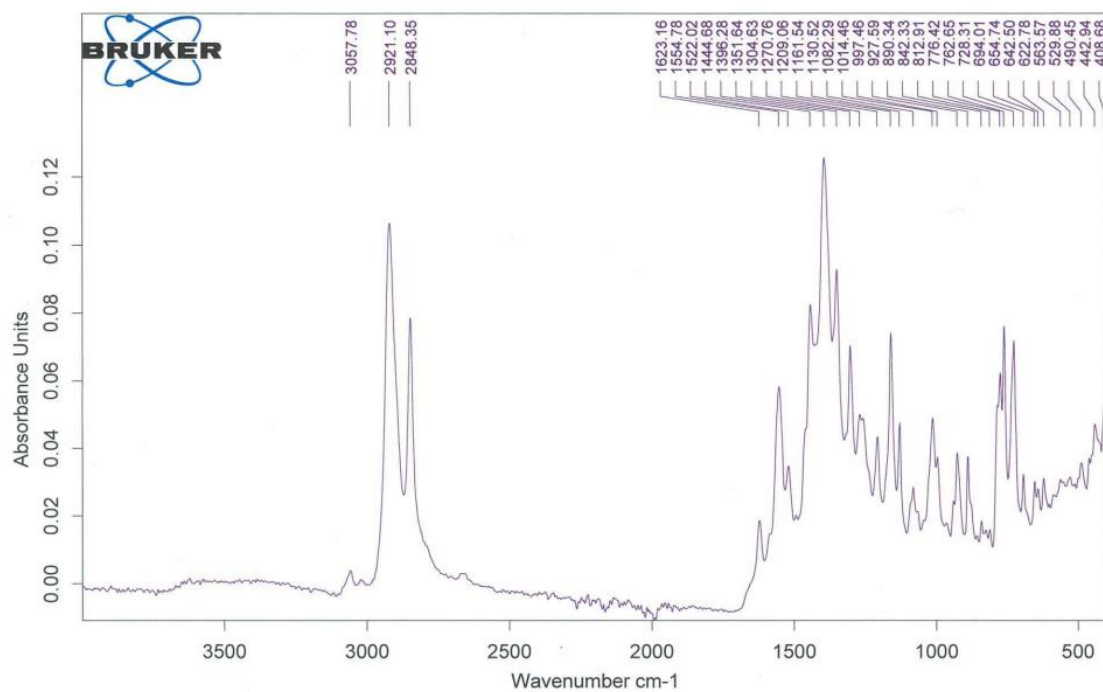
Supplementary Figure 4.3. ^1H - ^1H COSY NMR spectrum (500 MHz, C_6D_6) of $[(\text{BDI}^{\text{DicyP}})\text{SmI}]_2$ (**4.1**).



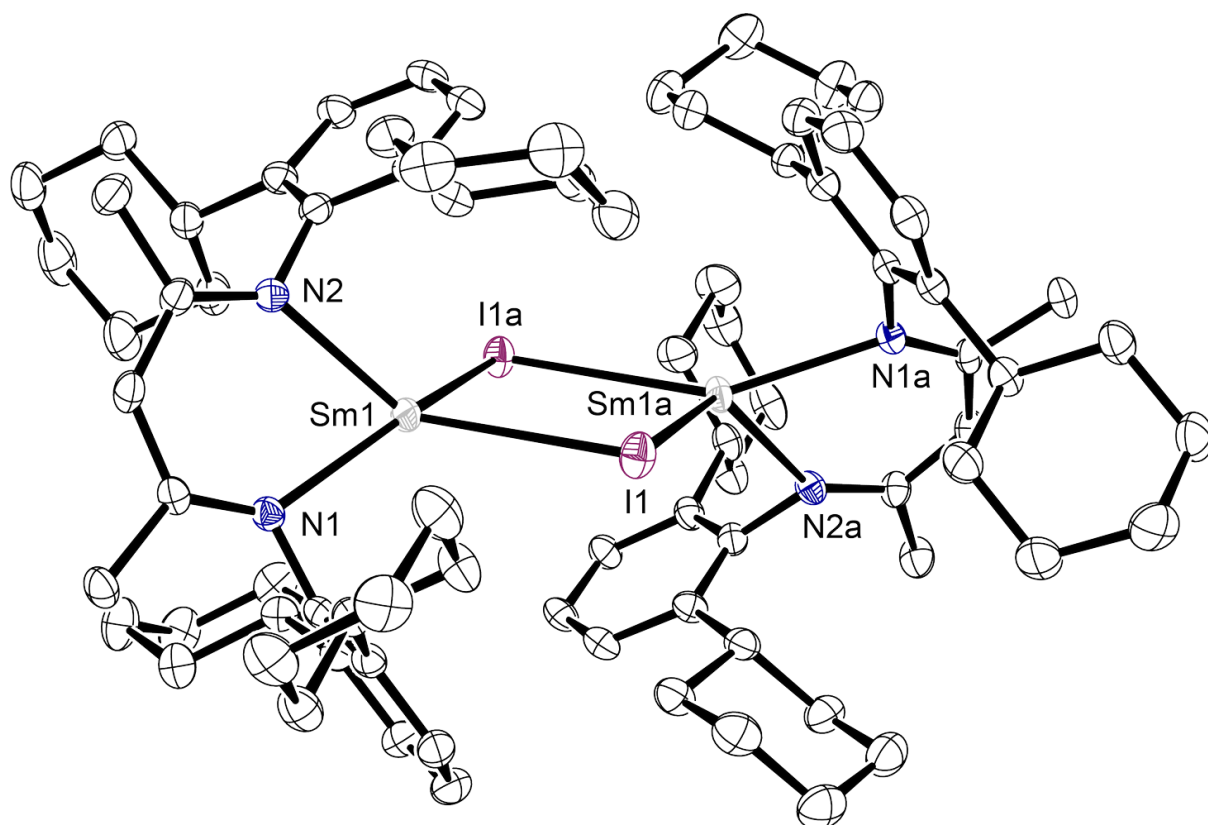
Supplementary Figure 4.4. ^1H - ^{13}C HSQC NMR spectrum (500 MHz, C_6D_6) of $[(\text{BDI}^{\text{DicyP}})\text{SmI}]_2$ (**4.1**).



Supplementary Figure 4.5. DEPT-135 ^{13}C NMR spectrum (126 MHz, C_6D_6) of $[(\text{BDI}^{\text{Dicyl}})\text{SmI}]_2$ (**4.1**).



Supplementary Figure 4.6. Infrared spectrum of $[(\text{BDI}^{\text{Dicyl}})\text{SmI}]_2$ (**4.1**).



Supplementary Figure 4.7. Ortep representation (30% probability ellipsoids) of $[(\text{BDI}^{\text{Dicyl}})\text{SmI}]_2$ (**4.1**). Hydrogen atoms have been omitted for clarity.

[(BDI^{Dicyp})SmCH(SiMe₃)₂] (4.2)

A red THF solution of KCH(SiMe₃)₂ (139.9 mg, 0.70 mmol) was added dropwise to a forest green THF solution of [(BDI^{Dicyp})SmI]₂ (602.9 mg, 0.35 mmol) while stirring and left to react for 20 minutes at room temperature. The resultant dark khaki green mixture was dried *in vacuo*, the residue extracted with hexane and filtered through celite. Brown crystals suitable for an X-ray diffraction experiment was obtained from a concentrated dark brown hexane solution at – 30 °C (400.0 mg, 64%).

¹H NMR (500 MHz, C₆D₆) δ 40.89 (br, 2H, Cy–CH₂), 30.72 (s, 2H, Cy–CH₂), 18.98 (s, 4H, Cy–CH₂), 18.44 (br, 2H, Cy–CH₂), 16.52 (s, 2H, Cy–CH₂), 9.53 (m, 4H, Cy–CH₂), 8.74 (s, 4H, Cy–CH₂), 8.23 (br, 4H, Cy–CH₂), 7.29 (m, 4H, ArH), 5.31 (m, 4H, Cy–CH₂), 4.96 (s, 2H, ArH), 3.65 (br, 4H, Cy–CH₂), 1.23 (br, 4H, Cy–CH₂), 0.93 (br, 4H, Cy–CH₂), –1.77 (s, 6H, NC(CH₃)CH), –8.72 (s, 18H, CH(SiMe₃)₂), –12.63 (s, 1H, NC(CH₃)CH), –54.92 (s, 0.3H, CH(SiMe₃)₂).

¹³C {¹H} NMR (126 MHz, C₆D₆) δ 214.9 (NC(CH₃)CH), 197.7 (C_{ipso}), 138.7 (C_{ortho}), 126.4 (C_{meta}), 124.4 (C_{para}), 57.1 (Cy–CH₂), 48.3 (Cy–CH₂ overlapping Cy–CH₂), 38.2 (Cy–CH₂ overlapping Cy–CH₂), 36.1 (Cy–CH₂ overlapping Cy–CH₂),

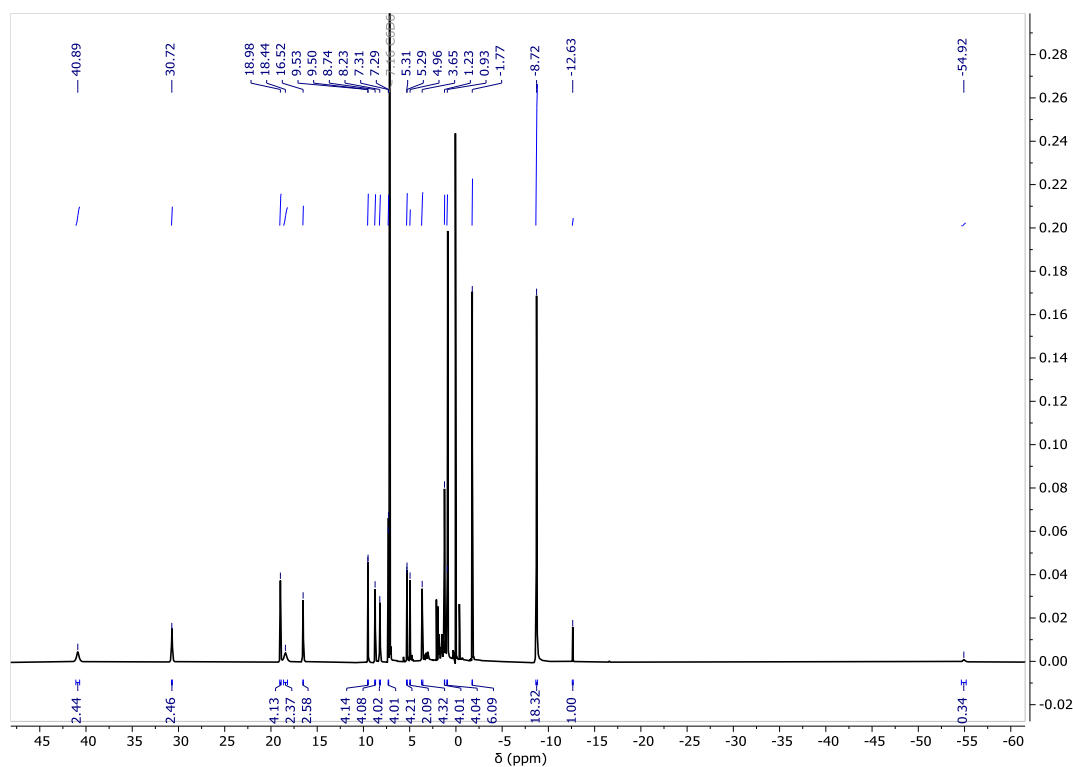
IR (cm^{–1}): 3062 (w), 3023 (w), 2920 (s), 2848 (s), 2667 (w), 1620 (w), 1554 (m), 1518 (w), 1493 (w), 1461 (m), 1445 (s), 1399 (s), 1351 (s), 1304 (m), 1254 (m), 1209 (m), 1162 (s), 1129 (m), 1080 (w), 1014 (m), 963 (w), 921 (w), 890 (w), 841 (m), 776 (m), 763 (m), 727 (m), 963 (w).

$\mu_{\text{eff}} = 3.70 \mu_{\text{B}}$ (C₆D₆, 22 °C).

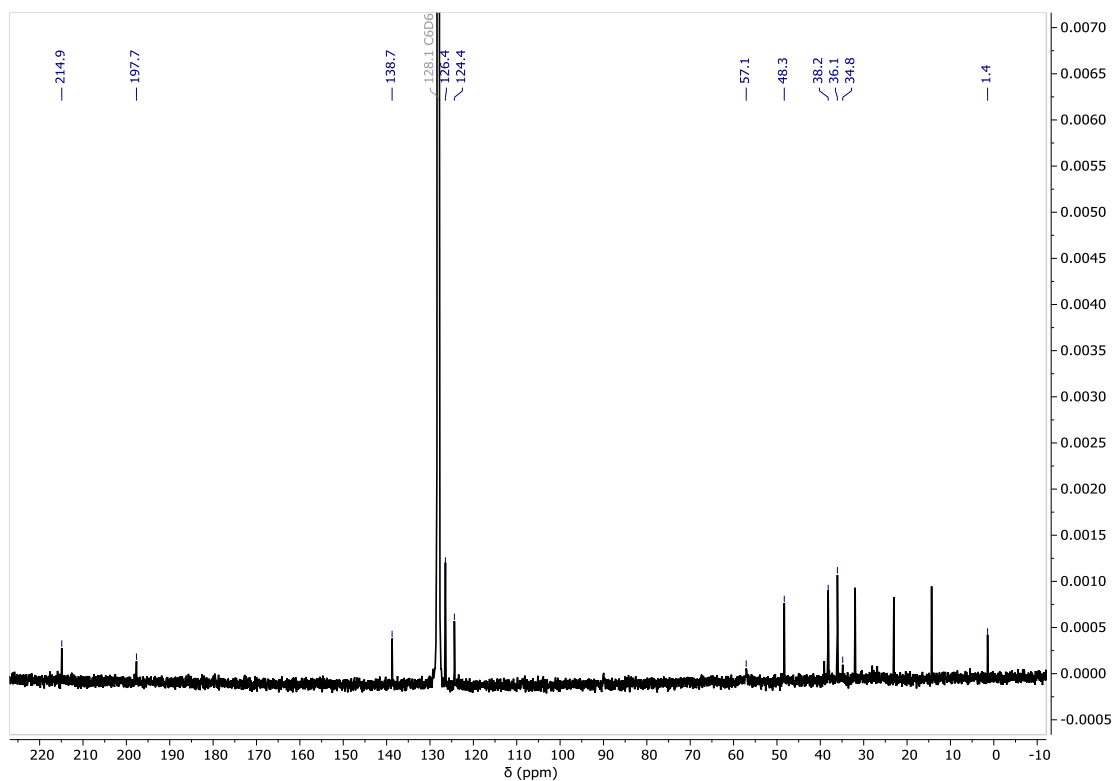
Elemental Analysis for [(BDI^{Dicyp})SmCH(SiMe₃)₂] (887.68 g mol^{–1}):

Calculated: C, 64.95; H, 8.63; N, 3.16%.

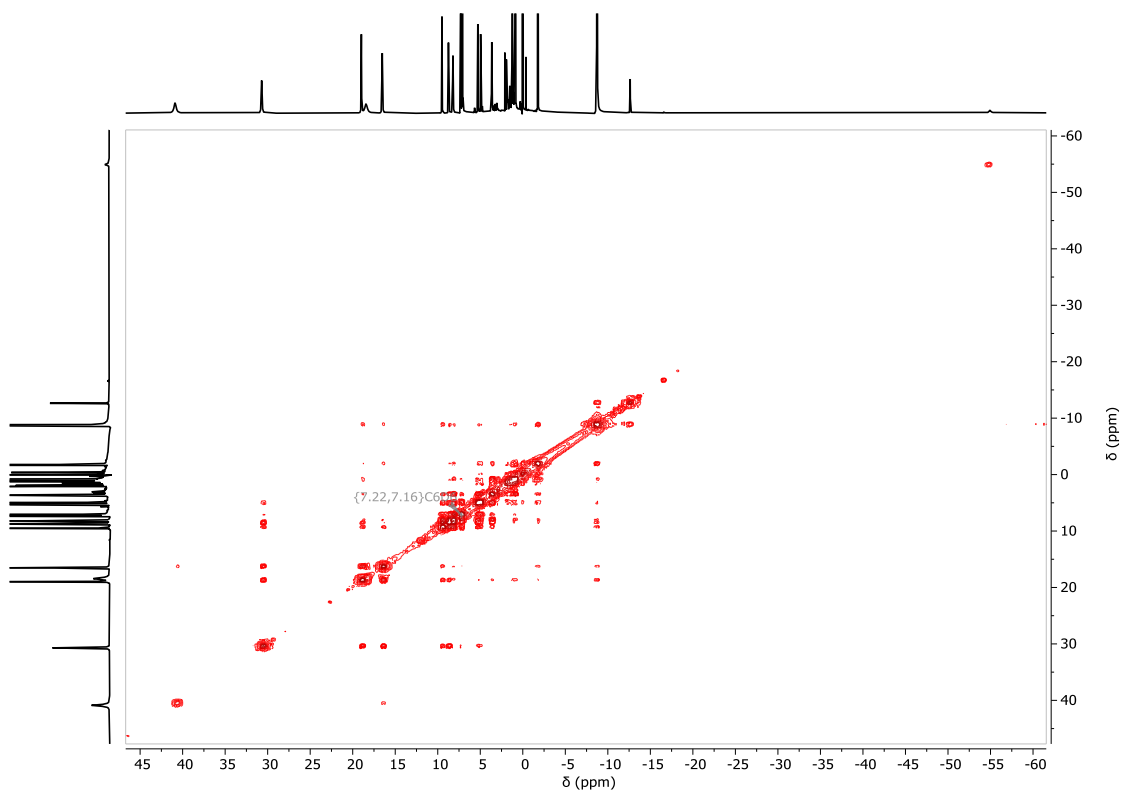
Found: C, 65.10; H, 8.58; N, 3.18%.



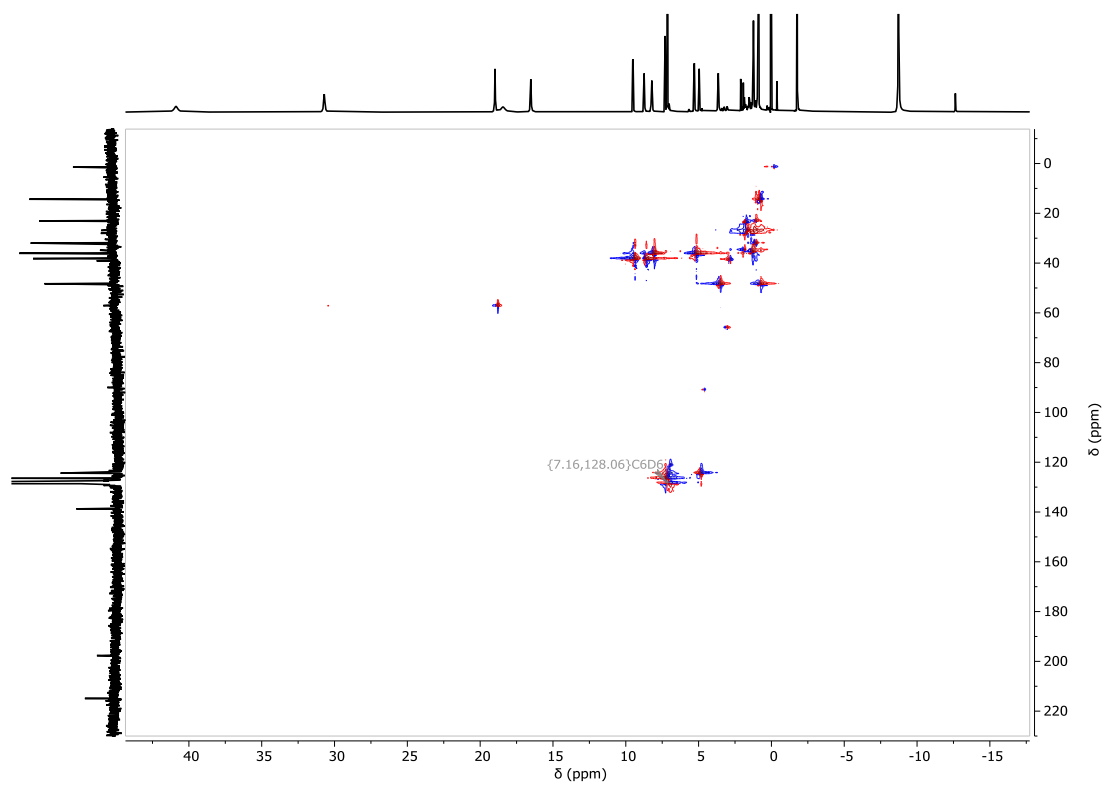
Supplementary Figure 4.8. ¹H NMR spectrum (500 MHz, C₆D₆) of [(BDI^{Dicyl})SmCH(SiMe₃)₂] (**4.2**).



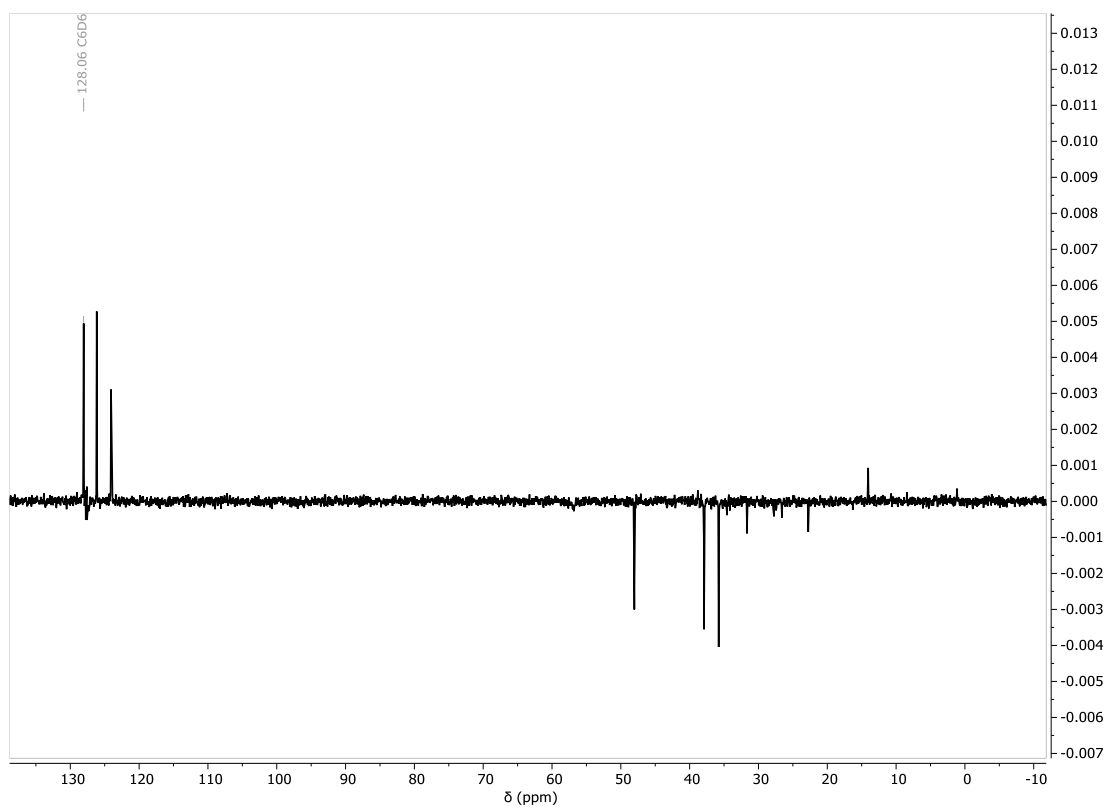
Supplementary Figure 4.9. ¹³C{¹H} NMR spectrum (126 MHz, C₆D₆) of [(BDI^{Dicyl})SmCH(SiMe₃)₂] (**4.2**).



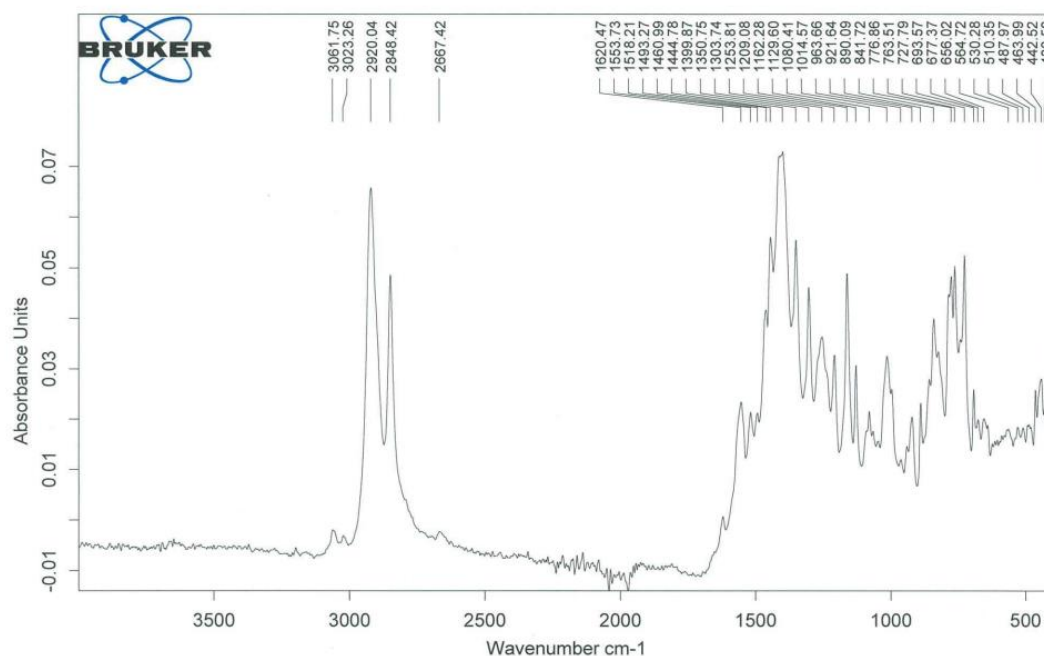
Supplementary Figure 4.10. ^1H - ^1H COSY NMR spectrum (500 MHz, C_6D_6) of $[(\text{BDI}^{\text{Dicyl}})\text{SmCH}(\text{SiMe}_3)_2]$ (**4.2**).



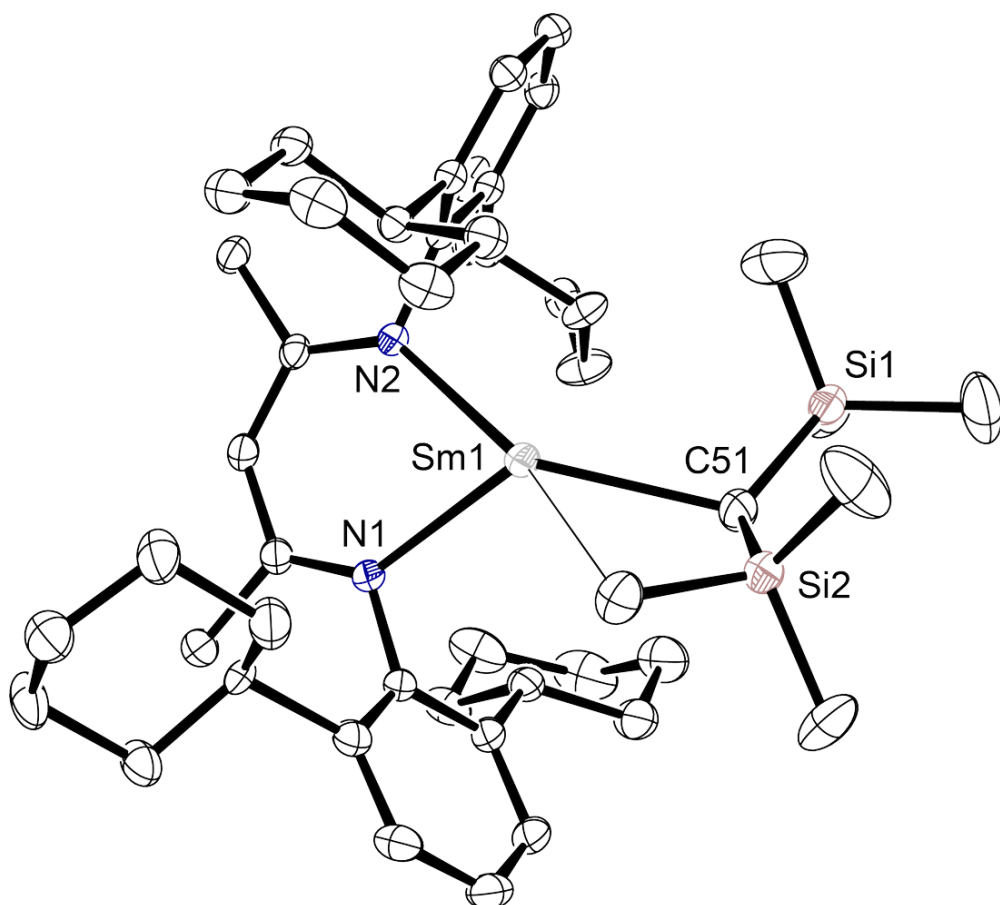
Supplementary Figure 4.11. ^1H - ^{13}C HSQC NMR spectrum (500 MHz, C_6D_6) of $[(\text{BDI}^{\text{Dicyl}})\text{SmCH}(\text{SiMe}_3)_2]$ (**4.2**).



Supplementary Figure 4.12. DEPT-135 ^{13}C NMR spectrum (126 MHz, C_6D_6) of $[(\text{BDI}^{\text{Dicyl}})\text{SmCH}(\text{SiMe}_3)_2]$ (**4.2**).



Supplementary Figure 4.13. Infrared spectrum of $[(\text{BDI}^{\text{Dicyl}})\text{SmCH}(\text{SiMe}_3)_2]$ (**4.2**).



Supplementary Figure 4.14. Ortep representation (30% probability ellipsoids) of $[(BDI^{DicyP})SmCH(SiMe_3)_2]$ (4.2). Hydrogen atoms have been omitted for clarity.

[(BDI^{Dicyp})Sm(μ -C₆H₆)Sm(BDI^{Dicyp})] (4.3)

a) A dark brown C₆H₆ solution containing [(BDI^{Dicyp})SmCH(SiMe₃)₂] (38.0 mg, 0.04 mmol) was added to an NMR tube fitted with a J. Youngs tap and heated to 60 °C overnight. The volatiles were removed *in vacuo*, the dark residual solid was re-dissolved into the minimum amount of toluene and left to crystallise at room temperature, giving dark green–brown plates suitable for an X-ray diffraction experiment (23.2 mg, 61.2%).

b) A dark brown C₆D₆ solution containing [(BDI^{Dicyp})SmCH(SiMe₃)₂] (30.0 mg, 0.03 mmol) was added to an NMR tube fitted with a J. Youngs tap and heated to 60 °C. Quantitative conversion to the reaction product was achieved after 2 days.

¹H NMR (500 MHz, C₆D₆) δ 20.36 (s, 3H, C₆H₆), 10.52 (s, 1H, NC(CH₃)CH), 6.58 (t, 2H, *J* = 7.7 Hz, *ArH*), 6.19 (d, 4H, *J* = 7.9 Hz, *ArH*), 5.29 (s, 6H, NC(CH₃)CH), 2.84 (m, 4H, Cy-CH₂), 1.73 (m, 4H, Cy-CH₂), 1.27 (m, 4H, Cy-CH₂), 0.95 (m, 8H, Cy-CH₂ overlapping Cy-CH₂), 0.44 (m, 4H, Cy-CH₂), -0.08 (m, 4H, Cy-CH₂), -0.33 (m, 4H, Cy-CH), -0.53 (m, 4H, Cy-CH₂), -1.33 (m, 4H, Cy-CH₂), -4.22 (m, 4H, Cy-CH₂).

¹³C{¹H} NMR (126 MHz, C₆D₆) δ 176.1 (NC(CH₃)CH), 149.6 (C_{ipso}), 141.3 (C_{ortho}), 123.9 (C_{para}), 123.7 (C_{meta}), 99.3 (NC(CH₃)CH), 40.5 (Cy-CH), 35.4 (Cy-CH₂ overlapping Cy-CH₂), 31.0 (Cy-CH₂ overlapping Cy-CH₂), 27.4 (Cy-CH₂ overlapping Cy-CH₂), 25.7 (Cy-CH₂ overlapping Cy-CH₂), 25.5 (Cy-CH₂ overlapping Cy-CH₂), 17.4 (NC(CH₃)CH).

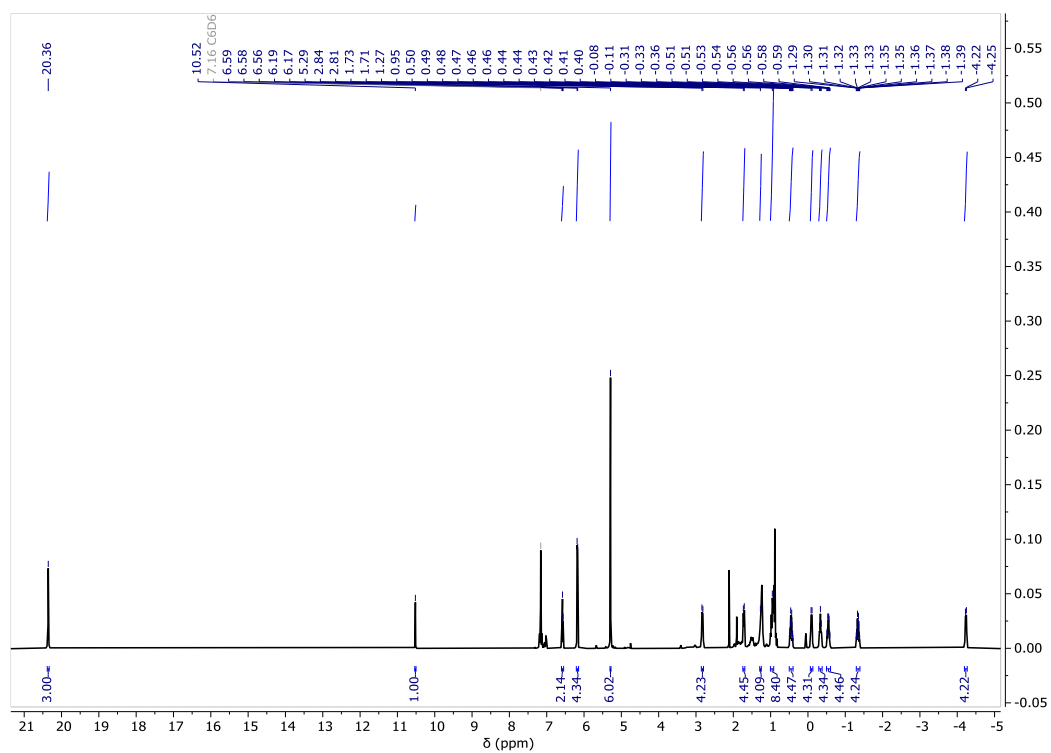
IR (cm⁻¹): 3062 (w), 2923 (s), 2849 (s), 1621 (m), 1551 (s), 1486 (w), 1445 (s), 1403 (m), 1353 (m), 1305 (w), 1260 (w), 1211 (w), 1165 (m), 1131 (w), 996 (s), 927 (s), 891 (s), 777 (s), 764 (s), 736 (s), 677(m).

$\mu_{\text{eff}} = 1.82 \mu_{\text{B}}$ (C₆D₆, 22 °C).

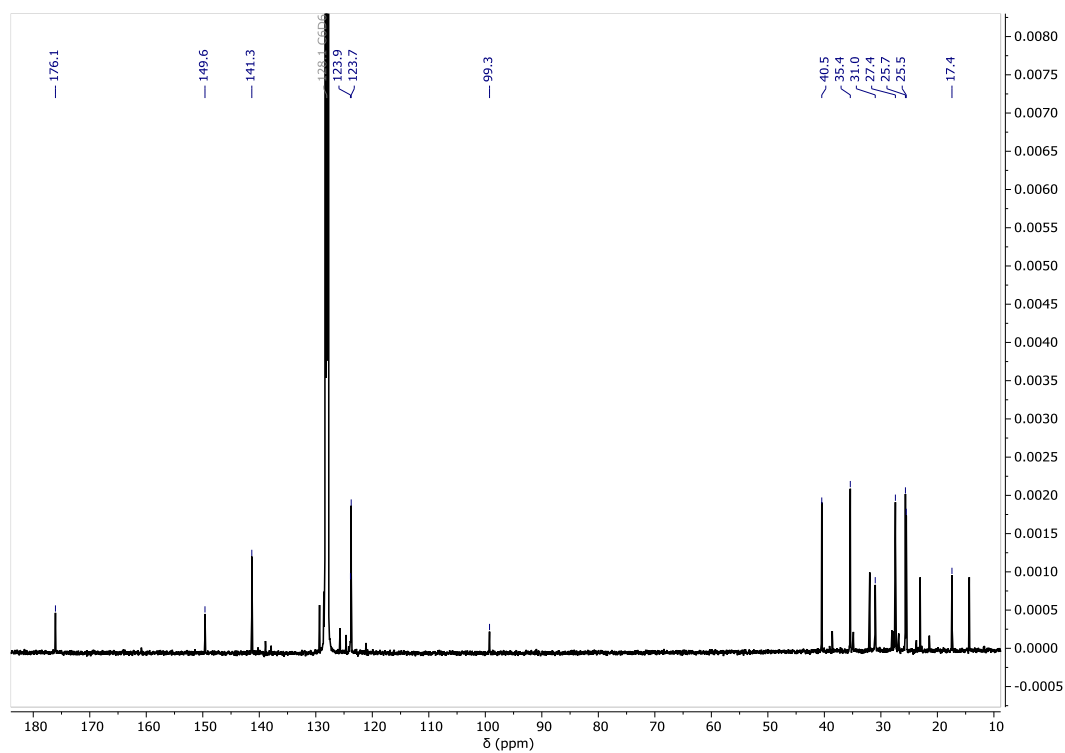
Elemental Analysis for [(BDI^{Dicyp})Sm(μ -C₆H₆)Sm(BDI^{Dicyp})] (1534.68 g mol⁻¹):

Calculated: C, 68.87; H, 7.88; N, 3.65%.

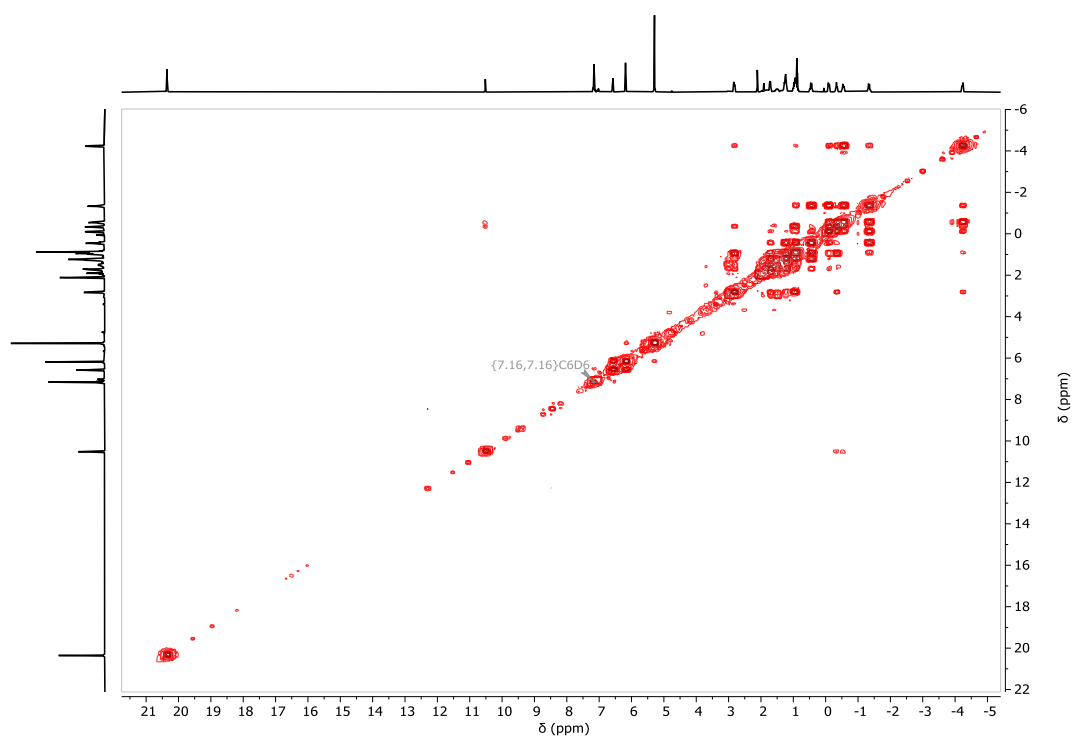
Found: C, 63.68; H, 7.89; N, 3.24%.



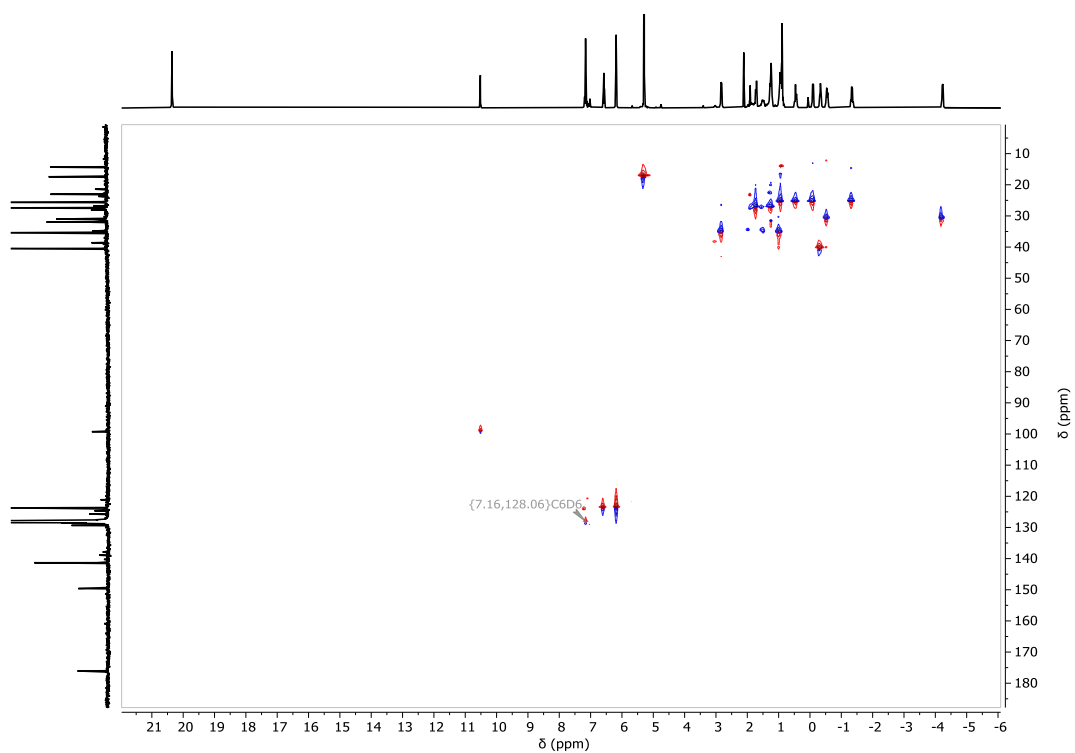
Supplementary Figure 4.15. ¹H NMR spectrum (500 MHz, C₆D₆) of [(BDI^{Dicyl})Sm(μ-C₆H₆)Sm(BDI^{Dicyl})] (**4.3**).



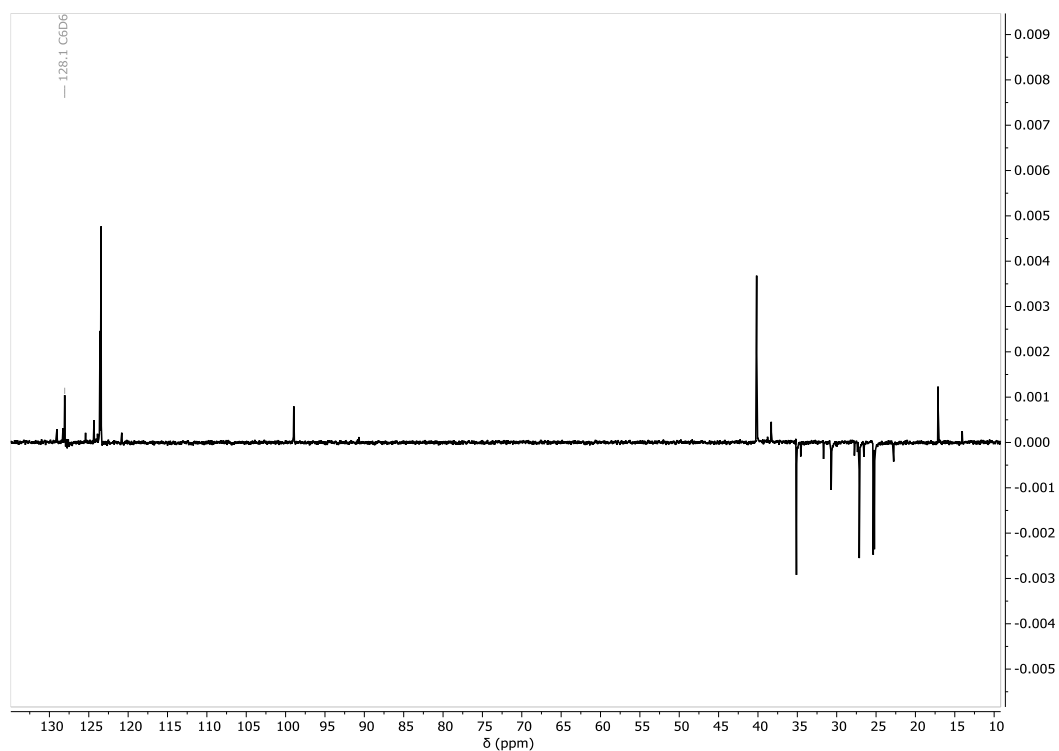
Supplementary Figure 4.16. ¹³C{¹H} NMR spectrum (126 MHz, C₆D₆) of [(BDI^{Dicyl})Sm(μ-C₆H₆)Sm(BDI^{Dicyl})] (**4.3**).



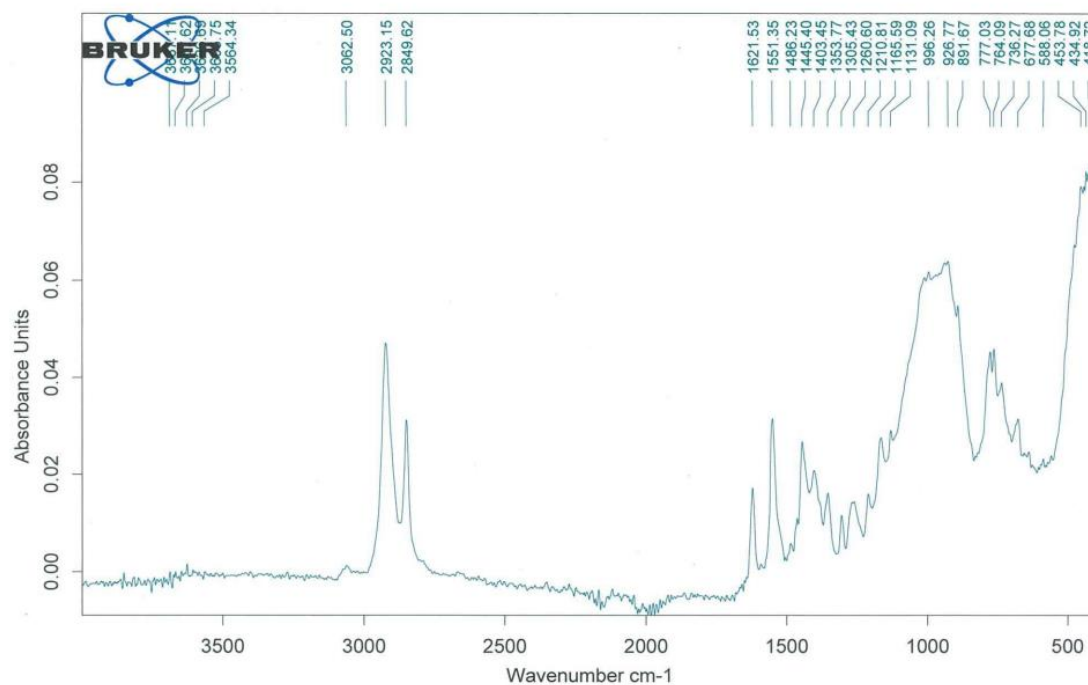
Supplementary Figure 4.17. ^1H - ^1H COSY NMR spectrum (500 MHz, C_6D_6) of $[(\text{BDI}^{\text{Dicyp}})\text{Sm}(\mu\text{-C}_6\text{H}_6)\text{Sm}(\text{BDI}^{\text{Dicyp}})]$ (**4.3**).



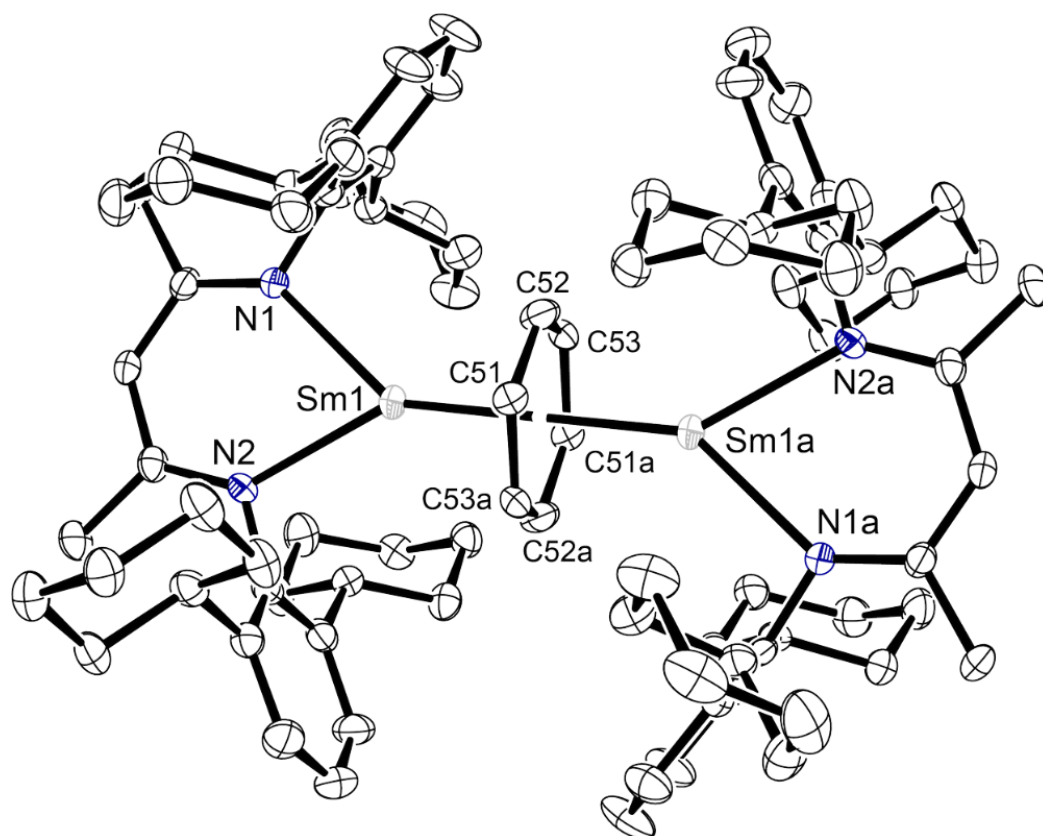
Supplementary Figure 4.18. ^1H - ^{13}C HSQC NMR spectrum (500 MHz, C_6D_6) of $[(\text{BDI}^{\text{Dicyp}})\text{Sm}(\mu\text{-C}_6\text{H}_6)\text{Sm}(\text{BDI}^{\text{Dicyp}})]$ (**4.3**).



Supplementary Figure 4.19. DEPT- ^{13}C NMR spectrum (126 MHz, C_6D_6) of $[(\text{BDI}^{\text{DicyP}})\text{Sm}(\mu\text{-C}_6\text{H}_6)\text{Sm}(\text{BDI}^{\text{DicyP}})]$ (**4.3**).



Supplementary Figure 4.20. Infrared spectrum of $[(\text{BDI}^{\text{DicyP}})\text{Sm}(\mu\text{-C}_6\text{H}_6)\text{Sm}(\text{BDI}^{\text{DicyP}})]$ (**4.3**).



Supplementary Figure 4.21. Ortep representation (30% probability ellipsoids) of $[(\text{BDI}^{\text{Dicyl}})\text{Sm}(\mu\text{-C}_6\text{H}_6)\text{Sm}(\text{BDI}^{\text{Dicyl}})]$ (**4.3**). Hydrogen atoms have been omitted for clarity.

$[(\text{BDI}^{\text{DicyP}})\text{Sm}(\mu\text{-C}_7\text{H}_8)\text{Sm}(\text{BDI}^{\text{DicyP}})]$ (4.4)

A dark brown toluene solution containing $[(\text{BDI}^{\text{DicyP}})\text{SmCH}(\text{SiMe}_3)_2]$ (26.7 mg, 0.03 mmol) was added to an NMR tube fitted with a J. Youngs tap and heated at 60 °C overnight. The resultant dark army green solution was decanted into a scintillation vial inside the glovebox and left to crystallise at room temperature, giving yellow plates suitable for an X-ray diffraction experiment (13.5 mg, 58%).

^1H NMR (500 MHz, C_6D_6) δ 22.72 (s, 1H, C_7H_8), 19.59 (s, 1H, C_7H_8), 16.70 (s, 0.5H, C_7H_8), 10.57 (s, 1H, $\text{NC}(\text{CH}_3)\text{CH}$), 6.42 (t, 2H, $J = 7.8$ Hz, ArH), 6.07 (d, 4H, $J = 7.9$ Hz, ArH), 5.22 (s, 6H, $\text{NC}(\text{CH}_3)\text{CH}$), 2.83 (m, 4H, Cy-CH_2), 1.78 (m, 4H, Cy-CH_2), 1.11 (m, 4H, Cy-CH_2), 1.01 (m, 4H, Cy-CH_2), 0.95 (m, 4H, Cy-CH_2), 0.51 (m, 4H, Cy-CH_2), 0.04 (m, 8H, Cy-CH_2 overlapping Cy-CH), -0.53 (m, 4H, Cy-CH_2), -0.98 (m, 4H, Cy-CH_2), -3.89 (m, 4H, Cy-CH_2), -10.85 (s, 1.5H, C_7H_8).

$^{13}\text{C}\{^1\text{H}\}$ NMR (126 MHz, C_6D_6) δ 175.9 ($\text{NC}(\text{CH}_3)\text{CH}$), 149.2 (C_{ipso}), 140.2 (C_{ortho}), 123.3 (C_{para}), 123.1 (C_{meta}), 99.1 ($\text{NC}(\text{CH}_3)\text{CH}$), 39.7 (Cy-CH), 34.9 (Cy-CH_2 overlapping Cy-CH_2), 30.9 (Cy-CH_2 overlapping Cy-CH_2), 27.2 (Cy-CH_2 overlapping Cy-CH_2), 25.5 (Cy-CH_2 overlapping Cy-CH_2 overlapping Cy-CH_2), 17.2 ($\text{NC}(\text{CH}_3)\text{CH}$).

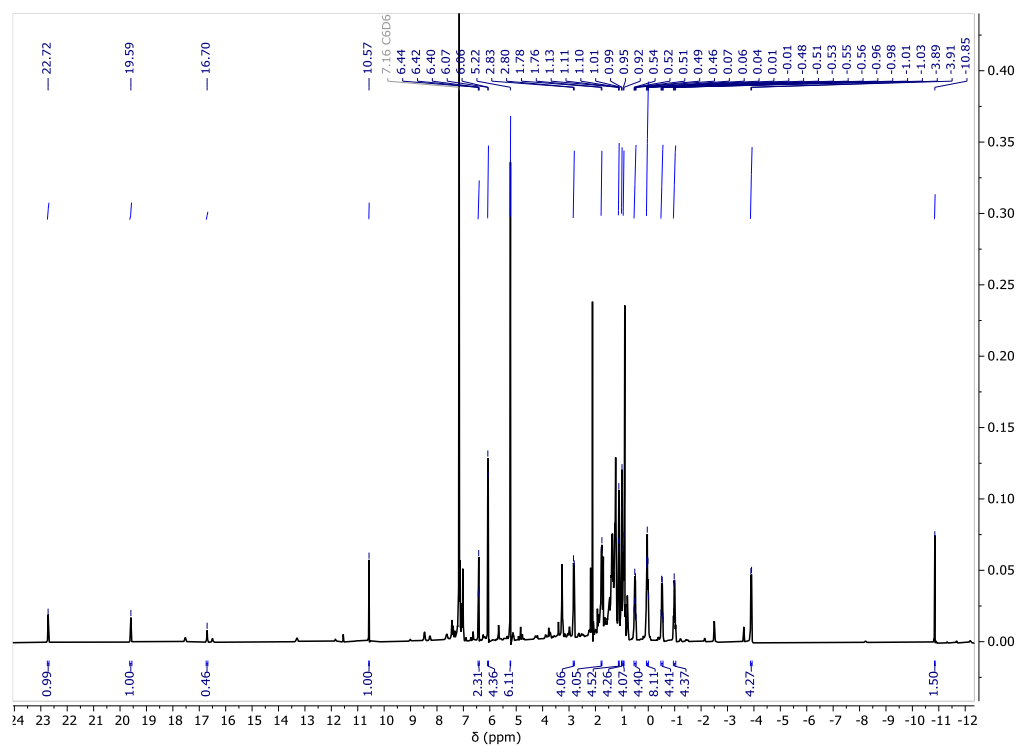
IR (cm^{-1}): 3056 (w), 2920 (s), 2848 (s), 1620 (s), 1550 (s), 1525 (m), 1484 (w), 1445 (s), 1397 (s), 1351 (s), 1302 (s), 1262 (s), 1211 (m), 1163 (s), 1130 (m), 1081 (w), 1018 (m), 997 (m), 926 (m), 890 (m), 842 (w), 775 (s), 763 (s), 733 (s), 694 (w).

$\mu_{\text{eff}} = 1.94 \mu_{\text{B}}$ (C_6D_6 , 22 °C).

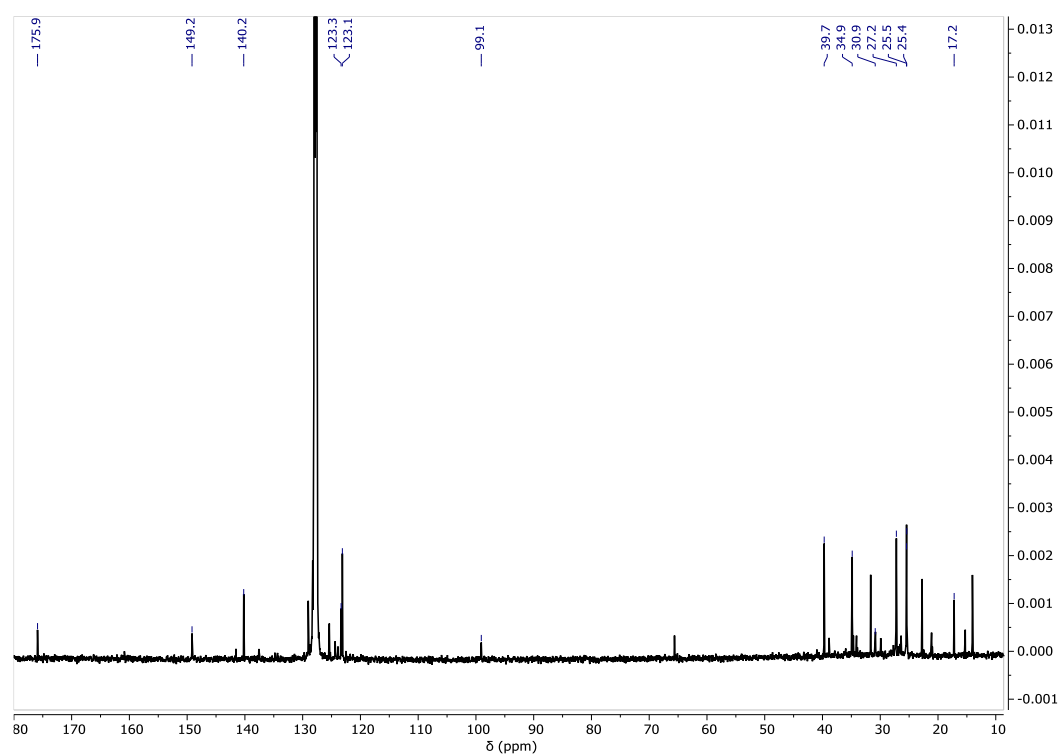
Elemental Analysis for $[(\text{BDI}^{\text{DicyP}})\text{Sm}(\mu\text{-C}_7\text{H}_8)\text{Sm}(\text{BDI}^{\text{DicyP}})]$ (1548.70 g mol^{-1}):

Calculated: C, 69.02; H, 7.94; N, 3.62%.

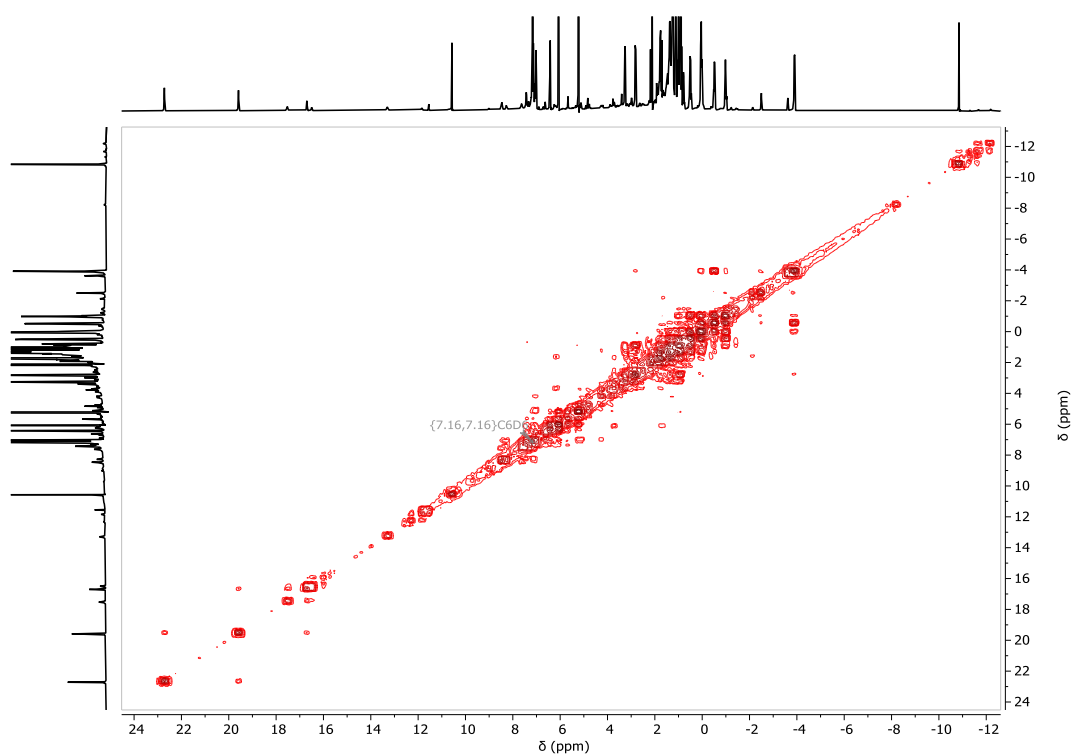
Found: C, 67.79; H, 8.00; N, 3.31%.



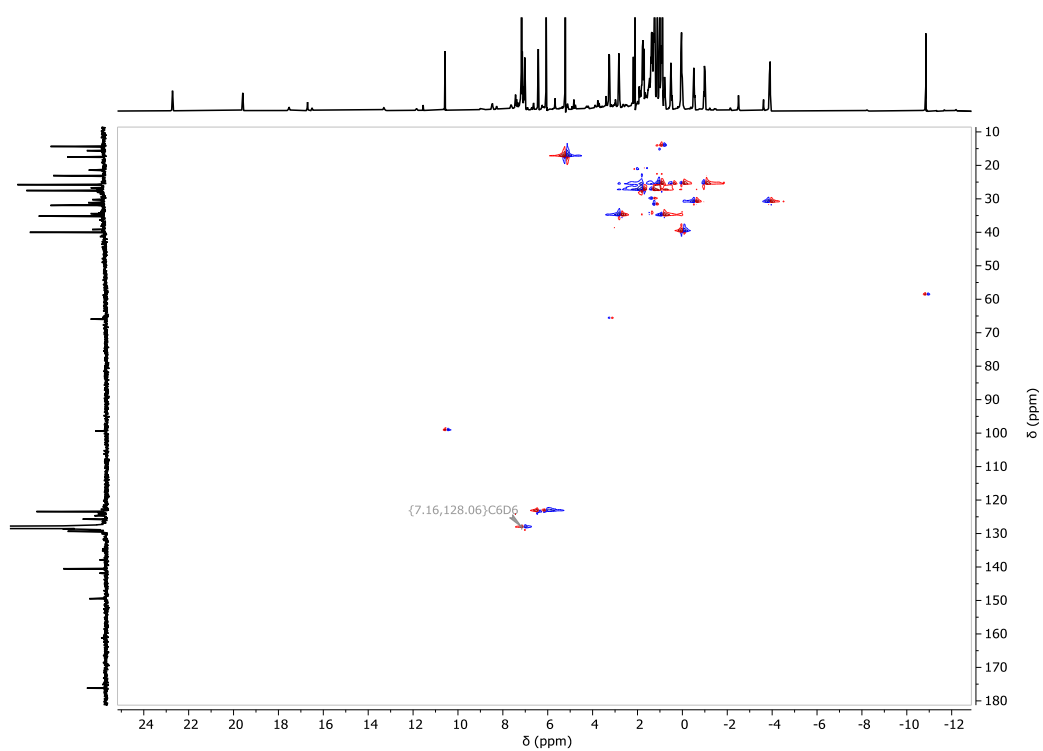
Supplementary Figure 4.22. ¹H NMR spectrum (500 MHz, C₆D₆) of [(BDI^{DicyP})Sm(μ-C₇H₈)Sm(BDI^{DicyP})] (4.4).



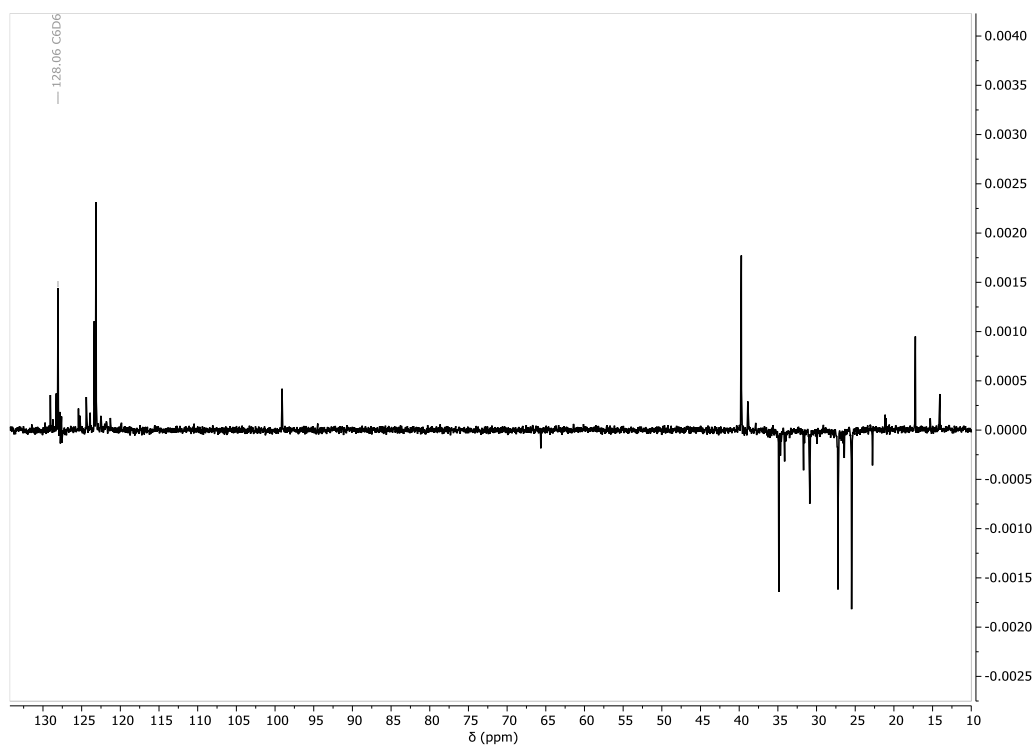
Supplementary Figure 4.23. ¹³C{¹H} NMR spectrum (126 MHz, C₆D₆) of [(BDI^{DicyP})Sm(μ-C₇H₈)Sm(BDI^{DicyP})] (4.4).



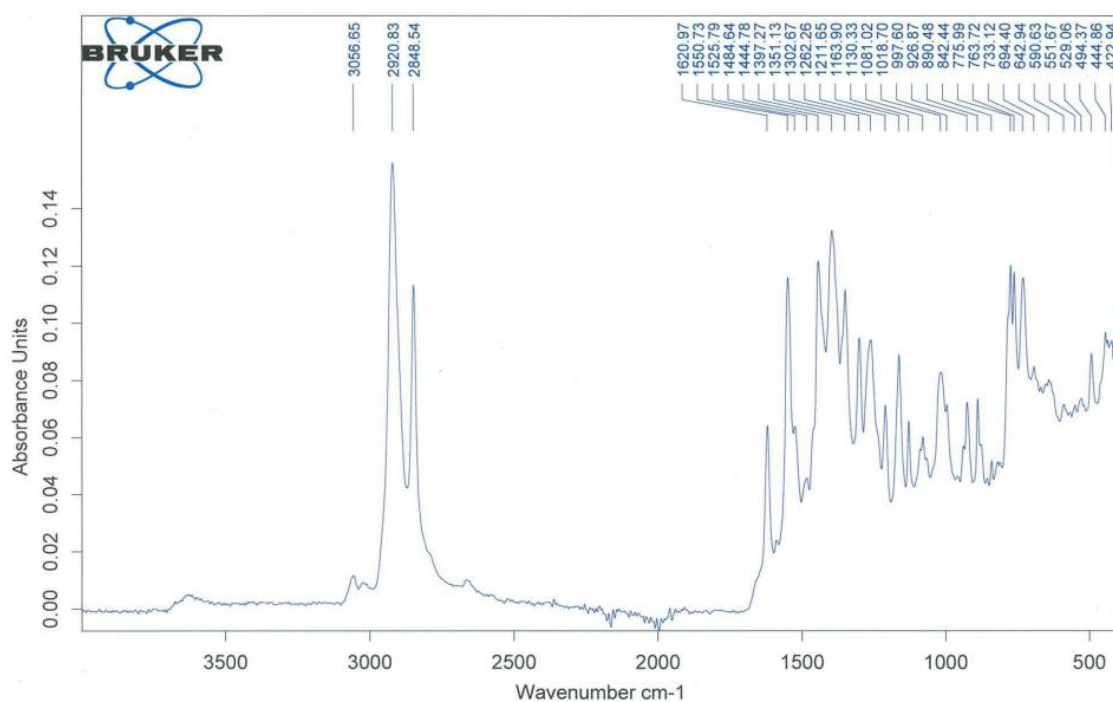
Supplementary Figure 4.24. ^1H - ^1H COSY NMR spectrum (500 MHz, C_6D_6) of $[(\text{BDI}^{\text{Dicyl}})\text{Sm}(\mu\text{-C}_7\text{H}_8)\text{Sm}(\text{BDI}^{\text{Dicyl}})]$ (**4.4**).



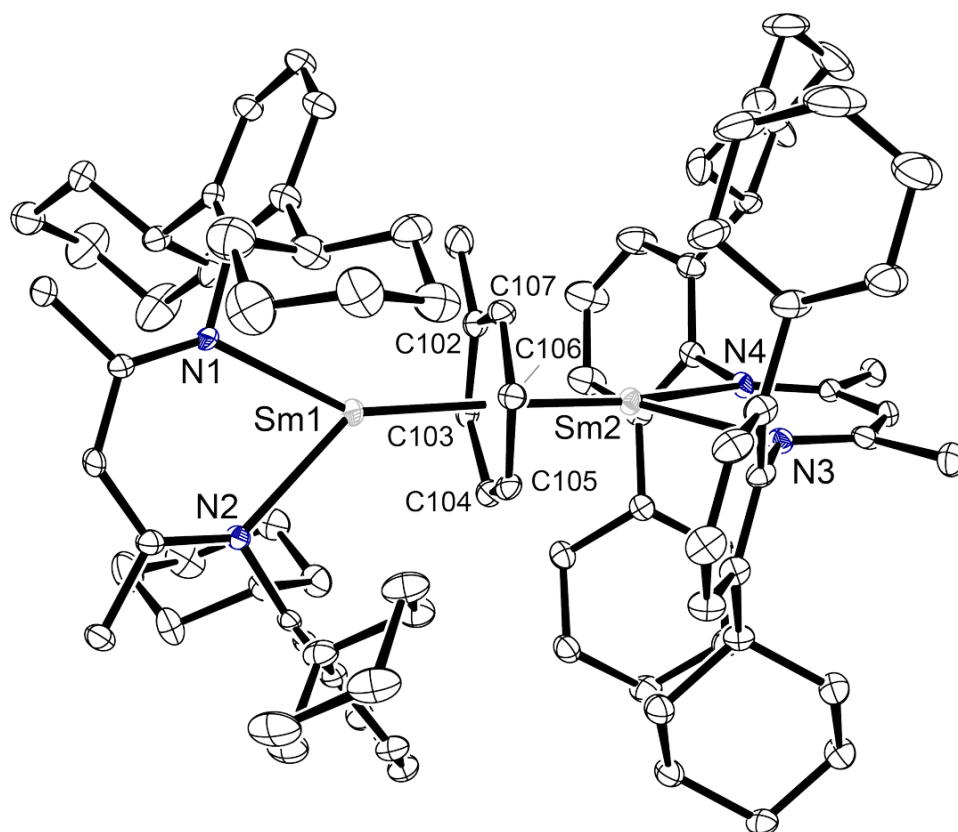
Supplementary Figure 4.25. ^1H - ^{13}C HSQC NMR spectrum (500 MHz, C_6D_6) of $[(\text{BDI}^{\text{Dicyl}})\text{Sm}(\mu\text{-C}_7\text{H}_8)\text{Sm}(\text{BDI}^{\text{Dicyl}})]$ (**4.4**).



Supplementary Figure 4.26. DEPT-135 ^{13}C NMR spectrum (126 MHz, C_6D_6) of $[(\text{BDI}^{\text{Dicyl}})\text{Sm}(\mu\text{-C}_7\text{H}_8)\text{Sm}(\text{BDI}^{\text{Dicyl}})]$ (4.4).



Supplementary Figure 4.27. Infrared spectrum of $[(\text{BDI}^{\text{Dicyl}})\text{Sm}(\mu\text{-C}_7\text{H}_8)\text{Sm}(\text{BDI}^{\text{Dicyl}})]$ (4.4).



Supplementary Figure 4.28. Ortep representation (30% probability ellipsoids) of $[(\text{BDI}^{\text{DicyP}})\text{Sm}(\mu\text{-C}_7\text{H}_8)\text{Sm}(\text{BDI}^{\text{DicyP}})]$ (4.4). Hydrogen atoms have been omitted for clarity.

[(BDI^{Dicyp})Sm(μ -C₆H₈Si)Sm(BDI^{Dicyp})] (4.5)

A colourless C₆D₆ solution of PhSiH₃ (6.46 mg, 0.06 mmol) was added to a dark brown C₆D₆ solution containing [(BDI^{Dicyp})SmCH(SiMe₃)₂] (53 mg, 0.06 mmol) in an NMR tube fitted with a J. Youngs tap. Monitoring of the reaction indicated complete consumption of the [(BDI^{Dicyp})SmCH(SiMe₃)₂] starting material instantaneously. The reaction mixture was decanted into a scintillation vial inside the glovebox and the solvent removed *in vacuo*. The residue was redissolved into the minimum amount of hexane, resulting in dark yellow plates suitable for an X-ray diffraction experiment (30.6 mg, 65%).

¹H NMR (500 MHz, C₆D₆) δ 24.88 (s, 1H, C₆H₅SiH₃), 17.29 (s, 1H, C₆H₅SiH₃), 13.08 (s, 0.5H, C₆H₅SiH₃), 10.57 (s, 1H, NC(CH₃)CH), 6.72 (t, 2H, *J* = 7.9 Hz, ArH), 6.36 (d, 4H, *J* = 7.6 Hz, ArH), 5.26 (s, 6H, NC(CH₃)CH), 2.79 (m, 4H, Cy-CH₂), 1.70 (m, 4H, Cy-CH₂), 1.12 (m, 8H, Cy-CH₂ overlapping Cy-CH₂), 1.01 (m, 4H, Cy-CH₂), 0.44 (m, 4H, Cy-CH₂), -0.14 (m, 4H, Cy-CH₂), -0.46 (m, 4H, Cy-CH₂), -0.99 (m, 4H, Cy-CH₂), -1.54 (m, 4H, Cy-CH₂), -2.78 (s, 1.5H, C₆H₅SiH₃), -4.33 (m, 4H, Cy-CH₂).

¹³C {¹H} NMR (126 MHz, C₆D₆) δ 176.2 (NC(CH₃)CH), 151.3 (C_{ipso}), 141.1 (C_{ortho}), 124.4 (C_{para}), 124.3 (C_{meta}), 100.0 (NC(CH₃)CH), 40.7 (Cy-CH), 35.1 (Cy-CH₂ overlapping Cy-CH₂), 31.3 (Cy-CH₂ overlapping Cy-CH₂), 27.4 (Cy-CH₂ overlapping Cy-CH₂), 25.6 (Cy-CH₂), 25.4 (Cy-CH₂ overlapping Cy-CH₂), 18.0 (NC(CH₃)CH).

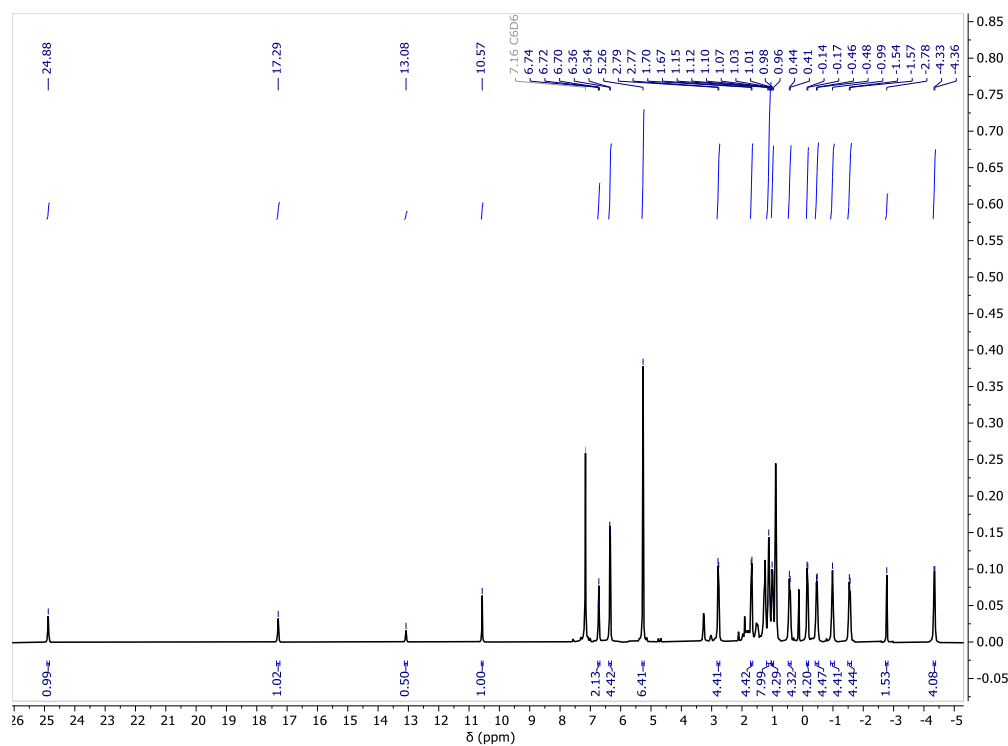
IR (cm⁻¹): 3058 (w), 2921 (s), 2848 (s), 2123 (w), 1621 (s), 1589 (w), 1550 (s), 1486 (w), 1445 (s), 1397 (s), 1352 (s), 1304 (s), 1262 (s), 1212 (m), 1165 (m), 1131 (m), 1080 (w), 1014 (m), 996 (m), 923 (s), 890 (s), 844 (s), 831 (m), 776 (s), 763 (s), 735 (s), 691 (s).

$\mu_{\text{eff}} = 1.78 \mu_{\text{B}}$ (C₆D₆, 22 °C).

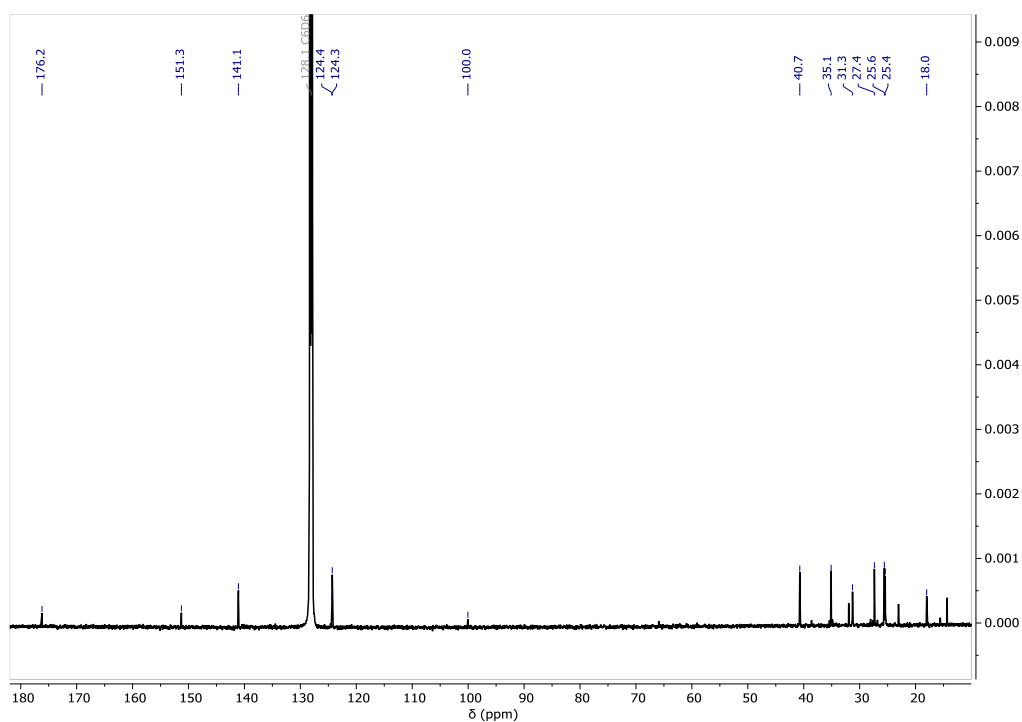
Elemental Analysis for [(BDI^{Dicyp})Sm(μ -C₆H₈Si)Sm(BDI^{Dicyp})] (1564.78 g mol⁻¹):

Calculated: C, 67.55; H, 7.86; N, 3.58%.

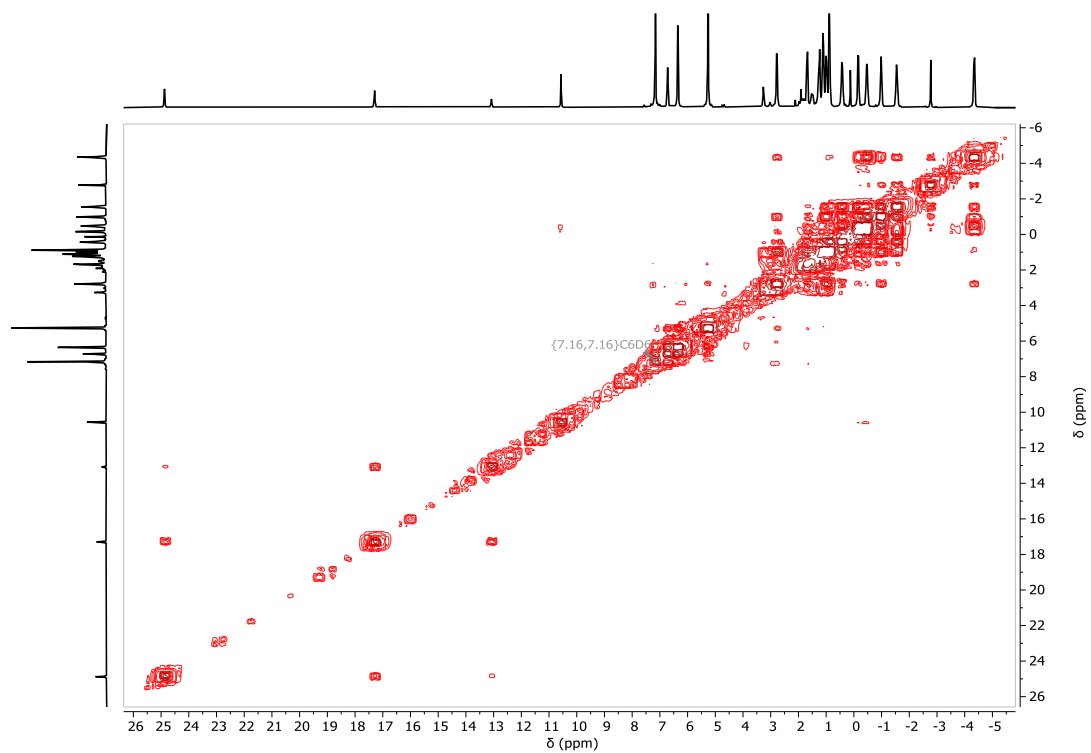
Found: C, 60.19; H, 7.23; N, 3.26%.



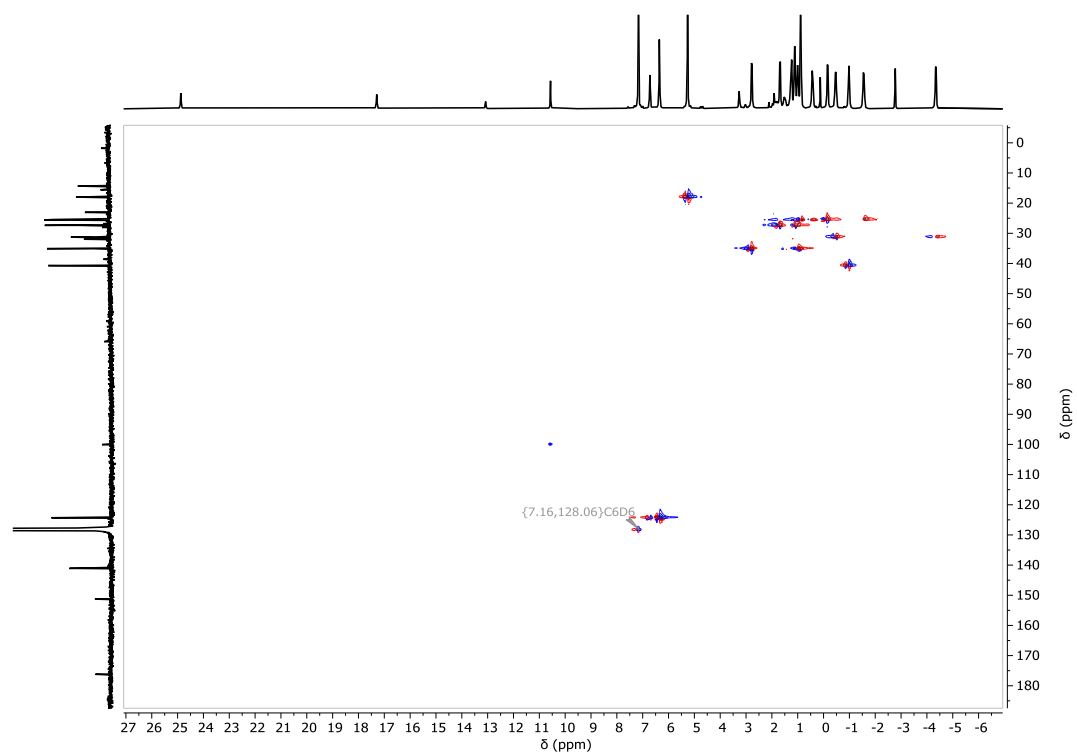
Supplementary Figure 4.29. ^1H NMR spectrum (500 MHz, C_6D_6) of $[(\text{BDI}^{\text{Dicyl}})\text{Sm}(\mu\text{-C}_6\text{H}_8\text{Si})\text{Sm}(\text{BDI}^{\text{Dicyl}})]$ (**4.5**).



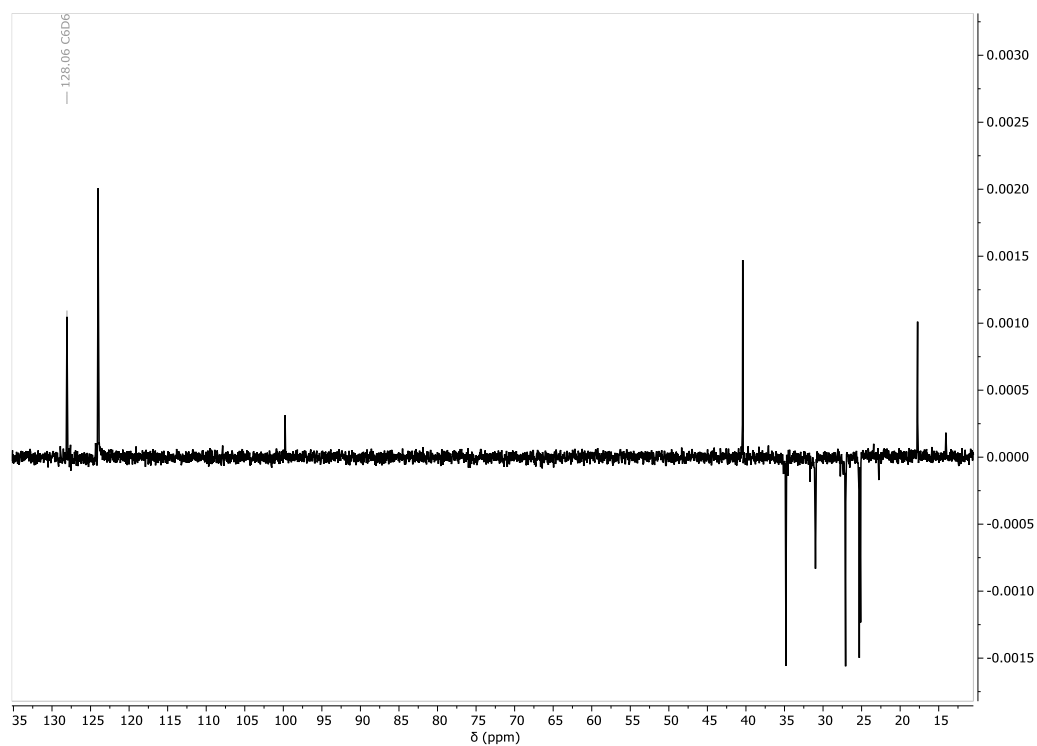
Supplementary Figure 4.30. $^{13}\text{C}\{^1\text{H}\}$ NMR spectrum (126 MHz, C_6D_6) of $[(\text{BDI}^{\text{Dicyl}})\text{Sm}(\mu\text{-C}_6\text{H}_8\text{Si})\text{Sm}(\text{BDI}^{\text{Dicyl}})]$ (**4.5**).



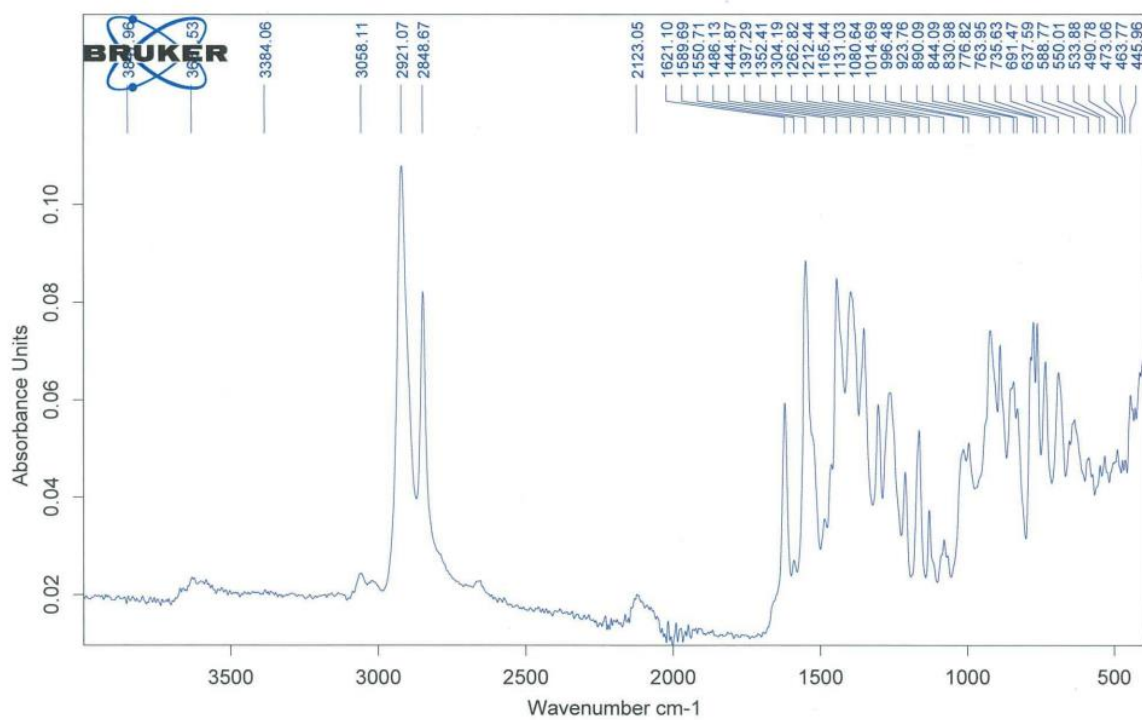
Supplementary Figure 4.31. ^1H - ^1H COSY NMR spectrum (500 MHz, C_6D_6) of $[(\text{BDI}^{\text{Dicyl}})\text{Sm}(\mu\text{-C}_6\text{H}_8\text{Si})\text{Sm}(\text{BDI}^{\text{Dicyl}})]$ (4.5).



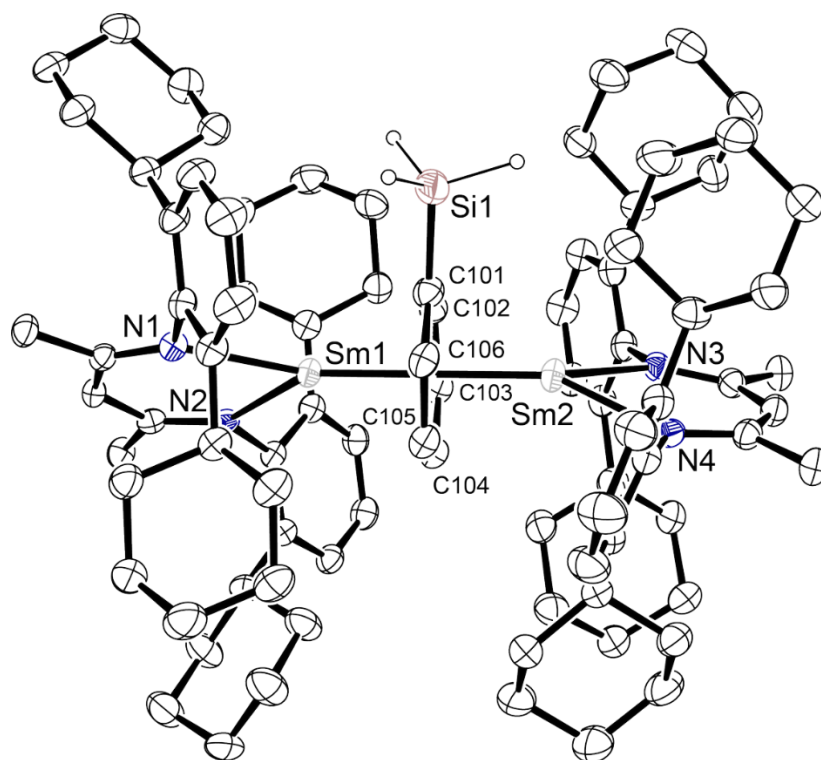
Supplementary Figure 4.32. ^1H - ^{13}C HSQC NMR spectrum (500 MHz, C_6D_6) of $[(\text{BDI}^{\text{Dicyl}})\text{Sm}(\mu\text{-C}_6\text{H}_8\text{Si})\text{Sm}(\text{BDI}^{\text{Dicyl}})]$ (4.5).



Supplementary Figure 4.33. DEPT-135 ^{13}C NMR spectrum (126 MHz, C_6D_6) of $[(\text{BDI}^{\text{DicyP}})\text{Sm}(\mu\text{-C}_6\text{H}_8\text{Si})\text{Sm}(\text{BDI}^{\text{DicyP}})]$ (**4.5**).



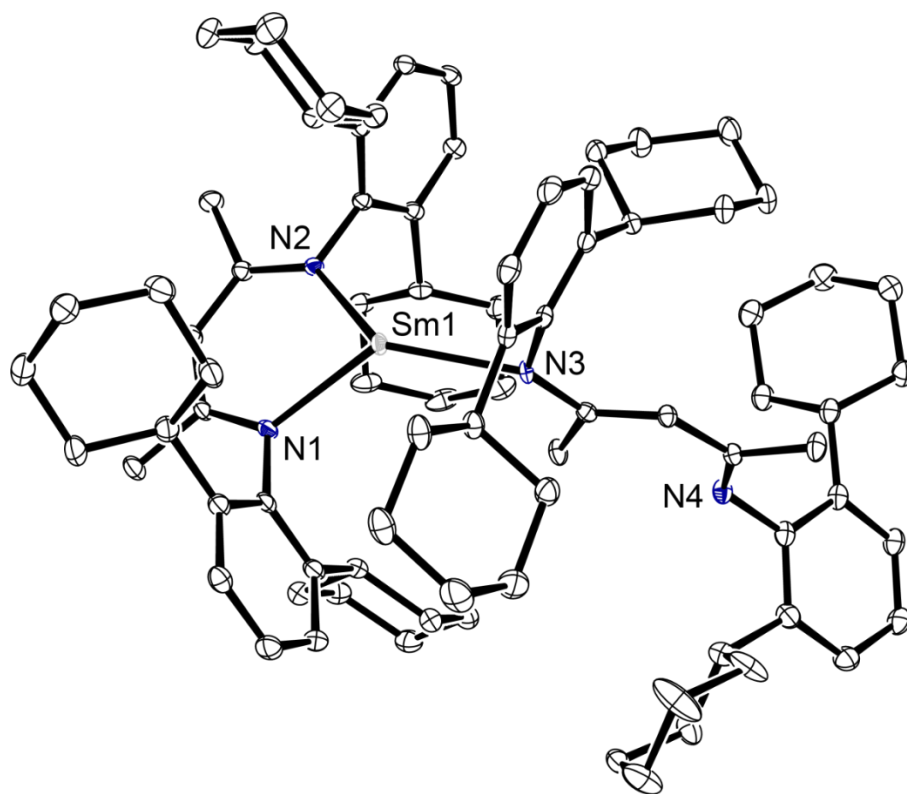
Supplementary Figure 4.34. Infrared spectrum of $[(\text{BDI}^{\text{DicyP}})\text{Sm}(\mu\text{-C}_6\text{H}_8\text{Si})\text{Sm}(\text{BDI}^{\text{DicyP}})]$ (**4.5**).



Supplementary Figure 4.35. Ortep representation (30% probability ellipsoids) of $[(\text{BDI}^{\text{DicyP}})\text{Sm}(\mu\text{-C}_6\text{H}_8\text{Si})\text{Sm}(\text{BDI}^{\text{DicyP}})]$ (**4.5**). Hydrogen atoms (except those on Si1) have been omitted for clarity.

Attempted synthesis of $[(\text{BDI}^{\text{Dicyp}})\text{Sm}(\mu\text{-C}_8\text{H}_{10})\text{Sm}(\text{BDI}^{\text{Dicyp}})]$

$[(\text{BDI}^{\text{Dicyp}})\text{SmCH}(\text{SiMe}_3)_2]$ (65 mg, 0.07 mmol) was dissolved in *p*-xylene inside an NMR tube fitted with a J. Youngs tap. The mixture was left to react over the weekend at room temperature, resulting in large dark crystalline blocks suitable for an X-ray diffraction experiment to deposit on the walls of the NMR tube.



Supplementary Figure 4.36. Ortep representation (30% probability ellipsoids) of $[(\text{BDI}^{\text{Dicyp}})_2\text{Sm}]$ (**4.6**). Hydrogen atoms have been omitted for clarity.

[(BDI^{Dicyp})Sm(μ -COT)] (4.7)

A faintly yellow hexane solution of COT (12.2 mg, 0.12 mmol) was added to a dark brown hexane solution containing [(BDI^{Dicyp})SmCH(SiMe₃)₂] (104.5 mg, 0.12 mmol) in scintillation vial inside the glovebox. Stirring for ca. 1h resulted in the formation of a yellow–brown solution with a pale–yellow suspension. Yellow blocks like crystals suitable for an X–ray diffraction experiment were obtained from a saturated toluene solution at room temperature (89.5 mg, 80.6%).

¹H NMR (500 MHz, C₆D₆) δ 8.11 (br, 8H, C₈H₈), 8.09 (m, 2H, J = 7.9 Hz, ArH), 7.70 (s, 1H, NC(CH₃)CH), 7.57 (d, 4H, J = 7.8 Hz, ArH), 3.61 (s, 6H, NC(CH₃)CH), 2.32 (m, 4H, Cy–CH₂), 1.36 (m, 4H, Cy–CH₂), 1.18 (m, 4H, Cy–CH₂), 0.70 (m, 4H, Cy–CH₂), 0.47 (m, 8H, Cy–CH₂ overlapping Cy–CH₂), 0.09 (m, 8H, Cy–CH₂ overlapping Cy–CH₂), –2.16 (m, 8H, Cy–CH₂ overlapping Cy–CH₂), –2.31 (m, 4H, Cy–CH).

¹³C{¹H} NMR (126 MHz, C₆D₆) δ 171.7 (NC(CH₃)CH), 153.7 (C_{ipso}), 13.6 (C_{ortho}), 126.7 (C_{meta}), 126.6 (C_{para}), 99.4 (NC(CH₃)CH), 84.9 (C₈H₈), 42.2 (Cy–CH), 34.9 (Cy–CH₂ overlapping Cy–CH₂), 32.5 (Cy–CH₂ overlapping Cy–CH₂), 27.0 (Cy–CH₂ overlapping Cy–CH₂), 25.5 (Cy–CH₂ overlapping Cy–CH₂), 25.4 (Cy–CH₂ overlapping Cy–CH₂), 21.1 (NC(CH₃)CH).

GC–MS: 303 (5.3%, –CH₃), 245 (7.1%, –SiMe₃), 230 (38.1%, –SiMe₃, –CH₃), 157 (93.8%, –SiMe₃, –SiMe₃, –CH₃), 131 (29.2%, –SiMe₃, –SiMe₃, –CH₃, –CH₃), 73 (100.0%, SiMe₃).

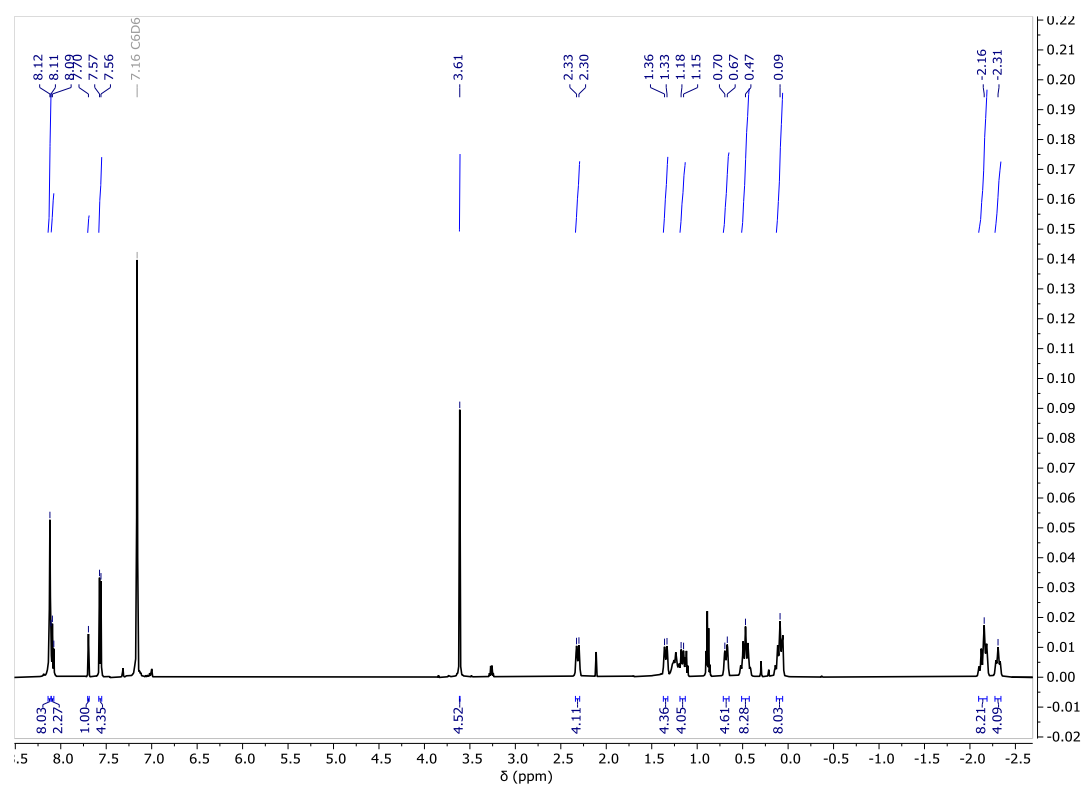
IR (cm^{–1}): 3056 (w), 3001 (w), 2921 (s), 2848 (s), 1621 (m), 1589 (w), 1548 (s), 1532 (s), 1485 (w), 1445 (s), 1395 (s), 1353 (s), 1302 (m), 1260 (m), 1213 (w), 1164 (m), 1130 (w), 1081 (w), 1027 (m), 997 (w), 926 (m), 891 (m), 832 (m), 789 (s), 776 (s), 764 (s), 736 (m), 736 (s), 704 (s), 671 (m), 627 (w).

μ_{eff} = 1.53 μ_{B} (C₆D₆, 22 °C).

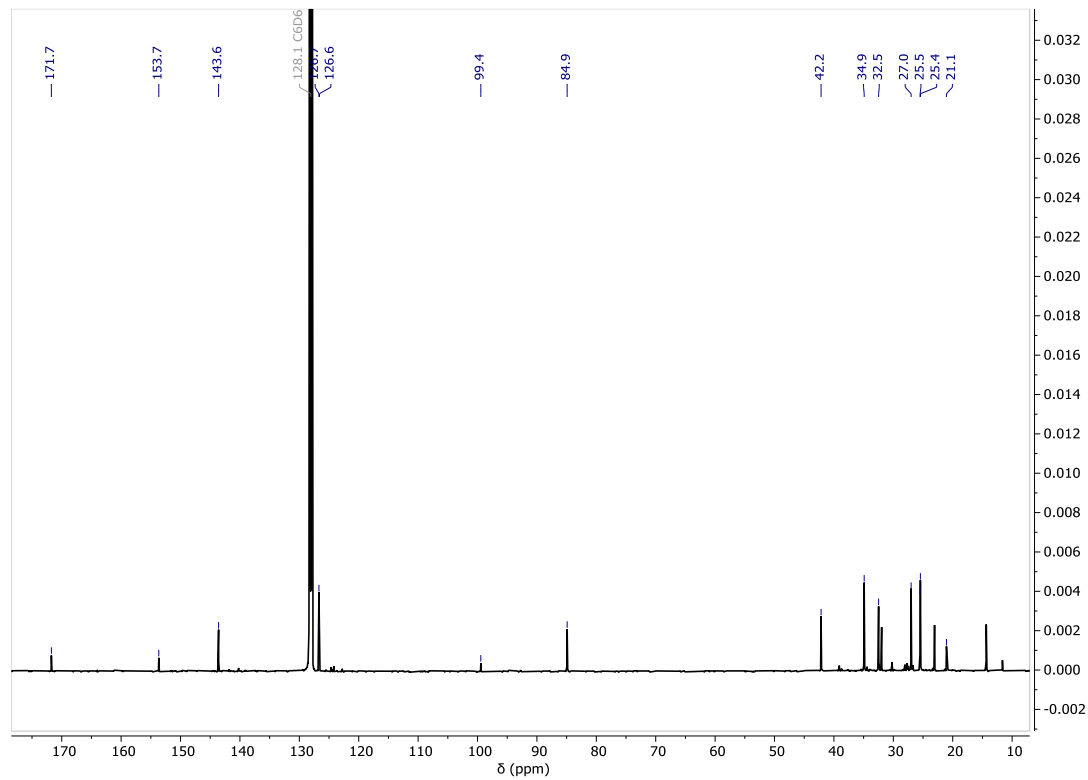
Elemental Analysis for [(BDI^{Dicyp})Sm(μ -COT)] (832.43 g mol^{–1}):

Calculated: C, 70.70; H, 7.87; N, 3.37%.

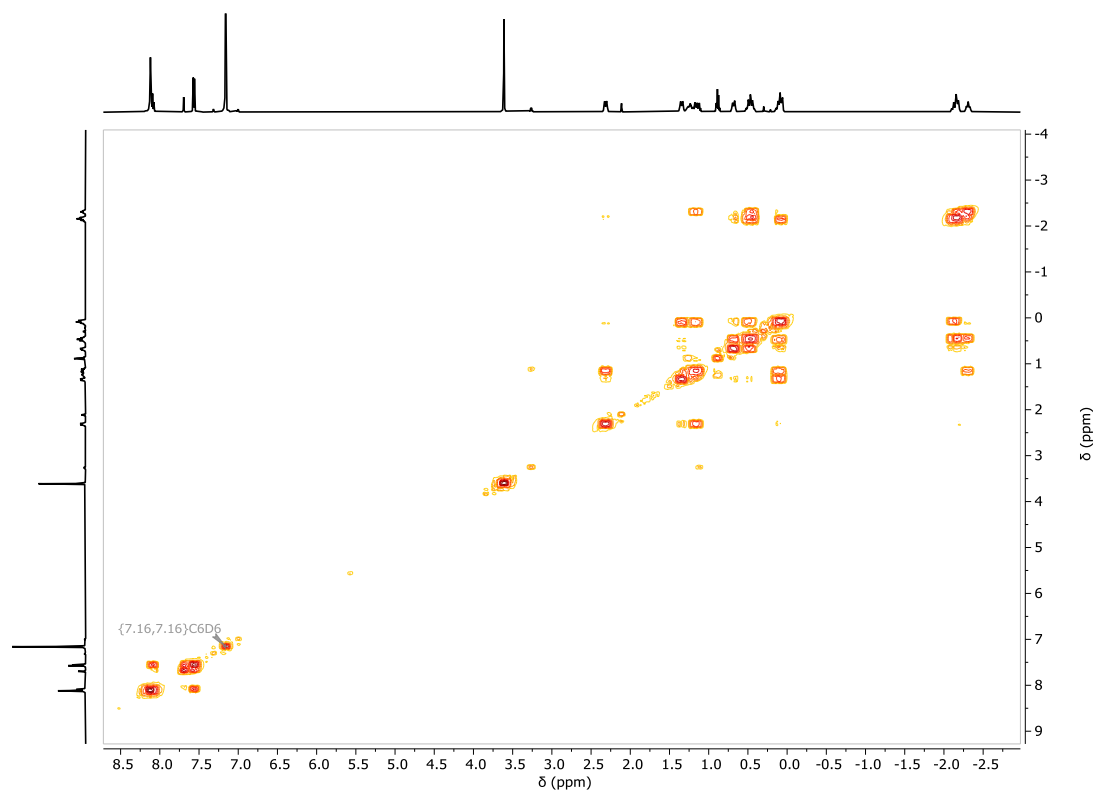
Found: C, 69.38; H, 8.12; N, 2.54%.



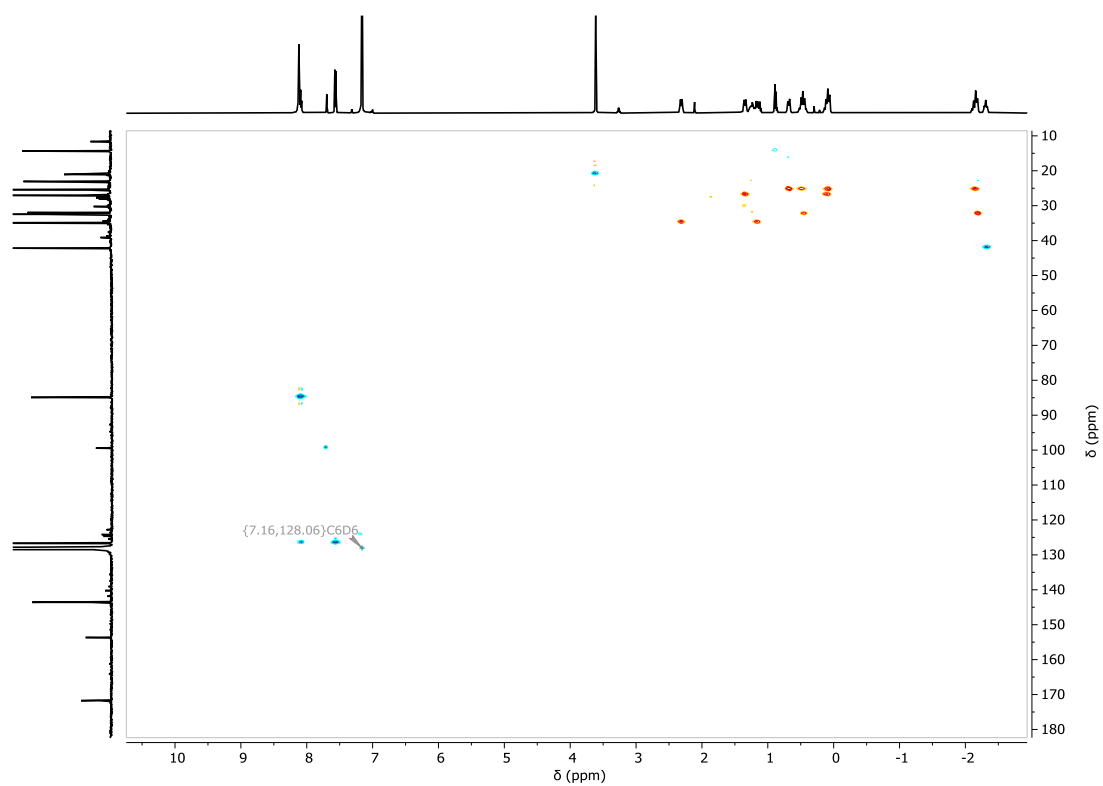
Supplementary Figure 4.37. ¹H NMR spectrum (500 MHz, C₆D₆) of [(BDI^{Dicyp})Sm(μ-COT)] (**4.7**).



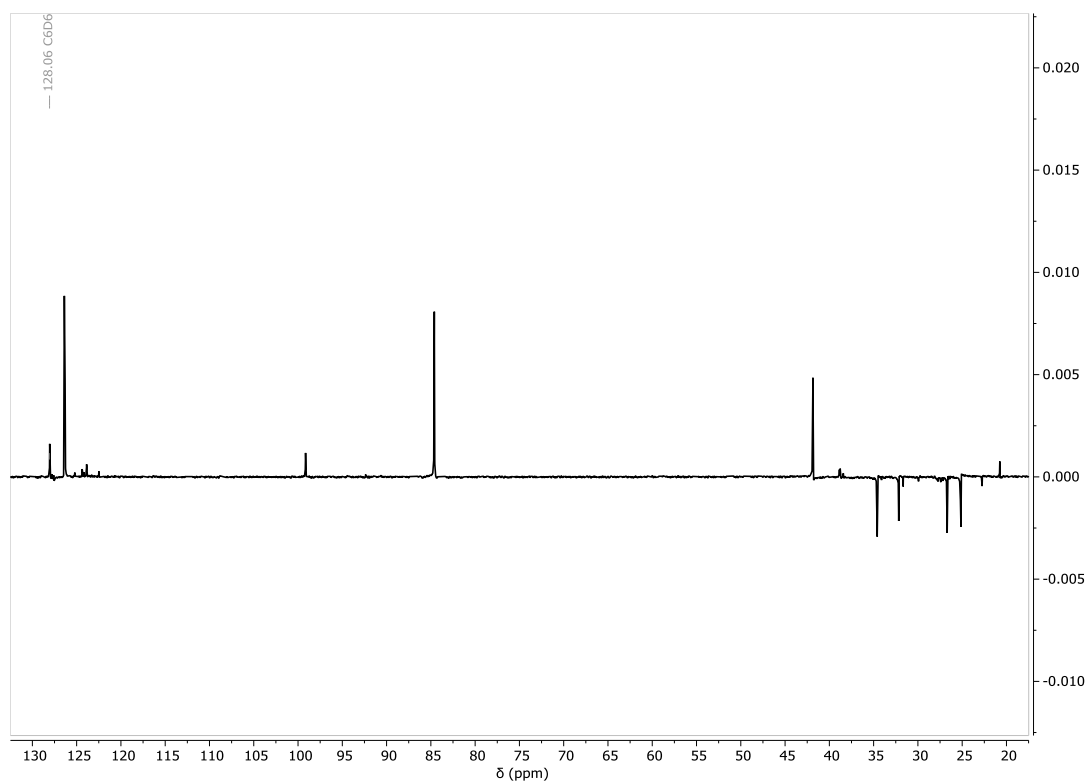
Supplementary Figure 4.38. ¹³C{¹H} NMR spectrum (126 MHz, C₆D₆) of [(BDI^{Dicyp})Sm(μ-COT)] (**4.7**).



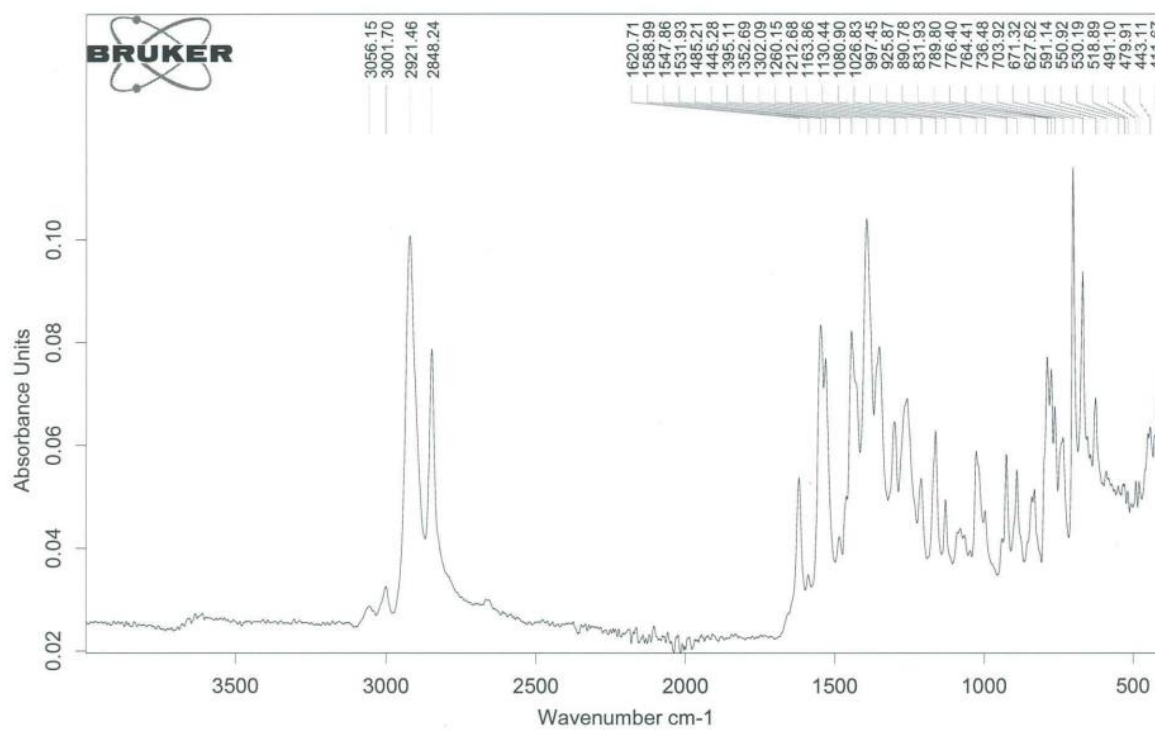
Supplementary Figure 4.39. ^1H - ^1H COSY NMR spectrum (500 MHz, C_6D_6) of $[(\text{BDI}^{\text{Dicyl}})\text{Sm}(\mu\text{-COT})]$ (**4.7**).



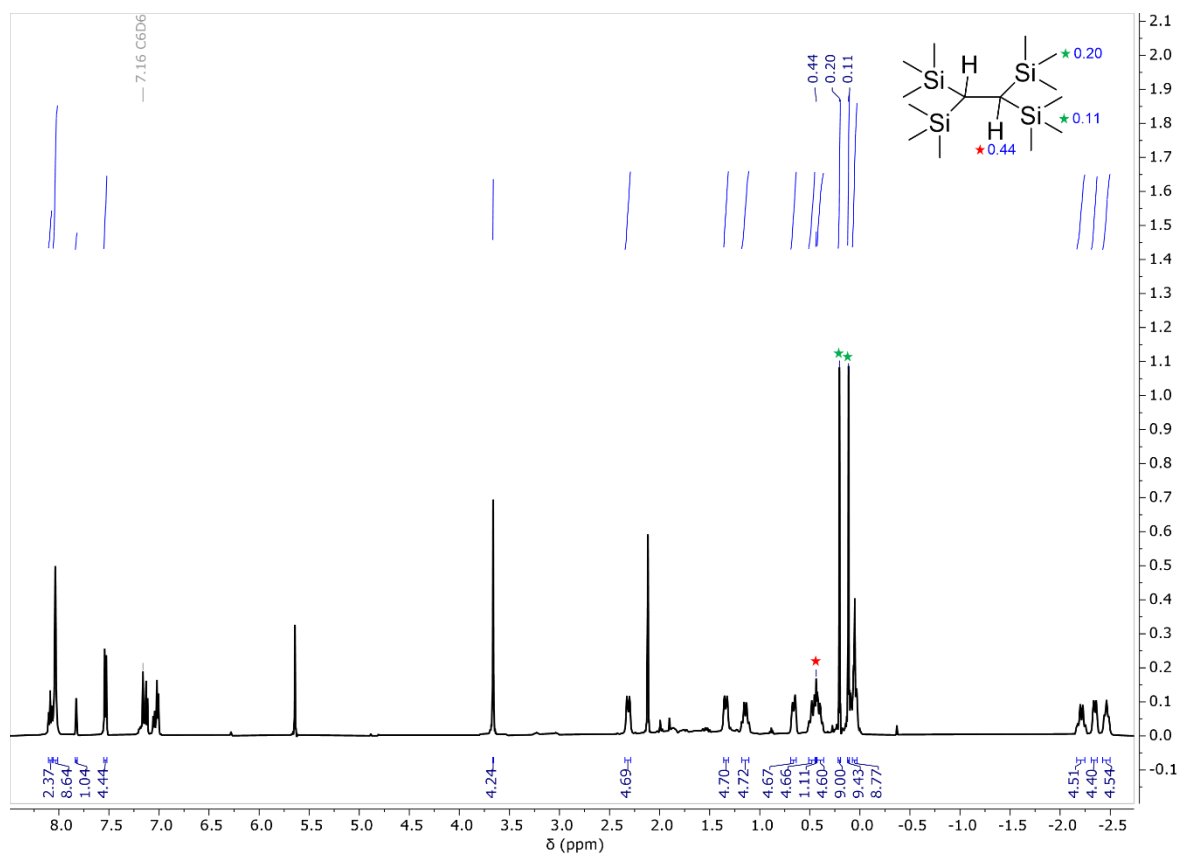
Supplementary Figure 4.40. ^1H - ^{13}C HSQC NMR spectrum (500 MHz, C_6D_6) of $[(\text{BDI}^{\text{Dicyl}})\text{Sm}(\mu\text{-COT})]$ (**4.7**).



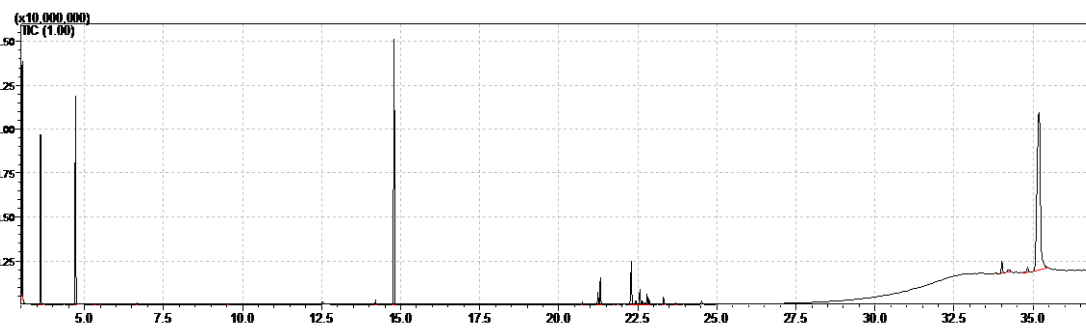
Supplementary Figure 4.41. DEPT-135 ^{13}C NMR spectrum (500 MHz, C_6D_6) of $[(\text{BDI}^{\text{Dicyclopentadienyl}})\text{Sm}(\mu\text{-COT})]$ (**4.7**).



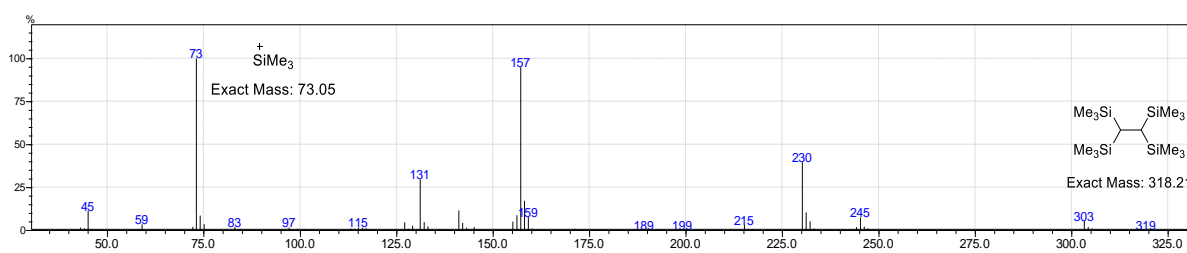
Supplementary Figure 4.42. Infrared spectrum of $[(\text{BDI}^{\text{Dicyclopentadienyl}})\text{Sm}(\mu\text{-COT})]$ (**4.7**).



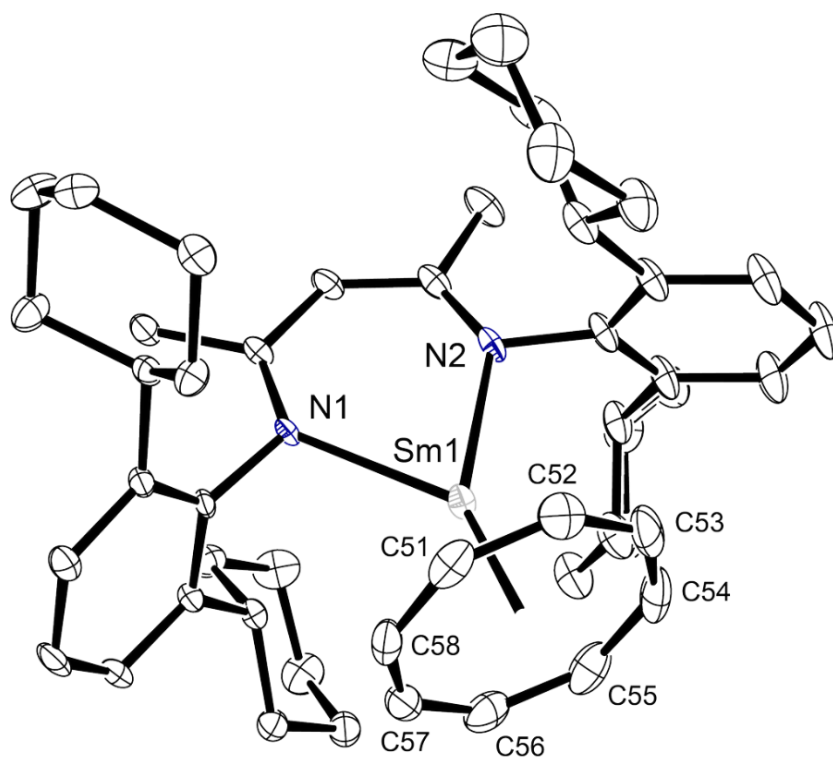
Supplementary Figure 4.43. ^1H NMR spectrum (500 MHz, C_6D_6) of $[(\text{BDI})^{\text{Dicyclopentadienyl}}\text{Sm}(\mu\text{-COT})]$ (**4.7**) in a 1:1 molar ratio with the organic by-product, 1,1,2,2-tetrakis(trimethylsilyl)ethane.



Supplementary Figure 4.44. GC-MS chromatogram of the reaction between **4.7** and COT, showing the peak for 1,1,2,2-tetrakis(trimethylsilyl)ethane (14.78 min).



Supplementary Figure 4.45. GC-MS trace showing the peak for 1,1,2,2-tetrakis(trimethylsilyl)ethane (14.78 min).

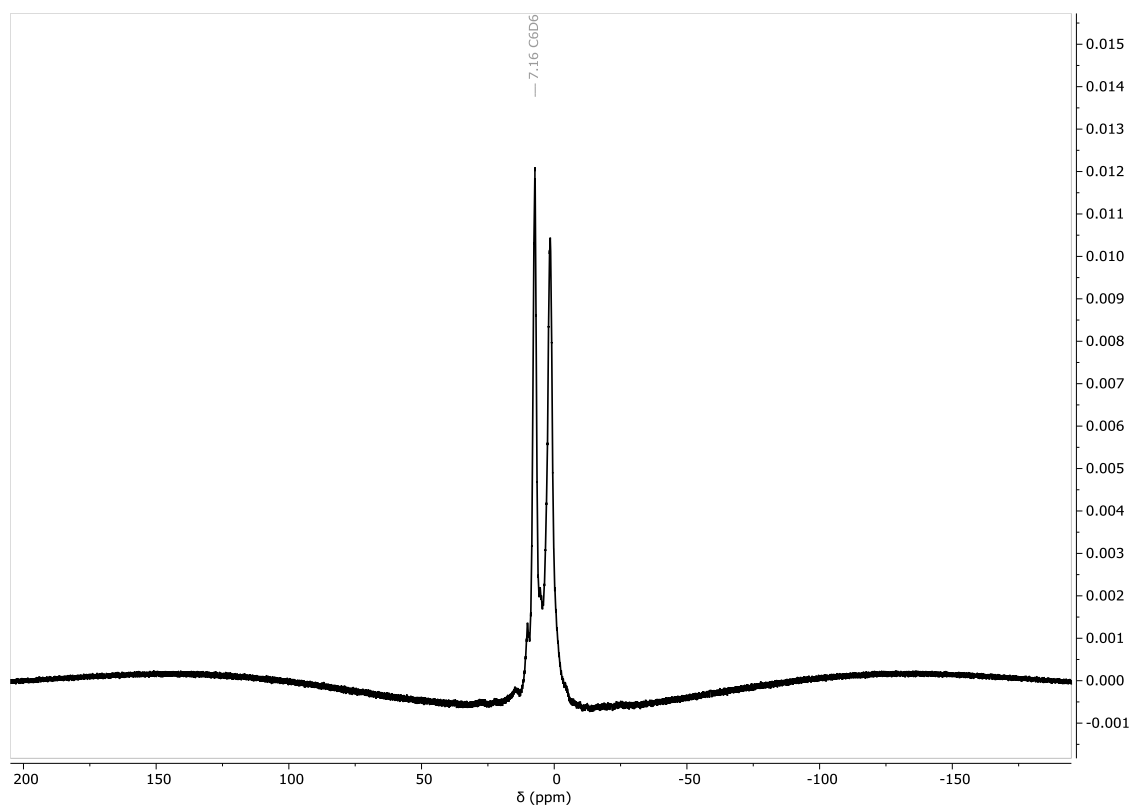


Supplementary Figure 4.46. Ortep representation (ellipsoid 30% probability) of $[(\text{BDI}^{\text{Dicyclopentadienyl}})\text{Sm}(\mu\text{-COT})]$ (**4.7**). Hydrogen atoms have been omitted for clarity.

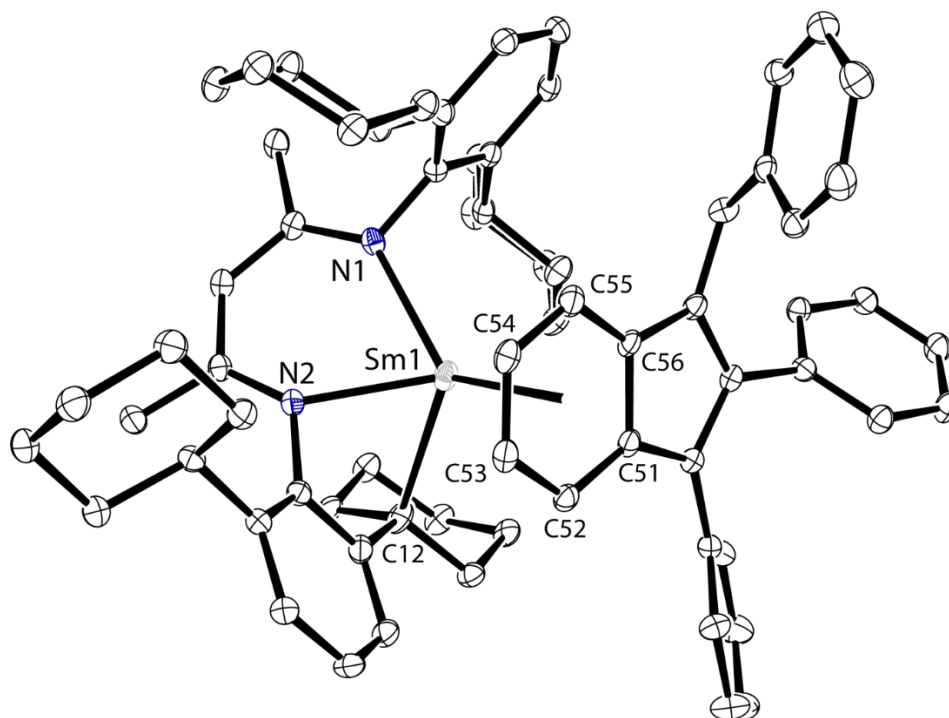
$[(\text{BDI}^{\text{DicyP}})\text{Sm}(\mu\text{-C}_{28}\text{H}_{21})]$ (4.8)

A colourless C_6D_6 solution of diphenylacetylene (38 mg, 0.21 mmol) was added to an J. Youngs tap NMR tube containing a dark green-brown C_6D_6 solution of $[(\text{BDI}^{\text{DicyP}})\text{Sm}(\mu\text{-C}_6\text{H}_6)\text{Sm}(\text{BDI}^{\text{DicyP}})]$ (82 mg, 0.05 mmol). Within 5 minutes at room temperature, the solution had turned a purple-red colour, however the reaction mixture was left overnight at room temperature. This afforded a dark red solution. The volatiles were removed under vacuum, and the crude product recrystallised from toluene, providing dark crystals suitable for an X-ray diffraction experiment after slow evaporation at room temperature.

The paramagnetic nature of $[(\text{BDI}^{\text{DicyP}})\text{Sm}(\mu\text{-C}_{28}\text{H}_{21})\text{Sm}(\text{BDI}^{\text{DicyP}})]$ hampered characterisation by multinuclear NMR spectroscopic techniques.



Supplementary Figure 4.47. ^1H NMR spectrum (500 MHz, C_6D_6) of $[(\text{BDI}^{\text{Dicyl}})\text{Sm}(\mu\text{-C}_{28}\text{H}_{22})]$ (**4.8**).



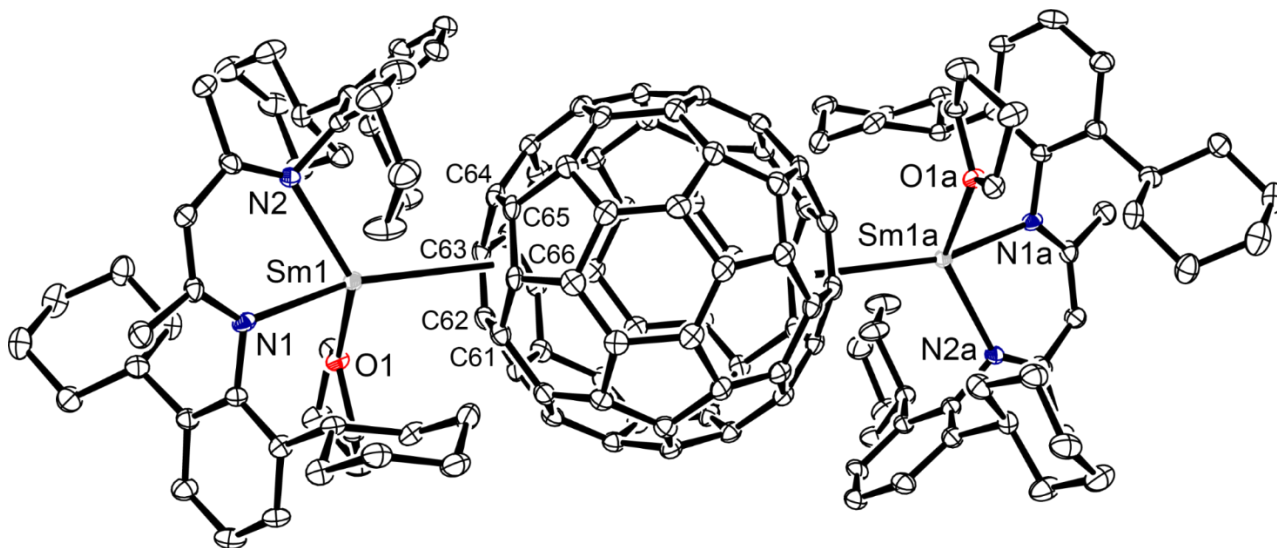
Supplementary Figure 4.48. Ortep representation (30% probability ellipsoids) of $[(\text{BDI}^{\text{Dicyl}})\text{Sm}(\mu\text{-C}_{28}\text{H}_{22})]$ (**4.8**). Hydrogen atoms have been omitted for clarity.

$[(\text{BDI}^{\text{DicyP}})(\text{THF})\text{Sm}(\mu\text{-C}_{60})\text{Sm}(\text{THF})(\text{BDI}^{\text{DicyP}})]$ (4.9)

a) A purple toluene solution containing fullerene (23 mg, 0.03 mmol) was added to a scintillation vial containing $[(\text{BDI}^{\text{DicyP}})\text{Sm}(\mu\text{-C}_6\text{H}_6)\text{Sm}(\text{BDI}^{\text{DicyP}})]$ (48 mg, 0.03 mmol) in toluene and the mixture was left to stir at room temperature overnight resulting in a brown solution and brown precipitate. The solution was filtered through Celite and left to slowly evaporate at room temperature, providing dark crystals suitable for an X-ray diffraction experiment.

b) A purple toluene solution containing fullerene (25 mg, 0.03 mmol) was added to a scintillation vial containing $[(\text{BDI}^{\text{DicyP}})\text{Sm}(\mu\text{-C}_6\text{H}_6)\text{Sm}(\text{BDI}^{\text{DicyP}})]$ (106 mg, 0.07 mmol) in toluene and the mixture was left to stir at room temperature overnight resulting in a brown solution and brown precipitate. The solution was filtered through Celite and left to slowly evaporate at room temperature, providing dark crystals suitable for an X-ray diffraction experiment.

The solubility of $[(\text{BDI}^{\text{DicyP}})\text{Sm}(\mu\text{-C}_{60})\text{Sm}(\text{BDI}^{\text{DicyP}})]$ hampered characterisation by multinuclear NMR spectroscopic techniques.

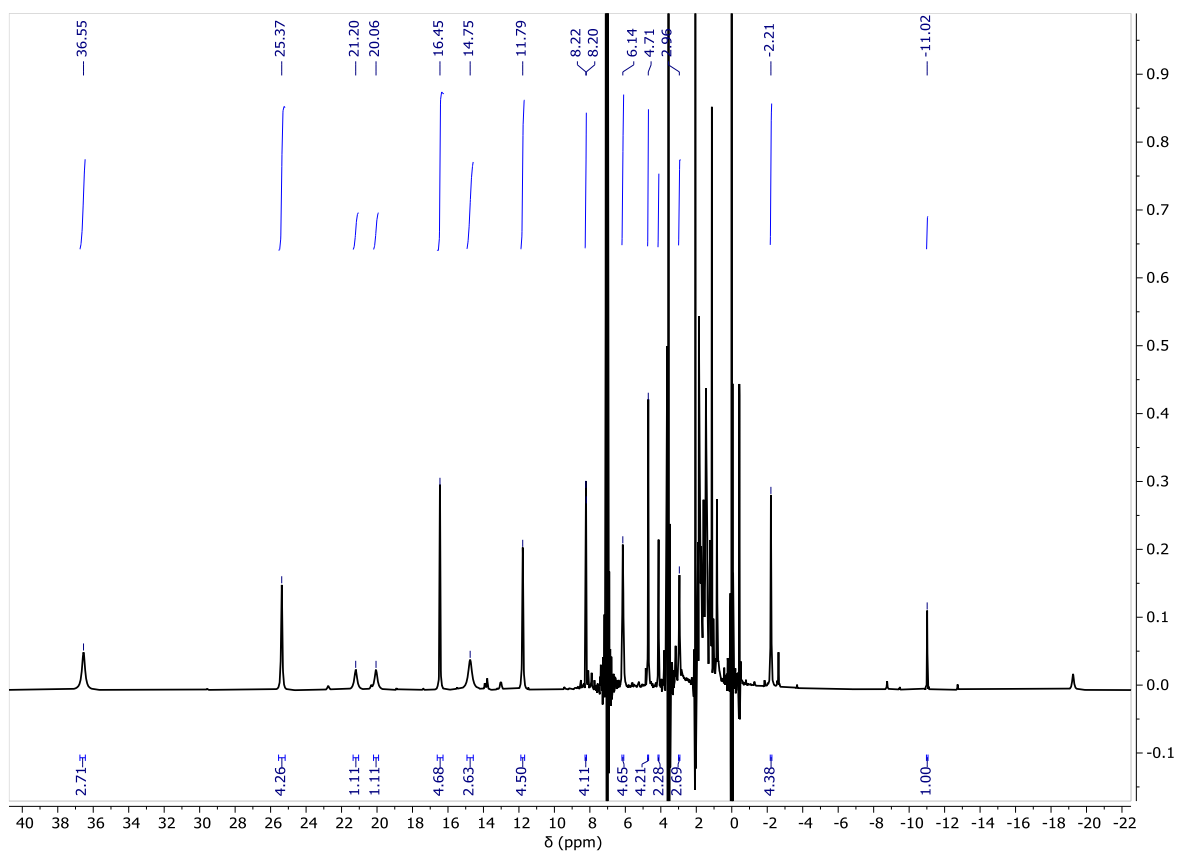


Supplementary Figure 4.49. Ortep representation (30% probability ellipsoids) of $[(\text{BDI}^{\text{DicyP}})(\text{THF})\text{Sm}(\mu\text{-C}_{60})\text{Sm}(\text{THF})(\text{BDI}^{\text{DicyP}})]$ (4.8). Hydrogen atoms have been omitted for clarity.

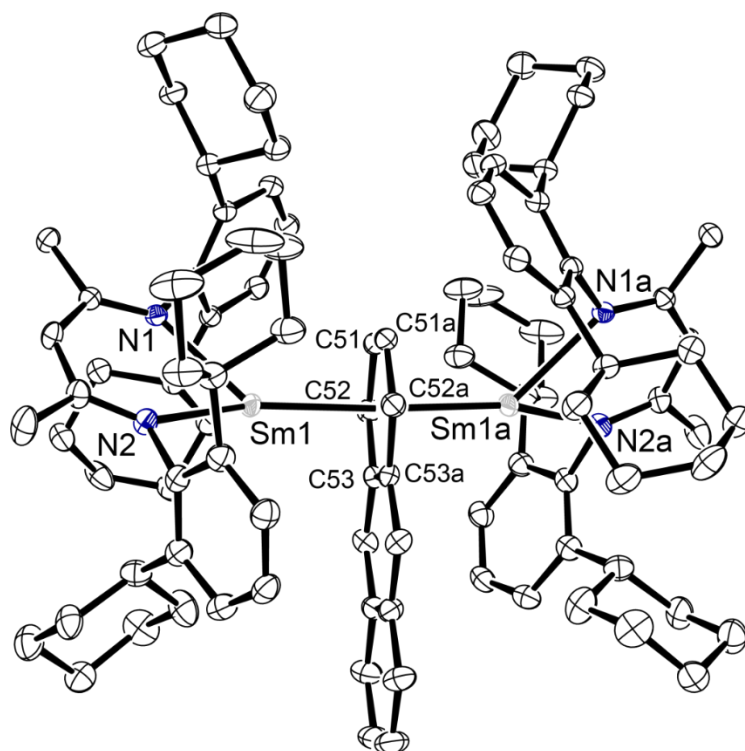
[(BDI^{Dicyp})Sm(μ -C₁₄H₁₀)Sm(BDI^{Dicyp})] (4.10)

A C₆D₆ solution of anthracene (4 mg, 0.02 mmol) was added to a J. Youngs tap NMR tube containing a C₆D₆ solution of [(BDI^{Dicyp})SmCH(SiMe₃)₂] (20 mg, 0.2 mmol). The mixture was heated for 48h at 60 °C, resulting in a blue-black solution. The volatiles were removed *in vacuo* and the crude product dissolved into toluene, affording dark crystals suitable for an X-ray diffraction experiment after slow evaporation at room temperature.

¹H NMR (500 MHz, C₆D₆) δ 36.55 (br, 2H), 25.37 (s, 4H), 21.20 (br, 1H, C₁₄H₁₀), 20.06 (br, 1H, C₁₄H₁₀), 16.45 (s, 4H), 14.75 (br, 2H, C₁₄H₁₀), 8.22 (s, 4H), 6.14 (s, 4H), 4.71 (s, 4H), 4.13 (s, 2H), 2.96 (s, 2H), -2.21 (s, 4H), -11.02 (s, 1H, NC(CH₃)CH).



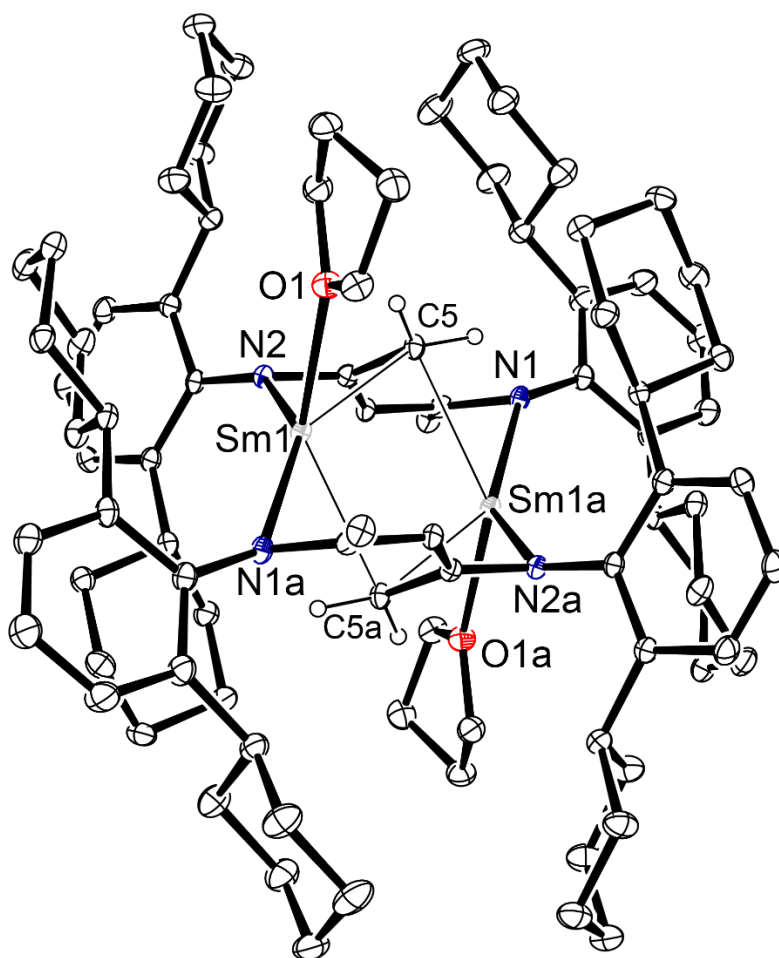
Supplementary Figure 4.50. ^1H NMR spectrum (500 MHz, C_6D_6) of the crude reaction mixture of $[(\text{BDI}^{\text{Dicyl}})\text{Sm}(\mu\text{-C}_{14}\text{H}_{10})\text{Sm}(\text{BDI}^{\text{Dicyl}})]$ (**4.10**).



Supplementary Figure 4.51. Ortep representation (30% probability ellipsoids) of $[(\text{BDI}^{\text{Dicyl}})\text{Sm}(\mu\text{-C}_{14}\text{H}_{10})\text{Sm}(\text{BDI}^{\text{Dicyl}})]$ (**4.10**). Hydrogen atoms have been omitted for clarity.

Attempted synthesis of $[(\text{BDI}^{\text{Dicyp}})\text{Sm}(\mu\text{-C}_{10}\text{H}_8)\text{Sm}(\text{BDI}^{\text{Dicyp}})]$

A colourless hexane solution of naphthalene (13 mg, 0.10 mmol) was added to a J. Youngs tap NMR tube containing $[(\text{BDI}^{\text{Dicyp}})\text{SmCH}(\text{SiMe}_3)_2]$ (92 mg, 0.10 mmol) in hexane and the mixture was heated for 1 week at 60 °C for 1 week. The resultant black-blue solution was left to crystallise at room temperature in a scintillation vial inside the glovebox, affording dark blocks suitable for a X-ray diffraction experiment.



Supplementary Figure 4.52. Ortep representation (30% probability ellipsoids) of compound **4.11**, isolated from the attempted synthesis of $[(\text{BDI}^{\text{Dicyp}})\text{Sm}(\mu\text{-C}_{10}\text{H}_8)\text{Sm}(\text{BDI}^{\text{Dicyp}})]$. Hydrogen atoms (except those on C5) have been omitted for clarity.

4.2 Single Crystal X-ray Diffraction Analysis

4.2.1 Crystal Structure Data and Refinement Details

All non-hydrogen atoms were refined anisotropically, unless specified below. Hydrogen atoms were placed at calculated positions and refined using a riding model, unless otherwise specified.

$[(\text{BDI}^{\text{DicyP}})\text{SmI}]_2$ (4.1)

There is an entire $[\text{L}_2\text{Sm}_2(\text{THF})]$ molecule and a toluene solvent molecule in the asymmetric unit (ASU). The coordinated THF molecule was disordered, so it was modelled in two parts, with occupancies freely refined to 0.7:0.3. The geometry of the minor component was restrained to be like the major component (SAME) and was refined isotropically. Additionally, one of the cyclohexyl side chains was also disordered, with occupancies freely refined to 0.51:0.49. The geometries of these disordered cyclohexyl rings were restrained to be like a well-ordered cyclohexyl ring (C18–C23) (SAME). The ADPs of C30/C130 were constrained to be equal (EADP) due to close proximity.

$[(\text{BDI}^{\text{DicyP}})\text{SmCH}(\text{SiMe}_3)_2]$ (4.2)

There is an entire molecule of $[\text{LSmCH}(\text{TMS})_2]$ in the ASU. The ADPs of one of the cyclohexyl groups (C36–C41) were initially very elongated, so were modelled as being disordered. These disordered cyclohexyl substituents were restrained to have the same geometry as the well-ordered side chain (C18–C23). Additionally, the ADPs of C36/C136 were constrained to be equal (EADP); and the phenyl-cyclohexane bonds (C35–C36/C136) were restrained to be equal between disorder parts (SADI). Two disordered and partial occupancy toluene molecules were evident from initial inspection of the electron density. Modelling of these molecules was unsatisfactory and given they were not part of the samarium complex, these were removed and the unmodelled electron density was instead accounted for using SQUEEZE, which yielded 138 electrons in a solvent accessible volume of 581 Å³. Note: 200 electrons expected for four toluene molecules in P1 unit cell.

$[(\text{BDI}^{\text{DicyP}})\text{Sm}(\mu\text{-C}_6\text{H}_6)\text{Sm}(\text{BDI}^{\text{DicyP}})]$ (4.3)

There is half of the $[\text{LSm}(\text{benzene})\text{SmL}]$ sandwich complex and half a toluene molecule in the ASU. The toluene molecule was located over an inversion centre; the entire toluene molecule was modelled at a fixed 50% occupancy, requiring PART -1 to ensure no bonding to its symmetry equivalent. Geometry controls were required for modelling this solvent molecule,

including distance restraints (SADI, ring to methyl) and ring geometry constraints (AFIX 66). Isotropic refinement of these atoms was also required.

$[(\text{BDI}^{\text{DicyP}})\text{Sm}(\mu\text{-C}_7\text{H}_8)\text{Sm}(\text{BDI}^{\text{DicyP}})]$ (4.4)

The entire $[\text{LSm}(\text{toluene})\text{SmL}]$ complex and a toluene solvent molecule were present in the ASU. One of the side chains was modelled as being disordered, with occupancies freely refined to 0.72:0.28. The geometry of both parts (C68–C73 and C168–C173) were restrained to be like well-behaved side chain (C62–C67) using SAME restraints. The ADPs of the associated anchor atoms C68/C168 were constrained to be the same using EADP, due to close proximity. The solvent toluene molecule was positioned over an inversion site, so the entire molecule was modelled at a fixed 50% occupancy and using PART -1 to prevent bonding to symmetry equivalent. This molecule required ring geometry constraints (AFIX 66) and a ring-methyl SADI restraint. The disordered components and solvent molecule were refined isotropically since refinement was unsatisfactory when anisotropic.

$[(\text{BDI}^{\text{DicyP}})\text{Sm}(\mu\text{-C}_6\text{H}_8\text{Si})\text{Sm}(\text{BDI}^{\text{DicyP}})]$ (4.5)

The entire $[\text{LSm}(\text{PhSiH}_3)\text{SmL}]$ sandwich complex was present in the ASU. The silane hydrogen atoms were not obvious in the electron density, presumably due to a combination of fast rotation of this group and longer Si–H bond distance. These hydrogen atoms were thus modelled using a combination of a geometry constraint (AFIX 134: idealised tetrahedral XH_3 group with H-atoms 'riding' on attached Si atom, X–H distance freely refined) and bond length restraints (DFIX). The idealised treatment of these atoms was deemed acceptable since the structure is consistent with other experimental data.

$[\text{BDI}^{\text{DicyP}}]_2\text{Sm}$ (4.6)

There is an entire molecule of $[(\text{L})_2\text{Sm}]$ and one and a half molecules of xylene in the ASU. The other half of the xylene molecule is generated through symmetry. One of the cyclohexyl groups (C62–C67) was modelled as being disordered, with occupancy allowed to freely refine to 0.71:0.29. The geometry of these disorder components was restrained to be like a well-behaved cyclohexyl group (C68–C73). Additionally, two pairs of atoms in the disorder (C62/C162 and C65/C165) had almost coincident coordinates and required ADP constraints (EADP) for stable refinement.

[(BDI^{Dicyp})Sm(μ -C₈H₈)] (4.7)

There are two [LSm(COT)] complexes and two toluene solvent molecules in the ASU. Both sidechains in one of the ligands is disordered (C72–C77 and C78–C83), which freely refined to occupancies of 0.61:0.39 and 0.59:0.41, respectively. The geometries of these cyclohexyl groups were restrained to be the same as a well-behaved cyclohexyl ring (C18–C23) (SAME). The carbon atoms in these groups (C72 and C78) that connect to the phenyl ring were constrained to have the same ADPs as their disorder counterparts (EADP), since these have almost identical coordinates - mostly affects attached proton placement. One of the cyclohexyl atoms (C81) and its disorder equivalent also are very close so required the same treatment. A rigid bond restraint was applied to two atoms (C117 and C118) in one of the COT molecules. One of the toluene molecules is disordered over two positions, freely refining to occupancies of 0.65:0.35. Both were restrained to have geometry like the other toluene molecule (SAME). Only the major component was refined anisotropically.

[(BDI^{Dicyp})Sm(μ -C₂₈H₂₁)] (4.8)

There is an entire molecule of [LSm(C₂₈H₂₁)] and one toluene molecule in the ASU. All non-H atoms were refined anisotropically, except for minor disorder component. One of the ligands cyclohexyl rings was modelled as being disordered over two positions, with occupancy freely refined to 0.76:0.24. The geometry of the two cyclohexyl ring disorder components were restrained to be like the well-behaved cyclohexyl ring (SAME). The positions of the methine carbon atoms (C12/C12b) were almost coincident, so their ADPs were constrained to be the same (EADP). Note: this carbon atom was modelled as being deprotonated, due to apparent bonding to the Sm centre. Finally, the phenyl-cyclohexyl bonds was restrained to be the same (SADI).

[(BDI^{Dicyp})Sm(μ -C₁₄H₁₀)Sm(BDI^{Dicyp})] (4.10)

There is half of the [LSm(C₁₄H₁₀)SmL] dimer and one molecule of benzene in the ASU. One of the cyclohexyl side chains was disordered. Occupancy allowed to freely refine to 0.66:0.34. The geometries of the disordered rings were (SAME) restrained to be consistent with a well behaved ring (C36–C41). Likewise, the benzene-cyclohexyl ring bonds were restrained to be the same (SADI).

[(BDI^{Dicyp})Sm(THF)]₂ (4.11)

There is a half of the [LSm(THF)]₂ dimer and two molecules of toluene in the ASU. Standard H-atom treatment, except two hydrogen atoms on the deprotonated methyl group (C5), which

coordinates to both samarium atoms in dimer. The positions of these two hydrogen atoms were allowed to freely refine, but the C–H bond lengths were restrained to be equal.

Supplementary Table 4.1. Crystal structure and refinement data for compounds **4.1** – **4.5**.

| | 4.1 | 4.2 | 4.3 | 4.4 | 4.5 |
|---|---|---|---|--|---|
| CCDC code | 2244280 | 2244279 | 2244281 | 2244283 | 2244282 |
| Empirical formula | C ₉₃ H ₁₃₀ I ₂ N ₄ OSm ₂ | C ₄₈ H ₇₆ N ₂ Si ₂ Sm | C ₉₅ H ₁₂₈ N ₄ Sm ₂ | C ₁₈₅ H ₂₅₂ N ₈ Sm ₄ | C ₈₈ H ₁₂₂ N ₄ SiSm ₂ |
| Formula weight (g mol ⁻¹) | 1874.50 | 887.63 | 1626.71 | 3189.33 | 1564.68 |
| Temperature (K) | 120 | 120 | 120 | 120 | 120 |
| Crystal system | Monoclinic | Triclinic | Monoclinic | Triclinic | Monoclinic |
| Space group | P 21/c | P -1 | P 21/n | P -1 | P 21/n |
| a (Å) | 21.6542(3) | 13.4370(6) | 15.4607(5) | 12.7661(4) | 13.6192(3) |
| b (Å) | 13.05450(10) | 13.8093(4) | 13.3650(5) | 15.0592(3) | 21.4581(5) |
| c (Å) | 31.8378(4) | 16.0202(5) | 20.7874(8) | 22.6085(6) | 26.8361(5) |
| α (°) | 90 | 95.108(3) | 90 | 103.3913(19) | 90 |
| β (°) | 106.6690(10) | 94.536(3) | 106.363(4) | 102.111(3) | 91.9663(17) |
| γ (°) | 90 | 110.091(3) | 90 | 95.965(2) | 90 |
| Volume (Å ³) | 8621.86(18) | 2761.48(18) | 4121.3(3) | 4080.65(19) | 7838.0(3) |
| Z | 4 | 2 | 2 | 1 | 4 |
| Calculated density (Mg/ m ³) | 1.444 | 1.068 | 1.311 | 1.298 | 1.326 |
| Absorption coefficient (mm ⁻¹) | 16.091 | 8.593 | 10.934 | 11.032 | 11.618 |
| F(000) | 3816 | 936 | 1700 | 1666 | 3264 |
| Crystal size (mm ³) | 0.209 x 0.113 x 0.026 | 0.271 x 0.180 x 0.167 | 0.138 x 0.108 x 0.024 | 0.079 x 0.059 x 0.017 | 0.181 x 0.092 x 0.022 |
| Theta range for data collection (°) | 3.683 to 73.235 ° | 3.434 to 73.430 ° | 3.982 to 73.162 ° | 3.684 to 77.442 ° | 3.846 to 73.356 ° |
| Index ranges | -26 ≤ h ≤ 26 -9 ≤ k ≤ 15 -39 ≤ l ≤ 39 | -16 ≤ h ≤ 16 -17 ≤ k ≤ 14 -19 ≤ l ≤ 19 | -18 ≤ h ≤ 17 -11 ≤ k ≤ 16 -25 ≤ l ≤ 25 | -15 ≤ h ≤ 15 -18 ≤ k ≤ 16 -27 ≤ l ≤ 28 | -16 ≤ h ≤ 13 -24 ≤ k ≤ 26 -33 ≤ l ≤ 33 |
| Reflections collected | 61306 | 33342 | 28615 | 52040 | 57514 |
| Independent reflections | 17159 R(int) = 0.0452 | 11011 R(int) = 0.0342 | 8182 R(int) = 0.0933 | 16301 R(int) = 0.0820 | 15646 R(int) = 0.0625 |
| Completeness to theta | 99.9 % | 100.0% | 99.9% | 100.0 % | 99.9% |
| Data/ restraints/ parameters | 17159/ 46/ 993 | 11011/ 13/ 536 | 8182/ 1/ 443 | 16301/ 37/ 902 | 15646/ 3/ 861 |
| Goodness-of-fit on F ² | 1.013 | 1.033 | 1.013 | 0.989 | 1.017 |
| Final R indices [I>2sigma(I)] | R1 = 0.0380 wR2 = 0.0931 | R1 = 0.0361 wR2 = 0.964 | R1 = 0.0633 wR2 = 0.1523 | R1 = 0.0481 wR2 = 0.1103 | R1 = 0.0548 wR2 = 0.1315 |
| R indices (all data) | R1 = 0.0458 wR2 = 0.0987 | R1 = 0.0388 wR2 = 0.0991 | R1 = 0.0956 wR2 = 0.1715 | R1 = 0.0696 wR2 = 0.1235 | R1 = 0.0754 wR2 = 0.1455 |
| Largest diff. peak and hole (e. Å ⁻³) | 1.418 and -1.716 | 0.912 and -1.197 | 1.442 and -1.296 | 1.361 and -2.012 | 1.266 and -1.151 |

Supplementary Table 4.2. Crystal structure and refinement data for compounds **4.6** – **4.8**, **4.10** and **4.11**.

| | 4.6 | 4.7 | 4.8 | 4.10 | 4.11 |
|---|---|---|---|--|---|
| CCDC code | | 2244284 | | | |
| Empirical formula | C ₉₂ H ₁₂₆ I ₂ N ₄ Sm | C ₅₆ H ₇₃ N ₂ Sm | C ₇₆ H ₈₅ N ₂ Sm | C ₁₀₈ H ₁₃₆ N ₄ Sm ₂ | C ₁₀₄ H ₁₄₄ N ₄ O ₂ Sm ₂ |
| Formula weight (g mol ⁻¹) | 1444.32 | 924.51 | 1176.80 | 1790.90 | 1782.92 |
| Temperature (K) | 120 | 120 | 120 | 120 | 120 |
| Crystal system | Triclinic | Triclinic | Triclinic | Monoclinic | Monoclinic |
| Space group | P -1 | P -1 | P -1 | P 2/c | P 21/c |
| a (Å) | 13.63220(10) | 14.7652(4) | 11.7577(3) | 15.22570(10) | 14.3119(2) |
| b (Å) | 14.6426(2) | 18.9329(4) | 15.6528(5) | 14.51340(10) | 11.4964(2) |
| c (Å) | 21.6272(2) | 19.0732(4) | 16.6512(4) | 20.75570(10) | 27.3211(4) |
| α (°) | 96.8450(10) | 78.597(2) | 80.896(2) | 90 | 90 |
| β (°) | 105.7490(10) | 68.502(2) | 81.122(2) | 100.4360(10) | 91.9560(10) |
| γ (°) | 102.3980(10) | 71.689(2) | 88.673(3) | 90 | 90 |
| Volume (Å ³) | 3985.10(8) | 4689.1(2) | 2989.64(14) | 4510.65(5) | 4492.67(12) |
| Z | 2 | 4 | 2 | 2 | 2 |
| Calculated density (Mg/ m ³) | 1.204 | 1.310 | 1.307 | 1.319 | 1.318 |
| Absorption coefficient (mm ⁻¹) | 5.876 | 9.676 | 7.709 | 10.042 | 10.094 |
| F(000) | 1542 | 1940 | 1234 | 1872 | 1872 |
| Crystal size (mm ³) | 0.136 x 0.107 x 0.066 | 0.173 x 0.103 x 0.039 | 0.116 x 0.060 x 0.041 | 0.297 x 0.149 x 0.091 | 0.118 x 0.065 x 0.065 |
| Theta range for data collection (°) | 3.466 to 73.465 ° | 3.537 to 72.431 ° | 3.805 to 72.744 ° | 3.737 to 72.491 ° | 4.172 to 72.253 ° |
| Index ranges | -16 ≤ h ≤ 16 -18 ≤ k ≤ 18 -23 ≤ l ≤ 26 | -18 ≤ h ≤ 18 -23 ≤ k ≤ 23 -23 ≤ l ≤ 22 | -14 ≤ h ≤ 12 -19 ≤ k ≤ 19 -20 ≤ l ≤ 17 | -18 ≤ h ≤ 18 -16 ≤ k ≤ 17 -16 ≤ l ≤ 25 | -17 ≤ h ≤ 17 -13 ≤ k ≤ 14 -33 ≤ l ≤ 30 |
| Reflections collected | 60346 | 150904 | 36958 | 44755 | 29649 |
| Independent reflections | 15925 R(int) = 0.0586 | 18453 R(int) = 0.0677 | 11770 R(int) = 0.0675 | 8874 R(int) = 0.0365 | 8810 R(int) = 0.0354 |
| Completeness to theta | 100.0 % | 99.9% | 99.9% | 100.0 % | 100.0% |
| Data/ restraints/ parameters | 15925/ 36/ 942 | 18453/ 142/ 1191 | 11770/ 37/ 739 | 8874/ 37/ 571 | 8810/ 1/ 513 |
| Goodness-of-fit on F ² | 1.051 | 1.024 | 1.058 | 1.040 | 1.077 |
| Final R indices [I>2sigma(I)] | R1 = 0.0339 wR2 = 0.0800 | R1 = 0.0369 wR2 = 0.0875 | R1 = 0.0510 wR2 = 0.1093 | R1 = 0.0281 wR2 = 0.0690 | R1 = 0.0310 wR2 = 0.0664 |
| R indices (all data) | R1 = 0.0383 wR2 = 0.0821 | R1 = 0.0426 wR2 = 0.0909 | R1 = 0.0647 wR2 = 0.1159 | R1 = 0.0319 wR2 = 0.0722 | R1 = 0.0380 wR2 = 0.0691 |
| Largest diff. peak and hole (e. Å ⁻³) | 0.778 and -0.963 | 2.355 and -2.183 | 1.601 and -2.518 | 0.976 and -1.209 | 1.030 and -0.731 |

4.3 Solid-State Magnetic Susceptibility Measurements

Magnetisation measurements, conducted by Simon Granville and Tane Butler, were made on compound **4.3** using a Quantum Design MPMS-5 Superconducting Quantum Interference Device (SQUID) magnetometer. A weighed sample of the compound was loaded into a diamagnetic glass tube and flame sealed under an argon atmosphere. The tube was cleaned by sonication in acetone and mounted inside a diamagnetic (plastic drinking straw) sample holder. Magnetisation measurements were made with the RSO sample transport, using individual scans of 4 cm length. Over this scan length, the longer plastic straw and glass tube are magnetically uniform, ensuring only the magnetic moment from compound **4.3** was detected. The resultant data was interpreted by Lujia Liu.

For the temperature-dependent susceptibility, a 1 T field was applied, and the measurements made while cooling from ambient (300 K) to 4 K. For the variable-field measurements at 4 K, the magnetisation was then measured as a function of applied field sweeping from 7 T to 0.

To fit the temperature-dependent susceptibility we used the Curie-Weiss equation:

$$\chi_m = \frac{C}{T - \theta_{CW}}$$

χ_m = molar magnetic susceptibility, C = Curie constant, θ_{CW} = Curie-Weiss temperature.

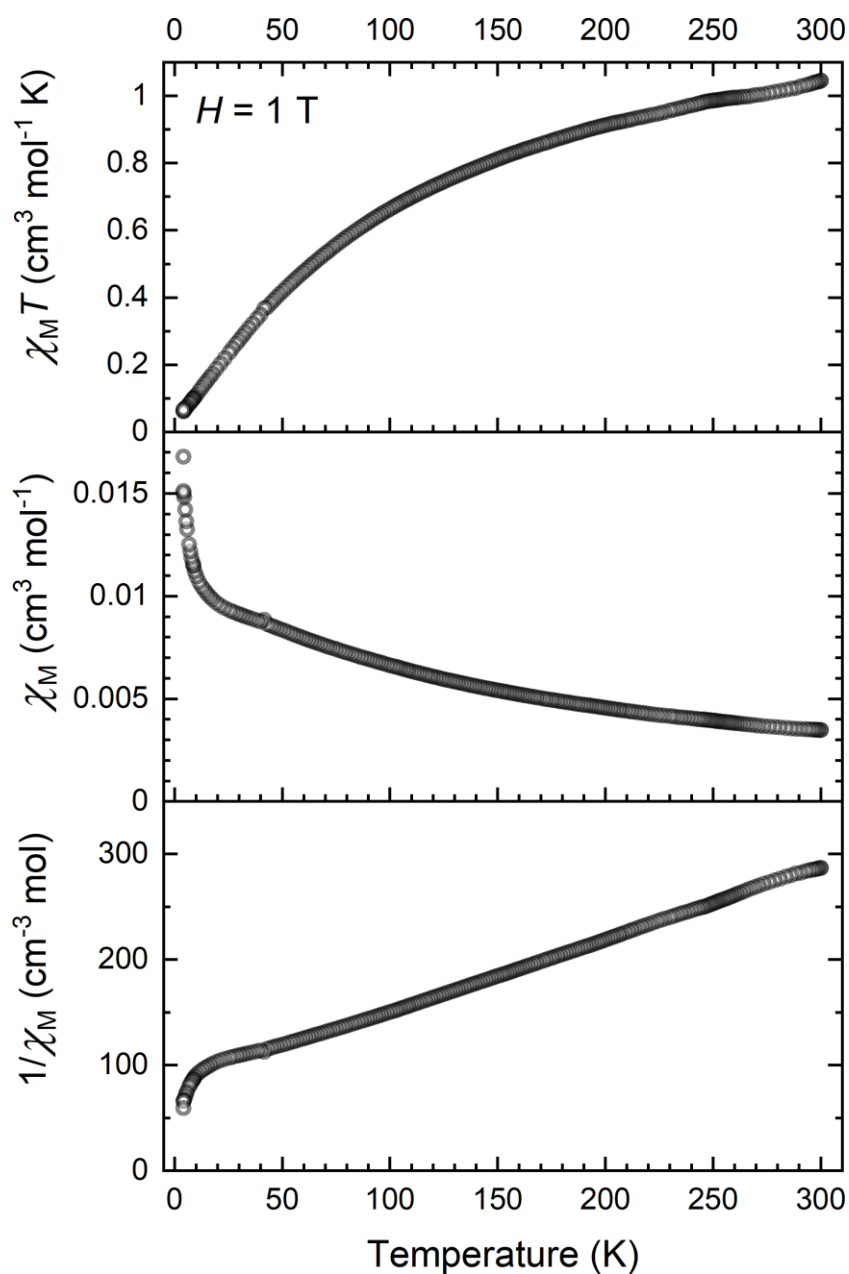
The effective magnetic moment was calculated by following:

$$\mu_{eff} = \sqrt{8C} \mu_B (\text{cgs units})$$

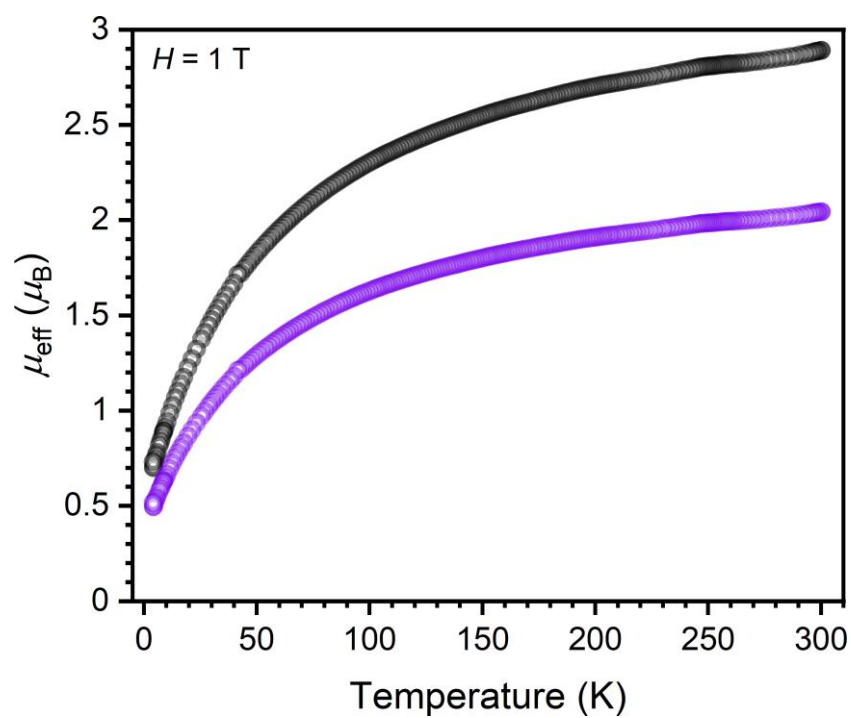
Exchange coupling constant between the two Sm^{3+} spins is estimated using the following equation:

$$\theta_{CW} = \frac{2J_{ex}}{3k_B} (g_j - 1)^2 J(J + 1)$$

where θ_{CW} is the Curie-Weiss temperature, J is the total angular momentum quantum number, J_{ex} is the exchange coupling constant, k_B is the Boltzmann constant, and $(g_j - 1)^2 J(J + 1)$ is the de Gennes factor. Here, a spin-orbit ground state of $J = 5/2$ and a g -factor of $g_j = 2/7$ were used to calculate J_{ex} . However, we note that this calculation only provides a rough estimate for the exchange coupling constant due to the proximity of higher order spin-orbit manifolds in Sm^{3+} .



Supplementary Figure 4.53. Field-cooled, variable-temperature magnetic susceptibility plots for **4.3** under an applied magnetic field strength of 1 T.

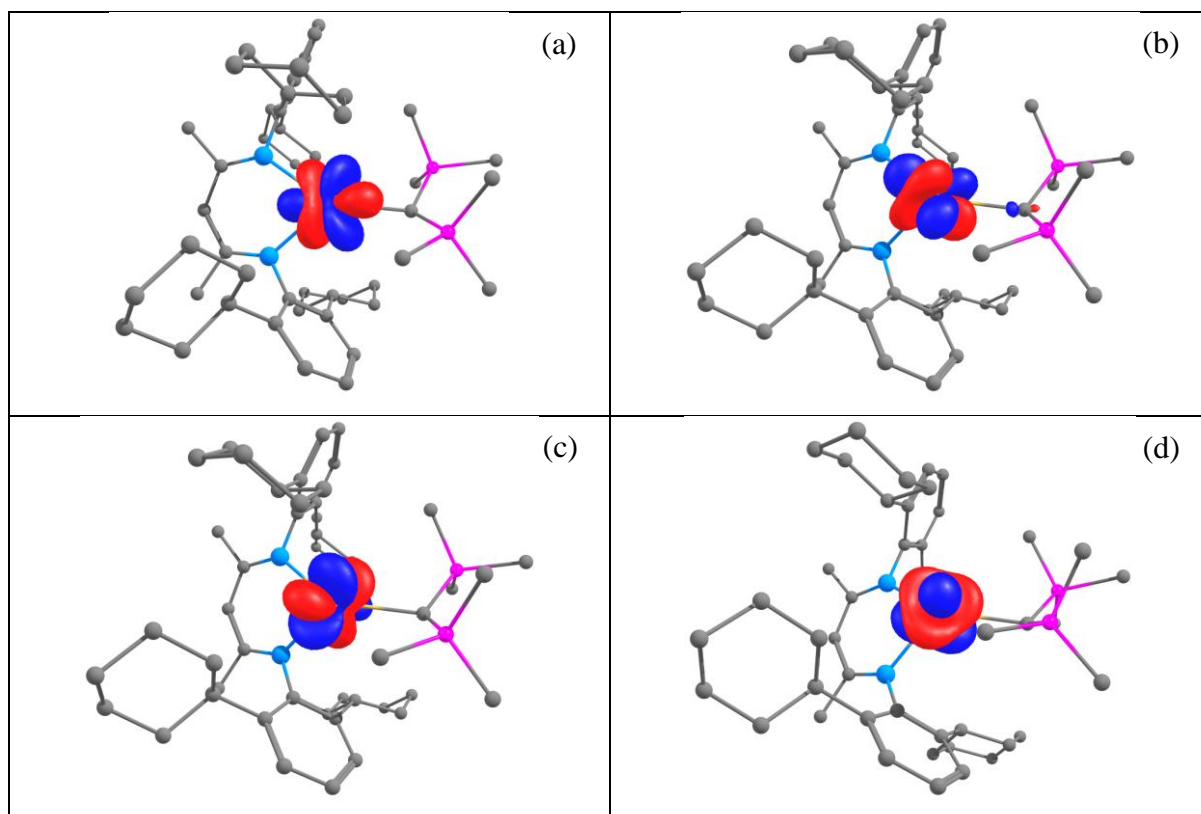


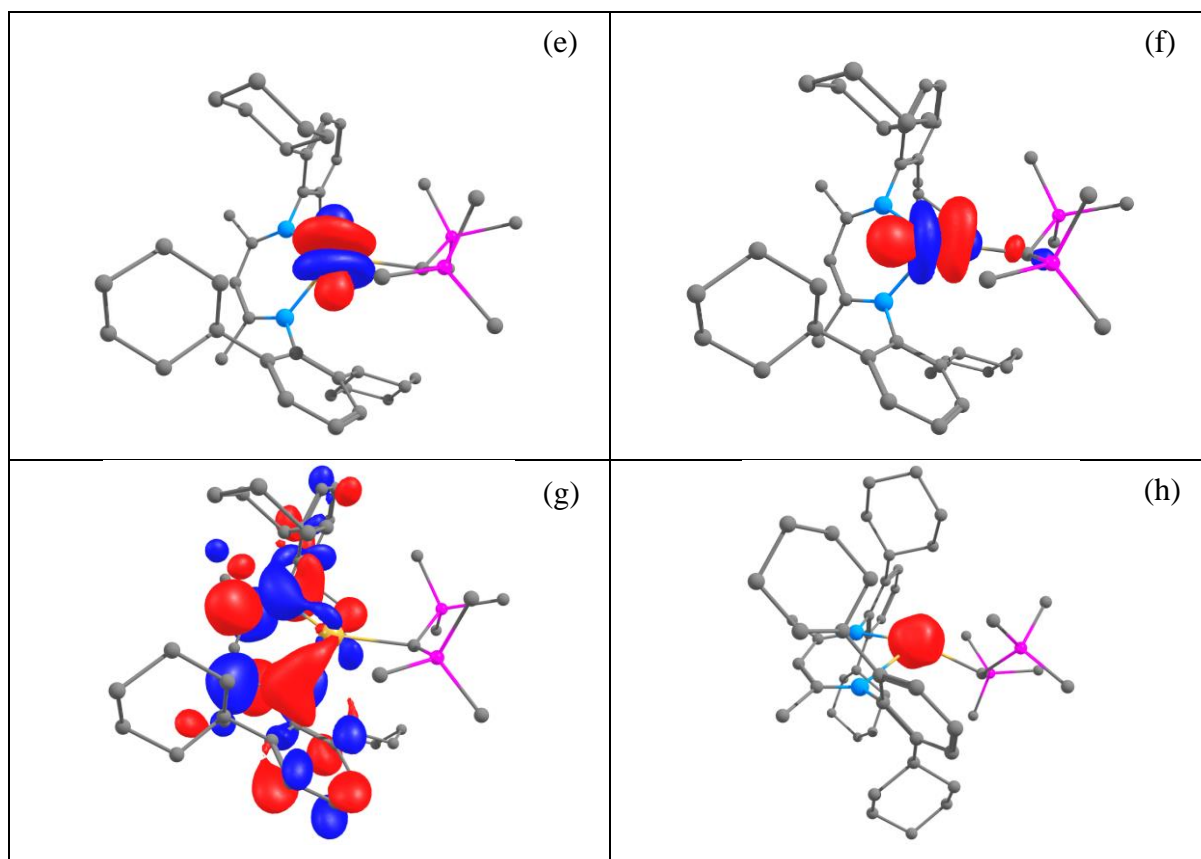
Supplementary Figure 4.54. Variable-temperature effective magnetic moment plot for **4.3** (grey) and for each Sm(III) ion (purple).

4.4 Computational Details

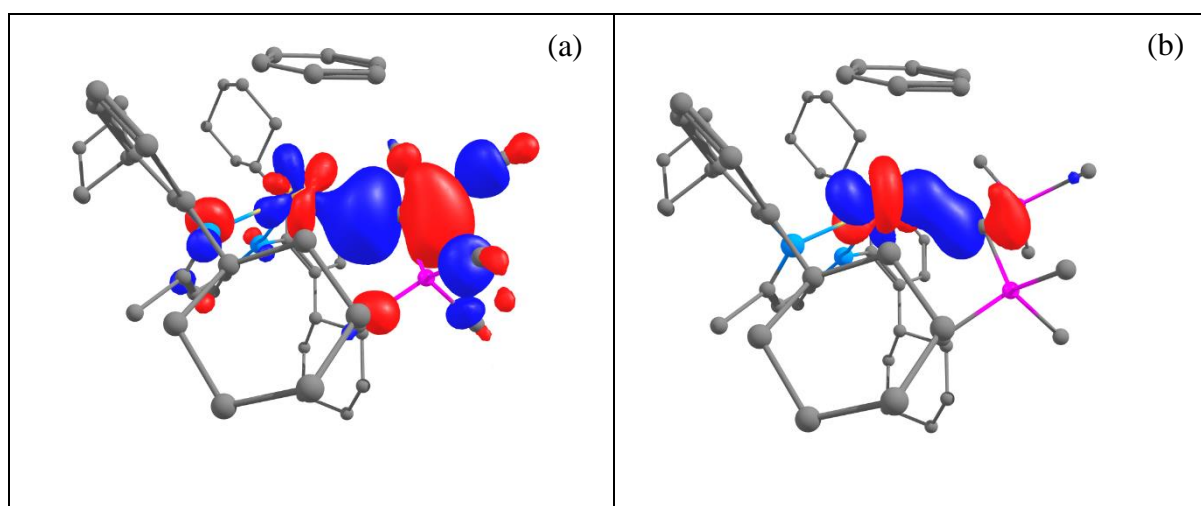
All computational calculations were conducted by Prof. Laurent Maron and Thayalan Rajeshkumar. The optimisation of reactants, transition states, IRC and products were carried out by employing DFT hybrid functional (B3PW91)¹⁰ along with small core pseudopotential Stuttgart basis set¹⁸⁻²⁰ for silicon (additional polarisation function²¹ is employed for silicon atoms), samarium atoms (large core for samarium atom is used to optimise appropriate structures) and Pople basis set (6-31G**) for the rest of the atoms.^{15, 22} Frequency calculations were performed to locate saddle points for transition state structures, minima for rest of the structures and for obtaining thermal corrections over the energies. All the calculations were performed using Gaussian 09 suite of programs.¹¹

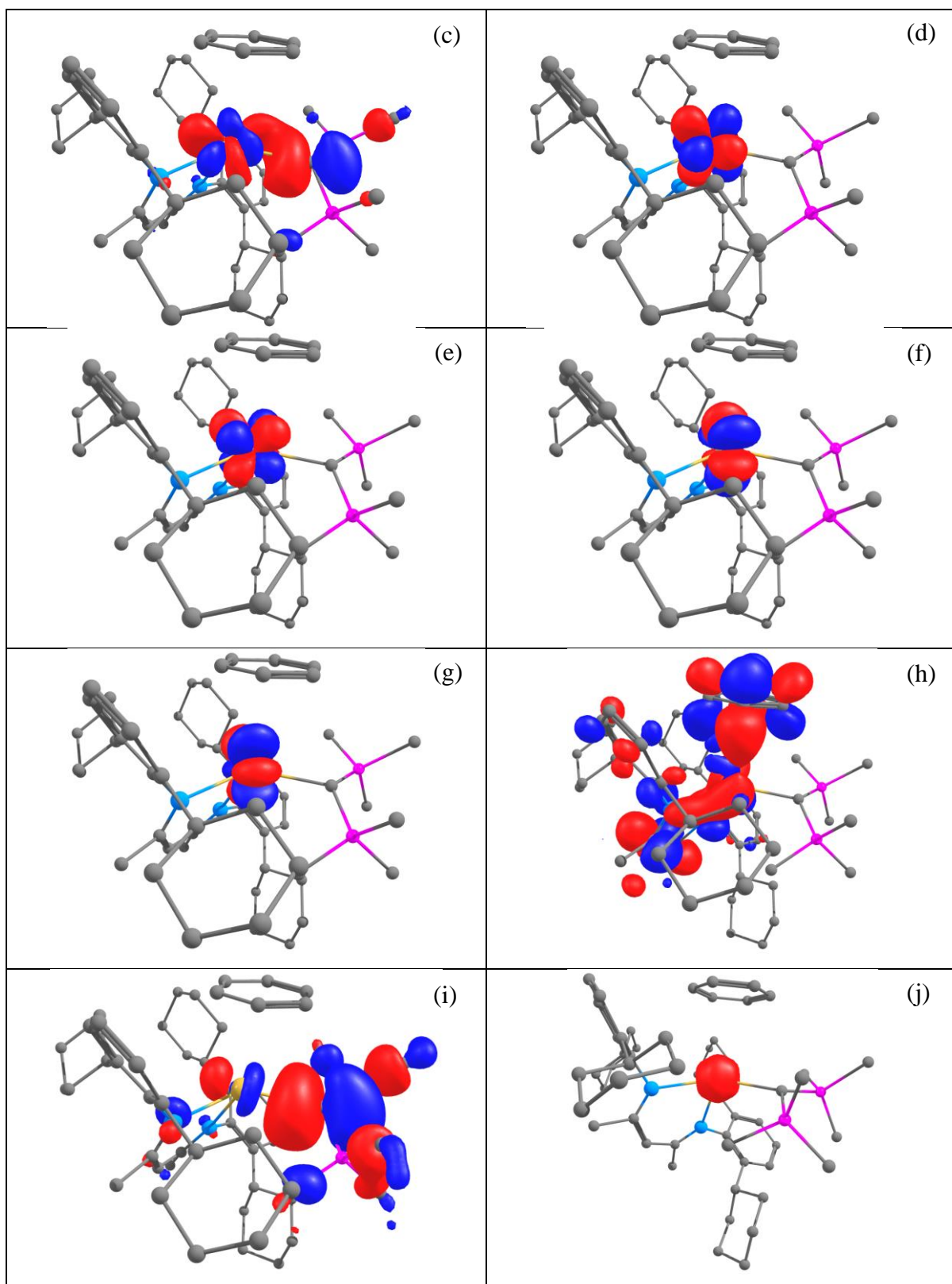
Supplementary Table 4.3. Crystal DFT computed MO's for **4.2**. (a) HOMO-5, (b) HOMO-4, (c) HOMO-3, (d) HOMO-2, (e) HOMO-1, (f) HOMO, (g) LUMO, (h) spin-density plot



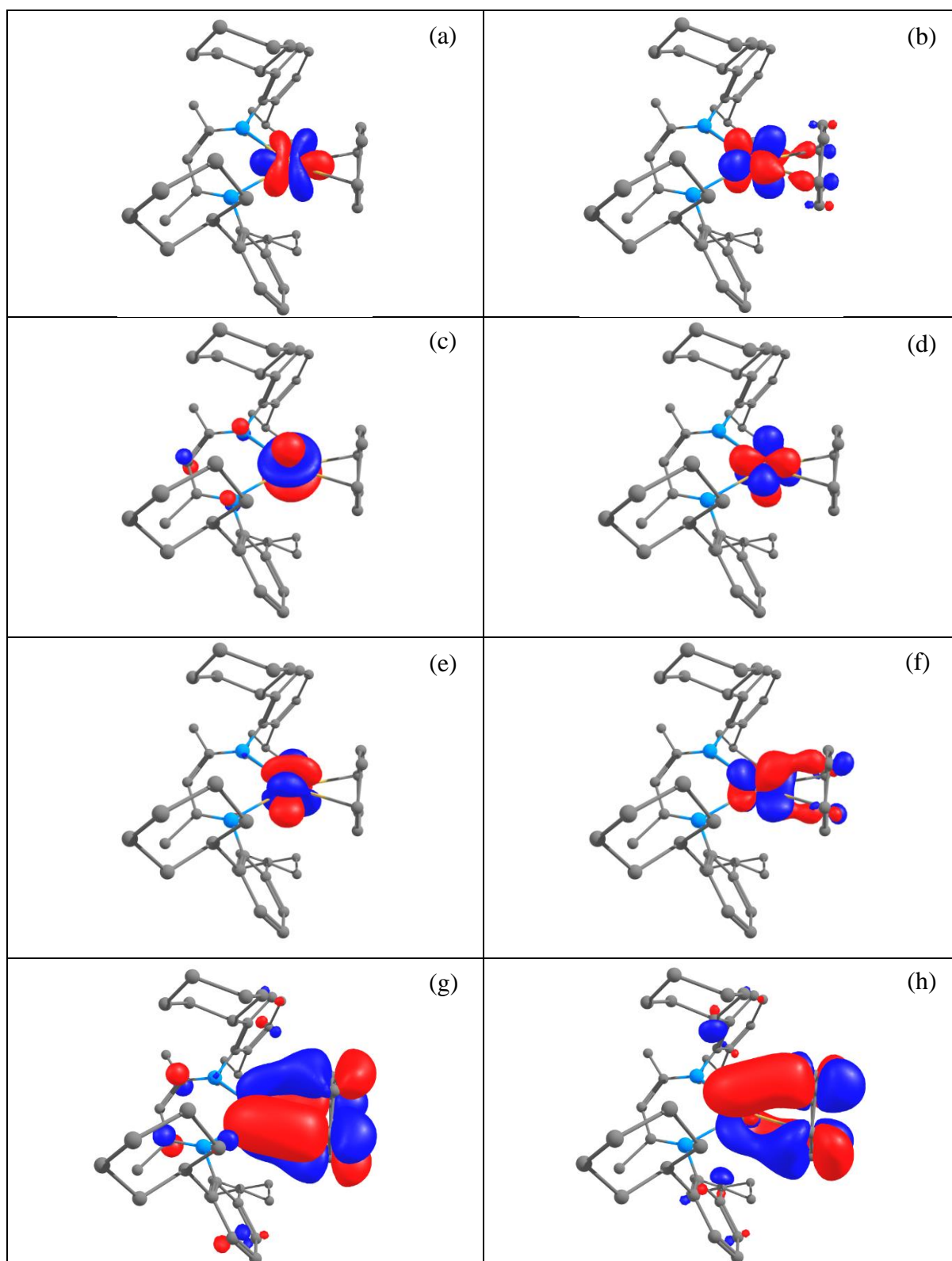


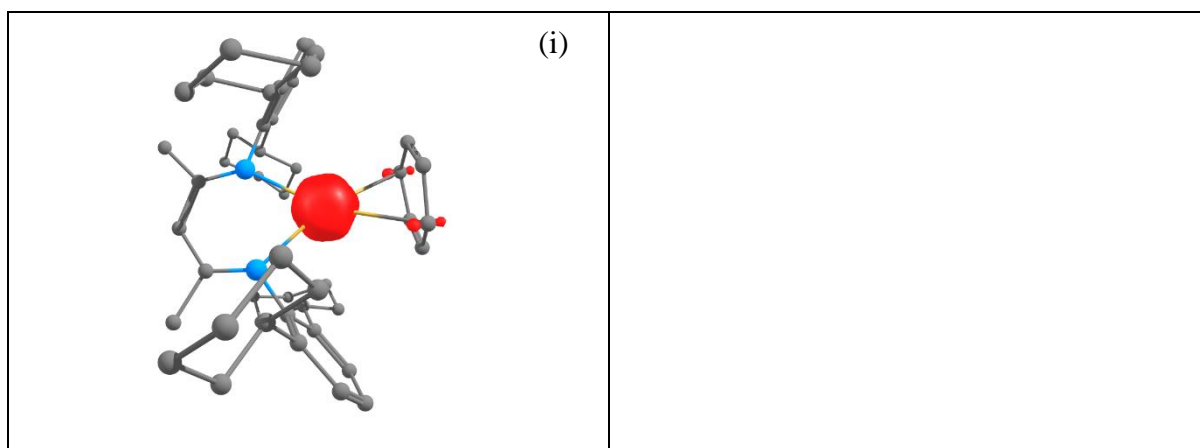
Supplementary Table 4.4. DFT computed MO's for **Int1**. (a) AMO-HOMO-6, (b) AMO-HOMO-5, (c) AMO-HOMO-4, (d) AMO-HOMO-3, (e) AMO-HOMO-2, (f) AMO-HOMO-1, (g) AMO-HOMO, (h) AMO-LUMO, (i) BMO-HOMO, (j) spin-density plot.



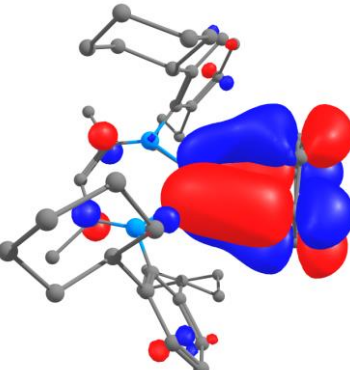


Supplementary Table 4.5. DFT computed MO's for **Int2**. (a) HOMO-6, (b) HOMO-5, (c) HOMO-4, (d) HOMO-3, (e) HOMO-2, (f) HOMO-1, (g) HOMO, (h) LUMO, (i) LUMO.





Supplementary Table 4.6. NBO analysis of Canonical Molecular Orbitals (CMO) for **Int2**.

| | | |
|---|---|---|
| HOMO, MO 200 (occ): orbital energy = -0.08843 a.u. 0.758*[199]: 3C (1)Sm1- C106- C112 -0.303*[195]: BD (2) C108- C110 -0.303*[187]: BD (2) C102- C104 |  | (0.89857) 3C (1)Sm1- C106- C112 (23.20%) 0.4816*Sm1 s(8.70%) p 0.01(0.05%) d10.40(90.51%) f0.08(0.73%) g0.00(0.01%) (38.54%) 0.6208* C106 s(1.13%) p87.14(98.85%) d 0.01(0.02%) (38.26%) 0.6186* C112 s(1.17%) p84.51(98.82%) d 0.01(0.02%) (0.91407) BD (2) C108- C110 (43.64%) 0.6606* C108 s(0.51%) p99.99(99.40%) d 0.18(0.09%) (56.36%) 0.7507* C110 s(0.51%) p99.99(99.43%) d 0.12(0.06%) (0.91358) BD (2) C102- C104 (43.70%) 0.6610* C102 s(0.52%) p99.99(99.38%) d 0.18(0.09%) (56.30%) 0.7503* C104 s(0.54%) p99.99(99.40%) d 0.12(0.06%) |
|---|---|---|

5.0 References

1. G. M. Richardson, T. Rajeshkumar, F. M. Burke, S. A. Cameron, B. Nicholls, J. Harvey, R. A. Keyzers, T. Butler, S. Granville, L. Liu, L. Maron and M. D. Anker, preprint out at *Nature Portfolio*, under vision (*Nat. Chem.*), **2023**.
2. G. M. Richardson, I. Douair, S. A. Cameron, J. Bracegirdle, R. A. Keyzers, M. S. Hill, L. Maron and M. D. Anker, *Nat. Comm.*, **2021**, 12 (1), 3147.
3. T. X. Gentner, B. Rösch, G. Ballmann, J. Langer, H. Elsen and S. Harder, S., *Angew. Chem. Int. Ed.*, **2019**, 58 (2), 607-611.
4. D. D. L. Jones, S. Watts and C. Jones, *Inorganics*, **2021**, 9 (9).
5. I. I. Oleinik, I. V. Oleinik, I. B. Abdrakhmanov, S. S. Ivanchev and G. A. Tolstikov, *Russ. J. Gen. Chem.*, **2004**, 74 (9), 1423-1427.
6. J. Cosier and A. M. Glazer, *J. Appl. Cryst.*, **1986**, 19 (2), 105-107.
7. O. V. Dolomanov, L. J. Bourhis, R. J. Gildea, J. A. K. Howard and H. Puschmann, *J. Appl. Cryst.*, **2009**, 42 (2), 339-341.
8. G. Sheldrick, *Acta Cryst. Sec. A*, **2008**, 64 (1), 112-122.
9. G. Sheldrick, *Acta Cryst. Sec. C*, 2015, 71 (1), 3-8.
10. A. D. Becke, *J. Chem. Phys.*, **1993**, 98 (7), 5648-5652.
11. M. J. Frisch, G. W. Trucks, H. B. Schlegel, G. E. Scuseria, M. A. Robb, J. R. Cheeseman, G. Scalmani, V. Barone, G. A. Petersson, H. Nakatsuji, X. Li, M. Caricato, A. Marenich, J. Bloino, B. G. Janesko, R. Gomperts, B. Mennucci, H. P. Hratchian, J. V. Ortiz, A. F. Izmaylov, J. L. Sonnenberg, D. Williams-Young, F. Ding, F. Lipparini, F. Egidi, J. Goings, B. Peng, A. Petrone, T. Henderson, D. Ranasinghe, V. G. Zakrzewski, J. Go, N. Rega, G. Zheng, W. Liang, M. Hada, M. Ehara, K. Toyota, R. Fukuda, J. Hasegawa, M. Ishida, T. Nakajima, Y. Honda, O. Kitao, H. Nakai, T. Vreven, K. Throssell, J. A. Montgomery, Jr., J. E. Peralta, F. Ogliaro, M. Bearpark, J. J. Heyd, E. Brothers, K. N. Kudin, V. N. Staroverov, T. Keith, R. Kobayashi, J. Normand, K. Raghavachari, A. Rendell, J. C. Burant, S. S. Iyengar, J. Tomasi, M. Cossi, J. M. Millam, M. Klene, C. Adamo, R. Cammi, J. W. Ochterski, R. L. Martin, K. Morokuma, O. Farkas, J. B. Foresman, and D. J. Fox, *Gaussian 09 Revision D.01*. **2016**.
12. W. Küchle, M. Dolg, H. Stoll and H. Preuss, *J. Chem. Phys.*, **1994**, 100 (10), 7535-7542.
13. X. Cao and M. Dolg, *J. Mol. Struct. (THEOCHEM)*, **2004**, 673 (1), 203-209.
14. X. Cao, M. Dolg and H. Stoll, *J. Chem. Phys.*, **2002**, 118 (2), 487-496.
15. R. Ditchfield, W. J. Hehre and J. A. People, *J. Chem. Phys.*, **1971**, 54, 724-728.
16. J. R. van den Hende, P. B. Hitchcock, S. A. Holmes, M. F. Lappert, W. P. Leung, T. C. W. Mak and S. Prashar, *J. Chem. Soc., Dalton Trans.*, **1995**, (9), 1427-1433.
17. G. B. Deacon, S. Hamidi, P. C. Junk, R. P. Kelly and J. Wang, *Eur. J. Inorg. Chem.*, **2014**, 2014 (3), 460-468.
18. A. Bergner, M. Dolg, W. Küchle, H. Stoll and H. Preuß, *Mol. Phys.*, **1993**, 80 (6), 1431-1441.
19. M. Dolg, H. Stoll and H. Preuss, *Theor. Chim. Acta*, **1993**, 85 (6), 441-450.
20. M. Dolg, H. Stoll, A. Savin and H. Preuss, *Theor. Chim. Acta*, **1989**, 75 (3), 173-194.
21. A. Höllwarth, M. Böhme, S. Dapprich, A. W. Ehlers, A. Gobbi, V. Jonas, K. F. Köhler, R. Stegmann, A. Veldkamp and G. Frenking, *Chem. Phys. Lett.*, **1993**, 208 (3), 237-240.
22. P. C. Hariharan and J. A. Pople, *Theor. Chim. Acta*, **1973**, 28 (3), 213-222.